

Keeping it cool: Mammal responses to microclimatic variation in disturbed Indonesian lowland forest



Helen Danielle Slater

Thesis submitted in partial fulfilment of the requirements for the
degree of PhD

May 2021



Department of Life and Environment Sciences

Faculty of Science and Technology

Bournemouth University

This copy of the thesis has been supplied on condition that anyone who consults it is understood to recognise that its copyright rests with its author and due acknowledgement must always be made of the use of any material contained in, or derived from, this thesis.

Abstract

The combined impacts of deforestation, forest fragmentation and climate change will push many mammal species towards extinction, unless appropriate long-term conservation measures are implemented. While most mammal conservation projects focus on protecting remaining primary habitat, it is also important to determine the long-term viability of populations in human-modified landscapes. Effective conservation requires a detailed understanding of species' responses to fragmentation and climate change, yet physiological and behavioural responses of mammals to forest edge effects and climatic variation remain poorly understood. This thesis combines field data and observations with mechanistic models of microclimate and biophysical models of animal bioenergetics to determine the impacts of forest edges and microclimate variation on mammals at a site of disturbed forest in the Sikundur region of Sumatra, Indonesia. First, I identify mammal-habitat associations and the impacts of edge effects on terrestrial mammals using occurrence data from remote camera traps and fine-scale data of climate and habitat structure measured from the field. Next, I implement and test the performance of two freely available mechanistic models of microclimate, 'NicheMapR' and 'microclimc', and determine the effects of vegetation structure on their performance. Finally, I utilise an existing biophysical model 'NicheMapR' to predict the impact of forest edges on metabolism and water balance of a Critically Endangered mammal, the Sumatran orang-utan, *Pongo abelii*. Negative impacts of both forest edges and increased temperatures were observed. Mammal occurrence declined with increasing temperatures, and mammal diversity was much lower at the forest edge compared to the interior, while biophysical modelling suggested that orang-utans are already experiencing thermal stress at frequent intervals for short periods of time, with the frequency of these periods being higher at the forest edge. There are notable climate variations in both space and time which are not captured by coarse scale macroclimate data or yearly averages, and my study showed how useful available microclimate models can be to predict localised temperatures using readily available data. The results demonstrate that disturbed and edge forests are still of value to mammal conservation, but that this usefulness varies depending on the target species. This is one of only a few studies to date which has utilised mechanistic modelling approaches in tropical forest and for terrestrial mammals to fully incorporate microclimatic variation and its effects on tropical forest mammals. These approaches are promising tools which can be used to determine the underlying

mechanisms of population responses to change, identify important local-scale threats to populations and appropriate mitigation strategies.

Table of contents

| | |
|---|----|
| Abstract | 3 |
| Table of contents | 5 |
| List of Figures | 9 |
| List of Tables..... | 13 |
| Acknowledgements | 16 |
| Author’s Declaration..... | 18 |
| Publications and conferences | 19 |
| Chapter 1 General Introduction | 21 |
| 1.1 Thesis aims and general overview | 24 |
| 1.2 Chapter overviews..... | 25 |
| 1.3 Study Location & Site description | 26 |
| Chapter 2 Mammals in The Anthropocene: Predicting Mammal Responses to Environmental Change..... | 30 |
| 2.1 Introduction..... | 30 |
| 2.2 Tropical mammals: Current status and future threats | 32 |
| 2.2.1 Conservation of tropical mammals..... | 34 |
| 2.3 Climate change & tropical mammals..... | 38 |
| 2.3.1 Predicting species ranges | 41 |
| 2.3.2 Limitations of existing approaches | 42 |
| 2.3.3 Adaptations to climate change..... | 44 |
| 2.4 Microclimates and their relevance to climate change responses | 46 |
| 2.4.1 Microclimate variability in forests..... | 47 |
| 2.4.2 Vertical microclimate gradients in forests | 47 |
| 2.4.3 Thermal buffering in forests | 48 |
| 2.5 Measuring & modelling microclimates..... | 49 |
| 2.5.1 Direct measurements & remote sensing | 49 |

| | | |
|-----------|---|----|
| 2.5.2 | Modelling microclimate..... | 50 |
| 2.6 | Using microclimates in predicting species responses to climate change.. | 51 |
| 2.7 | Summary and conclusions | 51 |
| Chapter 3 | Forest edge effects on microclimate and mammal activity in Sikundur, Sumatra. | 53 |
| Abstract | | 53 |
| 3.1 | Introduction..... | 54 |
| 3.2 | Objectives..... | 57 |
| 3.3 | Methods..... | 58 |
| 3.3.1 | Field data collection..... | 58 |
| 3.3.2 | Data analysis | 62 |
| 3.4 | Results..... | 65 |
| 3.4.1 | Objective 1) Comparing environmental conditions at different distances from the edge..... | 65 |
| 3.4.2 | Objective 2) Variation in mammal activity rates between distances. | 74 |
| 3.4.3 | Objective 3) Environmental predictors of mammal activity rates | 77 |
| 3.5 | Discussion | 82 |
| 3.5.1 | Differences in forest conditions and edge effects..... | 82 |
| 3.5.2 | Mammal activity | 83 |
| 3.5.3 | Remote monitoring of wildlife populations..... | 87 |
| 3.5.4 | Conservation Implications | 89 |
| 3.6 | Conclusion | 89 |
| Chapter 4 | Predicting microclimate in a heterogeneous tropical secondary forest in Sumatra, Indonesia..... | 91 |
| Abstract | | 91 |
| 4.1 | Introduction..... | 93 |
| 4.2 | Aim & Objectives | 97 |

| | | |
|-----------|---|-----|
| 4.3 | Methods..... | 97 |
| 4.3.1 | Location | 97 |
| 4.3.2 | <i>In situ</i> microclimate measurements | 97 |
| 4.3.3 | Vegetation & canopy structure | 99 |
| 4.3.4 | Microclimate modelling..... | 99 |
| 4.3.5 | Effects of canopy structure on microclimate variation and microclimate model performance..... | 101 |
| 4.4 | Results | 102 |
| 4.4.1 | Observed microclimate | 102 |
| 4.4.2 | Microclimate modelling..... | 102 |
| 4.4.3 | Vegetation structure..... | 108 |
| 4.4.4 | Vegetation effects on observed microclimate and model performance | 108 |
| 4.5 | Discussion | 116 |
| 4.5.1 | Vegetation structure & microclimate conditions | 116 |
| 4.5.2 | Microclimate model performance..... | 117 |
| Chapter 5 | A biophysical modelling approach to investigating edge effects on arboreal mammals: a case study of the Sumatran orangutan, <i>Pongo abelii</i> | 120 |
| | Abstract | 120 |
| 5.1 | Introduction..... | 122 |
| 5.2 | Aim & objectives | 126 |
| 5.3 | Methods..... | 127 |
| 5.3.1 | The endotherm model | 127 |
| 5.4 | Results | 130 |
| 5.5 | Discussion | 142 |
| Chapter 6 | General discussion | 148 |
| 6.1 | Structure and microclimate in secondary forests | 149 |

| | | |
|-------|---|-----|
| 6.2 | Edge effects on forest conditions and mammals..... | 150 |
| 6.3 | Microclimate modelling in secondary tropical forests..... | 151 |
| 6.4 | Applications of mechanistic models in mammal ecology and conservation 152 | |
| 6.5 | Conclusions & recommendations for future research..... | 154 |
| 6.5.1 | Future work..... | 155 |
| | References | 160 |
| | Appendix 3.1 R scripts to run generalized linear models and generalized linear mixed models of microclimate and forest structure effects on mammals..... | 205 |
| | Appendix 4.1 R scripts to run the NicheMapR microclimate model..... | 226 |
| | Appendix 4.2 R scripts to run the microclimc microclimate model | 284 |
| | Appendix 5.1 R scripts to run the NicheMapR endotherm model..... | 289 |

List of Figures

Unless otherwise stated, all figures and photographs contained within this document have been produced by the author of this thesis. All maps were created using ArcGIS® software by Esri. ArcGIS® and ArcMap™ are the intellectual property of Esri and are used herein under license. Copyright © Esri. All rights reserved. For more information about Esri® software, please visit www.esri.com.

- Figure 1.1: a) Location of the Sikundur region and the Leuser ecosystem in Sumatra, Indonesia, and b) the Aras Napal and Sikundur region located in North Sumatra. 28
- Figure 1.2: Corrugated iron fencing surrounding an orange plantation bordering the National Park at Aras Napal; several plantations in this area have fencing or some other barrier blocking access to/from the forest, but some have no fencing at all. 29
- Figure 1.3: A typical orange plantation close to the National Park at Aras Napal. 29
- Figure 3.1: Monitoring locations close to Aras Napal in the Sikundur region of the Gunung Leuser National Park (GLNP), North Sumatra province, Sumatra, Indonesia. The dark green line represents the border of the GLNP..... 59
- Figure 3.2: Typical conditions at the forest boundary. Farms and plantations adjacent to the forest generally extend right up to the forest edge, creating a very obvious boundary between the two land cover types. 59
- Figure 3.3: HOBO data logger used to measure microclimate conditions throughout the site at Aras Napal. 60
- Figure 3.4: SpyPoint Force Dark trail cameras were used to record mammal activity at each monitoring location..... 62
- Figure 3.5: The range of microclimate conditions recorded at different distances from the forest edge at Aras Napal. (a) Mean temperature for the whole sampling period; (b) mean temperature of each day; (c) minimum temperature of each day; (d) maximum temperature of each day; (e) mean light intensity of each day; and (f) maximum light intensity of each day..... 69
- Figure 3.6: Total height (m), bole height (m), and height:DBH ratio of trees recorded at different distances from the forest edge at Aras Napal. 73
- Figure 3.7: Number of trees per plot, DBH (cm), crown area (m²), and canopy connectivity (%) of trees recorded at different distances from the forest edge at Aras Napal. 74

| | |
|--|-----|
| Figure 3.8: Species accumulation curve showing number of mammal families detected with sampling effort in Aras Napal..... | 75 |
| Figure 3.9: Total number of detection events for each mammal Order detected at different distances from the forest edge at Aras Napal..... | 77 |
| Figure 3.10: GLM predictions (lines), with 95% confidence intervals (grey shading), and observed number of mammal detections against (a) maximum temperature, °C; (b) minimum temperature, °C; (c) tree height, m; and (d) DBH, cm on the total number of mammal detection events at Aras Napal. | 79 |
| Figure 3.11: Model predictions (lines) and observed values (points) of detection rates by mammal Order against (a) Maximum temperature, °C; (b) Tree height, m; and (c) Diameter at breast height, cm..... | 81 |
| Figure 4.1: Random sampling locations used to measure and predict microclimate at Sikundur. | 98 |
| Figure 4.2: Hourly variation in ambient air temperatures, °C, observed from data loggers and predicted by NicheMapR and microclimc..... | 104 |
| Figure 4.3: Range of temperatures for each location of a) observed values recorded from data loggers and b) values predicted by NicheMapR. Different heights are denoted by (1) bottom; (2) middle; and (3) top. | 105 |
| Figure 4.4: Observed and predicted values for ambient air temperature, °C, for all locations and heights at Sikundur (excluding points removed due to logger exposure to direct sunlight). (a) Observed (red) and NicheMapR predictions (black) of ambient temperature against day of year for the period October 2018 - October 2019; (b) Spearman’s correlation of NicheMapR predictions against observed values for temperature; (c) Observed (red) and microclimc predictions (black) of ambient temperature against day of year for the period October 2018 - October 2019; and (d) Spearman’s correlation of microclimc predictions against observed values for temperature..... | 106 |
| Figure 4.5: The range of values of forest structure variables collected from vegetation plots at Sikundur: (a) Total tree height, m; (b) bole height, m; (c) diameter at breast height, cm; (d) crown area, m; (e) crown depth, m; and (f) crown connectivity, % | 110 |
| Figure 4.6: Linear mixed model predictions (line) with 95% confidence intervals (grey shading) and observed values (points) of monthly mean temperature against a) | |

| | |
|--|-----|
| logger height, m; b) plot location; and c) calendar month on monthly mean temperatures recorded by data loggers at Sikundur. | 111 |
| Figure 4.7: Linear mixed model predictions (line) with 95% confidence intervals (grey shading) and observed values (points) of daily maximum temperature against a) logger height, m; b) plot location; and c) calendar month on daily maximum temperatures recorded by data loggers at Sikundur. | 111 |
| Figure 4.8: Linear mixed model predictions (line) with 95% confidence intervals (grey shading) and observed values (points) of root mean square error of NicheMapR temperature predictions against a) logger height, m; b) plot location; and c) calendar month on root mean square error of NicheMapR microclimate predictions at Sikundur. | 112 |
| Figure 4.9: Linear mixed model predictions (line) with 95% confidence intervals (grey shading) and observed values (points) of mean absolute error of NicheMapR temperature predictions against a) logger height, m; b) plot location; and c) calendar month on mean absolute error of NicheMapR microclimate predictions at Sikundur. | 112 |
| Figure 5.1: NicheMapR endotherm model predictions of core body temperature, dorsal fur temperature, metabolic rate, and water loss across a series of ambient temperatures for adult male, adult female, and juvenile orangutans when using estimates of basal metabolic rate based on the mouse-elephant curve of body mass against BMR. Zero values were produced when the endotherm model was unable to find a solution (i.e., it was not possible for the modelled organism to maintain their body temperature within the defined parameters for metabolic rate, panting and sweating). | 131 |
| Figure 5.2: NicheMapR endotherm model predictions of core body temperature, dorsal fur temperature, metabolic rate, and water loss across a series of ambient temperatures for adult male, adult female, and juvenile orangutans when using observed basal metabolic rates from Pontzer et al (2010). Zero values were produced when the endotherm model was unable to find a solution (i.e., it was not possible for the modelled organism to maintain their body temperature within the defined parameters for metabolic rate, panting and sweating). | 132 |
| Figure 5.3: Air temperatures, °C, predicted by NicheMapR and recorded from data loggers at 1.5m from the ground for the time period August – October 2019: (a) The | |

| | |
|--|-----|
| range of predicted and observed temperatures for each hour of the day; and (b) predicted temperatures against observed temperatures..... | 134 |
| Figure 5.4: (a) The number of days per year where maximum temperature predicted by NicheMapR exceeds the upper critical temperature, UCT of 32°C at 4 locations at the edge and the interior; and (b) the proportion of total time where temperatures predicted by NicheMapR exceed the UCT at 4 edge and 4 interior locations. Circles represent actual values, while diamonds represent the group means..... | 134 |
| Figure 5.5: NicheMapR predictions of metabolic rate, W, for different age/sex classes of orangutans at edge and interior locations at Sikundur when using inputs of basal metabolic rate from (a) estimates based on the mouse-elephant curve; and (b) observed values from Pontzer et al 2010. | 137 |
| Figure 5.6: NicheMapR predictions of water loss rate, g/h, for different age/sex classes of orangutans at edge and interior locations at Sikundur when using inputs of basal metabolic rate from (a) estimates based on the mouse-elephant curve; and (b) observed values from Pontzer et al 2010. | 138 |
| Figure 5.7: NicheMapR predictions of dorsal fur temperature, °C, for different age/sex classes of orangutans at edge and interior locations at Sikundur when using inputs of basal metabolic rate from (a) estimates based on the mouse-elephant curve; and (b) observed values from Pontzer et al 2010..... | 139 |
| Figure 5.8: Water loss rate, g/h, estimated by NicheMapR using observed values of metabolic rate from Pontzer et al 2010, against predicted air temperature, mid canopy, in °C, for (a) adult male; (b) adult female; and (c) juvenile orangutans.. | 141 |

List of Tables

| | |
|--|----|
| Table 3.1: Environmental variables collected from all monitoring locations at Aras Napal. | 63 |
| Table 3.2: Summary of microclimate variables collected at different distances from the forest edge at Aras Napal. N = number of cases, μ = mean, M = median, SD = standard deviation. | 66 |
| Table 3.3: Test statistics and Bonferroni adjusted P-values from post-hoc Dunn's pairwise comparisons of Tall (i.e., mean temperature, °C, for the whole sampling period) recorded at different distances from the forest edge at Aras Napal. Values which are significantly different following adjustment with $\alpha = 0.05$ are given in bold with an asterisk..... | 67 |
| Table 3.4: Test statistics and Bonferroni adjusted P-values from post-hoc Dunn's pairwise comparisons of T_{\max} (ie., maximum temperature, °C, for each day) recorded at different distances from the forest edge at Aras Napal. Values which are significantly different following adjustment with $\alpha = 0.05$ are given in bold with an asterisk. .. | 67 |
| Table 3.5: Test statistics and Bonferroni adjusted P-values from post-hoc Dunn's pairwise comparisons of Tday (i.e., mean temperature, °C, for each day), recorded at different distances from the forest edge at Aras Napal. Values which are significantly different following adjustment with $\alpha = 0.05$ are given in bold with an asterisk. | 67 |
| Table 3.6: Test statistics and Bonferroni adjusted P-values from post-hoc Dunn's pairwise comparisons of LI _{all} (i.e., mean light intensity, lux, for the whole sampling period) recorded at different distances from the forest edge at Aras Napal. Values which are significantly different following adjustment with $\alpha = 0.05$ are given in bold with an asterisk..... | 68 |
| Table 3.7: Test statistics and Bonferroni adjusted P-values from post-hoc Dunn's pairwise comparisons of LI _{day} (i.e., mean light intensity, lux, for each day) recorded at different distances from the forest edge at Aras Napal. Values which are significantly different following adjustment with $\alpha = 0.05$ are given in bold with an asterisk. .. | 68 |
| Table 3.8: Test statistics and Bonferroni adjusted P-values from post-hoc Dunn's pairwise comparisons of LI _{max} (i.e., maximum light intensity, lux, for each day) recorded at different distances from the forest edge at Aras Napal. Values which are significantly different following adjustment with $\alpha = 0.05$ are given in bold with an asterisk. .. | 68 |

| | |
|---|-----|
| Table 3.9: Summary of forest structure variables collected from plots at different distances from the forest edge at Aras Napal..... | 71 |
| Table 3.10: Test statistics and Bonferroni adjusted P-values from post-hoc Dunn's pairwise comparisons of mean tree height, m, recorded at different distances from the forest edge at Aras Napal. Values which are significantly different following adjustment with $\alpha = 0.05$ are given in bold with an asterisk..... | 72 |
| Table 3.11: Test statistics and Bonferroni adjusted P-values from post-hoc Dunn's pairwise comparisons of mean bole height, m, recorded at different distances from the forest edge at Aras Napal. Values which are significantly different following adjustment with $\alpha = 0.05$ are given in bold with an asterisk..... | 72 |
| Table 3.12: Test statistics and Bonferroni adjusted P-values from post-hoc Dunn's pairwise comparisons of the mean ratio of tree height to diameter at breast height, HDR, recorded at different distances from the forest edge at Aras Napal. Values which are significantly different following adjustment with $\alpha = 0.05$ are given in bold with an asterisk..... | 72 |
| Table 3.13: Checklist of mammals detected at Aras Napal with total number of detections and naïve occupancy (the proportion of sites with ≥ 1 detection events). | 76 |
| Table 3.14: Exponentiated coefficient estimates with standard errors in parentheses for the GLM with poisson distribution and log:link function testing the effects of environmental variables on the number of mammal detection events at Aras Napal. Significant effects ($\alpha = 0.05$) are highlighted in bold. | 78 |
| Table 3.15: Generalised linear mixed model (negative binomial) fit by the laplace approximation of total detection events according to environmental variables. Mammal Order is included as a random factor. Significant P-values ($\alpha = 0.05$) are highlighted in bold. | 80 |
| Table 4.1: Summary of observed temperatures from data loggers and predicted ambient air temperatures for each location and height sampled at Sikundur. | 103 |
| Table 4.2: Spearman's correlation, root mean square error, RMSE, and mean absolute difference, MAD, between temperatures, °C, recorded from data loggers and temperatures, °C, predicted by NicheMapR at individual sampling locations and heights at Sikundur. *** P<0.001 with Bonferroni adjustment. | 107 |
| Table 4.3: Summary of forest structure variables collected from vegetation plots at Sikundur..... | 109 |

| | |
|--|-----|
| Table 4.4: Results of the linear mixed model for effect of logger height (H) on monthly mean temperature recorded by data loggers at Sikundur, σ^2 denotes within group variance, while τ_{00} denotes between group variance of random effects. | 113 |
| Table 4.5: Results of the linear mixed model for effect of logger height on daily maximum temperature recorded by data loggers at Sikundur, σ^2 denotes within group variance, while τ_{00} denotes between group variance of random effects. | 114 |
| Table 4.6: Results of the linear mixed model for effect of logger height on root mean square error of microclimate predictions generated by NicheMapR for individual locations at Sikundur, σ^2 denotes within group variance, while τ_{00} denotes between group variance of random effects. | 115 |
| Table 4.7: Results of the linear mixed model for effect of logger height on mean absolute error of microclimate predictions generated by NicheMapR for individual locations at Sikundur, σ^2 denotes within group variance, while τ_{00} denotes between group variance of random effects. | 115 |
| Table 5.1: Input parameters and their sources used for the NicheMapR endotherm model for adult male, adult female and juvenile orangutans. | 128 |
| Table 5.2: Summary of temperatures recorded by data loggers, temperatures predicted by NicheMapR, and model performance at individual locations at Sikundur. | 135 |
| Table 5.3: NicheMapR endotherm model predictions for metabolic rate, W, water loss rate, g/h, and dorsal fur temperature, °C of adult male, female, and juvenile orangutans from individual sampling locations at Sikundur. | 140 |

Acknowledgements

Firstly, I would like to thank my supervisors Professor Amanda Korstjens and Dr Phillipa Gillingham. Your endless support, patience and guidance has been incredible throughout this PhD, and I couldn't have done this without you. I am so very grateful for the opportunities you have given me. I would also like to thank Professor Michael Kearney and Isobel Bramer for their advice and support in developing adapting the NicheMapR models and R scripts. Additionally, I would like to extend thanks to Professor Ross Hill and Harry Manley for their support and advice in spatial analysis and ArcGIS Pro. Thank you also to Dr. Andrew Whittington and Dr Demetra Andreou for their support and advice at the start of the project.

Special thanks go to Universitas Syiah Kuala, and in particular Dr Abdullah and Dini from the International Affairs office for their very warm hospitality, support, and guidance during my time in Indonesia, and their invaluable help and support in obtaining my research permits and visa. Additionally, I would like to thank RISTEK and Taman Nasional Gunung Leuser for granting me permission to conduct research in Indonesia. I would also like to thank Rudi Putra, Issa and the rest of the team at Forum Konservasi Leuser for their additional guidance and support, and for their tireless efforts to conserve the forests and wildlife of Sumatra.

My thanks also go out to the team at the Sumatran Orangutan Conservation Programme HQ in Medan, in particular to Dr Ian Singleton and Matt Nowak for their support and advice in conducting fieldwork, and for inviting me to work from the Sikundur research station. In particular I would like to thank Matt for his endless patience in helping me to solve problems with permits and field data collection, and for always being on hand for a chat and a beer during my time in Indonesia. I would also like to thank Graham Usher and Dave Dellatore for providing the UAV data. Thank you also to the field staff at Sikundur: Suprayudi, Riki, Ben, Winn, Argus, Ucok and Supri. Your knowledge and experience has been invaluable, and without you I would not have been able to complete my research. I would especially like to thank Supri and Ucok for going above and beyond in helping me collect my data and troubleshoot my methodologies. Also, I would like to thank Rusman, Nursal and the entire Aras Napal community for making me feel so incredibly welcome and at home during my time in Sumatra.

I would like to thank Bournemouth University for funding my research, as well as the BU GCRF fund and Research Impact funds which also helped to support my project costs. Additionally, I would like to thank the People's Trust for Endangered Species and the International Primatological Society for providing additional funding which was vital to covering various logistical costs involved in the project. Finally, I would like to thank Tempcon for providing sponsorship to purchase climate data loggers.

I would also like to thank the team at Invisible Flock for helping to bring some of my research to life in ways I would never be able to. In particular, I would like to thank Ben, Vic and Fletch for their help in developing and implementing equipment in the field, for helping me to set up the equipment in Sumatra, and for being lovely company for some of my time in the field.

I am also forever grateful to all of my fellow researchers and students with whom I shared my time in Indonesia. In particular, I want to thank Emma Hankinson and Nathan Harrison for their unwavering support and friendship. I would also like to thank Rosanna Consiglio for always having my back and believing in me. Finally, I would like to thank James Askew, Ziva Justinek Meidina Fitriana, Chiara Ripa and Lucy Twitcher for their friendship and support at various times throughout my PhD.

Thank you also to all my fellow post-graduate researchers at BU. In particular, I would like to thank Michelle, Hannah, Paul, Owen, Ramin, Heather & Sam for being wonderful officemates, who are always on hand for a silly chat over coffee and cake. Thank you also for continuing to support both me and each other throughout the past year, even though lockdowns have kept us away from campus. I am also forever grateful to my lovely friends Annie, Phoebe, Katie, Esraa, Georgie and Laura, who have never failed to support me and cheer me up even in the hardest of times.

Last, but most definitely not least, thank you so much to my Mum and Dad, my brother Alex, and my partner Darryl. You have all always had my back, believed in me, and motivated me to keep going. I would not have got this far without you. I love you all. Thank you especially to Darryl for not only humouring, but also sharing my animal obsession, and for always offering me support, love, and snacks to keep me going throughout this journey. I could not have done this without you. I love you.

Author's Declaration

The work for this thesis was carried out between September 2017 and May 2021 at the Department of Life and Environment Sciences, Faculty of Science and Technology, Bournemouth University. This work was conducted under the supervision of Professor Amanda Korstjens and Dr Phillipa Gillingham.

I declare that while registered as a PhD candidate at Bournemouth University, I have not been a registered candidate or enrolled as a student for an award of any other academic or professional institution. I furthermore declare that no material contained within this thesis has been used in any other submission for an academic award.

I declare that the work contained within this thesis is my own work. All materials, data, findings, and ideas presented here which are not my own have been fully and appropriately acknowledged throughout the document. Maps throughout this thesis were created using ArcGIS® software by Esri. ArcGIS® and ArcMap™ are the intellectual property of Esri and are used herein under license. Copyright © Esri. All rights reserved. For more information about Esri® software, please visit www.esri.com.

Publications and conferences

Peer-reviewed publications

Williams, K. A., **Slater, H. D.**, Gillingham, P., and Korstjens, A. H., (accepted; in press). Environmental factors are stronger predictors of primate species' distributions than basic biological traits. *International Journal of Primatology*.

Harrison, N. J., Hill, R. A., Alexander, C., Marsh, C. D., Nowak, M. G., Abdullah, A., **Slater, H. D.**, and Korstjens, A. H., 2020. Sleeping trees and sleep-related behaviours of the siamang (*Symphalangus syndactylus*) in a tropical lowland rainforest, Sumatra, Indonesia. *Primates*, 1, 3.

Slater, H. D., and Abdullah, A., 2020, February. The importance of forests as microclimate refuges for mammals in Sumatra. In *Journal of Physics: Conference Series* (Vol. 1460, No. 1, p. 012051). IOP Publishing. <https://iopscience.iop.org/article/10.1088/1742-6596/1460/1/012051/pdf>

Bramer, I., Anderson, B., Bennie, J., Bladon, A., Frenne, P. de, Hemming, D., Hill, R. A., Kearney, M. R., Korner, C., Korstjens, A. H., Lenoir, J., Marsh, C. D., Morecroft, M. D., **Slater, H. D.**, Suggitt, A. J., Zellweger, F., and Gillingham, P. K., 2018. Advances in Monitoring and Modelling Climate at Ecologically Relevant Scales. *Advances in Ecological Research*, 58, 101–161.

Korstjens, A. H., **Slater, H. D.**, and Hankinson, E., 2018. Predicting African primate species' responses to climate change. In: *Primatology, Biocultural Diversity and Sustainable Development in Tropical Forests*. Mexico City: UNESCO, 186–204.

Conference Presentations

Slater, H. D., Gillingham, P., Abdullah, A., and Korstjens, A. H., 2020. Edge effects, microclimate & mammal activity in Sumatra, Indonesia. Oral presentation for the Sci-Tech Post-Graduate Research Conference, Bournemouth University.

Slater, H. D. and Abdullah, A., 2019. The importance of forests as microclimate refuges for mammals in Sumatra. Oral presentation for The 1st Annual International Conference on Mathematics, Science and Technology Education, Universitas Syiah Kuala. Banda Aceh, Indonesia.

Slater, H. D., Gillingham, P., and Korstjens, A. H., 2019. Edge effects in secondary tropical forest: Microclimate and mammal occurrence. Poster presentation for the British Ecological Society Annual Meeting. Belfast.

Slater, H. D., Gillingham, P., and Korstjens, A. H., 2019. Voices in the Jungle: Using remote sensing to monitor forest biodiversity. Live research and poster exhibit for the 11th Annual Postgraduate Research Conference, Bournemouth University.

Slater, H. D., Williams, K. A., and Korstjens, A. H., 2016. Predicting species' responses to environmental change: biological traits and African primate biogeography. Oral presentation for the British Ecological Society Annual Meeting. Liverpool.

Korstjens, A. H., Williams, K. A., and **Slater, H. D.**, 2016. Predicting species' responses to environmental change: the biogeography of diurnal African primates. Oral presentation for the Joint meeting of the International Primatological Society and the American Society of Primatologists. Chicago.

Slater, H. D., 2016. Logging, forest structure and group densities of primates in North Sumatra, Indonesia. Poster presentation for the Primate Society of Great Britain Spring Meeting. University of York.

Slater, H. D. and Consiglio, R., 2014. The importance of forest structure on primate distributions in Sikundur, Sumatra, Indonesia. Poster presentation for the Primate Society of Great Britain Winter Meeting. University of Birmingham.

Chapter 1

General Introduction

Biodiversity loss and climate change are major global challenges. Current rates of biodiversity loss and climate change have exceeded the maximum threshold and threaten to undermine ecosystem stability, function, and provisioning of vital ecosystem services. Climate change and biodiversity loss interact with each other in a negative feedback loop; climate change will result in further biodiversity loss, while loss of species reduces ecosystem resilience and stability, making ecological processes more vulnerable to changes in climate. Halting current rates of biodiversity loss and reversing trends in declining wildlife populations is crucial to maintaining global ecological resilience. Tropical forests contain the largest proportion of global terrestrial biodiversity, as well as playing a key role sequestering atmospheric carbon and mitigating against anthropogenic climate change (Posa et al. 2011; Englhart et al. 2013; Astuti and McGregor 2015). Protection and restoration of tropical forest biomes is therefore integral to preserving biodiversity and mitigating against global climate change.

Biodiversity is now being lost rapidly; an estimated one million species are thought to be threatened with extinction (IPBES 2019). Current species extinction rates are around 100 to 1,000 times higher than the historical background rate estimated from the fossil record; these extinctions are mainly attributed to human activities, and this rate is expected to increase further throughout the 21st century (Mace et al. 2005). This is well above the maximum planetary boundary for biodiversity loss of ten times the natural rate proposed by Rockström et al. (2009). Current projections of future extinction rates have a wide range of uncertainty, in part due to a lack of data on species ecology (particularly dispersal and migration rates), but also because there is the potential for effective interventions to reduce extinction risk, including land-use management and climate mitigation (Pereira et al. 2010). We do not have enough long-term data to truly understand the full implications of biodiversity loss, but most evidence suggests that loss of biodiversity will result in reduced resilience and function of ecosystems globally. Additionally, the loss of biodiversity will have implications for other Earth systems, including hydrological cycles, nutrient cycles, and climate change (Mace et al. 2014).

The effects of climate change are becoming increasingly evident and will further exacerbate biodiversity declines. The current concentration of global atmospheric Carbon has already well exceeded the planetary boundary and is now likely to lead to irreversible climate change (Rockström et al. 2009). Arctic sea ice, mountain glaciers, and sea levels have already changed notably from their Holocene state as a result of climate change (IPCC 2007). Climate affects species by determining their range, abundance at a given location, phenology and influencing microhabitat use and energy budgets. Climate-related local extinctions have already been recorded in hundreds of species, with the tropics having a considerably higher rate of local extinctions compared with temperate regions (Wiens 2016). Tropical regions, including Southeast Asia and Indonesia are considered ‘hotspots’ of climate change vulnerability, due to the large number of species and taxa which are predicted to be negatively impacted (Pacifci et al. 2015). These regions contain a high proportion of endemic and already threatened species which can be considered especially vulnerable to climate change, since they are facing heightened ecological pressure from habitat loss and/or persecution and hunting by humans (Urban 2015). The question of how species will respond to both future climate change and land use change must be addressed in order to develop forward-thinking biodiversity management strategies which will remain effective in the long-term (Jones et al. 2016).

Tropical forests are vital to maintaining global biodiversity. They are among the most threatened ecosystems and human activities are fundamentally altering the abiotic conditions within them. Indonesia has one of the highest rates of forest loss globally, with a large proportion of this loss occurring on the island of Sumatra. Tree cover loss in Sumatra totalled 104,700km² between 2001-2017, equivalent to a loss of 29.2% since 2000 and CO₂ emissions of 1.04 billion tonnes (Global Forest Watch 2018). In Sumatra, much of the remaining primary forest now exists within protected areas, which have become ‘islands’ of intact habitat in a sea of human-dominated landscapes; this is problematic for large mammals which exist at low densities, range over large distances, and require large tracts of intact, quality habitat (Nyhus and Tilson 2004b). Agricultural land around protected areas has negative effects on biodiversity by eroding the quality of matrix habitat, limiting the potential for dispersal and migration, and introducing harmful edge effects in remaining forest fragments (Laurance et al. 2014). In order to plan effective conservation strategies, we must first fully understand the synergistic effects of both climate change and human disturbance.

Microclimate refuges are areas which species can use to minimise their exposure to sub-optimal extremes, thereby allowing them to persist even when macroclimate conditions become unfavourable (Suggitt et al. 2018). Climatic conditions within primary forests have been shown to be decoupled from macroclimate, usually having cooler and more stable (i.e., higher minimum and lower maximum temperatures) conditions than non-forested areas (de Frenne et al. 2019). Additionally, forests are highly heterogenous and contain many microhabitats and microclimates which species can utilise to avoid extreme climate conditions, thereby reducing their extinction risk (Suggitt et al. 2018). It is generally assumed that disturbance and fragmentation of forests will reduce the decoupling effect within forests, however, there is growing evidence suggesting that secondary forests are still resilient to changes in macroclimate conditions and will still provide species with microclimate refuges (Blonder et al. 2018; Senior et al. 2018). Few microclimate studies to date have directly measured the extent to which species actually utilise microclimates to avoid unfavourable conditions (Senior 2020). Determining the role of microclimate refuges and identifying important refuges should be a priority of conservation research to inform long-term spatial planning of habitat protection and identify the most important features to consider when planning reforestation or restoration of disturbed forests.

Mammals are a key component of tropical forest ecosystems, playing major roles in vegetation community structure and plant-animal interactions. Many conservation projects centre on large-bodied, charismatic mammals, using them as ‘umbrella’ species to conserve whole ecosystems, with the assumption that protecting them will, by default, benefit many other species with which they co-exist (Branton and Richardson 2011). Large mammals are generally wide-ranging, more sensitive to disturbance and require large expanses of intact, high quality and heterogeneous habitat, which makes them especially vulnerable to deforestation and climate change (Davidson et al. 2017). Larger bodied and more conspicuous mammals are often easier to monitor compared with other taxa, meaning that they can be used as indicators for ecosystem health and to measure the success of conservation measures in reducing declines and facilitating population recovery (Jones and Safi 2011). Larger bodied mammals fare particularly poorly in the face of environmental change, with rapid population declines and local extinctions reported for a large proportion of species (WWF 2018). Our understanding of mammal vulnerability to climate change is still very limited, and much of it based on assumptions

developed from studies of other taxa, which are likely to have very different relationships with their environment than mammals (Paniw et al. 2021).

Most conservation research currently focusses on mitigating against immediate threats such as habitat loss and hunting; there are limited data on climate change impacts on mammals. The research which has been conducted only focusses on broad scale patterns in species-environment relationships (Guisan et al. 2013). This has limited value to locally implemented conservation plans. Most threatened mammals require immediate short-term conservation actions and can be difficult to justify more long-term strategies to combat climate change (Tulloch et al. 2016). There is little point in protecting a species against climate change if they will become extinct due to hunting or habitat loss before they are affected by climate. Most conservation strategies also focus on preserving ‘pristine’ habitats, such as primary rainforest; however, this is no longer a realistic goal, and cannot be solely relied upon to maintain biodiversity (Meijaard 2017). Most of the Earth’s land surface is now impacted in some way by human activities. It is therefore vital that conservation strategies incorporate disturbed and human dominated landscapes, which will become increasingly important to maintaining biodiversity in the near future.

1.1 Thesis aims and general overview

In this thesis, I aim to investigate the potential conservation importance of an area of regenerating secondary forest in Sumatra, Indonesia, as a potential microclimate refuge from climate change for endangered mammals. I determine the impacts of forest disturbance and edge effects on microclimate and mammal activity by utilising observational measurements of microclimate conditions, mammal behaviour and habitat use combined with mechanistic and biophysical models to predict microclimate conditions and mammal bioenergetics along a gradient moving from the forest edge and into the interior. The thesis will comprise six chapters in total. This current chapter (chapter 1) serves as a general introduction to provide a background and rationale for the research, followed by an in-depth literature review in chapter 2, three data chapters (chapters 3 – 5), and, finally, a general discussion in chapter 6 to summarise the findings and suggest future directions in this area of research.

1.2 Chapter overviews

Chapter 2: Mammals in the Anthropocene: predicting mammal responses to environmental change.

This chapter provides a review of existing literature on microclimate research in tropical forests and how it relates to mammal responses to environmental change and mammal conservation. First, I review the current status of tropical forest mammals and efforts to conserve them. I then give an overview of existing attempts to predict how they might respond to future climate change and human disturbance. I also review the importance of forest microclimates in facilitating species responses to climate change and summarize existing evidence for this. Finally, I highlight the role of predictive models in conservation planning, identify existing barriers to their successful integration into management strategies, and discuss how models can be developed further to improve their accessibility and relevance to conservation practitioners.

Chapter 3: Measuring edge effects on forest microclimate and mammal activity

In this chapter I determine links between forest structure (recorded in vegetation plots) microclimate (recorded with data loggers), and mammal activity (recorded by motion-activated trail cameras), using generalized linear models. This provides insight into habitat characteristics which are most favourable for different types of mammals and determine how fragmentation and edge effects impact microclimate conditions and mammal activity.

Chapter 4: Comparing mechanistic approaches to modelling microclimate variations in a secondary tropical forest.

In this chapter I test and compare the performance of two mechanistic microclimate models: NicheMapR and microclimc. This provides empirical evidence for the accuracy of these newly developed models in tropical secondary forests and identify the effects of different aspects of vegetation structure (e.g., canopy height, canopy cover, connectedness) on the models' ability to accurately predict microclimate. Few studies have tested these models in disturbed tropical forests, and this is the first time that they have been tested in lowland tropical forests in Indonesia.

Chapter 5: A biophysical modelling approach to investigating edge effects on arboreal mammals: a case study of the Sumatran orangutan, *Pongo abelii*

In this chapter I use a biophysical model to predict the potential ecophysiological consequences of edge effects on a Critically Endangered ape, the Sumatran orangutan. I use the NicheMapR endotherm model to predict and compare orangutan metabolic rates from locations at the forest edge and in the interior. Very few studies to date have applied NicheMapR (or its earlier counterpart NicheMapper) to primate species, and this is the first instance that biophysical models have been applied to a great ape. The outputs of this model can be used as inputs in further mechanistic models of orangutan responses to fragmentation and climate change; for example, time budget models to predict fitness and survival, or individual-based models of habitat use and ranging behaviour. These types of mechanistic models will give better local scale predictions of habitat suitability under future scenarios for climate change and land use, since they can incorporate physiological and behavioural adaptations to climate change.

Chapter 6: General discussion

In this final chapter, I reiterate the main aim and broad questions of my research, summarise my main findings, and suggest ideas for future directions. I discuss the implications of forest edge effects and human disturbance in secondary forests for mammal responses to climate change. I examine how well existing models of microclimate and animal responses to climatic conditions can be applied for mammals in tropical secondary forests and suggest how they can be refined to be more generally applicable for locations and species which are data deficient. I also highlight how future ecological research can be implemented to provide quality empirical data to support long-term conservation planning.

1.3 Study Location & Site description

The study was conducted in the Sikundur region, located within the Leuser ecosystem, at the boundary of the Gunung Leuser National Park, GLNP, in the North Sumatra province of Sumatra, Indonesia (Figure 1.1). This is an area of secondary lowland forest which was selectively logged until the area was afforded full legal protection with its designation as the Gunung Leuser National Park in 2004 (YOSL-OIC

2009). Due to its proximity to the National Park boundary, the area is still subject to occurrences of illegal logging and hunting of wildlife (Roth et al. 2020). The Sikundur Biodiversity Monitoring Station, managed by the Sumatran Orangutan Conservation Programme, SOCP, is situated in this region; The Sikundur team have been carrying out monitoring and conservation work, mainly focussing on great apes and other primates, since 2013.

Adjacent to the forest in the Sikundur region is the village of Aras Napal. This is a small community consisting of around 150 households. Subsistence and smallholder agriculture are the predominant land uses in the area outside of the protected forest, while the area to the North of the village comprises larger rubber and oil palm plantations. The larger plantations are not owned and managed by Aras Napal residents, although several residents from the village do work on these plantations to supplement their income from their own farms. Most households in Aras Napal own smallholder farms (around 1-2 hectares usually), which is their main source of income. Many of these are located directly adjacent to the forest (Figure 1.2). Orange trees are the dominant crop plant (Figure 1.3). Unlike other areas in Sumatra, particularly to the North in the Aceh province (Abdullah et al. 2019), there are few reports of conflict between large mammals (especially tigers and elephants) and people here. Elephants are reported to come into agricultural land near the village, but generally cause minimal damage, and do not appear to forage in smallholder plantations, although they do cause notably more damage in rubber and oil palm, which appear to contain more favourable food items for them. The biggest problems caused by wildlife are from smaller mammals, mainly pigs and macaques, which are reported to frequent farms adjacent to the forest on a daily basis and can cause significant damage and loss to orange crops. Some larger farms have small patches of other crops, including corn and other fruits (mainly rambutan and durian). There have been reports of an unflanged male orangutan entering these farms during the fruiting season in order to forage in these patches. Attitudes towards the forest and its wildlife are generally favourable. During the course of this study, we discovered some evidence of hunting in the protected area close to the village (e.g., camera trap footage of people, snares, tracks, and remnants of camps in the forest), although few people reported hunting when asked about their activities in the forest during surveys. Currently, there is insufficient data to detail how often hunting takes place, who is responsible for these activities, which species are being harvested and to what extent, or how this is affecting populations in the area.

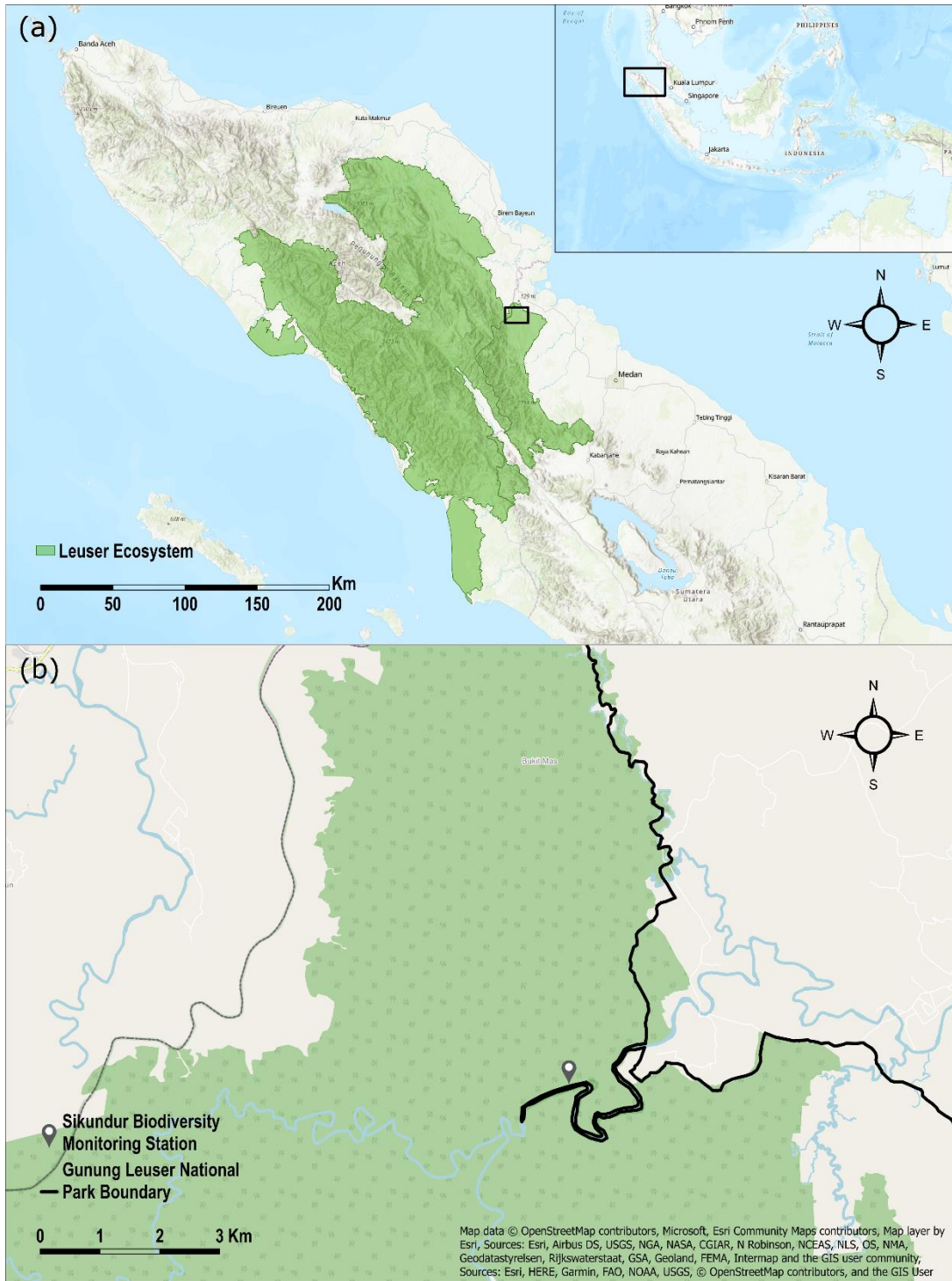


Figure 1.1: a) Location of the Sikundur region and the Leuser ecosystem in Sumatra, Indonesia, and b) the Aras Napal and Sikundur region located in North Sumatra.



Figure 1.2: Corrugated iron fencing surrounding an orange plantation bordering the National Park at Aras Napal; several plantations in this area have fencing or some other barrier blocking access to/from the forest, but some have no fencing at all.



Figure 1.3: A typical orange plantation close to the National Park at Aras Napal.

Chapter 2

Mammals in The Anthropocene: Predicting Mammal Responses to Environmental Change.

2.1 Introduction

Addressing the current biodiversity crisis is a major priority for ecologists and conservation biologists, with species being lost at an unprecedented rate; around 1 million species are now considered threatened with extinction (IPBES 2019). Effective long-term conservation of tropical species is hindered by a lack of understanding of how species can adapt and persist in human-modified landscapes, and limited ability to predict how abundance, community composition, and ecological processes will be impacted by environmental changes (Gardner et al. 2009a). Improvements in methods for monitoring and modelling wildlife population dynamics will be instrumental in reaching targets for biodiversity conservation and climate change mitigation in the tropics. This review summarises the status of tropical mammals and current conservation methods, details existing knowledge of their responses to environmental change, and discusses how predictive models of species responses can be improved to increase their relevance and applicability to conservation efforts on the ground.

The tropics, and tropical forests in particular, contain a high proportion of threatened species (Myers et al. 2000). Tropical forests contain more than two thirds of the world's terrestrial species, despite covering less than 10% of the global land surface (Gaston 2000; Bradshaw et al. 2009). Tropical biodiversity hotspots are predicted to be especially vulnerable to environmental change since a large proportion of their biodiversity comprises rare, endemic species with limited geographic ranges (Malcom et al. 2006). A larger proportion of tropical species are also habitat or dietary specialists with narrower thermal niches than temperate species, making them less able to adapt to the significant environmental changes caused by either habitat loss and conversion or climate change (Trew and Maclean 2021). Despite their highly threatened status, tropical biodiversity hotspots are still relatively underrepresented in studies of climate change impacts and species responses to long term environmental change (de los Ríos et al. 2018); filling in this knowledge gap will enhance the success of management strategies for tropical ecosystems.

Mammals comprise a significant portion of tropical biomass and their removal from ecosystems will have long-term implications on ecosystem functioning, many of which are poorly understood (Galetti and Dirzo 2013). The most important roles mammals play in maintaining ecosystem health in the tropics can be summarised as: 1) grazing; 2) seed dispersal; 3) creation of open areas and pathways; 4) influencing population densities of competitor and prey species. Grazing by herbivores prevents dominance of more competitive, generalist plants, thereby enhancing understory plant species richness (Camargo-Sanabria et al. 2014). Wide-ranging herbivores, such as elephants, rhinoceroses, and primates, feed on a diverse array of plant species and range over large distances, making them highly effective seed dispersers (Campos-Arceiz and Blake 2011; Muñoz et al. 2017). Large-bodied mammals shape ground vegetation by stripping leaves and bark, breaking stems, small branches and even pushing over entire trees, creating trails which are used by other animals (Cristoffer and Peres 2003). Carnivores influence population dynamics and behaviour of their prey and limit overgrazing, thereby enhancing understorey diversity (e.g., the reintroduction of wolves to Yellowstone National Park resulted in reduced grazing by elk, creating a trophic cascade which benefitted many other species, including beavers, bison, and birds; Ripple and Beschta 2012). Large-bodied mammals tend to exist at low densities and range over large distances, meaning that they require large tracts of intact, well-connected, high-quality habitat. Conservation plans focussing on large mammals will therefore benefit many other forest dwelling species by proxy. Successful long-term management of mammals and their habitat will ensure the continued stability and function of tropical forest ecosystems.

Ecologists can provide empirical evidence from field data and predictive models to inform conservation planning and mitigation against threats such as habitat loss and climate change. Currently, most conservation work aims to address the most immediate threats to wild populations, such as habitat loss or unsustainable hunting, however it is becoming increasingly important to incorporate the effects of long-term climate change into conservation strategies (Sutherland et al. 2018). Modelling of global patterns in species biogeography is a common tool in planning conservation at large spatial scales, e.g., by identifying global hotspots of biodiversity, threatened species, and vulnerability to threats such as climate change (Myers et al. 2000; Mittermeier et al. 2011). While a great deal of work has focussed on improving the accuracy and power of predictive models in determining potential species responses to environmental changes, uptake of these improved models by conservation planners and practitioners remains limited

(Tulloch et al. 2016). Much of the climate change research to date has focussed on broad scale patterns in species range dynamics and does not provide information at local scales, which is most useful to planning conservation on the ground (Serra-Diaz and Franklin 2019). Developing models which can be downscaled to provide information on ecological process at smaller scales, along with improving their accessibility to decision makers and conservation practitioners, will enable improved evidence-based conservation strategies that are safeguarded against future threats to populations (Stalenberg 2019).

2.2 Tropical mammals: Current status and future threats

Mammals are a highly threatened taxon. Around 22% of mammals are threatened with extinction according to their IUCN red list status (IUCN 2014). A particularly important region is South East Asia, which has the highest proportion of actually & potentially threatened species, and one of the highest rates of deforestation and habitat loss globally (Sodhi et al. 2010; Davidson et al. 2017). On average, terrestrial mammals are directly impacted by human activities across 51% of their range; this percentage is much higher for species found predominantly in tropical forests (Allan et al. 2019). Their already threatened status, combined with relatively slow reproductive rates and generation times makes them particularly vulnerable to climate change, and they are therefore a particular focus of conservation efforts (WWF 2018). Habitat loss and fragmentation are the most immediate and obvious threats to tropical forest mammals (Tilman et al. 2017); however, hunting and the wildlife trade, human-wildlife conflict, non-native species, and climate change also represent significant threats to tropical biodiversity. Small population sizes, low genetic diversity, and a limited ability to move across human dominated landscapes will make it harder, if not impossible, for many threatened mammals to adapt to the growing threat of climate change, by limiting their ability to adapt or shift their ranges as climatic conditions change.

Most mammal species declines are attributed to habitat loss from deforestation, which is proportionally highest in South East Asia, where an estimated 2.5 million hectares of rainforest is lost each year (Bradshaw et al. 2009). Rates of forest loss in tropical countries are accelerating with rapid industrialisation and expansion of commercial agriculture to fulfil global demand for products such as palm oil, rubber, coffee, and cocoa (Laurance 2004; Curtis et al. 2018). Agricultural expansion often further increases other pressures on remaining habitat by increasing hunting, timber extraction, and introduction of non-

native species within adjacent primary forests (Gardner et al. 2009a; Barlow et al. 2016; Mynářová et al. 2016; Burkett-Cadena and Vittor 2017; Clark et al. 2018). Disturbed or selectively logged forest varies significantly from primary forest in its physical habitat structure and species composition, with generally lower canopy height, reduced canopy connectivity, lower species richness, fewer specialist species, a lack of large emergent trees and more canopy gaps (Kakati et al. 2009; Hamard et al. 2010; Norris et al. 2010; Reiners et al. 2015). These physical changes fundamentally alter the biotic and abiotic environment within disturbed forests, causing notable changes in climatic conditions, species interactions and food availability under forest canopies (Scott et al. 2005; Dent and Wright 2009; Blonder et al. 2018).

Habitat loss and climate change will act synergistically to profoundly impact tropical ecosystems and populations (Brodie 2016). The impacts of extensive fragmentation of primary tropical forests on forest-dwelling mammals are numerous. Firstly, as the ratio of edge to interior forest increases, edge effects in remaining forest fragments will become more pronounced, leading to notable changes in the biophysical conditions within forests (Arroyo-Rodríguez et al. 2017; Pfeifer et al. 2017). Secondly, fragmented landscapes have variable connectivity between remaining habitat patches, and mammals often have limited ability to move between patches (Senior et al. 2019). Loss of connectivity and anthropogenic disturbance have already significantly reduced average movement by mammals, resulting in reduced dispersal distances and limiting the ability of mammals to shift their ranges as climate change alters the area of climatically suitable habitat, i.e., their 'climate space' (Tucker et al. 2018). It is estimated that even after shifting their ranges as much as current forest cover allows, tropical species would still experience an average temperature increase of 0.77-2.6°C (Senior et al. 2019). Thirdly, mammals in fragmented habitats are more likely to enter the human-dominated matrix. Degraded and fragmented forests are resource-poor, and it is harder for large bodied, wide-ranging mammals to locate adequate resources to survive and avoid anthropogenic landscapes (Kinnaird et al. 2003). The resulting human-wildlife interactions can be costly; people experience loss of income, increased stress and uncertainty, injury or even death, while wildlife often suffer from higher parasite loads, inadequate nutrition, and increased mortality due to persecution or attempts to protect lands. Better understanding of species range dynamics in the context of both fragmentation and climate change will be instrumental in accurately forecasting species movements, vulnerability to climate

change, and risks of human-wildlife conflict; information which will be invaluable to planning appropriate mitigation measures.

There is still a great deal of uncertainty in long-term predictions of species future population and range dynamics. Currently, very little is known about the capacity for mammals to adapt to climate change within their present geographic ranges. Accurate predictions of future climate space will depend on models which can incorporate the impacts of both land use and climate change on the distribution of suitable habitat, as well as species' adaptive capacity within their current range. A better understanding of species-environment relationships and how these will determine their responses to both habitat loss and climate change will enable scientists to make accurate and powerful predictive models which can provide empirical evidence to support conservation planning (Dawson et al. 2011).

2.2.1 Conservation of tropical mammals

Planning appropriate conservation measures requires detailed knowledge of species' current and former ranges, as well as their ecological requirements and habitat preferences. Conservation strategies can generally be divided into three main categories: protection of remaining primary habitat, restoration of degraded or converted habitat and reintroduction or translocation of captive bred or wild individuals (Wilson et al. 2014). Conservation projects are generally stretched thin on the ground and struggling to cover large areas with limited resources, meaning that it is essential to allocate resources where they are most needed and where they can be utilised most effectively (Hannah and Lovejoy 2007). There is growing concern that current conservation measures will not be adequate to prevent extinction of threatened species over the coming century, as habitat loss continues, and the effects of climate change become more pronounced (Iwamura et al. 2013; Bonebrake et al. 2018). Conservation strategies can be improved by incorporating information on local scale threats and ecological processes, inclusion of local communities and socioeconomic issues, and a better understanding of species ranges to improve ecological representation in protected area networks (Daily et al. 2009). Recent advancements in remote sensing and modelling techniques are now able to provide much of the required information, however these methods require further development and standardisation to make them more widely applicable and accessible to practitioners (Choi et al. 2019; Stalenberg 2019). Good quality empirical data, coupled

with accurate and reliable predictions of species distributions and responses to change, helps to identify areas which should be prioritised for protection, are most suitable for restoration, and are most appropriate for reintroductions.

2.2.1.1 Habitat protection

Protection of remaining primary habitat is one of the most important goals of any conservation programme. This is commonly achieved through the designation of protected areas, and implementation of legal restrictions on potentially damaging activities such as forest clearance, resource extraction and hunting. Protected area networks will only be effective tools for long-term conservation provided they are representative of the target species current and future ranges (Pringle 2017). The current extent of protected areas is most often based on assumptions regarding species distributions and habitat preferences and are biased towards areas which are relatively cheap and easy to protect from development (Venter et al. 2014); however, it is not ecologically representative and is not considered adequate to protect threatened species from further declines or climate change (Pimm et al. 2014). A large proportion of the range of many threatened mammals falls outside of current protected area networks (e.g., around 75% of orangutans are observed outside of protected areas; Meijaard and Wich 2007). In many cases, current protected area networks are predicted to become defunct as climate space shifts (Struebig et al. 2015; Oliver et al. 2016). Additionally, it is imperative that connectivity is established and maintained between protected areas to allow for dispersal and gene flow among metapopulations, as well as facilitate range shifts following climate change (Wiens et al. 2011; Fung et al. 2017; Saura et al. 2018). Species distribution models, and their predictive power in determining future species ranges, are instrumental in reviewing and updating protected area networks to ensure that they cover an adequate area to protect biodiversity under present conditions and following future environmental changes (Wiens et al. 2011; Struebig et al. 2015).

Effective management and enforcement to prevent illegal activities which negatively impact biodiversity are also crucial to protected area effectiveness (Poor, Frimpong, et al. 2019). Even species which are not directly exploited are often impacted by illegal activities such as logging or hunting, for example, snares used to catch Least Concern species, such as deer or wild pigs, also result in deaths of protected species; (Bisi et al. 2019). Unfortunately, many protected areas lack sufficient funding or resources for

effective management and enforcement (Bruner et al. 2004). Some protected areas cover large expanses or geographic borders, making effective enforcement and management even more challenging (Hannah and Lovejoy 2007). Legislation alone is rarely adequate to prevent illegal exploitation in protected areas; conservationists must include the communities that live there in all aspects of management, from planning to enforcement (Yuliani et al. 2018). Quantitative data on the extent and nature of smallholder agriculture, especially on illegally cleared land, will help to identify the underlying causes of illegal forest clearance at the edge of protected areas. Protected areas will be essential in providing species with refuges from anthropogenic threats; nevertheless, they alone will not be sufficient to preserve biodiversity (Meijaard et al. 2012).

2.2.1.2 Forest Restoration

Restoration of degraded or cleared forest is increasingly utilised as a conservation tool, particularly in landscapes which have been cleared illegally. Anthropogenic and secondary forest landscapes now represent a significant portion of remaining forested areas (Dent and Wright 2009). Previously, these areas have been dismissed as having limited conservation value since they contain lower abundance and species richness than primary forests; however, there is growing evidence that these landscapes are still valuable for biodiversity, provided they are well managed (e.g., Marshall et al. 2006; Barlow et al. 2007; Bernard and Marshall 2020). While monoculture plantations support relatively low numbers of species compared with primary forest, selectively logged forest and agroforests still maintain high levels of biodiversity (Costantini et al. 2016). Agroforests can be beneficial for some threatened mammals (e.g., orangutans, Ancrenaz et al. 2015; and elephants, Nummelin 1990; Rood et al. 2010; Collins 2018). Integrated approaches, which combine community managed smallholder agriculture with protection or restoration of forested areas, have proven to be successful in maintaining endangered populations and biodiversity (Abram et al. 2015; Azhar et al. 2015). Increasing and maintaining connectivity in fragmented forests will enable wide ranging mammals to move between patches, thereby facilitating dispersal and gene flow. Restoration sites in agroforestry mosaics can also act as effective refuges helping to facilitate species range driven by climate change (Braidwood et al. 2018). When implementing wildlife corridors and reforestation it is essential to consider the habitat requirement of the target species, for example, arboreal species, such as orangutans and gibbons, will require well connected and taller canopies for locomotion and resting sites (McGregor et al. 2014;

Davies et al. 2017). With proper planning and management, reforestation and improving connectivity in fragmented landscapes will be an effective medium- and long-term strategy in conserving mammals and promoting sustainable development in tropical countries.

2.2.1.3 Reintroduction & translocation

Reintroductions or translocations are common conservation interventions in cases where local extinctions occur, or where an environment becomes so degraded that it can no longer support a viable population. Conservation NGOs allocate a great deal of resources to the rescue, rehabilitation, and relocation of animals from unsuitable environments (Pyke and Szabo 2018). This action is necessary when individuals become stranded in human-dominated landscapes or in forest fragments which are too small to support them. Orangutans, for example, will remain within their home range, even once the forest has been cleared, while elephants frequently utilise agricultural areas, either to feed on crops or move between forest patches (Russon 2002; Abdullah et al. 2019). These animals often become problematic through crop foraging, destruction of property or aggressive behaviour towards people (Nyhus and Tilson 2004a). In some cases, NGOs can remove individuals before they are captured or killed, however, they often require costly and lengthy medical care for injuries, malnutrition, or disease and cannot always be successfully relocated (Campbell-Smith et al. 2012). Stranded individuals may also be taken and kept illegally as pets in unsuitable conditions. Confiscated individuals, especially those who have been captive since a young age, require a great deal of rehabilitation before they are able to survive in the wild (Wilson et al. 2014). Releasing ex-captive animals can be problematic in areas with existing wild populations, especially in species with complex social structures, such as primates or elephants (Yeager 1997; Russon 2009). Safeguarding reintroduced populations against future threats requires reliable forecasting of future land use and climate change and their potential impacts, e.g., an area which is likely to become climatically unsuitable in the future is not a good reintroduction site. Translocation is a costly conservation strategy, which does not address the underlying causes of habitat loss and illegal hunting and is therefore ineffective without more long-term conservation actions to preserve and restore suitable habitat and allow populations to manage themselves (Wilson et al. 2014). Knowledge of past species distributions and habitat suitability assessments are vital in identifying

potential reintroduction sites, and real-time monitoring is essential to determine the success and long-term viability of reintroduced populations.

2.3 Climate change & tropical mammals

The impacts of climate change on mammals are going to become more pronounced over the coming century, and it is now a major focus of conservation research is to predict species' responses to future climate change in order to develop and improve long-term conservation strategies. Around 7.9% of mammal species are predicted to become extinct as a direct result of climate change (Urban 2015), while over 80% are expected to experience significant range contractions (Pacifci et al. 2015). Based on existing literature, around 47% of terrestrial non-flying mammals have already experienced negative impacts of climate change in at least part of their range, and this proportion will most likely increase with further climate change (Pacifci et al. 2017). Climate is a major factor in phenology, disease dynamics, community composition, behaviour, habitat use and species biogeography. Species must either shift their range to remain in climatically suitable areas, adapt to climate change *in situ*, or become extinct (Pecl et al. 2017). Climate change responses vary by species, with some benefitting from climate change, while others suffer negative impacts. Conservation planning frequently assumes that species distributions and habitat preferences will remain stationary, however, over the next century, accelerating climate change will result in dynamic changes to ecosystems at the community, species, and individual level (Hodgson et al. 2009). Differing responses of individual species makes predicting responses to environmental change challenging and identifying the most threatened species will require development of predictive models that can fully incorporate all factors that influence population dynamics and survival, including climatic tolerance and adaptive capacity of species, and other anthropogenic threats.

The rate and extent of anthropogenic climate change will fall outside of the historic or natural range of variability, meaning that mass extinctions are probable (Hodgson et al. 2009). Much of the tropics are predicted to experience a temperature increase as much as 50% higher than the global average (Graham et al. 2016). The likelihood and severity of extreme weather events, including tropical cyclones, flooding and drought is predicted to increase. As well as leading to direct mortality (e.g., the Bramble Cay melonys is the first documented case of a mammalian extinction directly linked to climate change;

Waller et al., 2017), climate change will alter vegetation composition and structure in forests, thereby influencing canopy processes such as evapotranspiration, leaf turnover, and plant growth and mortality, leading to changes in climate conditions and the availability of food, shade, and predation cover (O'Grady et al. 2011). Climate change impacts are predicted to be mostly negative for mammal populations and will compound existing threats (Trisurat et al. 2014). For example, the potential cultivation zone for oil palm in South East Asia is projected to expand notably with climate change, and the projected resulting forest loss is 3-4 times higher than projections which do not consider climate change, thereby potentially reducing the range of tropical mammals by 47-67% (Brodie 2016). Climate also strongly influences disease dynamics, with increased temperatures being linked to increased transmission and prevalence of internal parasites (Lv et al. 2011; Haider et al. 2017). Species which are already threatened will face further pressure from climate change, which will likely intensify other threats. Understanding the impacts of climate change and how they will interact with existing threats to wildlife populations is therefore essential to planning appropriate mitigation.

Most medium to large-bodied mammals in the tropics will be negatively impacted due to their biological traits and ecological requirements (Schloss et al. 2012; Pacifici et al. 2017). Species in the tropics are assumed to be less able to adapt to climate change *in situ*, since they are used to a relatively stable climate and likely have a much narrower fundamental niche than temperate species, making them especially vulnerable to climate change (Urban et al. 2012; Korstjens and Hillyer 2016). Additionally, tropical species already exist much closer to their maximum tolerance thresholds than temperate species (Deutsch et al. 2008). The nonlinear relationship between temperature and metabolic rates means that species in already warm climates will experience greater metabolic impacts and thermal stress with every degree of warming compared to those in cooler regions (Dillon et al. 2010; Rezende and Bozinovic 2019). Due to their limited adaptive capacity, notable range contractions are predicted for most mammals in the Tropics (Schloss et al. 2012).

Larger bodied animals tend to require larger areas of intact habitat, have complex nutritional requirements, lower fecundity, and slower generation times (Lister and Stuart 2008). This results in slower recovery from population losses, e.g., from hunting or extreme weather events such as drought or forest fires and limits their ability to adapt to changing climates by shifting their phenology or geographic range (Boutin and Lane

2014). Around 30% of terrestrial mammals have potential spread rates which are lower than the global mean velocity of climate change, meaning that they will be unable to track climate change (Santini et al. 2016). In many cases the observed rate of phenological change is mismatched between mammals and plants, with many mammals unlikely to be able to shift their phenology as quickly as their food species, thereby reducing fitness in species which rely on seasonally available resources and synchronisation with plant phenology (Boutin and Lane 2014; Korstjens and Hillyer 2016). Range shifts have been observed in other vertebrate taxa (mainly birds; Thomas and Lennon 1999; Chen et al. 2011), however there is limited direct evidence of climate driven range shifts in mammals, particularly in tropical lowlands (Lenoir and Svenning 2015). Even where climate space is predicted to expand mammals will be limited in their ability to shift their ranges at a pace in keeping with the velocity of climate change (Santini et al. 2016; Senior et al. 2019).

Differing responses of individual species to climate change will result in novel species assemblages and interspecific interactions with major implications for ecosystem functioning and species fitness (Bonebrake et al. 2018). For example, increased temperatures in forest canopies are predicted to increase epiphyte mortality, with knock-on effects for canopy structure and species which utilise epiphytes (Nadkarni and Solano 2002). Species specific differences in dispersal ability and sensitivity to environmental change will result in novel community assemblages, where previously allopatric species are brought together while sympatric species are separated (Urban et al. 2012). Additionally, climate change results in behavioural changes, for example shifts in arboreal behaviour in forests (Scheffers et al. 2013), or shifts from diurnal to nocturnal behaviour (Levy et al. 2019), which will have implications for community interactions. When determining how communities will respond to climate change, it is also important to consider species traits, local climate and ecological pressures (Lenoir and Svenning 2015).

Consistent global estimates of species extinction risk and distributions under future climate change are needed to highlight the most vulnerable species and areas which should be prioritised for protection and mitigation strategies (Urban 2015). Recently, much research has focussed on climate change impacts on species biogeography, however, there still remain significant biases in the existing literature, with tropical systems and endotherms both being vastly underrepresented (Urban 2015; Feeley et al.

2017). There is little information on the effects of climate change on community composition, species interactions and other ecological processes which will affect species survival (Urban et al. 2012; Cavaleri et al. 2015). Most work to date also does not account for adaptations in physiological or behavioural thermoregulation to increased temperatures (Reside et al. 2018).

2.3.1 Predicting species ranges

Species distribution models, or SDMs, are most often used to determine species-environment relationships and project these to predict a species' future range following climate change. SDMs fall into two main categories: correlative models (or bioclimate envelope models) and mechanistic models. Correlative distribution models incorporate current or past observations of environmental conditions and species presence/absence or abundance data to infer habitat requirements and estimate the maximum and minimum extremes at which a species can survive in a given habitat. Mechanistic models, on the other hand, are process-based models which use information about a species' ecophysiology to predict the environmental conditions under which they can survive (Kearney and Porter 2009). Species biogeography will undergo major shifts as the area of climatically suitable land (or climate space) available to species changes. Generally, species are expected to alter their habitat and microclimate preferences and shift into higher latitudes and elevations, although they will be limited in their ability to do this by habitat loss and dispersal limitations. To date, most published models predicting mammal distributions under climate change have focussed on temperate regions, however, it is likely that tropical mammals will be disproportionately affected by climate change, in part because many tropical mammals are reliant on forested habitats. The ranges of forest dwelling species are limited not just by their own thermal tolerances, but by the distribution of forest cover. When considered separately, deforestation has a greater impact on mammal ranges than climate change, however when both drivers are combined, the effect is much more severe (Trisurat et al. 2014). Based on climate change projections alone, 11-36% of mammal species in Borneo are predicted to lose at least 30% of their range by 2080, however when deforestation is also considered this proportion increases to 30-49% (Struebig et al. 2015).

Increasingly, more work has focussed on investigating the underlying mechanisms behind species-environment relationships in order to identify environmental factors

influencing habitat suitability and species survival. Time budget models can be used to incorporate behavioural responses to climate and other factors, such as human disturbance and resource availability into assessments of habitat suitability, extinction risk, animal movement, dispersal capacity and distribution models (e.g., Lehmann et al. 2008; Korstjens et al. 2010; 2018; Carne et al. 2012). Individual- or agent-based models can also be used to investigate how species might alter their behaviour based on climate and can incorporate behavioural thermoregulation strategies (Bryson et al. 2007). These approaches can be used to determine key factors which impact survival, rather than simply identifying areas as suitable or unsuitable (Carne et al. 2012). Dynamic energy budget theory can be used to take this one step further (e.g., NicheMapR; Kearney and Porter 2017a), by also incorporating physiological responses to climate, and allowing the inclusion of thermoregulatory responses, such as sweating, panting, or seeking shade, which might allow species to tolerate extremes in temperature (Porter et al. 2010).

2.3.2 Limitations of existing approaches

To date, most climate change research is focussed on species range dynamics, relying on correlating current ranges with coarse-scale environmental layers, and fails to adequately account for other factors influencing species biogeography (Ehrlén and Morris 2015; Reside et al. 2018). Models predicting species responses to climate change perform much better when considering other factors which are important in determining species distributions alongside climate (e.g., human activities, species traits and interspecific interactions), however most published studies still consider the effects of climate and land use separately. This is a particular issue for tropical species and forest specialists, which are particularly threatened by habitat loss and fragmentation due to deforestation (Davidson et al. 2017). Anthropogenic barriers and slow dispersal velocity will prevent species from shifting their ranges; however, these are often not included in climate envelope models (Hellmann et al. 2012). Climate change will trigger a shift in the area occupied by forest biomes, and this effect will be exacerbated by changes in human land use (Noss 2001). The area currently occupied by tropical forest biomes is predicted to be 55-80% less by 2100 (Asner et al. 2010). Relying on range predictions from correlative models alone can lead to over- or under-estimation of species extinction risk, resulting in inadequate conservation measures (Serra-Diaz and Franklin 2019). A holistic approach, incorporating mechanistic and biophysical models, and knowledge of ecological

requirements and the effects of human disturbance, is required to develop and adapt the most effective conservation measures.

Conclusions regarding climate change vulnerability are also often based on oversimplified assumptions, which do not factor in climate variability at finer spatial and temporal scales (Trew and Maclean 2021). While it is true that macroclimate conditions in tropical forests are, on average, less variable, with narrower extremes than temperate zones, there are still notable fluctuations in microclimate across time and space. Mammal survival will be determined by the duration and frequency of their exposure to extreme temperatures, rather than directly by increases in macroclimate averages (Enriquez-Urzelai et al. 2020). Most mammals will be able to tolerate exposure to sub-optimal conditions at least temporarily and can utilise microclimate variations to limit their exposure, for example by shifting their activities to a different time of day, or by utilising cooler parts of the forest (Jucker et al. 2018). Additionally, ambient air temperature is not the only important environmental variable in determining survival at a given location. Other variables, such as solar radiation, are often more important for mammal thermoregulation, however these variables are not adequately accounted for in most predictive models. Not accounting for fine-scale climate variation can result in overestimation of extinction risk and in areas which may be instrumental to species persistence being overlooked.

Distribution models are limited by the quality of input used to parameterise them (Milling et al. 2018). Correlative approaches use climate information from large scale global datasets, and fine scale climate variation is not considered when determining future habitat suitability. Currently available climate data tend to be unrepresentative of conditions below forest canopies, yet this is rarely accounted for in distribution models (Bramer et al. 2018). These data are usually interpolated from meteorological weather stations, which are spread across relatively large spatial scales and are designed to limit the effect of local climate influences, such as vegetation or topography (Frey, Hadley, and Betts 2016). Weather stations also have relatively poor coverage in most tropical countries (World Meteorological Organization 2020). This mismatch between coarse-grained macroclimate datasets and the scale at which organisms experience their environment limits the performance and applicability of species distribution models at smaller spatial scales (Fuller et al. 2010), resulting in inaccurate predictions of species ranges and extinction risk, and a potential misallocation of resources. Ignoring variations

in local climate will result in areas of suitable habitat being missed, and therefore not prioritised for protection. Accurate prediction of species responses to future change in tropical forest requires an understanding of micro-climate variation within the forest canopy, and SDMs for tropical species must incorporate fine-scale variation to effectively predict responses to future environmental change.

2.3.3 Adaptations to climate change

The underlying mechanisms of species responses to climate change and range shifts are poorly understood. Phenotypic changes in physiology and behaviour will be the first response of individual organisms to climate change, before macroevolutionary changes or range shifts occur (Nogués-Bravo et al. 2018). The role of thermoregulatory responses in facilitating species survival and determining their thermal tolerance thresholds are relatively understudied in climate change predictions (Fuller et al. 2010; Stalenberg 2019). There are very few empirical data available on phenotypic plasticity or the energetic costs associated with climate change in wild mammals (Stalenberg 2019). Incorporating phenotypic plasticity in thermoregulation into models predicting species responses will improve their power and ability to identify key mechanisms driving extinction risk from climate change.

Mammals can cope, at least temporarily, with temperature extremes through physiological responses, such as sweating and panting, however these can be energetically costly, thereby limiting their benefit in allowing animals to cope longer-term. Physiological adaptations which can reduce the costs of thermoregulation are relatively unknown for mammals but have been observed in some species. Some primates have lower basal metabolic rates to cope with unpredictable or seasonal fluctuations in temperature and resource availability (Fuller et al. 2010; Turner 2020). Heterothermy, i.e., allowing a wider range of maximum and minimum body temperatures in warmer conditions, has been observed in possums and Arabian Oryx (Mitchell et al. 2002; Hetem et al. 2012). Selective brain cooling is another physiological adaptation which has been observed in even-toed ungulates and some large cats which may play a role in regulating body temperature and preventing water loss from evaporative cooling in arid environments (Schino and Troisi 1990; McFarland et al. 2015).

Mammals can also control their exposure to extreme temperatures, or cope with the increased metabolic demands of thermoregulation in higher temperatures, by altering

their behaviour. Some mammals have been observed altering their daily activity patterns and switching to more nocturnal patterns of behaviour to allow for reduced activity during hotter parts of the day (Levy et al. 2019). Other species have altered their social behaviours, vervet monkeys and long-tailed macaques, for example, change their preference for huddling partners in cooler temperatures, becoming less choosy when temperatures become dangerously low (Kelley et al. 2016); lemurs also utilise sunning and huddling behaviours to keep warm during low temperatures (Eppley et al. 2016). Habitat use and sleeping site selection have also been noted to vary with temperature. Bamboo lemurs were observed to sleep on the ground either in burrows or open sites, with site choice being more strongly linked to ambient temperatures than predation or parasite risk (Evans 2009). Microbats in Australia demonstrated strong preferences for urban bat boxes based on their microclimate properties rather than the presence of parasites (Takemoto 2004). Terrestrial behaviour in African great apes is linked to climate, with terrestrial behaviour increasing during the dry season when temperatures in the upper canopy are higher (Valencia et al. 2016; Harrison and Noss 2017).

Mammals in tropical forests may also utilise microclimate refuges (areas within forest canopies which are offset and/or decoupled from macroclimate, which are likely to be less affected by climate change and often have fewer extreme fluctuations in temperature) to avoid suboptimal extremes. Tropical forest refugia have been instrumental in facilitating species survival during past climate change events, in part contributing to their high levels of biodiversity and endemic specialists (Suggitt et al. 2018; Enriquez-Urzelai et al. 2020). The availability of different microclimates in heterogenous habitats significantly reduces predicted extinction risks from contemporary climate change in some species, however this requires testing in more taxa (Morelli et al. 2016). There are currently no standard guidelines for identification and management of potential refuges (Hylander et al. 2015). Further information is needed on the ability of species to tolerate temperature changes within their current range, and the degree to which microclimates in forests will be decoupled from macroclimate changes in the future (Gillingham et al. 2012). Identifying potential refuges for species will identify locations and key microhabitats which should be prioritised for protection to ensure the long-term survival of species under future climate change.

2.4 Microclimates and their relevance to climate change responses

The spatial scale of climate data used significantly impacts the outcome of species distribution models predicting responses to climate change (Osborne et al. 2004). Climate change projections tend to be based on macroclimate data at spatial resolutions of 1km² or larger. Organisms will experience climate at much smaller resolutions than this. There are substantial variations within each grid square of these climate data layers. Temperatures at finer spatial scales vary by around 9°C on average (Pincebourde et al. 2016). Broadly defined, microclimate refers to fine-scale variations in climate which are decoupled from the background atmosphere or macroclimate (Bramer et al. 2018). Organisms in heterogenous environments with high levels of spatial and temporal variation in microclimate will therefore have different levels of exposure and vulnerability to extreme temperatures than what is predicted by coarse-scale models. (Zellweger et al. 2019; Kearney et al. 2020)

It is widely known that elevation, topography, and vegetation can strongly influence climate, hence weather stations tend to be placed away from vegetation and topographical features. The effects of topography and elevation are fairly well documented, however there is limited empirical data available on the relationship between vegetative characteristics and climate at finer spatial scales (Lembrechts et al. 2019). Vegetation mainly affects climate in tropical regions through increased evapotranspiration and increased latent heat flux between the Earth's surface and atmosphere, thereby cooling surface temperatures and increasing humidity and precipitation (Davis et al. 2019). The extent of cooling exerted by vegetation is related to moisture availability and seasonality of precipitation, with the effect being greatest during dry seasons when water availability is lowest (Frey, Hadley, Johnson, et al. 2016a; de Frenne et al. 2019). A better understanding of the relationship between vegetation, topography and fine-scale microclimate will enable modelling of the microclimate across broad spatiotemporal extents and at high resolutions (Nakamura et al. 2017). Collecting detailed data on topography, vegetation and climate over large spatial extents is not feasible for most ecological studies, however, developments in remote sensing and modelling methods have made it possible to generate accurate predictions of microclimate conditions for most terrestrial locations on Earth (Zellweger et al. 2019; Kearney et al. 2020). These datasets can now be incorporated into SDMs to improve their performance and reliability in predicting species responses to climate change.

2.4.1 Microclimate variability in forests

Tropical forests have a complex and diverse physical vegetation structure, coupled with often rugged terrains, leading to highly variable microclimates. Forests have been shown to have lower average and maximum temperatures, and higher minimum temperatures than non-forested areas (Senior et al. 2018). This decoupling effect is greater at higher magnitudes of macroclimate temperature change (de Frenne et al. 2019). At finer scales, forest canopies affect the amount of solar radiation reaching the ground, limiting wind exposure, intercepting precipitation, and retaining humidity; this results in a complex set of interactions between physical vegetation characteristics (e.g., tree height, canopy density, large emergent trees, presence of epiphytes and lianas) and microclimate (Senior et al. 2018). Little is known about microclimate processes under forest canopies, and particularly in secondary or selectively logged forests (Scheffers et al. 2014). Generally, it is assumed that degradation and fragmentation will degrade the buffering effect of forests and reduce the availability of cooler microclimate refuges whilst increasing variability and extremes, however there is some evidence suggesting that secondary forests maintain similar climatic conditions and availability of refuges to primary forests (Scheffers et al. 2013).

2.4.2 Vertical microclimate gradients in forests

The relationship between latitudinal and altitudinal climate gradients and biodiversity are well known, however finer scale gradients exist which are poorly known. Within forests with complex strata, vertical gradients in microclimate can be much steeper than those across elevation and latitude. For example, observed temperature change in the 20m between the understorey and upper canopy in forest in the Phillipines was much greater than the observed change over a 200m elevation gradient (Scheffers et al. 2014). Arboreal species may be able to adapt to climate change through vertical shifts in the canopy or using buffered microhabitats as refuges from climatic extremes, for example, rainforest frog assemblages become increasingly dominated by arboreal species with increasing altitude (Scheffers et al. 2013). As the climate becomes warmer less tolerant species will likely be pushed towards the cooler and wetter conditions on the ground and this will have major implications for species interactions and community dynamics (Vanwallegem and Meentemeyer 2009). Understanding the implications of this in terms of long-term species survival and adaptation to climate change requires further long-term monitoring of species behaviour and vertical changes in structure and microclimate. A

great deal of forest ecology and science is biased towards the understorey, and there is still a major knowledge gap on upper canopy processes and biodiversity.

2.4.3 Thermal buffering in forests

Microhabitats within forests can be resilient to extreme variations in macro-scale climate, and species can exploit this to avoid climatic extremes and persist following climate change (Suggitt et al. 2018). Microhabitats were up to 3.9°C cooler on average and had reduced maximum temperatures of up to 3.5°C compared with macro-scale ambient temperatures, based on 36 published studies across the tropics; this buffering effect is strongest in the tropical lowlands where temperature is most variable (Scheffers et al. 2014). It is known that forest structure can significantly affect understorey climate, but the nature of this relationship is not understood well enough to enable accurate prediction of spatial and temporal microclimate variation across heterogenous forest landscapes (Bramer et al. 2018). Combining recent methodological developments, such as airborne LiDAR, with ground microclimate sensors enables robust assessment of how topography and vegetative structure influences climate at finer spatial scales. Additionally, the key mechanisms determining population tolerances to climate change are poorly understood, and for most species it is not known how well they will be able to adapt *in situ* or shift their range under climate change (Nogués-Bravo et al. 2018). Accurately predicting future extinction risk and species responses to environmental change requires combining fine-scale physical models of the environment with robust models of species responses to climate change.

Macroclimate buffering in tropical forests will be impacted by the effects of disturbance and fragmentation. Reductions in canopy cover result in increased penetration of solar radiation and reduced evaporative water loss, which leads to hotter, drier average conditions, with more extreme diurnal variations (Stevens et al. 2015; Gaudio et al. 2017). Disturbed forests in Malaysian Borneo have more variable and warmer microclimates on average compared with primary forest, with maximum temperatures in disturbed forest exceeding those recorded at the nearest weather station by 5 – 10°C (Blonder et al. 2018). Another study in Borneo recorded temperatures in logged and plantation forests that were 2.5 – 6.5°C higher than in primary forests (Hardwick et al. 2015). As forests become more fragmented, edge effects will become more pronounced, leading to further changes in forest microclimates (Broadbent et al.

2008). Approximately 70% of global forested areas are now found within 1km of a forest edge (Haddad et al. 2015), therefore data on the direction and extent of microclimate changes brought on by edge effects in forests, especially secondary forests, is urgently needed.

2.5 Measuring & modelling microclimates

Recent advances have been made in studying microclimates and incorporating these data into ecological studies. There are now publicly available datasets of fine scale topography and climate (e.g., Microclim, Maclean et al. 2019), however the accuracy and applicability of these in certain regions, such as the tropics, are insufficiently tested. The increasing availability of automated and remote sensing equipment has made it more viable to collect microclimate data across larger temporal and spatial scales. Microclimate can be measured directly *in situ*, inferred from remote sensing data, interpolated between weather stations or sensors, downscaled from macroclimate measurements, or predicted using process-based or mechanistic models. Appropriate methods to measure microclimate will depend on the study organism and the temporal and spatial scale of the study (Bramer et al. 2018). More information is needed on the performance of microclimate models in different environments, including heterogenous tropical forest canopies.

2.5.1 Direct measurements & remote sensing

Automated sensors which can be left to autonomously record and store data on microclimatic conditions are now readily available, making it possible to measure microclimate at high spatial and temporal resolutions. There are now a wide range of sensors which can record multiple microclimate variables, and these all differ in their ease of use, accuracy, and price range. The most appropriate sensors and survey design will depend on the variable of interest, the process or organism being studied and resource constraints of the project (Bramer et al. 2018). Although automated sensors are relatively cheap per unit, it is still costly to deploy them over a large area or for long periods of time, meaning that most studies are carried out over short periods and/or small geographic extents (Zellweger et al. 2019). Due to the wide range of equipment available and the fact that microclimate measurements in ecological studies are relatively new, the methods employed are varied and usually specific to a site or case study, and it is therefore difficult to scale up measurements to make broader conclusions about microclimate patterns

(Bramer et al. 2018). In order to understand broader scale patterns, *in situ* measurements should be carried out over the long term or combined with historical weather station data.

Remote sensing can be used to directly measure climate, either with thermal satellite imagery or portable infra-red cameras attached to unmanned aerial vehicles. High resolution satellite data is now available for most locations, while drone technology is rapidly becoming more accessible and less expensive (e.g., Koh and Wich 2012). The advantage of remotely sensed data over gridded climate data is that each pixel in a layer represents a direct measurement, rather than being interpolated from weather station data (Lembrechts et al. 2019). There are limitations to this method; most measurements have limited spatial or temporal extents, and satellite data is limited by cloud cover, especially in tropical rainforests. Remote sensing data often do not capture climate variation at very fine scales which are most relevant to organisms' responses to climate change (Choi et al. 2019).

2.5.2 Modelling microclimate

The cost and effort to set up and maintain sensor networks to directly measure microclimate across the large spatial and temporal extents required for species distribution modelling are beyond the scope of most studies. Instead, modelling approaches can be used to generate microclimate input data using a combination of field data and statistical models to predict microclimate. Previous microclimate models have either been indirectly downscaled from macroclimate data (e.g., Flint and Flint 2012; Dingman et al. 2013; Meineri and Hylander 2017), or directly interpolated from field measurements (e.g., Vanwalleghem and Meentemeyer 2009c; Ashcroft and Gollan 2011; Slavich et al. 2014; Frey et al. 2016b). Microclimate models have the advantage of being able to provide long term and high-resolution climate predictions across a large area, however they still require good quality datasets for predictor variables which can accurately capture microclimate variation, such as topography or vegetation, and are also limited by the extent and quality of input data. Mechanistic models (e.g., Kearney, Isaac, et al. 2014; Kearney and Porter 2017; Maclean et al. 2019; Kearney et al. 2020) downscale or interpolate climate data based on physical processes, enabling them to incorporate effects of fine-scale topography, vegetation, and substrate on climate. Such mechanistic models have the potential to enable accurate predictions of microclimate conditions for any terrestrial location globally.

2.6 Using microclimates in predicting species responses to climate change

To date, relatively few species distribution models have incorporated microclimate data, although those which do have shown a marked improvement in their ability to accurately map species ranges compared with those using macroclimate data (e.g., plant species in Northern Scandinavia, Lembrechts et al. 2019; ground beetles in the UK, Gillingham et al. 2012; plant species in Australia, Ashcroft et al 2008). Higher resolution climate data will be able to capture microclimate refuges which might otherwise be missed if only using macroclimate (Maclean et al. 2015; Briscoe et al. 2016). Using data at finer spatio-temporal resolutions also allows for better forecasting of the effects of temporary extremes in weather, such as heatwaves or drought, which may not be captured by macroclimate datasets (Briscoe et al. 2016). Using microclimate predictions can also help to identify and incorporate other factors, besides temperature, that might limit survival, such as water and energy balance (e.g., Kearney et al. 2013; 2016; Mathewson et al. 2017; Fitzpatrick et al. 2019).

2.7 Summary and conclusions

Forests will provide species with temporary refuges from climate extremes, potentially facilitating persistence with climate change, and identifying these refuges is a priority in conservation biology. The true extent of their refugial capacity is poorly known. More data is needed to test the direction and extent of the decoupling between microclimate conditions in forests and background macroclimate, and to understand how this effect will be affected as the macroclimate changes. The extent to which refuges can buffer against extreme weather events, such as heatwaves, should also be explored. Identifying potential refuges for protection is a priority in conservation biology. As well as identifying existing refuges, it will also be beneficial to identify important characteristics of refuges (e.g., canopy height, connectivity, or structural complexity) to provide guidance for restoration and reforestation.

Microclimate research can provide valuable evidence to support conservation planning. Direct measurements of microclimate are valuable in providing location-specific insight into species habitat preferences, providing evidence to support planning of restoration sites, wildlife corridors and agroforests (Lembrechts et al. 2019). Microclimate models can provide data over large geographic and temporal extents using

freely available datasets on topography, and without direct microclimate measurements. Microclimate models do however require testing in a wider variety of locations and environments before they can be more widely implemented. Improvements in availability and accessibility of autonomous monitoring equipment and mechanistic models of microclimate is increasing their use in ecological research.

More work is required to encourage the uptake of SDM outputs into long term conservation action. This includes further development of models which can be adapted to the species, population, or location of interest and tailored to include impacts of other relevant local threats, e.g., hunting pressure, logging, agriculture etc. (Tulloch et al. 2016). The development of more sophisticated and complex distribution models is beneficial to improving understanding of processes which shape species biogeography at large scales; however, they do not necessarily help to inform conservation planning. Correlative models can be overly simplistic and do not work so well at smaller spatial scales, limiting their use in making management decisions at the local scale. Mechanistic approaches can overcome this, but many models require detailed input data on species life histories and physiology which is often not available for rare species, leading to high levels of uncertainty in predictions (Kearney et al. 2016). The complexity of mechanistic and biophysical models can also be off-putting for practitioners who do not have in-depth knowledge of bioenergetics and ecophysiology (Stalenberg 2019). Advances in remote sensing technologies and a better understanding of the relationship between species basic traits and climate can help to further improve models, while further development of mechanistic models to make them more widely applicable and accessible will ensure that conservation programmes are able to benefit from advances in modelling species distributions.

Chapter 3

Forest edge effects on microclimate and mammal activity in Sikundur, Sumatra.

Abstract

Tropical forests are becoming increasingly fragmented, and as deforestation continues the proportion of edge habitat in forest-dwelling tropical mammal ranges will increase. Abiotic conditions at forest edges are influenced by the adjacent open human-dominated agricultural areas, often leading to warmer and drier average conditions, and more extreme fluctuations in temperature; these effects can be evident as much as 2km into forest fragments. It is generally assumed that these changes will have negative impacts on forest-dwelling mammals, however there are few empirical studies which explicitly test this. This chapter investigates variations in microclimate and mammal occurrence in relation to forest structure and edge effects using remote monitoring data. Automated sensors were used to record temperature and light levels from locations at varying distances from the forest edge, moving from adjacent smallholder orange plantations to 2km into the interior. Forest structure was recorded within 25 x 25m plots at the same locations. The number of detection events by remote camera traps was used as a proxy to monitor occurrence of terrestrial mammals. Daily mean and maximum temperatures were significantly higher at the forest edge compared to the interior, with this effect persisting up to 1km into the forest. Mammal occurrence and diversity was notably lower close to the forest edge. Responses to forest edges differed between mammal orders, with some species preferring the edge habitat and others avoiding the edge together. These results suggest that abiotic changes in forests brought on by edge effects have negative impacts on mammals, but the extent of this effect varies by species.

3.1 Introduction

Forest dwelling species in the tropics must adapt to increasingly fragmented and human-dominated landscapes. It is estimated that around 70% of global forested areas now lie within 1km of a forest edge (Haddad et al. 2015), and this proportion is likely to increase with continued human population growth and rising demand for natural resources and agricultural land. Protected areas and forest reserves often result in ‘hard’ edges between forest patches and the surrounding human-dominated matrix, i.e., farmland, road, or clear-felled areas (Ries et al. 2004). These often-contrasting environments exerting influence on each other creates a gradient in abiotic conditions at the boundary (Bolt et al. 2018). Loss of large trees and an increase in vegetation turnover at the boundary results in increased penetration of solar radiation, increased desiccation, warmer average temperatures, and higher temperature variability at forest edges; this effect has been observed up to 1km into forest patches (Laurance 2004; Pohlman et al. 2007; Campbell et al. 2017), although few studies to date have investigated edge effects along continuous gradients, or directly linked abiotic changes to mammal habitat use.

Edges alter habitat quality in remaining forest patches and reduce functional connectivity between them by limiting animal movement and dispersal, thereby impacting community composition, population dynamics and species persistence in fragmented environments (Zurita et al. 2012). Fragmented secondary forests typically have lower canopy cover and connectivity, and greater structural heterogeneity with more gaps than primary forests, meaning that the interior of fragments is less sheltered from external macroclimate influences, and edge effects are therefore likely to extend further into the forest interior (Ewers and Banks-Leite 2013), although there is little information available to demonstrate this. Furthermore, changes in forest microclimate will potentially impact on their ability to shelter animals from the effects of recent climate change, however very few studies to date have considered the synergistic impacts of habitat fragmentation and climate change on the behaviour and survival of forest-dwelling species.

Edge effects change both the biotic and abiotic conditions within forest fragments, thereby altering forest microclimates and potentially impacting on the capacity of forests to provide microclimate refuges for vulnerable species under future climate change (Gardner et al. 2009b). Identifying these refuges is a priority of conservation scientists to

ensure that current protected area networks will be effective in the long term to facilitate biodiversity conservation (Thomas and Gillingham 2015). Forest remnants have acted as refugia for species during past climate change events and are expected to do so throughout present anthropogenic climate change (Ashcroft 2010). Large areas with continuous forest cover have been shown to have a cooler and less variable microclimate compared with the background macroclimate (de Frenne et al. 2019); however, the true extent and direction of changes to forest microclimate conditions caused by fragmentation and human disturbance is poorly understood. Selective logging within forest patches usually targets the largest trees, resulting in canopy gaps and altering micro-climatic conditions through increased exposure of the understorey to light radiation, wind, and precipitation (Blonder et al. 2018). Additionally, forest fragments adjacent to human landscapes are often more exposed to further exploitation by people, such as small-scale timber extraction or hunting, which in turn further alters the conditions within forest patches (Poor, Jati, et al. 2019; Saiful and Latiff 2019). Determining how habitat fragmentation affects the relationship between micro- and macro-climatic conditions in tropical forests is an important step in identifying potential microclimate refuges, particularly in secondary forest, which has now replaced primary forest across a large proportion of tropical mammal ranges (Dent and Wright 2009; Matos et al. 2020).

Predicting species responses to climate change requires knowledge of how the abiotic environment will change, as well as species habitat preferences and their fundamental niche. Responses of forest-dwelling mammals to edges are highly variable and depend on multiple factors, including taxonomic class, species traits (such as generalist/specialist, dietary breadth, body size, fecundity, ranging distance), matrix type and permeability, anthropogenic hunting pressure, fragment size, connectivity, and fragment quality (Da Silva et al. 2015; Estrada et al. 2016; Wittmann et al. 2016). There are many studies documenting edge effects on vegetation structure, composition, and microclimate, but information on how they impact large vertebrate communities is limited, and even fewer studies have considered edge effects associated with logging and other land use changes (Brodie et al. 2015). Large mammals have been observed to avoid the forest boundary by up to 3km in Sumatran forests (Kinnaird et al. 2003). In general, it is reported that habitat specialists are more negatively impacted by edge effects than generalists, while species which can exploit the matrix (e.g., by crop foraging) respond positively to forest edges (Pfeifer et al. 2017). Forest specialists, carnivores and larger bodied species have a lower probability of presence in small forest patches (Keinath et al. 2017), while wide-ranging

species have been shown to have a higher extinction risk in small fragments than those with smaller home ranges (Woodroffe and Ginsberg 1998). On the other hand, wide-ranging species are more likely to be able to move between remaining patches, resulting in a lower extinction risk than species which move less (Crooks et al. 2017). The variation in species responses makes it challenging to accurately predict how a given species might respond to fragmentation and the resulting edge effects. This challenge is further exacerbated by the lack of robust, up to date information on species distributions and habitat preferences.

A major challenge in wildlife conservation is the lack of data on the distribution, abundance, and habitat requirements of threatened species. Knowledge is often based on old surveys (i.e., more than 20 years old), educated guesses and assumptions based on expert knowledge and habitat suitability assessments, or simply does not exist (IUCN 2021). Many species distribution models are prone to over- or under-estimate extinction risk due to inappropriately scaled environmental data, or low-quality species distribution data (Elith and Leathwick 2009). Furthermore, there is a tendency to group heterogeneous landscapes into uniform blocks of categorical land units, but this is not always appropriate; logging intensity in secondary forest, for example, can vary greatly depending on accessibility and regional management policy (Wearn et al. 2017). Unfortunately, quality data is lacking for most endangered species (Burivalova et al. 2019); threatened mammal populations are challenging to monitor, particularly those living in remote, inaccessible regions, such as tropical forests. Large mammals tend to live at low population densities and range over great distances. As a result of these challenges, traditional field monitoring techniques which are based on direct observations by field researchers, such as line transects or point counts, require substantial survey effort to produce robust and accurate population estimates, and it is not feasible for most research projects to continue this in the long-term (Stephenson 2019). Long-term species monitoring provides valuable data for conservation planning, by highlighting priority species and habitats for protection, areas with high risk of human-wildlife conflict, and ideal locations for wildlife corridors and release of captive-bred/rehabilitated animals. Unfortunately, the high levels of cost and effort required for long term monitoring of threatened species means that wildlife monitoring projects are often short-term, and research is biased towards a select few locations with established field stations and/or habituated animals. Furthermore, research on wild animals is not necessarily concerned with answering questions relating to conservation (Sheil 2001). The spatial and temporal

extent of information required for conservation planning is often beyond the scope and constraints of ecological research projects, meaning they have limited applicability in conservation practice.

Since conservation is all-too-often limited by severe resource constraints, it is hugely important to plan and allocate resources in the most efficient and cost-effective way. High levels of error in species distribution models can lead to areas being assigned inappropriate levels of protection and this therefore limits their usefulness in practical conservation. For example, species distribution models using coarse scale macroclimate data could predict local extinctions at a location and miss potential microclimate refugia, resulting in that area being ‘written off’ for conservation (Gillingham et al. 2012).

Emerging remote monitoring technologies can be harnessed for wildlife research to answer questions relevant to species conservation. Recent advances have made these technologies much more feasible and affordable options in wildlife monitoring programmes. Autonomous networks of remote sensors can generate huge amounts of data on biodiversity, species richness, abundance, distribution, and behaviour, and require far less survey effort than traditional field survey methods (Steenweg et al. 2017). Remote monitoring methods can be utilised to answer questions about spatial ecology and can support conservation planning by providing better insight into species’ habitat requirements, helping to identify local-scale population threats, and enabling more effective management of human-wildlife interactions (Wrege et al. 2017; Stephenson 2019). For example, real time monitoring can be used to develop automated proximity alerts when animals are moving towards agricultural lands to enable landowners and conservation practitioners to be better prepared for crop foraging events and reduce the likelihood of injuries or fatalities to both people and wildlife (Wall et al. 2014). As with all emerging technologies, care should be taken when integrating them into long term projects, since there are currently no standardised protocols for implementation of remote monitors such as camera traps.

3.2 Objectives

This chapter aims to record edge effects on temperatures, forest structure and mammal activity rates in tropical mature secondary forest. Furthermore, it will explore the potential of emerging remote technologies to be implemented in long term population

monitoring of threatened species and provide robust, up-to-date data to improve the accuracy and application of predictive species distribution models for conservation planning. This will provide a better understanding of edge effects in secondary tropical forest and identify habitat preferences of threatened mammals in Sumatra. These data can inform conservation planning by highlighting which habitat characteristics are most important for determining mammal occurrence.

1. Measure and compare forest structure and microclimate conditions at different distances from the forest edge.
2. Record how mammal activity changes with distance from the forest edge.
3. Determine which environmental variables are most important in driving variation in mammal activity rates.

3.3 Methods

3.3.1 Field data collection

3.3.1.1 Location

Data were collected from Aras Napal and the Sikundur region on the boundary of the Gunung Leuser National Park (GLNP) in the North Sumatra province of Sumatra, Indonesia (see chapter 1, section 2, for a full description of the site). Monitoring locations were set up at 500m intervals along four 2km transects starting within orange plantations at the park boundary and extending into the interior (see

Figure 3.1 –

Figure 3.2). Starting locations at the forest boundary were chosen within farms once landowner permission had been obtained. Transect routes, with points at 500m intervals were then generated in ArcGIS Pro. Where possible, monitoring locations were set up within 50m of these generated points. In some cases, points had to be moved further due to landscape features, such as streams or rivers, which could not be crossed on foot. Final monitoring locations are shown in Figure 3.1. Data collection took place over a 60-day period from August – October 2019. To avoid disturbance-related changes in animal behaviour, vegetation characteristics at the plots were measured at the end of the monitoring period.

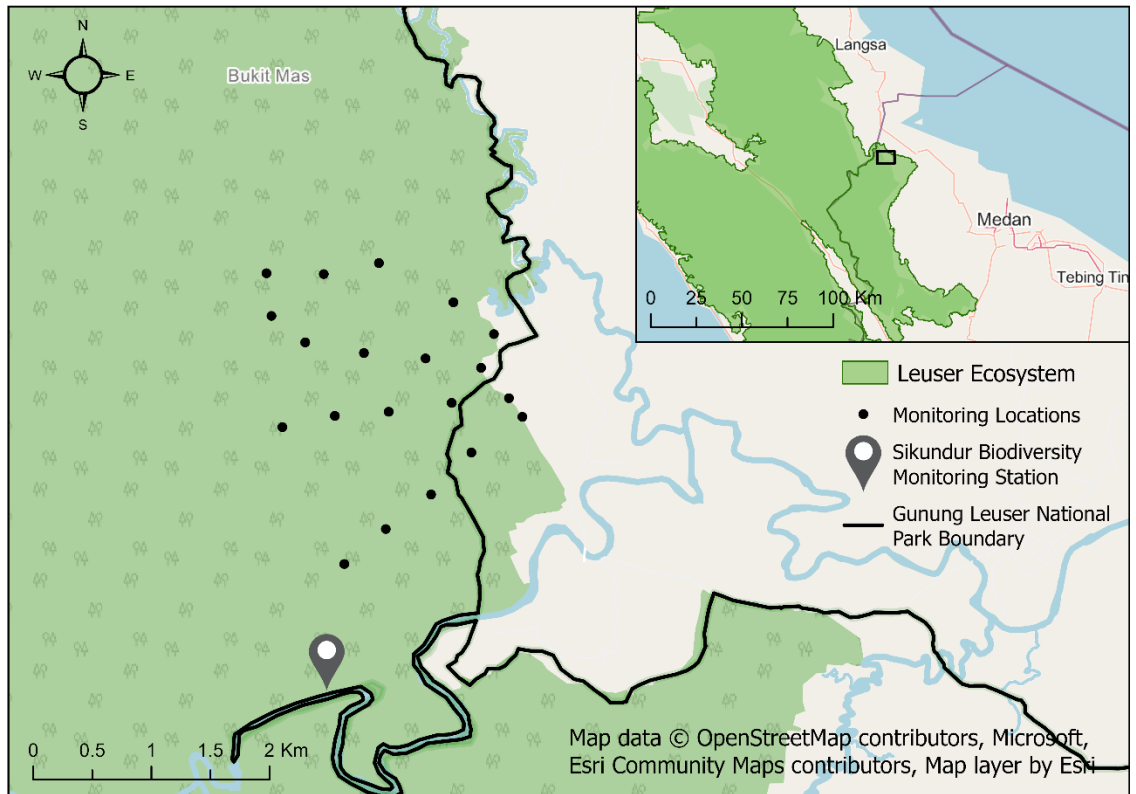


Figure 3.1: Monitoring locations close to Aras Napal in the Sikundur region of the Gunung Leuser National Park (GLNP), North Sumatra province, Sumatra, Indonesia. The dark green line represents the border of the GLNP.



Figure 3.2: Typical conditions at the forest boundary. Farms and plantations adjacent to the forest generally extend right up to the forest edge, creating a very obvious boundary between the two land cover types.

3.3.1.2 Microclimate

At each monitoring location Onset HOBO UA-002-08 8K Pendant Waterproof Temperature & Light Intensity Loggers (Figure 3.3) were used to record ambient temperature ($^{\circ}\text{C}$) and light intensity (lux). Sensors were secured at approximately 1.5m and programmed to autonomously record temperature and light intensity at 30-minute intervals. A software issue at the beginning of the sampling period meant that it was not possible to set up data loggers from the start, therefore microclimate data were only collected for 49 days. To prevent greenhouse effects from direct sunlight, sensors were placed in a well shaded location. At the end of the monitoring period sensors were collected and data extracted using HOBOWare software. Climate variables were summarised into T_{all} (mean temperature for the whole sampling period); T_{day} (mean temperature of each day); T_{max} (maximum temperature of each day); T_{min} (minimum temperature of each day); Li_{all} (mean light intensity for the whole period), Li_{day} (mean light intensity for each day); and Li_{max} (maximum light intensity for each day).



Figure 3.3: HOBO data logger used to measure microclimate conditions throughout the site at Aras Napal.

3.3.1.3 Forest Structure

Forest structure was recorded within 25x25m plots at all monitoring locations. Within each plot, the total number of trees with a diameter at breast height (DBH) of more than 10cm was recorded, and structural data were collected from each of these trees. Circumference at breast height (cm) was recorded using a measuring tape around the trunk, and diameter was calculated using the following formula, where D = tree diameter, cm; and c = tree circumference, cm:

$$D = \frac{C}{\pi}$$

Total height (m) and bole height (m) were measured using a Haglof Vertex IV instrument. The height to DBH ratio (HDR) was calculated by dividing the total height by the DBH. Crown width (m) was measured using tape measures from the ground to the nearest 10cm in both North-South and East-West directions. Crown area (m^2) was estimated using the following formula, where A = crown area, m^2 :

$$A = \pi \times \left(\left(\frac{N - S \text{ width}}{2} \right) \times \left(\frac{E - W \text{ width}}{2} \right) \right)$$

Canopy connectivity was estimated as a percentage of the crown which connected with neighbouring crowns.

3.3.1.4 Mammal activity

SpyPoint Force Dark remote trail cameras (Figure 3.4) were placed at each monitoring location and left for at least 60 days. Cameras were secured at a height of approximately 50cm facing towards an animal trail, salt lick or stream bed which was most likely to be frequented by medium to large-bodied animals. Cameras were set to take one image followed by 30 seconds of video when triggered by movement. Monitoring locations were visited only once, approximately halfway through the sampling period, to replace batteries and memory cards. At the end of the monitoring period cameras were collected and images sorted into separate directories for each transect and camera location.



Figure 3.4: SpyPoint Force Dark trail cameras were used to record mammal activity at each monitoring location.

3.3.2 Data analysis

3.3.2.1 Comparing forest conditions

Data from all transects were pooled and grouped by distance from the National Park boundary (i.e., 0km, 0.5km, 1km, 1.5km and 2km). All environmental variables show a non-normal distribution; therefore, non-parametric tests were used to check for differences between variables at each distance. A Kruskal-Wallis test was used to test for a significant difference between groups, followed by post-hoc Dunns multiple pairwise tests to identify which groups were significantly different. P-values were adjusted using a sequential Bonferroni correction to account for multiple comparisons and reduce the risk of false positives. Analyses were performed in R version 4.0.0 (R Core Team 2020). See Table 3.1 for a full list of environmental variables which were tested for differences between distances.

Table 3.1: Environmental variables collected from all monitoring locations at Aras Napal.

| Variable | Description(units) |
|-------------------|---|
| T _{all} | Mean temperature recorded for the whole sampling period (°C) |
| T _{day} | Mean temperature per day (°C) |
| T _{max} | Maximum temperature recorded each day (°C) |
| T _{min} | Minimum temperature recorded each day (°C) |
| Li _{all} | Mean light intensity recorded for the whole sampling period (lux) |
| Li _{max} | Maximum light intensity recorded each day (lux) |
| Total height | Total tree height for each tree (m) |
| Bole height | Height to the first major branch for each tree (m) |
| Number of trees | Total number of trees DBH>10cm per plot |
| DBH | Diameter at breast height for each tree (cm) |
| HDR | Height to DBH ratio for each tree |
| Crown area | Estimated crown area for each tree (m ²) |
| Connectivity | Estimated connectivity for each tree (%) |

3.3.2.2 Mammal activity rates

After being sorted into location and camera directories camera trap images were reviewed and recorded species were identified. Metadata tags containing the identified species were assigned to each image using the image management software Digikam (digiKam 2021). Standardised common names from the Integrated Taxonomic Information System database (ITIS 2021) were used to ensure long-term usability of image metadata in future research projects. Identifying species by metadata tagging is

advantageous since it facilitates exchange of data between researchers and allows for inter-observer comparisons where more than one observer is identifying images. The `recordTable` function from the R-package `camtrapR` (Niedballa et al. 2016) was used to extract image metadata and tabulate all detection events, excluding those of people and non-mammals. A minimum delta time (i.e., time difference between two subsequent detection events of the same species at the same location) of 1 hour was applied to ensure temporal independence between detection events.

A species accumulation curve was derived to show the accumulation of species as the number of sampling days increases in order to check that the sampling period was long enough to capture all mammals in the community. The “`specaccum`” function from the R package “`vegan`” was used to obtain this (Oksanen et al. 2019), using the equation from Roeland Kindt’s exact accumulator method, as recommended within the `vegan` package documentation.

3.3.2.3 Determining environmental drivers of mammal activity

The total number of mammal detections was used as a proxy for overall mammal activity at each location. This was used as the response variable in a Generalized Linear Model (GLM) to test the effect of environmental variables on the number of mammal detections. A correlation matrix was used to check for co-linearity among the predictor variables. Where variables had a correlation coefficient above 0.7, only one variable was chosen to be included in the model. The analysis was performed using the R package ‘`MASS`’ (Venables and Ripley 2002). Since the response variable comprises discrete count data which cannot be negative, the model was fitted with a Poisson distribution and `log`: link function. The ‘`dredge`’ function from the R package ‘`MuMIn`’ (Barton 2020) was then used to select which combination of variables produced the best model performance based on their Akaike Information Criterion (AIC).

A Generalized Linear Mixed Model (GLMM) was then fitted to the number of detections of each mammal Order, with Order included as a random effect. The analysis was run with the R package ‘`glmmTMB`’ (Brooks et al. 2017). As in the GLM, independent variables were first selected using a correlation matrix, and the ‘`dredge`’ function was used to select the best combination of variables based on the model AIC criterion. The GLMM was also fitted with a negative binomial distribution since the response variable are counts and the data are over dispersed.

3.4 Results

3.4.1 Objective 1) Comparing environmental conditions at different distances from the edge

3.4.1.1 Microclimate

Summaries of microclimate variables are shown in Table 3.2. Mean T_{all} across all locations was $25.54^{\circ}\text{C} \pm 2.25$ (Table 3.2). T_{all} varied significantly between distances from the edge (*Kruskal-Wallis* $\chi^2 = 152.71$, $df = 4$, $P < 0.01$; Figure 3.5 and Table 3.2). Post-hoc comparisons indicate that T_{all} was highest at the National Park boundary ($\mu = 26.07^{\circ}\text{C}$), and lowest at 1km into the forest ($\mu = 25.24^{\circ}\text{C}$). T_{all} was significantly higher at 0.5km than 1.5km and 2km, while there was no significant difference between 1.5km and 2km (see

Table 3.3 for post-hoc test statistics and Bonferroni adjusted P-values). The results indicate a similar pattern in T_{max} , which also varied significantly between distances (*Kruskal-Wallis* $\chi^2 = 274.18$, $df = 4$, $P < 0.01$; Figure 3.5 and Table 3.2). Post-hoc comparisons indicated that T_{max} was highest at the National Park boundary ($\mu = 31.35^{\circ}\text{C} \pm 2.64$), and lowest at 1km ($\mu = 28.05^{\circ}\text{C} \pm 1.15$). T_{max} was higher at 0.5km than 1km and 1.5km and there was no difference between 2km and 0.5km or 1.5km (see Table 3.4 for Dunn's test statistics and Bonferroni adjusted P-values). T_{day} also varied significantly between distances (*Kruskal-Wallis* $\chi^2 = 93.37$, $df = 4$, $P < 0.01$; Figure 3.5 and Table 3.2), with post-hoc tests indicating that T_{day} was significantly higher at the National Park boundary ($\mu = 26.03^{\circ}\text{C} \pm 1.00$), and significantly lower at 1km from the boundary than all other distances ($\mu = 28.05 \pm 1.15^{\circ}\text{C}$; see Table 3.5 for Dunn's pairwise tests and Bonferroni corrected P-values). T_{min} did not vary between distances (*Kruskal-Wallis* $\chi^2 = 6.34$, $df = 4$, $P = 0.18$; Figure 3.5 and Table 3.2), therefore further post-hoc comparisons were not carried out.

Mean light intensity recorded across the whole site and sampling period was $1079.88 \text{ lux} \pm 2921.8$ (Table 3.2). Li_{all} , Li_{day} and Li_{max} varied significantly between distances (*Kruskal-Wallis* $\chi^2 = 262.59$, $df = 4$, $P < 0.01$; *Kruskal-Wallis* $\chi^2 = 330.30$, $df = 4$, $P < 0.01$; *Kruskal-Wallis* $\chi^2 = 292.39$, $df = 4$, $P < 0.01$ respectively; also see Figure 3.5 and Table 3.2). Li_{all} , Li_{day} and Li_{max} were highest at the National Park boundary ($\mu = 2977.28 \text{ lux} \pm 2197.77$; $\mu = 2911.78 \text{ lux} \pm 2191.67$; $\mu = 16034.14 \text{ lux} \pm 10930.88$ respectively) and lowest at 1km ($\mu = 469.68 \text{ lux} \pm 206.35$; $\mu = 471.55 \text{ lux} \pm 224.09$; $\mu = 2565.25 \text{ lux} \pm$

1127.97 respectively) into the forest. There was no difference in light intensity at 0.5km, 1.5km and 2km (see Table 3.6 -

Table 3.8 for all Dunn’s pairwise test statistics and Bonferroni adjusted P-values).

Table 3.2: Summary of microclimate variables collected at different distances from the forest edge at Aras Napal. *N* = number of cases, μ = mean, *M* = median, *SD* = standard deviation.

| Distance from forest edge, km | All locations pooled | 0 km | 0.5 km | 1 km | 1.5 km | 2 km |
|------------------------------------|----------------------|----------------------|---------------------|---------------------|---------------------|---------------------|
| Mean Temperature, °C | <i>N</i> = 42135 | <i>N</i> = 8012 | <i>N</i> = 8529 | <i>N</i> = 8538 | <i>N</i> = 8546 | <i>N</i> = 8510 |
| | μ = 25.54 | μ = 26.07 | μ = 25.38 | μ = 25.24 | μ = 25.55 | μ = 25.48 |
| | <i>M</i> = 25.12 | <i>M</i> = 25.90 | <i>M</i> = 25.30 | <i>M</i> = 25.27 | <i>M</i> = 25.56 | <i>M</i> = 25.48 |
| | <i>SD</i> = 2.25 | <i>SD</i> = 0.48 | <i>SD</i> = 0.31 | <i>SD</i> = 0.22 | <i>SD</i> = 0.14 | <i>SD</i> = 0.10 |
| Daily mean temperature, °C | <i>N</i> = 908 | <i>N</i> = 181 | <i>N</i> = 182 | <i>N</i> = 182 | <i>N</i> = 182 | <i>N</i> = 182 |
| | μ = 25.53 | μ = 26.03 | μ = 25.37 | μ = 25.23 | μ = 25.55 | μ = 25.49 |
| | <i>M</i> = 25.60 | <i>M</i> = 26.01 | <i>M</i> = 25.43 | <i>M</i> = 25.31 | <i>M</i> = 25.58 | <i>M</i> = 25.54 |
| | <i>SD</i> = 0.68 | <i>SD</i> = 1.00 | <i>SD</i> = 0.75 | <i>SD</i> = 0.67 | <i>SD</i> = 0.69 | <i>SD</i> = 0.68 |
| Daily maximum temperature, °C | <i>N</i> = 908 | <i>N</i> = 181 | <i>N</i> = 182 | <i>N</i> = 182 | <i>N</i> = 182 | <i>N</i> = 182 |
| | μ = 34.30 | μ = 31.35 | μ = 28.77 | μ = 28.05 | μ = 29.06 | μ = 29.00 |
| | <i>M</i> = 34.69 | <i>M</i> = 31.88 | <i>M</i> = 28.36 | <i>M</i> = 27.96 | <i>M</i> = 29.15 | <i>M</i> = 29.05 |
| | <i>SD</i> = 2.26 | <i>SD</i> = 2.64 | <i>SD</i> = 1.80 | <i>SD</i> = 1.15 | <i>SD</i> = 1.20 | <i>SD</i> = 1.26 |
| Daily minimum temperature, °C | <i>N</i> = 908 | <i>N</i> = 181 | <i>N</i> = 182 | <i>N</i> = 182 | <i>N</i> = 182 | <i>N</i> = 182 |
| | μ = 22.70 | μ = 23.07 | μ = 23.08 | μ = 23.17 | μ = 23.24 | μ = 23.19 |
| | <i>M</i> = 22.72 | <i>M</i> = 23.10 | <i>M</i> = 23.10 | <i>M</i> = 23.20 | <i>M</i> = 23.20 | <i>M</i> = 23.20 |
| | <i>SD</i> = 0.76 | <i>SD</i> = 0.80 | <i>SD</i> = 0.79 | <i>SD</i> = 0.74 | <i>SD</i> = 0.74 | <i>SD</i> = 0.73 |
| Light intensity, lux | <i>N</i> = 42135 | <i>N</i> = 8012 | <i>N</i> = 8529 | <i>N</i> = 8538 | <i>N</i> = 8546 | <i>N</i> = 8510 |
| | μ = 1079.88 | μ = 2977.28 | μ = 752.71 | μ = 469.68 | μ = 660.94 | μ = 728.91 |
| | <i>M</i> = 0.00 | <i>M</i> = 2750.28 | <i>M</i> = 597.18 | <i>M</i> = 422.60 | <i>M</i> = 646.00 | <i>M</i> = 707.49 |
| | <i>SD</i> = 2921.80 | <i>SD</i> = 2197.77 | <i>SD</i> = 512.47 | <i>SD</i> = 206.35 | <i>SD</i> = 110.11 | <i>SD</i> = 204.36 |
| Daily mean light intensity, lux | <i>N</i> = 42135 | <i>N</i> = 181 | <i>N</i> = 182 | <i>N</i> = 182 | <i>N</i> = 182 | <i>N</i> = 182 |
| | μ = 1077.65 | μ = 2911.78 | μ = 749.39 | μ = 471.55 | μ = 662.19 | μ = 733.32 |
| | <i>M</i> = 1082.72 | <i>M</i> = 2215.94 | <i>M</i> = 574.64 | <i>M</i> = 439.53 | <i>M</i> = 645.28 | <i>M</i> = 708.41 |
| | <i>SD</i> = 264.58 | <i>SD</i> = 2191.67 | <i>SD</i> = 504.32 | <i>SD</i> = 224.09 | <i>SD</i> = 221.38 | <i>SD</i> = 269.98 |
| Daily maximum light intensity, lux | <i>N</i> = 908 | <i>N</i> = 181 | <i>N</i> = 182 | <i>N</i> = 182 | <i>N</i> = 182 | <i>N</i> = 182 |
| | μ = 27139.23 | μ = 16034.14 | μ = 4218.77 | μ = 2565.25 | μ = 3671.46 | μ = 4052.96 |
| | <i>M</i> = 28933.50 | <i>M</i> = 15155.70 | <i>M</i> = 3100.00 | <i>M</i> = 2411.10 | <i>M</i> = 3444.50 | <i>M</i> = 3788.90 |
| | <i>SD</i> = 6145.11 | <i>SD</i> = 10930.88 | <i>SD</i> = 2931.08 | <i>SD</i> = 1127.97 | <i>SD</i> = 1339.68 | <i>SD</i> = 1811.38 |

Table 3.3: Test statistics and Bonferroni adjusted P -values from post-hoc Dunn's pairwise comparisons of Tall (i.e., mean temperature, °C, for the whole sampling period) recorded at different distances from the forest edge at Aras Napal. Values which are significantly different following adjustment with $\alpha = 0.05$ are given in bold with an asterisk.

| | 0.5km | 1km | 1.5km | 2km |
|-------|---|---|---|---|
| 0km | Z = -9.31 P < 0.01* | Z = 11.11 P < 0.01* | Z = 4.18 P < 0.01* | Z = 6.05 P < 0.01* |
| 0.5km | | Z = 1.83 P = 0.68 | Z = -5.22 P < 0.01* | Z = -3.30 P = 0.01* |
| 1km | | | Z = 7.04 P < 0.01* | Z = -5.12 P < 0.01* |
| 1.5km | | | | Z = 1.91 P = 0.56 |

Table 3.4: Test statistics and Bonferroni adjusted P -values from post-hoc Dunn's pairwise comparisons of T_{max} (i.e., maximum temperature, °C, for each day) recorded at different distances from the forest edge at Aras Napal. Values which are significantly different following adjustment with $\alpha = 0.05$ are given in bold with an asterisk.

| | 0.5km | 1km | 1.5km | 2km |
|-------|--|---|--|---|
| 0km | Z = -12.11 P < 0.01* | Z = 15.84 P < 0.01* | Z = 9.17 P < 0.01* | Z = 9.58 P < 0.01* |
| 0.5km | | Z = 3.73 P < 0.01* | Z = -2.94 P = 0.03* | Z = -2.52 P = 0.12 |
| 1km | | | Z = 6.67 P < 0.01* | Z = -6.24 P < 0.01* |
| 1.5km | | | | Z = 0.42 P = 1.00 |

Table 3.5: Test statistics and Bonferroni adjusted P -values from post-hoc Dunn's pairwise comparisons of T_{day} (i.e., mean temperature, °C, for each day), recorded at different distances from the forest edge at Aras Napal. Values which are significantly different following adjustment with $\alpha = 0.05$ are given in bold with an asterisk.

| | 0.5km | 1km | 1.5km | 2km |
|-------|---|--|--|---|
| 0km | Z = -7.28 P < 0.01* | Z = 9.09 P < 0.01* | Z = 4.89 P < 0.01* | Z = 5.77 P < 0.01* |
| 0.5km | | Z = 1.82 P = 0.69 | Z = -2.39 P = 0.17 | Z = -1.50 P = 1.00 |
| 1km | | | Z = 4.21 P < 0.01* | Z = -3.31 P < 0.01* |
| 1.5km | | | | Z = 0.89 P = 1.00 |

Table 3.6: Test statistics and Bonferroni adjusted P -values from post-hoc Dunn's pairwise comparisons of LI_{all} (i.e., mean light intensity, lux, for the whole sampling period) recorded at different distances from the forest edge at Aras Napal. Values which are significantly different following adjustment with $\alpha = 0.05$ are given in bold with an asterisk.

| | 0.5km | 1km | 1.5km | 2km |
|-------|---|--|--|--|
| 0km | $Z = -10.91$ $P < 0.01^*$ | $Z = 15.80$ $P < 0.01^*$ | $Z = 10.36$ $P < 0.01^*$ | $Z = 9.21$ $P < 0.01^*$ |
| 0.5km | | $Z = 4.96$ $P < 0.01^*$ | $Z = -0.57$ $P = 1.00$ | $Z = -1.72$ $P = 0.85$ |
| 1km | | | $Z = 5.54$ $P < 0.01^*$ | $Z = -6.68$ $P < 0.01^*$ |
| 1.5km | | | | $Z = -1.15$ $P = 1.00$ |

Table 3.7: Test statistics and Bonferroni adjusted P -values from post-hoc Dunn's pairwise comparisons of LI_{day} (i.e., mean light intensity, lux, for each day) recorded at different distances from the forest edge at Aras Napal. Values which are significantly different following adjustment with $\alpha = 0.05$ are given in bold with an asterisk.

| | 0.5km | 1km | 1.5km | 2km |
|-------|---|--|--|--|
| 0km | $Z = -12.24$ $P < 0.01^*$ | $Z = 17.64$ $P < 0.01^*$ | $Z = 11.42$ $P < 0.01^*$ | $Z = 9.71$ $P < 0.01^*$ |
| 0.5km | | $Z = 5.41$ $P < 0.01^*$ | $Z = -0.82$ $P = 1.00$ | $Z = -2.52$ $P = 0.12$ |
| 1km | | | $Z = 6.23$ $P < 0.01^*$ | $Z = -7.92$ $P < 0.01^*$ |
| 1.5km | | | | $Z = -1.70$ $P = 0.90$ |

Table 3.8: Test statistics and Bonferroni adjusted P -values from post-hoc Dunn's pairwise comparisons of L_{max} (i.e., maximum light intensity, lux, for each day) recorded at different distances from the forest edge at Aras Napal. Values which are significantly different following adjustment with $\alpha = 0.05$ are given in bold with an asterisk.

| | 0.5km | 1km | 1.5km | 2km |
|-------|---|--|--|--|
| 0km | $Z = -11.28$ $P < 0.01^*$ | $Z = 16.71$ $P < 0.01^*$ | $Z = 10.26$ $P < 0.01^*$ | $Z = 8.95$ $P < 0.01^*$ |
| 0.5km | | $Z = 5.44$ $P < 0.01^*$ | $Z = -1.02$ $P = 1.00$ | $Z = -2.31$ $P = 0.21$ |
| 1km | | | $Z = 6.46$ $P < 0.01^*$ | $Z = -7.75$ $P < 0.01^*$ |
| 1.5km | | | | $Z = -1.30$ $P = 1.00$ |

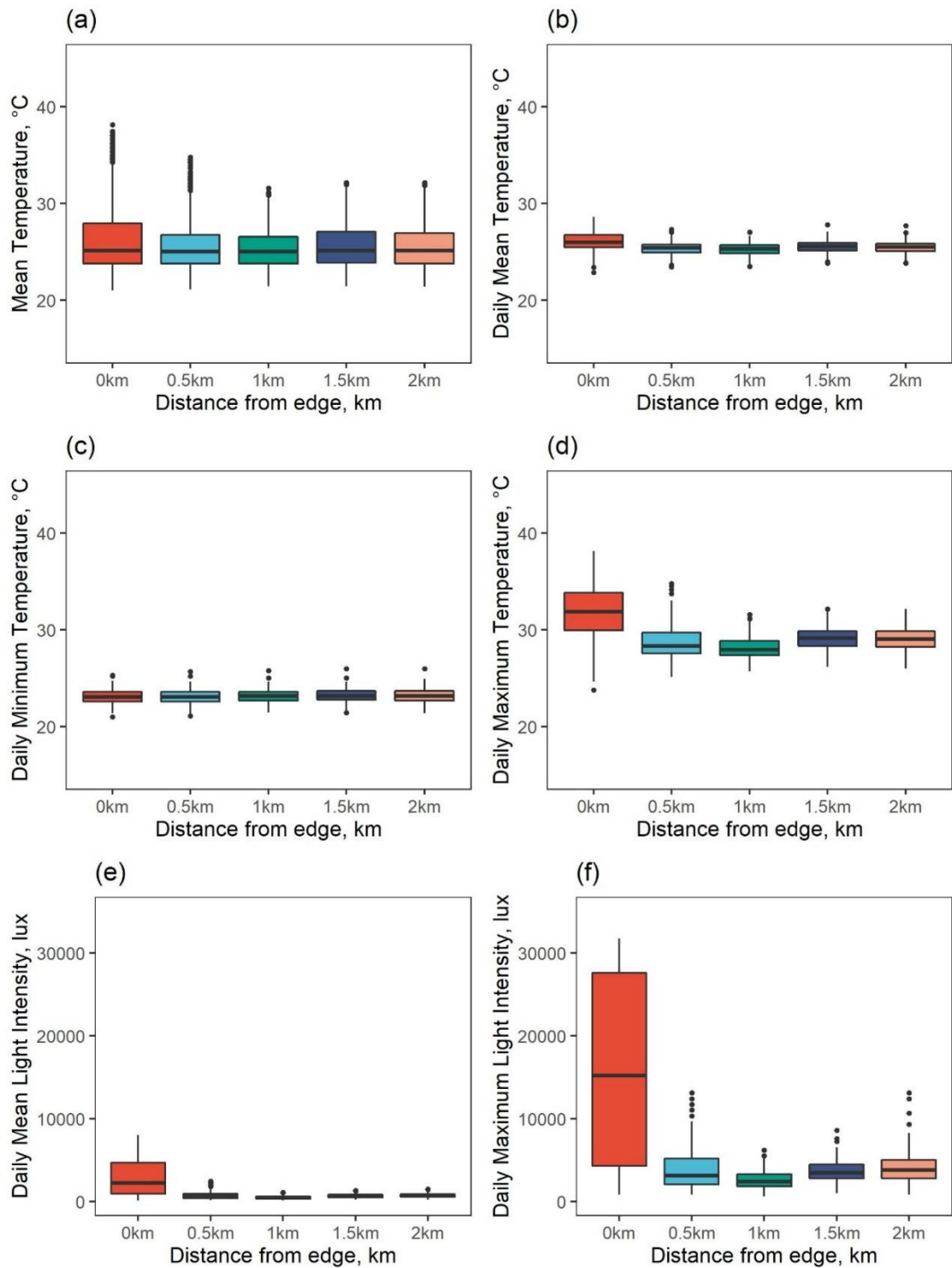


Figure 3.5: The range of microclimate conditions recorded at different distances from the forest edge at Aras Napal. (a) Mean temperature for the whole sampling period; (b) mean temperature of each day; (c) minimum temperature of each day; (d) maximum temperature of each day; (e) mean light intensity of each day; and (f) maximum light intensity of each day

3.4.1.2 Forest Structure

Forest structure variables are summarised in Table 3.9. Trees were generally smaller, with relatively low total height ($\mu = 19.45\text{m} \pm 8.27$) and DBH ($\mu = 33.45\text{cm} \pm 13.58$),

compared with what would be expected in primary tropical forest; DBH did not vary between distances (*Kruskal-Wallis* $\chi^2 = 4.0188$, $df = 4$, $P = 0.40$). There was a significant difference in tree height between distances (*Kruskal-Wallis* $\chi^2 = 11.59$, $df = 4$, $P = 0.02$), however post-hoc tests only indicated a marginally significant difference between 0.5km and 1km after adjusting for multiple comparisons with Bonferroni correction (see Table 3.10 for all pairwise comparisons), with 0.5km having lower tree height ($\mu = 17.44\text{m} \pm 6.79$) than 1km ($\mu = 21.83\text{m} \pm 8.51$). The mean HDR across the whole site was 61.03 ± 42.01 . HDR varied significantly between distances (*Kruskal-Wallis* $\chi^2 = 26.52$, $df = 4$, $P < 0.01$), with post-hoc tests indicating that the HDR was significantly lower at the National Park boundary ($\mu = 24.25 \pm 13.71$) compared with all other distances, apart from 0.5km ($\mu = 31.76 \pm 16.62$). There were no further significant differences between any other distances (see

Table 3.11 for all pairwise comparisons).

Average bole height across the whole site was $10.71\text{m} \pm 6.03$. Bole height varied significantly between distances (*Kruskal-Wallis* $\chi^2 = 23.941$, $df = 4$, $P < 0.01$). Trees measured at the National Park boundary had a lower bole height ($\mu = 8.06\text{m} \pm 4.61$) than those measured at all other distances. Additionally, trees at 0.5km had a lower bole height ($\mu = 9.13\text{m} \pm 4.90$) than trees at 1km ($\mu = 12.68\text{m} \pm 6.85$). There was no difference in bole heights recorded at 1km, 1.5km and 2km (see

Table 3.12 for all pairwise comparisons).

The average crown area across the whole site was $44.86 \text{ m}^2 \pm 36.74$, and there was no evidence of any significant variation between distances (*Kruskal-Wallis* $\chi^2 = 6.6232$, $df = 4$, $P = 0.16$). The average number of trees per plot was 10.85 ± 3.41 . The number of trees within a plot did not vary between distances (*Kruskal-Wallis* $\chi^2 = 3.74$, $df = 4$, $P = 0.44$). Canopy connectivity was generally low ($\mu = 45.00\% \pm 23.33$), with average connectivity estimates being below 50% at all distances, there was no evidence for a significant difference in canopy connectivity between distances (*Kruskal-Wallis* $\chi^2 = 1.44$, $df = 4.00$, $P = 0.84$).

Table 3.9: Summary of forest structure variables collected from plots at different distances from the forest edge at Aras Napal.

| Distance from forest edge | All locations pooled | 0 km | 0.5 km | 1 km | 1.5 km | 2 km |
|-------------------------------|-----------------------------|-----------------------------|-----------------------------|-----------------------------|-----------------------------|-----------------------------|
| Number of trees | $N = 20$ | $N = 5$ |
| | $\mu = 10.85$ | $\mu = 12.13$ | $\mu = 13.50$ | $\mu = 11.23$ | $\mu = 10.71$ | $\mu = 11.11$ |
| | $M = 11.5$ $SD = 3.41$ | $M = 13.00$ $SD = 1.18$ | $M = 14.00$ $SD = 2.38$ | $M = 12.00$ $SD = 1.58$ | $M = 11.00$ $SD = 2.70$ | $M = 10.00$ $SD = 3.61$ |
| Tree height, m | $N = 217$ | $N = 48$ | $N = 52$ | $N = 44$ | $N = 35$ | $N = 38$ |
| | $\mu = 19.45$ | $\mu = 17.48$ | $\mu = 17.44$ | $\mu = 21.83$ | $\mu = 21.43$ | $\mu = 20.08$ |
| | $M = 17.70$ $SD = 8.27$ | $M = 16.35$ $SD = 6.34$ | $M = 16.30$ $SD = 6.79$ | $M = 18.65$ $SD = 8.51$ | $M = 18.20$ $SD = 10.37$ | $M = 19.30$ $SD = 8.98$ |
| Bole height, m | $N = 217$ | $N = 48$ | $N = 52$ | $N = 44$ | $N = 35$ | $N = 38$ |
| | $\mu = 10.71$ | $\mu = 8.06$ | $\mu = 9.13$ | $\mu = 12.68$ | $\mu = 12.24$ | $\mu = 12.51$ |
| | $M = 10.10$ $SD = 6.08$ | $M = 7.30$ $SD = 4.61$ | $M = 8.70$ $SD = 4.90$ | $M = 12.10$ $SD = 6.85$ | $M = 11.00$ $SD = 6.84$ | $M = 13.2$ $SD = 5.67$ |
| Diameter at breast height, cm | $N = 217$ | $N = 48$ | $N = 52$ | $N = 44$ | $N = 35$ | $N = 38$ |
| | $\mu = 33.45$ | $\mu = 34.62$ | $\mu = 30.11$ | $\mu = 38.69$ | $\mu = 32.49$ | $\mu = 31.36$ |
| | $M = 38.20$ $SD = 13.58$ | $M = 29.60$ $SD = 13.26$ | $M = 26.10$ $SD = 9.98$ | $M = 28.64$ $SD = 33.28$ | $M = 27.06$ $SD = 14.55$ | $M = 28.65$ $SD = 11.40$ |
| Height:DBH ratio | $N = 217$ | $N = 48$ | $N = 52$ | $N = 44$ | $N = 35$ | $N = 38$ |
| | $\mu = 61.03$ | $\mu = 24.25$ | $\mu = 31.76$ | $\mu = 66.14$ | $\mu = 38.03$ | $\mu = 40.64$ |
| | $M = 62.07$ $SD = 42.01$ | $M = 22.28$ $SD = 13.71$ | $M = 30.79$ $SD = 16.62$ | $M = 63.78$ $SD = 17.71$ | $M = 38.03$ $SD = 14.83$ | $M = 41.43$ $SD = 15.25$ |
| Crown area, m ² | $N = 217$ | $N = 48$ | $N = 52$ | $N = 44$ | $N = 35$ | $N = 38$ |
| | $\mu = 44.86$ | $\mu = 24.25$ | $\mu = 38.09$ | $\mu = 53.76$ | $\mu = 50.76$ | $\mu = 37.31$ |
| | $M = 33.93$ $SD = 36.74$ | $M = 22.28$ $SD = 13.71$ | $M = 28.88$ $SD = 29.37$ | $M = 38.57$ $SD = 45.83$ | $M = 37.48$ $SD = 42.74$ | $M = 29.32$ $SD = 29.26$ |
| Canopy connectivity, % | $N = 217$ | $N = 48$ | $N = 52$ | $N = 44$ | $N = 35$ | $N = 38$ |
| | $\mu = 45.00$ | $\mu = 44.27$ | $\mu = 44.23$ | $\mu = 44.43$ | $\mu = 43.86$ | $\mu = 48.68$ |
| | $M = 45.00$ $SD = 25.33$ | $M = 40.00$ $SD = 20.68$ | $M = 40.00$ $SD = 24.22$ | $M = 45.00$ $SD = 23.33$ | $M = 45.00$ $SD = 20.37$ | $M = 52.50$ $SD = 28.18$ |

Table 3.10: Test statistics and Bonferroni adjusted P-values from post-hoc Dunn's pairwise comparisons of mean tree height, m , recorded at different distances from the forest edge at Aras Napal. Values which are significantly different following adjustment with $\alpha = 0.05$ are given in bold with an asterisk.

| | 0.5km | 1km | 1.5km | 2km |
|-------|----------------------|-----------------------|-----------------------|----------------------|
| 0km | Z = 0.17 P = 1.00 | Z = -2.52 P = 0.12 | Z = -1.76 P = 0.78 | Z = 6.05 P = 0.98 |
| 0.5km | | Z = 2.73 P = 0.06 | Z = 1.95 P = 0.51 | Z = 1.86 P = 0.63 |
| 1km | | | Z = 0.59 P = 1.00 | Z = 0.74 P = 1.00 |
| 1.5km | | | | Z = 0.13 P = 1.00 |

Table 3.11: Test statistics and Bonferroni adjusted P-values from post-hoc Dunn's pairwise comparisons of mean bole height, m , recorded at different distances from the forest edge at Aras Napal. Values which are significantly different following adjustment with $\alpha = 0.05$ are given in bold with an asterisk.

| | 0.5km | 1km | 1.5km | 2km |
|-------|-----------------------|---|--------------------------------------|---|
| 0km | Z = -1.13 P = 1.00 | Z = -3.81 P < 0.01* | Z = -2.98 P = 0.03* | Z = -3.71 P < 0.01* |
| 0.5km | | Z = 2.78 P = 0.05* | Z = 2.00 P = 0.46 | Z = 2.71 P = 0.07 |
| 1km | | | Z = 0.59 P = 1.00 | Z = -0.04 P = 1.00 |
| 1.5km | | | | Z = -0.61 P = 1.00 |

Table 3.12: Test statistics and Bonferroni adjusted P-values from post-hoc Dunn's pairwise comparisons of the mean ratio of tree height to diameter at breast height, HDR, recorded at different distances from the forest edge at Aras Napal. Values which are significantly different following adjustment with $\alpha = 0.05$ are given in bold with an asterisk.

| | 0.5km | 1km | 1.5km | 2km |
|-------|-----------------------|---|---|---|
| 0km | Z = -2.33 P = 0.20 | Z = -4.13 P < 0.01* | Z = -4.21 P < 0.01* | Z = -3.67 P < 0.01* |
| 0.5km | | Z = 1.92 P = 0.54 | Z = -2.14 P = 0.32 | Z = -1.55 P = 1.00 |
| 1km | | | Z = 0.33 P = 1.00 | Z = 0.29 P = 1.00 |
| 1.5km | | | | Z = 0.59 P = 1.00 |

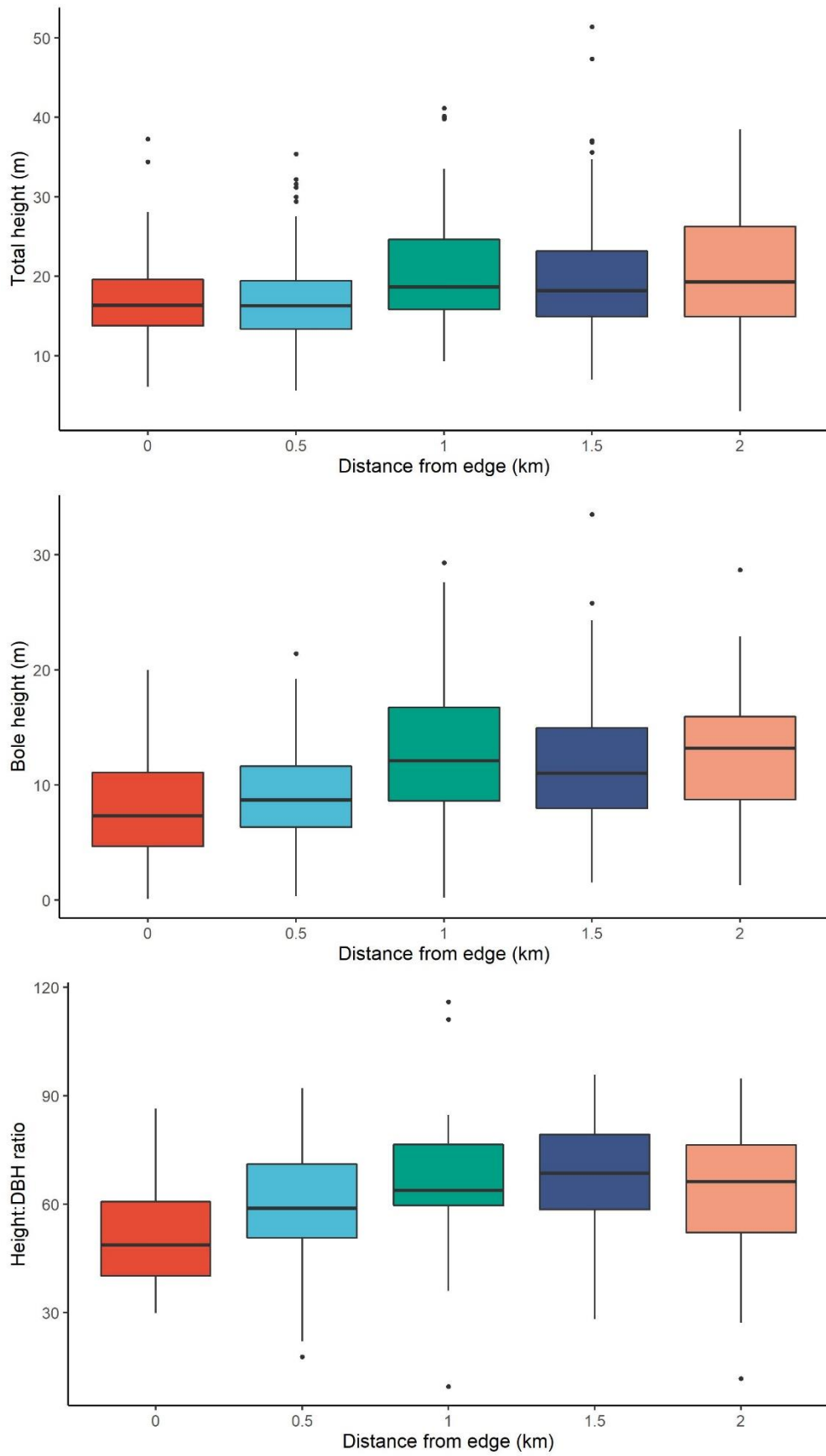


Figure 3.6: Total height (m), bole height (m), and height:DBH ratio of trees recorded at different distances from the forest edge at Aras Napal.

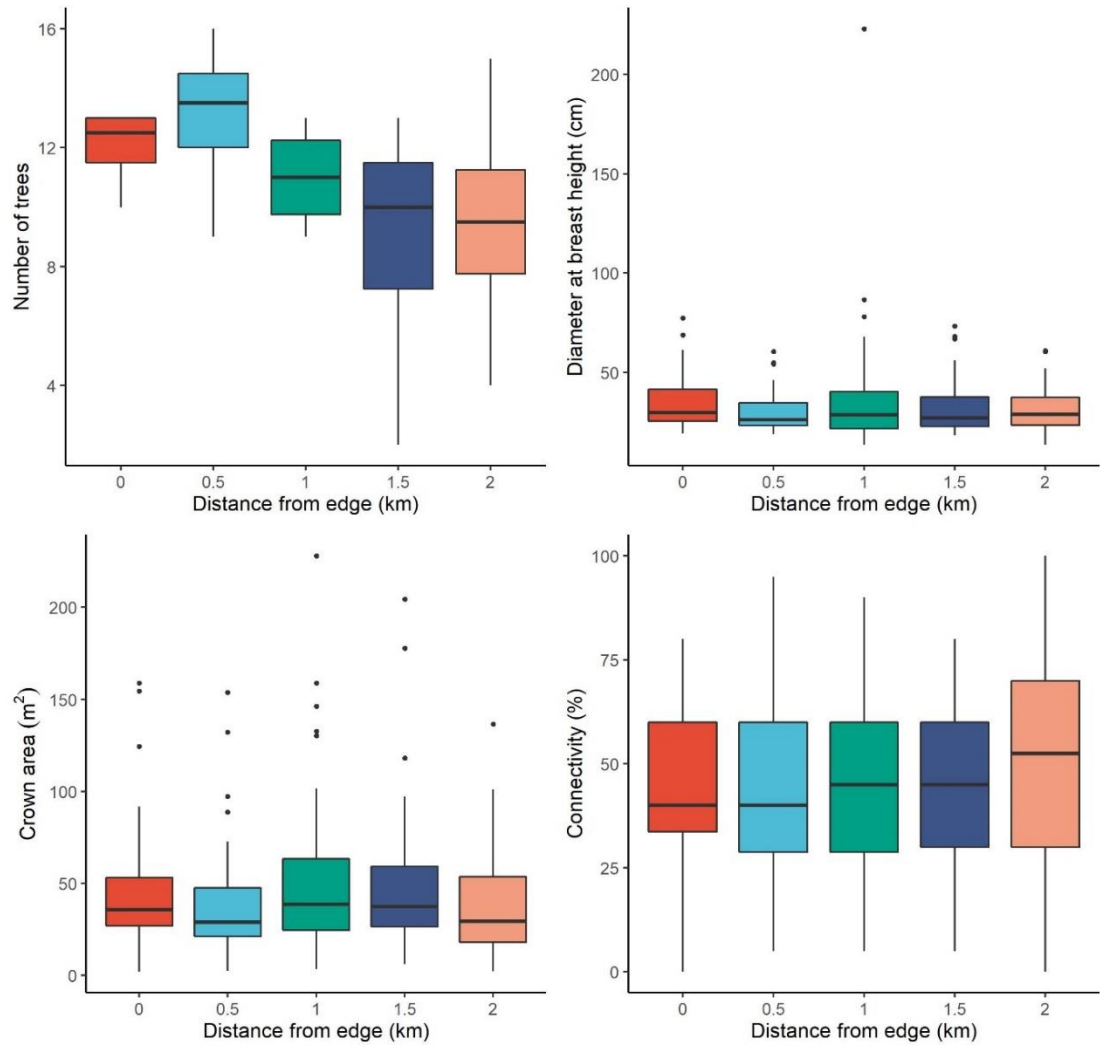


Figure 3.7: Number of trees per plot, DBH (cm), crown area (m²), and canopy connectivity (%) of trees recorded at different distances from the forest edge at Aras Nepal.

3.4.2 Objective 2) Variation in mammal activity rates between distances

Out of 20 camera traps deployed, one malfunctioned and recorded incorrect timestamps on images meaning that they could not be included in the analysis. The remaining 19 cameras yielded a total of 1079 sampling days (mean of 56.8 days per camera), 1384 images, and 300 mammal detection events. 16 mammal species were identified across 14 families and six orders (see Table 3.13). It was not possible to identify animals in the families Muridae (mice and rats) and Sciuridae (squirrels) to species level. The number of families detected at each location ranged from 1-10. Three families had fewer than five detections, while five had more than 20. The species accumulation curve (Figure 3.8) shows that by around 200 total sampling days, 12 out of 14 families had been detected, indicating that the sampling effort was adequate to capture all present and

detectable species. To increase sample sizes, all further analyses were performed at the Order level.

A Pearson's chi-squared test was used to test the hypothesis that there was a significant association between mammal Order occurrence and distance from the forest edge. The number of detection events of each mammal Order were not equal between distances ($\chi^2 = 75.324$, $df = 20$, $p < 0.01$; see Figure 3.9). Primate detections were higher towards the National Park boundary, and elephants were detected only within 1km from the edge and not further into the forest. Moonrats were only detected at distances greater than 1000m and carnivores were not detected at 0m. Ungulates and rodents were detected at all distances but had a much higher detection rate at 1000m than any other distance.

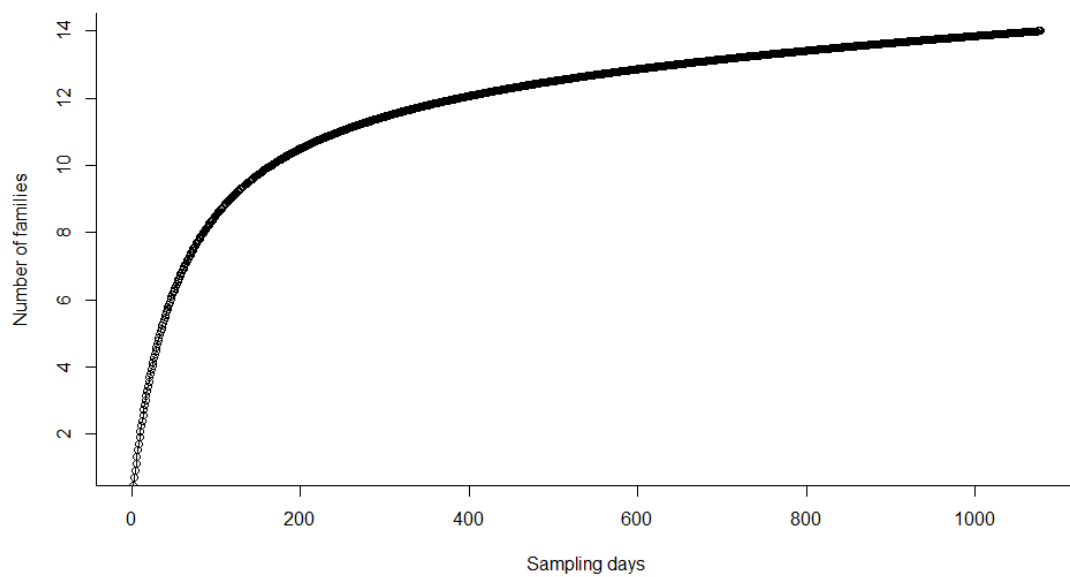


Figure 3.8: Species accumulation curve showing number of mammal families detected with sampling effort in Aras Nepal.

Table 3.13: Checklist of mammals detected at Aras Napal with total number of detections and naïve occupancy (the proportion of sites with ≥ 1 detection events).

| Class | Order | Family | Species | Scientific name | IUCN status | Population trend | Detection events | Naïve occupancy | |
|----------|----------------|----------------|-----------------------------|--------------------------------------|--|------------------|------------------|-----------------|------|
| Mammalia | Erinaceomorpha | Erinaceidae | Moonrat | <i>Echinosorex gymnura</i> | LC | unknown | 16 | 0.21 | |
| | | Primates | Cercopithecidae | Long-tailed macaque | <i>Macaca fascicularis</i> | LC | decreasing | 1 | 0.05 |
| | | | Cercopithecidae | Pig-tailed macaque | <i>Macaca nemestrina</i> | VU | decreasing | 83 | 0.79 |
| | | | Cercopithecidae | Thomas's langur | <i>Presbytis thomasi</i> | VU | decreasing | 2 | 0.05 |
| | Carnivora | Ursidae | Sun bear | <i>Helarctos malayanus</i> | VU | decreasing | 2 | 0.11 | |
| | | Mustelidae | Oriental short-clawed otter | <i>Amblonyx cinereus</i> | VU | decreasing | 1 | 0.05 | |
| | | Herpestidae | Collared mongoose | <i>Herpestes semitorquatus</i> | NT | decreasing | 1 | 0.05 | |
| | | Herpestidae | Short-tailed mongoose | <i>Herpestes brachyurus</i> | NT | decreasing | 5 | 0.11 | |
| | | Prionodontidae | Banded linsang | <i>Prionodon linsang</i> | LC | decreasing | 5 | 0.16 | |
| | | Felidae | Sumatran tiger | <i>Panthera tigris ssp. sumatrae</i> | CR | decreasing | 1 | 0.05 | |
| | | Proboscidea | Elephantidae | Sumatran elephant | <i>Elephas maximus ssp. sumatranus</i> | CR | decreasing | 11 | 0.21 |
| | Artiodactyla | Suidae | Wild boar | <i>Sus scrofa</i> | LC | Unknown | 23 | 0.53 | |
| | | Tragulidae | Lesser oriental chevrotain | <i>Tragulus kanchil</i> | LC | unknown | 48 | 0.47 | |
| | | Cervidae | Sambar | <i>Rusa unicolor</i> | VU | decreasing | 3 | 0.16 | |
| | | Cervidae | Southern red muntjac | <i>Muntiacus muntjack</i> | LC | decreasing | 37 | 0.26 | |
| | Rodentia | Muridae | Rat | -- | -- | -- | 9 | 0.26 | |
| | | Muridae | Mouse | -- | -- | -- | 44 | 0.16 | |
| | | Hystriidae | Malayan porcupine | <i>Hystrix brachyura</i> | LC | decreasing | 16 | 0.37 | |
| | | Sciuridae | Squirrel | -- | -- | -- | 17 | 0.37 | |

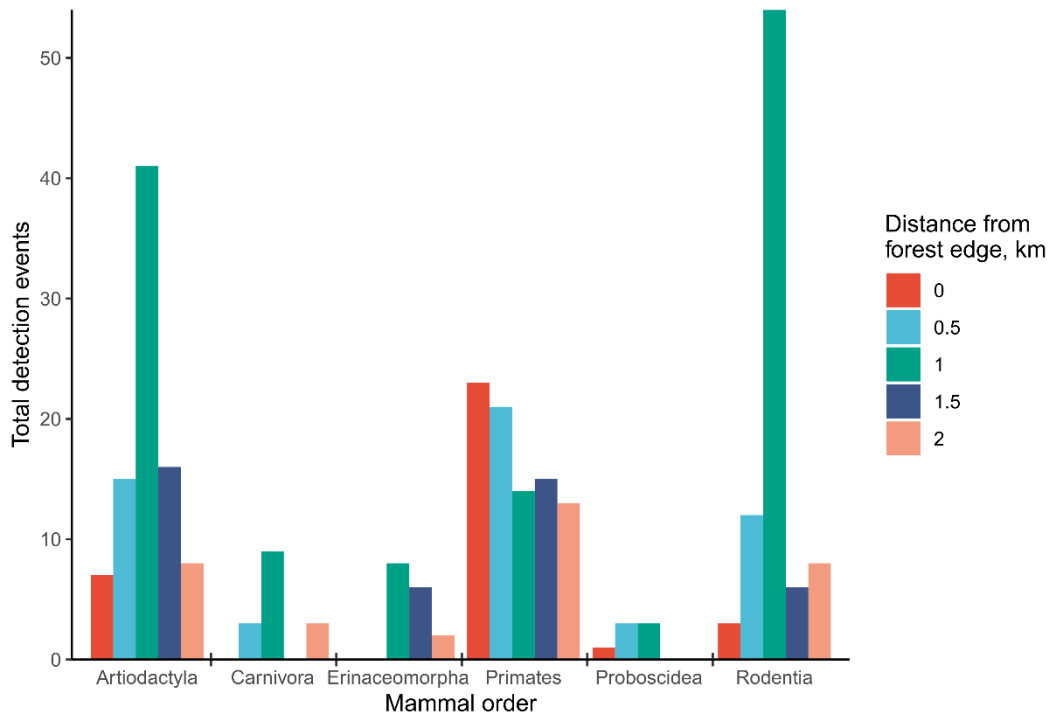


Figure 3.9: Total number of detection events for each mammal Order detected at different distances from the forest edge at Aras Napal.

3.4.3 Objective 3) Environmental predictors of mammal activity rates

3.4.3.1 Overall mammal detections

All microclimate variables except for T_{\min} were very highly correlated, accordingly only T_{\max} and T_{\min} were used in the models. T_{\max} was selected since it was shown to be the most variable between locations and is likely to be a more important constraint to diurnal terrestrial mammals than mean temperature. Total height and bole height were also strongly correlated; consequently, only total height was used in the analysis. There were no correlations between other forest structure variables, therefore these were all included in the model. The best model performance was obtained with the variables T_{\max} , T_{\min} , tree height and DBH (see Table 3.14 for model outputs). The deviance in mammal detection rates explained by this model was 27.72%. Model predictions and raw data of the detection rate against predictor variables are shown in Figure 3.10. The number of detections decreased with maximum and minimum temperatures, with a decrease in detection events of 0.88 and 0.32 for every 1°C increase. Number of detections also decreased with tree height, with a reduction of 0.90 for every 1m increase in height. DBH increased the number of detections by 1.20 for every 1cm increase in diameter.

Table 3.14: Exponentiated coefficient estimates with standard errors in parentheses for the GLM with poisson distribution and log:link function testing the effects of environmental variables on the number of mammal detection events at Aras Napal. Significant effects ($\alpha = 0.05$) are highlighted in bold.

| | Model 1 |
|--------------------------------------|--|
| (Intercept) | 851952702838.02 * (10.72) |
| Maximum temperature, °C | -0.88 *** (0.03) |
| Minimum temperature, °C | -0.32 * (0.48) |
| Tree height, m | -0.90 *** (0.02) |
| Diameter at breast height, cm | 1.20 *** (0.03) |
| N | 19 |
| AIC | 172.43 |
| BIC | 177.15 |
| Pseudo R2 | 0.92 |

*** $p < 0.001$; ** $p < 0.01$; * $p < 0.05$.

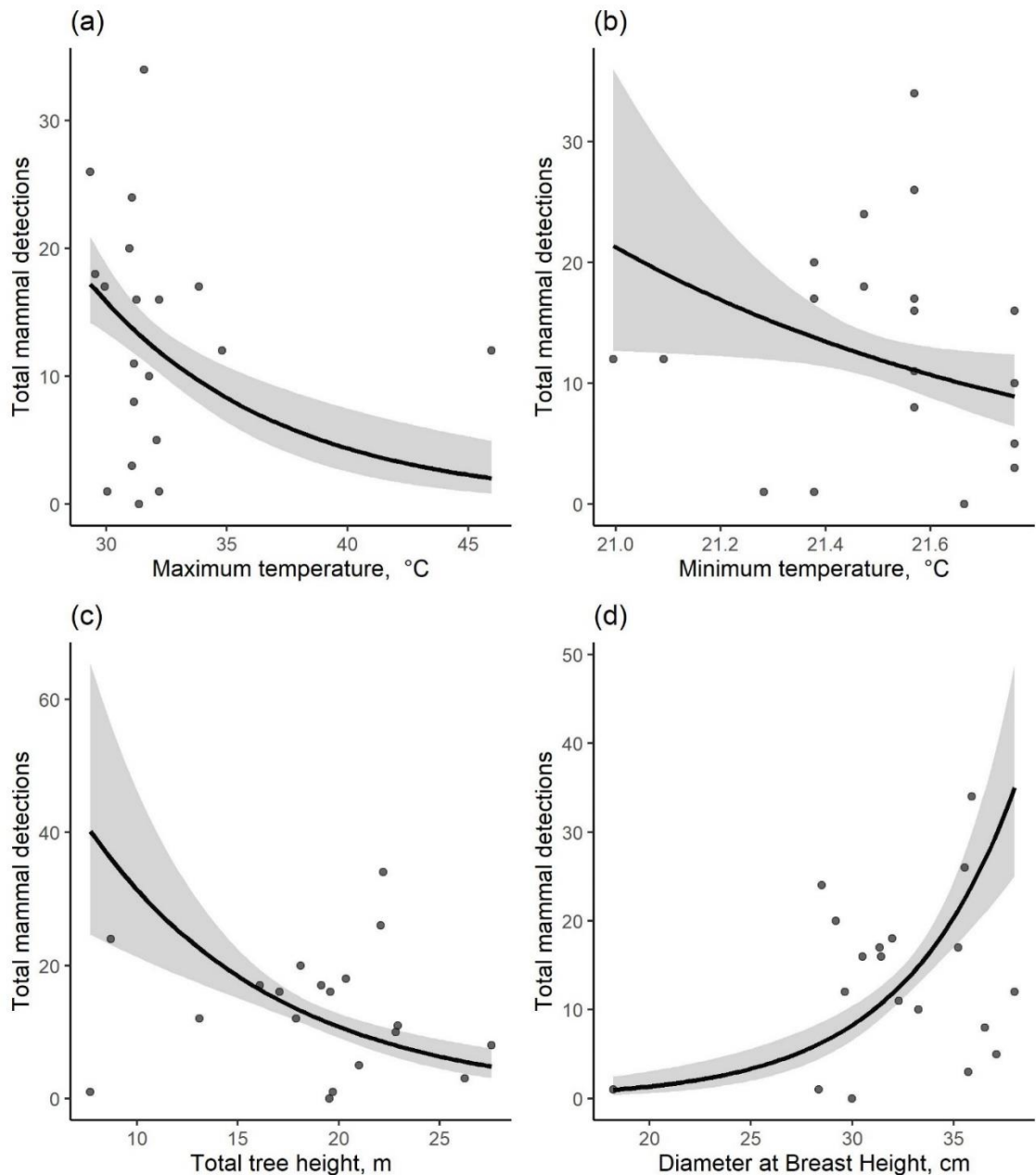


Figure 3.10: GLM predictions (lines), with 95% confidence intervals (grey shading), and observed number of mammal detections against (a) maximum temperature, °C; (b) minimum temperature, °C; (c) tree height, m; and (d) DBH, cm on the total number of mammal detection events at Aras Napal.

3.4.3.2 Number of detections for each mammal Order

The best model performance was obtained using T_{\max} , tree height, and DBH. Model outputs are given in Table 3.15 and model predictions with raw data of the detection rate for each Order against predictor variables are shown in Figure 3.11. T_{\max} and tree height were negatively correlated with the number of detections (Figure 3.11a & b). DBH was positively correlated to the number of detections (Figure 3.11c).

Table 3.15: Generalised linear mixed model (negative binomial) fit by the laplace approximation of total detection events according to environmental variables. Mammal Order is included as a random factor. Significant P-values ($\alpha = 0.05$) are highlighted in bold.

| Predictors | Number of detections | | |
|--|-----------------------|--------------------|------------------|
| | Incidence Rate Ratios | CI | p |
| (Intercept) | 0.55 | 0.02 – 17.79 | 0.738 |
| Maximum temperature, °C | 0.87 | 0.78 – 0.96 | 0.006 |
| Tree height, m | 0.85 | 0.77 – 0.95 | 0.004 |
| Diameter at breast height, cm | 1.31 | 1.14 – 1.50 | <0.001 |
| Random Effects | | | |
| σ^2 | 1.13 | | |
| τ_{00} order | 0.94 | | |
| ICC | 0.45 | | |
| N _{order} | 6 | | |
| Observations | 114 | | |
| Marginal R ² / Conditional R ² | 0.194 / 0.560 | | |

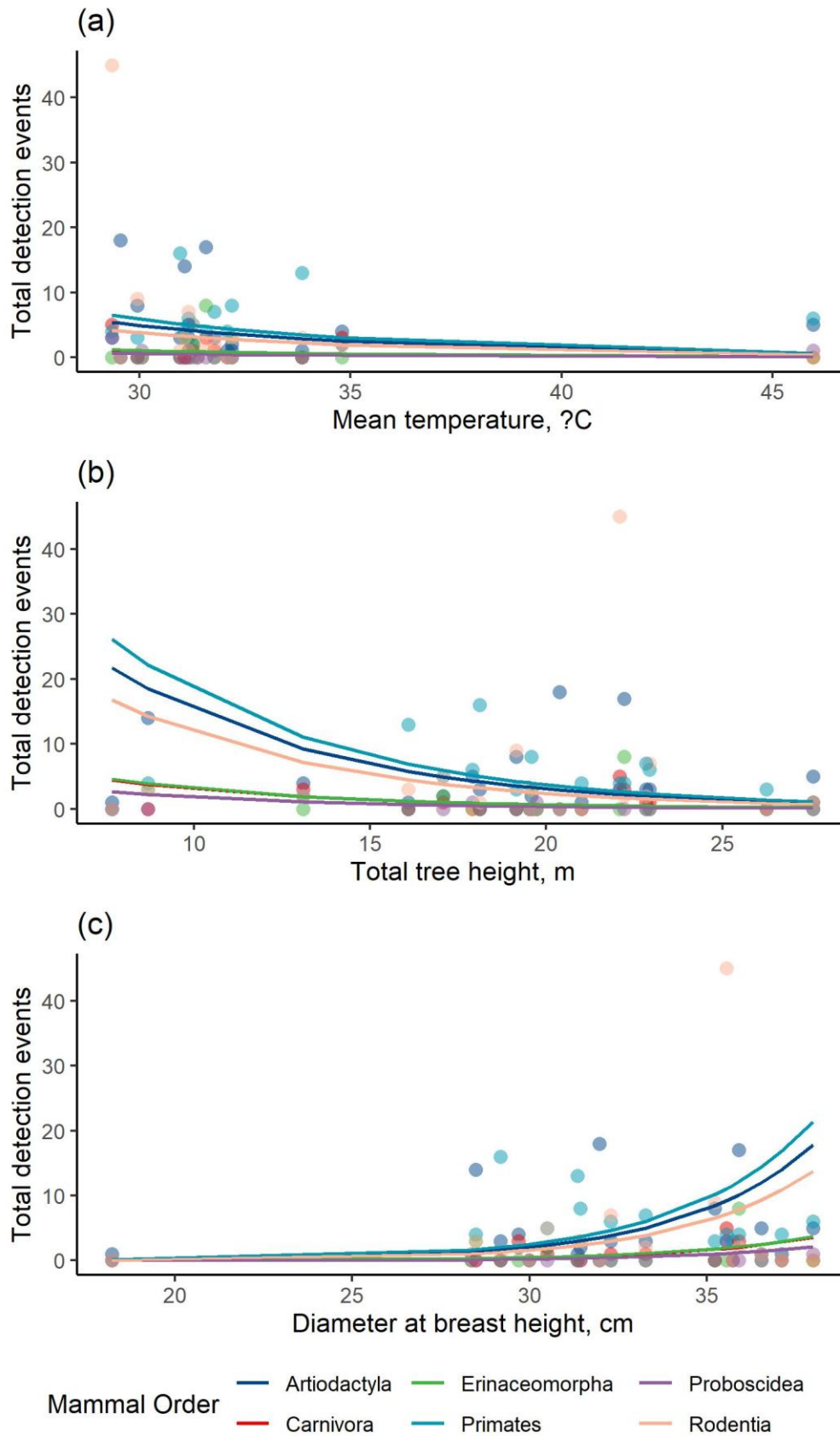


Figure 3.11: Model predictions (lines) and observed values (points) of detection rates by mammal Order against (a) Maximum temperature, °C; (b) Tree height, m; and (c) Diameter at breast height, cm.

3.5 Discussion

3.5.1 Differences in forest conditions and edge effects

Overall, temperatures and solar radiation were notably higher at the forest edge. In particular the daily maximum temperature was much higher at the edge compared with all other monitoring locations in the forest interior. This result indicates that increased temperature is driven by an increase in the penetration of light radiation into the canopy from the adjacent orange plantations, which have substantially lower vegetation cover. The fact that there was no variation in daily minimum temperature between distances further supports this since night-time temperatures were not affected by proximity to the forest edge. Forests are expected overall to dampen heat loss but considering the continued relatively high temperatures at night in this region, such an effect is not as pronounced as expected in, for example higher altitude forests. Although there was some statistically significant variation within the forest interior, these differences were far less pronounced than those between the edge and interior. Temperatures were also generally higher at 0.5km than those recorded further into the forest, demonstrating that edge effects are influencing conditions up to 0.5 -1km into the forest. These results are consistent with other data from tropical forests (e.g., Broadbent et al. 2008), although research in this area is limited given that most studies use discrete categories such as forest and non-forest (Zurita et al. 2012). Further measurements at a finer spatial scale are needed to identify exactly how far edge effects continue to influence understorey conditions and determine how closely temperature is correlated with proximity to the edge.

Vegetation structure did not seem to vary much along transects. Total height was uniformly low, even 2km into the protected forest. This is most likely a result of historic logging at the site, during which time most of the large emergent trees were removed (Priatna et al. 2000). HDR was lowest at the edge, indicating that trees at the edge have a wider girth in relation to their top height. There are a number of potential explanations for this and given that tree species data are not available and the relationship between height and DBH varies greatly both within and between tree species (Mugasha et al. 2013), it is difficult to draw conclusions. Generally, younger trees would be expected to have a higher HDR, since it is expected that young trees would favour upwards growth in order to reach the top of the canopy (Sumida et al. 2013). Historic logging would have targeted tall, wide trees with a lower HDR; presently there are few large emergent trees found throughout the site, and in particular there are virtually none located close to the

forest boundary. As a result, there is possibly a bias towards tree species with relatively low HDR, since these would not be favourable for harvesting.

These levels of variation in both structure and climate at relatively small spatial scales highlight the importance of considering local scale climate when modelling species' habitat preferences. Significant differences in temperature and light radiation were detected within less than one km, and these differences are potentially ecologically significant for forest dwelling animal species. Open access climate datasets are usually only available at scales much larger than an animal's body size or even their average home range. The highest available resolution for WorldClim (Hijmans et al. 2015), for example, is 30 seconds (or roughly 1km² at the equator), if climate for this study had been inferred from the WorldClim database rather than being directly measured, the small-scale differences noted here would not have been detected.

3.5.2 Mammal activity

The proportions of each mammal Order detected varied with distance from the National Park edge. This is unsurprising, given that some species will be better able to cope with forest edge conditions, and are known to utilise the adjacent human dominated landscape (Segan et al. 2016). Other species will be less tolerant of human disturbance and changes to forest conditions. The number of species detected was lower at the forest edge, with only five species (pigs, long and pig-tailed macaques, elephants, and squirrels) being detected compared with 8-13 species elsewhere. Most of the species detected at the edge are known to utilise agricultural lands (Love et al. 2017; Castillo-Contreras et al. 2018; Ruppert et al. 2018), while those which did not occur at the edge, such as carnivores and moonrats, are reportedly less able to exploit human dominated land (Michalski and Peres 2005; Brodie et al. 2015; Farris et al. 2017; Brozovic et al. 2018; Wynn-Grant et al. 2018). The results indicate that human influence plays a significant role in the species richness, abundance, and composition of the mammal community in this area. For many species, forest edges have a notable negative impact, and forest reserves or conservation set asides will need to be large enough to ensure species are able to avoid them. Large carnivores, such as tigers and sun bears, for example, will need a buffer area of at least 1.5km, and corridors will have to be wider than this to ensure that these species will use them. Many reserves in agricultural landscapes are not large enough to provide this and are therefore unable to support these species in the long-term. This highlights that while

set asides and remnants in agricultural mosaics can be valuable for biodiversity, they cannot replace continuous primary forests in conserving many large mammals (Barlow et al. 2007; Gibson et al. 2011).

Monkeys and pigs had the highest naïve occupancy, with both families being detected at 79% and 53% of all sites respectively. This will be due in part to pigs and the terrestrial pig-tailed macaque being more readily detected by camera traps, however both species are habitat generalists, and also known to utilise agricultural lands (Linkie et al. 2007). Conversion to agriculture is frequently reported to favour these species, since it provides them with a competitive advantage over forest specialists through enhanced foraging opportunities in croplands (Hill 2017; Castillo-Contreras et al. 2018). Daily crop foraging events by both pigs and monkeys have been reported within all plantations close to the National Park in Aras Napal, and the detection rate was higher for both species close to the Park boundary. Both monkeys and pigs appear to be relatively abundant throughout the whole area, and do not seem to be suffering a negative impact of human activities in this region. Despite clear evidence (on camera traps, K. Hodder & A. Korstjens 2020 unpublished) of near daily human hunting activity in the areas near the forest edge (mostly within 1km).

Elephants were only detected within 1km of the forest edge. All detection events were also associated with incidents involving elephants moving into the adjacent plantations, as reported by landowners from Aras Napal. Little is known regarding the abundance and demographics of the elephant population in the region, although recent unpublished data estimates that there is a population of around 78 individuals in the region and that they are also observed further inwards from the edge (Collins 2018). Additionally, interviews with Aras Napal residents suggest that there are at least one or two family-groups consisting of 10-15 individuals, and several solitary male bulls regularly utilising the forest and adjacent oil palm plantations. The camera trap data from this study confirms the presence of at least one family group in the area, since all detection events showed a group of individuals, including at least one juvenile (additional camera trap evidence in January 2020 also confirmed the presence of a young solitary bull, K. Hodder and AHK unpublished). All detection events occurred at camera locations where the camera was situated on a large trail, which usually led towards the forest edge. This suggests that the elephants in this area will generally avoid forest close to the edge, except to utilise the adjacent plantation land. Collins (2018) reported similar findings in this area based on

dung distribution, with elephants occurring more frequently close to human-dominated areas. This situation requires further monitoring, since it has the potential to turn into a conflict between plantation owners and elephants, although currently the reported levels of elephant crop foraging remain relatively low. More extensive monitoring which focusses on this population and extends further into the protected forest is needed to provide detailed information on how many groups/individuals are present in the area, whether they are connected to other elephant populations and the extent to which they are reliant on crop foraging to survive in the region.

Deer were detected most frequently at 1km from the edge, and at relatively low numbers elsewhere. Inspection of the raw data shows that this result is biased due to an outlier, where there were 16 detection events for Red Muntjac deer at one location at 1km, even after the data had been pruned to include only one observation per species per hour. This is likely due to this camera location being situated close to either a sleeping site or foraging site. Due to the low detection rate, it is difficult to identify a trend in deer occurrence; however, they appear to demonstrate a preference for interior over the forest edge, where hunters are more common. Other studies have reported similar findings, with deer in Borneo demonstrating a preference for interior forest (Brodie et al 2015).

Detection rates of carnivores, particularly large-bodied carnivores, were uniformly low, and no carnivores were detected at the National Park edge. This result is expected, large carnivores are generally found at low density and range over great distances, therefore their probability of detection at a given location is very low. Reports of carnivore incursions into the neighbouring plantations and village are rare; most plantations near the edge are fenced and patrolled regularly by either people or dogs, which will deter most wild carnivores. The results here indicate that carnivores respond negatively to forest edges, although this should be interpreted with caution due to the overall low detection rate across the site. Mammalian carnivores, particularly those with larger body sizes, are considered especially sensitive to disturbance (Crooks 2002; Heim 2011; Gerber et al. 2012; Farris et al. 2017). A camera trap study of large mammals in Borneo found that mammalian carnivores avoided the forest edge and demonstrated a strong preference for primary forest (Brodie et al. 2015).

The results found here suggest that mammals are more likely to be detected in cooler locations in the forest. The mean temperature, daily maximum temperature and amount

of light radiation were significantly lower at 1km compared with all other locations. Locations at this distance also had, on average, a much higher mammal detection rate. Both the GLM and GLMM indicated that higher maximum and minimum temperatures lead to a reduction in mammal detection rate, and this negative relationship remained consistent across mammal Orders. This could either be because mammals are less active in warmer temperatures (Korstjens et al. 2010) and therefore less likely to be detected by camera traps, or because they are actively avoiding warmer regions in the forest. The only way to test this would be through real time monitoring of animal movement and microclimate as experienced by the animal. It would not be possible to do this non-invasively, and my research permit in Indonesia only covered non-invasive, observational research; additionally, I did not have sufficient resources to safely sedate and tag potentially dangerous wild mammals.

Total tree height was negatively associated with mammal detections, while DBH was positively associated. The model considers these variables together, so more trees with a taller height and lower DBH result in a lower detection rate, while more trees with a lower height, but larger DBH would result in a higher detection rate. A plot with a high average HDR (i.e. a small DBH relative to the average height) would suggest a higher proportion of young trees, since younger trees tend to favour upwards growth to reach a competitive height, before switching to favour trunk growth. This result suggests that mammals do not favour areas with a high proportion of very young trees. These results are comparable with those reported from a camera trap study from the Udzungwa Mountains in Tanzania, which found a negative association between the stem density of small trees (DBH 5-10cm) and the abundance of several medium sized mammals, while the stem density of large trees (DBH >10cm) had a positive effect on several medium sized mammals (Martin et al. 2015). While it is well documented that mammal species richness is reduced in secondary compared with primary forest, very few studies have examined the relationship between vegetation structure and large mammals in detail.

While clear relationships between temperature, tree height and tree diameter and mammal detections were found, the observed effect sizes were relatively small. There are other edge-related factors, besides temperature and light, which are also likely to be important drivers of mammal detections. For example, the level of human activity in the forest could influence both the density and detectability of animals. Mammals in areas with high levels of human disturbance have been observed to exhibit more vigilant

behaviour and spend less time in areas with high human footprint (e.g., wolverines, Stewart et al 2016), thereby reducing their detection probability in these areas. Differences in species composition and therefore food availability at the edge will also influence the distribution of species, and the effects of abiotic changes at the forest edge could therefore be indirect. Carnivores, for example, will be influenced by the distribution of prey species, such as deer, which are preferred prey for tigers (Allen, Sibarani and Krofel 2020) and were detected less at locations near the forest edge. Further work is necessary to fully identify which edge-related changes are most important for different mammal species. To fully understand the role of abiotic edge effects in determining mammal abundance across the site, it will be necessary to conduct further monitoring to increase the number of samples for each mammal species detected and allow for interspecies comparisons, as well as incorporate data on other factors which may vary with distance from the edge, such as measures of human activity (e.g., foot traffic or distance to settlements/main trails/roads) and food availability. Unfortunately, the sample numbers in this study are too low to perform more detailed analysis, such as occupancy modelling or other inferential approaches, which would allow for interspecies comparisons by accounting for imperfect detection, and differences in detection probability between species (Martin et al. 2015). This would give more detailed insights into how each species is impacted by environmental disturbance and how disturbance will influence the community structure and functional diversity of forests. This study does provide a useful baseline for which species are using the forest, and those which appear to be more affected by environmental changes brought on by edge effects at the park boundary.

3.5.3 Remote monitoring of wildlife populations

Camera traps are widely utilised to remotely monitor elusive animals in challenging conditions, such as tropical forest. Several other studies have demonstrated the usefulness of camera trapping in monitoring terrestrial forest mammals (Ahumada et al. 2013; Brodie et al. 2015; Martin et al. 2015; Rovero et al. 2017). The species accumulation curve indicates that the sampling effort of this study was adequate to capture most of the present and detectable species in the area. Gathering data using traditional field surveys would have required substantially more survey effort, with separate survey designs likely being required for each species of interest; for example, surveying elephant populations involves monitoring dung along line transects over a minimum of several months (Walsh

et al. 2001). Camera traps are limited in that they have a small effective detection area and can only capture a snapshot of a forest community; however, they are a hugely beneficial addition to monitoring programmes as they are still more likely than a human to detect elusive and nocturnal species (Caravaggi et al. 2017; Stephenson 2019). It is also important to separate observational processes, such as differential detection probabilities across animal guilds and habitat types, from ecological ones, to allow comparisons between studies and determine patterns at the landscape scale (Wearn et al 2017). With further development of standardised protocols for data collection, storage and sharing, remote camera technologies can be utilised to develop a global network of biodiversity monitoring with high spatial and temporal resolution, which will be instrumental in achieving targets for biodiversity conservation (Steenweg et al. 2017).

If implemented effectively, remote sensing methods can help fill knowledge gaps in high biodiversity tropical regions and for elusive and rare species. Most conservation actions aim to mitigate threats, reduce population declines and facilitate population recovery. Wildlife monitoring is a necessary step in assessing the outcomes of these actions. While remote monitoring offers many opportunities for wildlife research and conservation by facilitating collection of these data, it is most effective when integrated into a well-structured plan with clear goals, standardized protocols and should be complemented by data collected by people on the ground (Stephenson 2019). The lack of a standard methodological framework for the collection and analysis of remote monitoring data makes it difficult for practitioners who are unfamiliar with the technologies to properly implement them, and for researchers to scale up conclusions or draw comparisons between studies, locations or populations (Steenweg et al. 2017). Effective biodiversity monitoring programmes require clear protocols for survey design, data collection, storage and sharing, as well as consideration of the target species and actual project objectives, which indicators are appropriate to determine success, as well as the practicalities of the project, including the feasibility of beneficiaries to continue applying these methods for long term monitoring (Stephenson 2019). If appropriate care is taken to ensure that monitoring projects and equipment are suitable for the local conditions, focal species and research questions, remote monitoring technologies are promising tools which can provide long-term, high-quality datasets on wildlife populations.

3.5.4 Conservation Implications

The Sikundur region represents key habitat to many species of conservation concern. A total of 17 mammal species were detected, seven of which are threatened with extinction (i.e. listed as Vulnerable, Endangered or Critically Endangered on the IUCN red list), with a further three species being listed as Near Threatened (IUCN 2014). Apart from three species (with unknown population trends), all identified species have a decreasing population trend (IUCN 2014). This demonstrates that, despite the history of degradation, this area is still supporting a number of species of conservation importance; this includes the Critically Endangered and endemic Sumatran elephant and Sumatran tiger. This further supports a growing body of evidence showing that secondary forests are essential to conserving tropical biodiversity (Dent and Wright 2009). Other secondary forest sites with a similar disturbance history to Sikundur, i.e. selectively logged and connected to primary forest, have a species richness and composition which closely resembles that in old growth forest, and recover rapidly following abandonment (Dunn 2004). While curbing deforestation and protecting remaining primary forest must remain a key aim of conservation, the reality is that up to 60% of the world's remaining forest cover comprises degraded or secondary forest, with 42 tropical countries now having a greater area of secondary forest than old growth forest; therefore, degraded, or secondary forests are critical to maintaining biodiversity in the future (Dent and Wright 2009).

3.6 Conclusion

This chapter aimed to test the hypotheses that forest structure and microclimate would vary significantly with distance from the forest edge, and that this variation would be associated with changes in mammal activity. Temperature and levels of light radiation in the understorey were significantly higher at the forest edge, and this effect is significant at least 500m from the boundary. Canopy structure did not appear to change much with distance from the edge; this is likely a result of historical selective logging, which would have removed most of the large emergent trees. Implementing long term monitoring of the forest conditions along this ecotone would provide a better insight into how edge effects and the resulting microclimatic changes influence forest regeneration in the area. Species richness, composition, and abundance of medium to large-bodied terrestrial mammals varied notably with distance to the forest edge. Monkeys, pigs, and elephants seemed to show a preference for edge habitat, while deer, moonrats and carnivores appear to suffer negative impacts from forest edges. These results highlight the importance of

considering the spatial extent of edge effects on target conservation species, and the individual ecological requirements of different species. Reserves and corridors designed to provide refuges and connectivity between patches for mammals must provide a buffer which is large enough to protect them from harmful edge effects, this will need to be more than 1km for some species.

The results also highlight the potential of remote camera traps for monitoring elusive forest fauna; however, care should be taken when incorporating remote sensors into conservation monitoring programmes, and when scaling up camera trap data to larger spatial and temporal extents. The major limitation with the data collected here is that it is not possible to use inferential statistics, such as occupancy modelling or mark-recapture, which account for differences in detection probability. This would be possible with further sampling effort in the future, enabling us to determine the landscape scale ecological processes which drive mammal distribution and habitat use within tropical secondary forest in Sumatra. Future work should focus on continued monitoring of the mammal populations identified here following standardised protocols to enable collation of data between studies, and further monitoring at a finer spatial scale of the microclimatic gradient between the forest and adjacent plantations.

Chapter 4

Predicting microclimate in a heterogeneous tropical secondary forest in Sumatra, Indonesia

Abstract

Ecological studies are increasingly incorporating fine-scale climate data to better understand species-environment relationships; however, collecting such data over large geographic and temporal extents in the field is costly, time-consuming, and often constrained by resource and funding limitations. Climatic conditions in tropical forests are on average cooler and less variable than the ambient macroclimate. However, the complex physical structure of forest canopies results in notable fine-scale variations in temperature. Fine-scale microclimate variations are not captured by macroclimate data which are interpolated from weather stations and are most commonly used in climate-envelope models of species' distributions. There have been increasing efforts to develop mechanistic models which use a process-based approach to predict microclimate by downscaling from macroclimate data measured by weather stations based on vegetation and topography. These models can provide data at more relevant ecological scales for modelling species-environment relationships. While they have been tested extensively in the temperate forests in the US and UK, and arid regions of Australia, they have yet to be tested in a tropical rainforest setting. This chapter tests the performance of two available microclimate models, NicheMapR and microclimc, in predicting below-canopy temperatures within a disturbed forest in the Sikundur region of Sumatra, Indonesia. Predictions of air temperature at hourly intervals over 365 days were generated for 3 different heights from the top of the canopy at 15 random locations. Predictions were then tested against observed values recorded by automated data loggers, which were programmed to record temperature and light intensity at hourly intervals for 365 days continuously from October 2018 – October 2019. Temperatures varied significantly across the sites, and between heights, with temperatures increasing with increasing height above ground (i.e., lower distance to the top of the canopy). Both microclimate models performed well at predicting temperatures with similar errors to those found by previous studies in other environments, although NicheMapR produced lower error values. Model errors increased with increasing height above ground, suggesting that the models require

further parameterisation to fully capture vertical canopy gradients in tropical forests. These results demonstrate that existing mechanistic models perform well at predicting below-canopy conditions in tropical forests. These models are promising tools which can be used to provide detailed climate inputs to provide a better understanding of species-environment relationships at finer scales.

4.1 Introduction

Correlative species distribution models (SDMs) are commonly used to determine species extinction risks and potential future ranges under different climate change scenarios, but these are limited by the quality of input data. Correlative approaches are useful for answering questions about broad-scale species biogeography, but they have limited applicability at smaller spatial scales, where most conservation planning and action takes place. Typically, SDMs use open-access coarse scale climate datasets which have been downscaled from data grids collected from meteorological weather stations, such as WorldClim (Faye et al. 2014). This is potentially problematic, particularly in the case of tropical forest species. Firstly, there is limited weather station coverage across much of the Tropics compared with temperate regions, meaning that the accuracy and reliability of these datasets is limited in these regions (Daly 2006; World Meteorological Organization 2020). Secondly, weather stations are spread across spatial scales which are far larger than those at which organisms are experiencing climate (Bramer et al. 2018). Finally, traditional weather stations measure free air temperature following standard meteorological recording guidelines. As such, they are situated 1-2m above ground in open areas away from climate forcing factors, such as vegetation and topographical features which are not representative of the environments experienced by forest species (Bramer et al. 2018). Global climate predictions which have been interpolated from weather stations have been shown to differ markedly from locally recorded temperatures, particularly in heterogeneous tropical landscapes (Faye et al. 2014). Therefore, for most published SDMs, the input data used do not accurately reflect the actual conditions experienced by forest dwelling organisms, and, as a result, important patterns and processes which are occurring on smaller spatial scales are mostly overlooked (Gardner et al. 2019). More ecological studies need to consider the scale of the environmental data they use, and how relevant it is to the organism, system, or process in question.

Tropical forests will play a key role in facilitating mammal responses to climate change, by providing refuges allowing them to avoid the increases in extreme climate conditions predicted for the tropics (Blonder et al. 2018). Canopy-climate interactions in dense tropical forests result in higher rainfall and local climatic conditions which are decoupled from the macroclimate. Tropical forests are, on average, cooler, wetter, and less variable compared with those recorded by meteorological weather stations (Fauset et al. 2020). This means that forests will function as buffers against future climate change

(de Frenne et al. 2019). Additionally, mature forests are highly complex, heterogeneous environments with substantial fine-scale spatial variation in topography and vegetation structure, both of which result in highly variable climatic conditions within the forests, thereby providing microclimate refuges that species can utilise to avoid sub-optimal extremes (Scheffers et al. 2014). These microclimate refuges are arguably more important for larger bodied endotherms, where extinction risk due to climate change will be determined mainly by the frequency and duration of their exposure to extreme temperatures, rather than overall changes in average conditions (Rezende et al. 2014).

Conservationists often emphasise preserving remaining primary forest habitat to maintain biodiversity; however, the importance of secondary and regenerating forests is becoming increasingly evident (Dent and Wright 2009). A large proportion of threatened species' ranges now comprise secondary forests, although the long-term viability of populations in these landscapes is poorly known. Climate buffering and availability of microclimate refuges in secondary forests could be compromised, compared to those in primary forests, as a result of reduced canopy cover and edge effects in fragmented landscapes (Bramer et al. 2020), however there are data to suggest that microclimate conditions within secondary forests remain comparable to those in primary forests, meaning that they are equally buffered from macroclimate changes, and still maintain sufficient heterogeneity to support high levels of biodiversity (Senior et al. 2018). Determining the relationship between canopy structure, microclimate and background macroclimate in secondary forests will enable identification of potential microclimate refuges which will facilitate mammal responses to climate change.

Microclimates influence species physiology, behaviour, and ecological interactions. They can act as a buffer for organisms against long-term changes, as well as provide refuges for species, enabling them to avoid sub-optimal extremes (Suggitt et al. 2018). Microclimates are defined generally as fine scale variations in climate at spatial resolutions below 100m which are, at least temporarily, decoupled from mean macroclimate (Bramer et al. 2018). This is particularly important for species in the tropics, where most organisms have narrower thermal tolerances and exist closer to their maximum tolerance threshold than temperate species (Khaliq et al. 2014). While microclimates have been of interest to ecologists for some time (Geiger 1971; Oke 1987), there are still relatively few studies which incorporate fine-scale habitat and climate data when determining species-environment relationships and/or predicting species responses

to climate change. A review by Suggitt et al. (2011) found that only two out of 48 studies related to climate envelope modelling published between 2004 and 2008 used habitat data with a resolution of under 1km. This is particularly true for the tropics, where the geographic bias in high-resolution climate data towards temperate regions has impeded studies of microclimate ecology (Jucker et al. 2020). For example, none of the published species distribution models for large Sumatran mammals (e.g., Hedges et al. 2005; Wich et al. 2016; Poor et al. 2019) include fine-scale habitat or climate data. Identifying potential microclimate refuges for mammals is key to generating robust and reliable predictions of their extinction risk and future distributions with climate change.

Measuring and modelling microclimates is becoming increasingly easier with technological advances that allow for relatively low-cost equipment and easy storage and sharing of large datasets (e.g., Lembrechts et al. 2020). Autonomous sensors in the field or remote sensing technologies can be harnessed to directly measure climate conditions at high resolutions across large spatial and temporal extents with relatively little survey effort (e.g., Ashcroft and Gollan 2011a; Still et al. 2019). Much microclimate research to date has focussed on specific regions, such as the UK, US, and parts of Australia, which have high weather station and satellite coverage, and are relatively easily accessible to establish and maintain sensor networks (Bramer et al. 2018). There is still, however, a relative lack of data from the tropics. Despite the increased accessibility of microclimate monitoring, lack of funding and accessibility are major limiting factors of ecological research projects in the tropics (Jucker et al. 2020). Establishing sensor networks over large spatial extents and maintaining them long-term in order to adequately interpolate microclimate in tropical forests will likely remain unfeasible for some time, therefore it is essential to develop models which can reliably generate microclimate predictions from existing coarse-scale datasets.

Studies using microclimate variables either directly interpolate microclimate from in situ measurements (e.g., Dobrowski et al. 2009; Fridley 2009; Vanwalleghem and Meentemeyer 2009; Ashcroft and Gollan 2011; Ashcroft et al. 2012; Slavich et al. 2014; Frey, Hadley, and Betts 2016) or predict indirectly through downscaling of coarse-grained macroclimate data grids (e.g., Flint and Flint 2012; Dingman et al. 2013; McCullough et al. 2016; Meineri and Hylander 2017). Attempts to interpolate between field data or downscale global macroclimate data both typically rely on assumptions based on the predictor variables used and how they influence microclimate, such as

topography, soil conditions and vegetation structure and cover. Although, global data on the first two variables is available, quality data on vegetation structure and its influence on microclimate is limited, and local climate processes beneath tropical forest canopies in particular are poorly understood (Bramer et al. 2018). Low weather station coverage, resource constraints and poor accessibility in these regions results in low quality macroclimate data for downscaling, and limited ability to collect *in situ* data for interpolation.

There are now several mechanistic models available which can generate microclimate predictions for any location globally by downscaling macroclimate data using a process-based approach, which considers the effects of topography and vegetation structure (e.g., Kearney et al. 2014; Kearney and Porter 2017; Maclean et al. 2019; Kearney et al. 2020). Process-based, or mechanistic, microclimate models, which use input data on topography and vegetation obtained from remote sensing (i.e., satellite imagery, aerial photogrammetry, or LiDAR) are likely to produce more reliable estimates of microclimate conditions, since they consider processes which drive local climate variations, such as the effects of topography, vegetation, and shading (Kearney et al. 2014). Combined with the increasing accessibility of remote sensing technology to collect detailed data on 3D landscape structure over large areas, mechanistic models are a promising tool for predicting fine-scale variations in climate. These models are being increasingly utilised in studies of species-climate relationships since they can perform well without requiring extensive data collection to provide input parameters (e.g., Kearney and Porter 2009; Kearney et al. 2016). Mechanistic models have been applied and tested in a number of contexts, including mapping microclimate in the UK, the US and Australia (Kearney et al. 2014; Maclean et al. 2017; Fitzpatrick et al. 2019; Kearney 2019), and predicting distributions of both ectotherms (Kearney and Porter 2004; Enriquez-Urzelai et al. 2019) and endotherms (e.g., Porter and Kearney 2009; Mathewson et al. 2017), but have yet to be tested in a tropical rainforest setting, or be applied in predicting climate space for large tropical mammals. Given the limitations of ecological studies in the tropics, the ability to generate microclimate predictions with high spatial and temporal resolutions across large areas will vastly improve our ability to identify current species-environment relationships and make inferences on how these might change in the future.

4.2 Aim & Objectives

This chapter tests the performance of remote sensing and mechanistic modelling approaches to determine microclimate conditions underneath forest canopies in secondary tropical forest. The ability to model climate conditions at fine scales will improve our ability to identify potential microclimate refuges within tropical forests, without the need for costly and time-consuming field surveys on the ground.

1. Determine temperature variation in time and over 3D space in a secondary tropical forest by recording temperature and light intensity at hourly intervals using autonomous data loggers deployed at 15 randomly generated points throughout the study site over a continuous 1-year period.
2. Determine the reliability of temperatures predicted by the mechanistic microclimate models by comparing predictions of hourly microclimate conditions for each of these points to the *in situ* observed temperature measurements.
3. Compare the performance of two different mechanistic models in predicting below canopy temperature variations.
4. Determine whether vegetation characteristics affect the ability of mechanistic models to predict below canopy temperatures.

4.3 Methods

4.3.1 Location

Fifteen sampling points were randomly generated using ArcGIS Pro software (ESRI 2010), with a minimum distance of 100m between them to prevent spatial autocorrelation between points. A location within 50m (to account for accessibility) of each of these points was then chosen to sample microclimate and vegetation structure. Final sampling locations are shown in Figure 4.1.

4.3.2 *In situ* microclimate measurements

Temperature, °C and light intensity recorded from each sampling location using automated HOBO Onset temperature and light pendant loggers, placed at different heights in the tree canopy. HOBO pendant loggers are able to record temperatures and relative light levels between -20 and 70°C and 0 – 320,000 lux respectively, with an accuracy of $\pm 0.53^{\circ}\text{C}$ from 0 – 50°C. A catapult was used to launch a weighted rope into the canopy. Three sensors were secured to this rope at 5m intervals and raised into the

canopy until the first sensor was as close to the top of the tree as possible. The actual height above ground of the logger was then measured in metres using a Haglöf Vertex IV ultrasound laser range finder (Haglöf Sweden AB [haglofsweden.com]). Loggers were programmed to record temperature (°C) and light intensity (lux) at hourly intervals starting at 5pm on the day of deployment and were left to record for a 12-month period, providing coverage of both the wet and dry seasons. Loggers were revisited once during the sampling period to replace any which had failed, and once at the end of the period to collect them and remove the ropes from the forest. Once collected, climate data were cleaned to remove false highs where increased temperatures were recorded due to the logger being exposed to direct sunlight. Instances where the recorded light intensity exceeded 32,000 lux, or where temperature increased by more than 5°C between consecutive hourly recordings were removed along with the two datapoints immediately following them. A Kruskal-Wallis test was performed using R version 4.0.0 (R Core Team 2020) to compare temperatures recorded at each location.

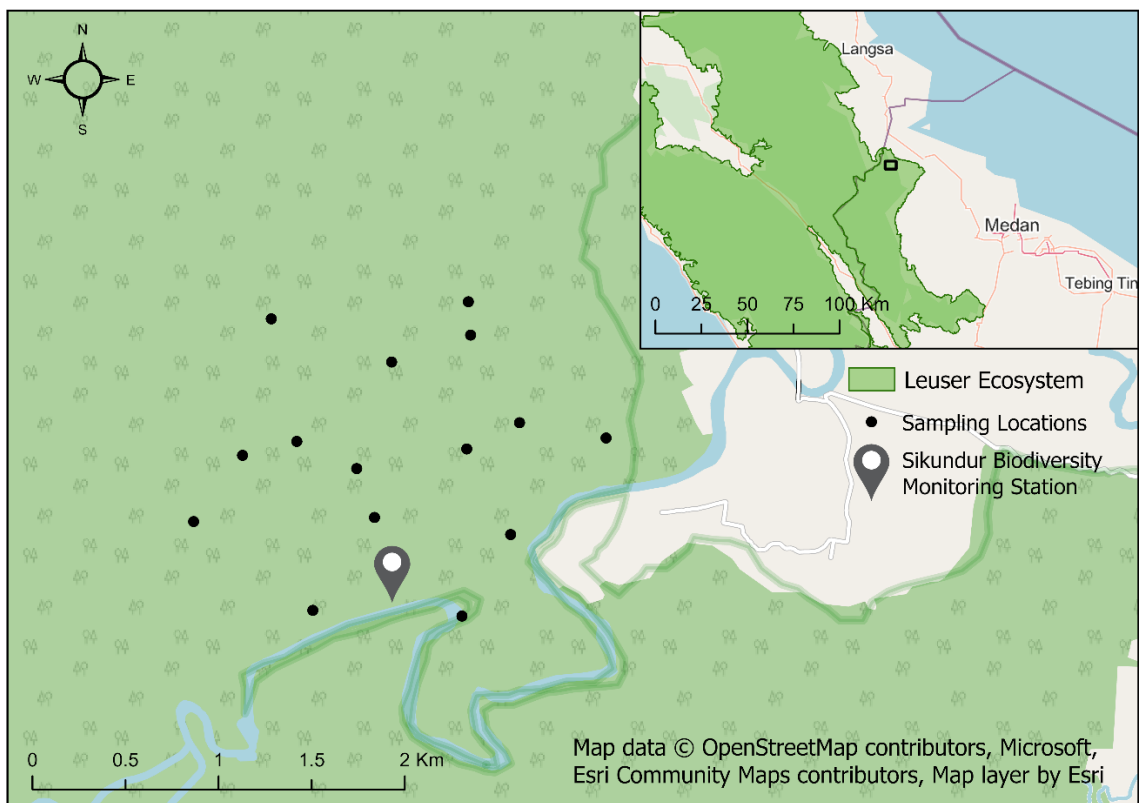


Figure 4.1: Random sampling locations used to measure and predict microclimate at Sikundur.

4.3.3 Vegetation & canopy structure

Canopy structure was recorded using 25 x 25m vegetation plots. Using the tree in which data loggers were placed as the origin, all trees within a 12.5m radius with a diameter at breast height (DBH) of more than 10cm were recorded. For each tree with a DBH of more than 10cm the following data was recorded: DBH (cm), calculated from the circumference of the trunk using a measuring tape at 1.3m (or above any large roots or buttresses); total height (m) and height to first major bole (m), measured using a Haglof vortex laser range finder; crown area (m²), estimated by measuring the crown along the N-S and E-W axes with a measuring tape on the ground; estimated percentage canopy connectivity. DBH was used to calculate basal area (m²) for individual trees, using the formula:

$$BA = \frac{\pi \times DBH^2}{40000}$$

Variables were summarised per plot as follows: unweighted mean height; mean bole height; mean DBH; mean basal area; mean crown area; mean crown depth; mean canopy connectivity; and total number of trees with DBH >10cm. In addition to the unweighted mean height, Lorey's height (the mean height of trees weighted by their basal area) was calculated using the `lorey.height` function in the 'sitreeE' package in R (Antón Fernández 2019). Lorey's height is frequently used in uneven-aged forest stands since it is less affected by loss of smaller trees than the unweighted mean height (Pourrahmati et al. 2018).

4.3.4 Microclimate modelling

Microclimate predictions were generated for all sampling locations and heights using two different packages for mechanistic microclimate modelling in R version 4.0.0 (R Core Team 2020); firstly, the microclimate model from NicheMapR (Kearney and Porter 2017), and secondly, `microclimc` (Maclean and Klinges 2021). Unlike NicheMapR, which is more general purpose, `microclimc` has been specifically designed to model below canopy microclimate, by incorporating more detailed input parameters for vegetation structure, including plant-area index, vegetation thickness and canopy height.

4.3.4.1 NicheMapR

Input variables on terrain and vegetation shading were manually included in the model to account for local climate forcing effects at each location. Terrain variables were obtained from the Shuttle Radar Topography Mission digital elevation model (SRTM DEM), with a 30m (1 arc-second) resolution. To reduce processing times, the SRTM DEM raster was first clipped to the study region in ArcGIS. Continuous data layers on slope ($^{\circ}$) and aspect ($^{\circ}$) for the whole site were generated from the SRTM DEM in SAGA-GIS (Conrad et al. 2015) using the ‘Slope, Aspect, Curvature’ function, found within the ‘Terrain Analysis’ toolbox under ‘Morphometry’. Vegetation shading was calculated using a digital surface model, DSM, with a resolution of 25.7 cm² per cell, developed from overlapping images taken over pre-programmed routes by unmanned aerial vehicles, UAVs, in 2015-2016 by Marsh (2019). The ‘Potential Incoming Solar Radiation’ function in SAGA-GIS (found within the ‘Terrain Analysis’ library, under ‘Lighting, Visibility’) was used to create a continuous data layer of total insolation (kWh/m²) across the whole site based on shading by neighbouring trees from the UAV DSM. The resulting data layer was overlaid with the SRTM DEM in ArcGIS and the ‘Point Sampling’ tool was used to extract values for elevation (m), slope ($^{\circ}$), aspect ($^{\circ}$), and total insolation (kWh/m²) for each sampling location. Total insolation was converted into a percentage of the insolation recorded at areas with no vegetation cover, this percentage was then subtracted from 100 to give the percentage shading to be used as the maximum shade in NicheMapR. The ‘micro_global’ function in NicheMapR was then used to generate hourly predictions of microclimate conditions over 365 days for all logger locations (15 points, with three heights per point, to give 45 sampling locations in total).

4.3.4.2 Microclimc

The climate forcing data required to run the microclimc model were interpolated to hourly intervals from the National Centers for Environmental Predictions global reanalysis dataset (NOAA Physical Sciences Laboratory 2021), which provides macroclimate data at 6-hourly intervals on a ~200km x 200km grid, using the function ‘hourlyNCEP’ from the ‘microclima’ R package (Maclean et al. 2019). These data were then reformatted to be used with microclimc using the ‘hourlyNCEP_convert’ function. Daily precipitation data were obtained from NCEP using the microclima function ‘dailyprecipNCEP’. Vegetation geometry parameters (plant-area index, vegetation

thickness, proportion of dead and live leaves, relative turbulence intensity) were derived based on habitat type (evergreen broadleaf forest) using the ‘habitatvars’ function in microclimc. The function outputs for canopy height were overwritten to include the recorded average tree height from each sampling location. The microclimate model was then run in steady-state mode using the function ‘runwithNMR’ to predict below canopy microclimate predictions at hourly time intervals for all sampling locations and heights.

4.3.4.3 Microclimate model validation

Model outputs were compared against logger data. Firstly, the ‘metrics’ R-package (Hamner and Frasco 2018) was used to calculate the root mean square error, RMSE, and mean absolute error, MAE, between model predictions and observed values of ambient air temperature, °C, for all data points pooled and at each individual location and height. RMSE and MAE were also calculated for each month of data collection for all individual locations and heights. The base R package ‘stats’ was then used to perform a Spearman’s rank correlation on predicted and observed values of ambient temperature at each location. RMSE, MAE and correlation coefficients were used to determine which model performs best at predicting hourly microclimate.

4.3.5 Effects of canopy structure on microclimate variation and microclimate model performance

Linear Mixed Models, LMMs (Harrison et al. 2018) were used to analyse the relationship between forest structure and observed monthly mean temperatures, observed daily maximum temperatures and model errors produced by NicheMapR. The models included plot-level canopy structure variables (number of trees with DBH >10cm per plot; mean DBH, cm; Lorey’s height, m; unweighted mean tree height, m; mean bole height, m; mean basal area, m²; mean crown depth, m; mean crown area, m²; and mean canopy connectivity, %) and logger height, m, as fixed effects; and month and sampling location as random intercepts. Vegetation variables were first checked for co-linearity using Pearson’s correlations. Variables which were significantly highly correlated ($r > 0.6$; $P < 0.05$) were not included in the LMM. The ‘dredge’ function from the MuMin R-package (Barton 2020) was used to determine which combination of fixed effects produced the best performing models based on their second order Akaike Information Criterion, AIC_c.

4.4 Results

4.4.1 Observed microclimate

Out of a total of 45 deployed data loggers at 15 locations, 3 were either lost or failed, resulting in no data. Of the remaining loggers, 18 failed partway through the sampling period due to either a hardware fault, low battery, or lightning strike, thereby only yielding data for a partial year; 23 loggers successfully recorded for a full year. Data loggers collected a total of 273,343 data points for temperature and light intensity at hourly intervals from October 2018 - October 2019, excluding points which were filtered out due to sunlight exposure. After filtering out values where the logger was exposed to direct sunlight, observed temperatures ranged from 17.47°C to 44.46°C, with a median of 25.02°C and a mean of 26.27°C (Figure 4.2 and Table 4.1). Observed temperatures were found to vary significantly between all 45 locations (KW $X^2 = 4758.7$, $df = 14$, $P < 0.01$; Figure 4.3a).

4.4.2 Microclimate modelling

Both microclimate model was run successfully for hourly intervals over 365 days at 45 points (3 heights across 15 locations) resulting in 394,200 data points for each model. NicheMapR Predictions of ambient temperatures ranged from 20.68°C to 33.50°C, with a median of 23.61°C and a mean of 25.28°C (Figure 4.2 and Table 4.1). Predicted temperatures varied significantly between sampling locations (KW $X^2 = 951.03$, $df = 14$, $P < 0.01$; Figure 4.3b). Microclimc predictions of ambient temperature was 24.92°C, with a median of 24.48°C and a range of 19.28 – 36.74°C (Figure 4.2 and Table 4.1). Predicted temperatures varied significantly between locations (KW $X^2 = 1742.7$, $df = 14$, $P < 0.01$; figure 4.3c). After accounting for points which were lost due to either failure, loss or sun exposure of the data logger, there were a total of 261,360 data points with both observed and predicted values for air temperature from both models.

Table 4.1: Summary of observed temperatures from data loggers and predicted ambient air temperatures for each location and height sampled at Sikundur.

| Location | Height, m | Dates when logger active | Temperature, °C | | | | | | | | | | | | | | |
|----------|-----------|--------------------------|-----------------|-------|-------|-------|------|-----------|-------|-------|-------|------|------------|-------|-------|-------|------|
| | | | Observed | | | | | NicheMapR | | | | | microclimc | | | | |
| | | | n | Mean | Max | Min | SD | n | Mean | Max | Min | SD | n | Mean | Max | Min | SD |
| 1 | 25 | 03/10/18 - 15/02/19 | 2656 | 25.47 | 40.07 | 20.14 | 3.30 | 8760 | 25.49 | 32.84 | 21.29 | 3.49 | 9432 | 25.12 | 35.63 | 20.33 | 1.88 |
| | 30 | 03/10/18 - 06/10/19 | 7881 | 26.16 | 39.96 | 17.48 | 3.68 | 8760 | 25.33 | 32.74 | 21.09 | 3.52 | 9432 | 25.17 | 36.12 | 20.38 | 1.92 |
| | 35 | 03/10/18 - 06/10/19 | 2760 | 25.53 | 39.50 | 17.67 | 3.20 | 8760 | 25.20 | 32.65 | 20.91 | 3.55 | 9432 | 25.21 | 36.45 | 20.42 | 1.94 |
| 2 | 18 | 01/10/18 - 06/10/19 | 8285 | 26.70 | 43.12 | 18.33 | 3.98 | 8760 | 25.47 | 32.71 | 21.34 | 3.43 | 9432 | 25.04 | 35.01 | 20.17 | 1.85 |
| | 23 | Failed/lost | * | * | * | * | * | 8760 | 25.25 | 32.58 | 21.05 | 3.48 | 9432 | 25.11 | 35.76 | 20.23 | 1.89 |
| | 28 | 01/10/18 - 06/10/19 | 8736 | 26.00 | 36.40 | 18.24 | 2.88 | 8760 | 25.07 | 32.47 | 20.82 | 3.52 | 9432 | 25.16 | 36.23 | 20.29 | 1.93 |
| 3 | 24 | 14/09/18 - 08/10/19 | 8786 | 26.41 | 43.72 | 18.24 | 3.69 | 8760 | 25.70 | 33.32 | 21.36 | 3.63 | 9432 | 25.11 | 35.56 | 20.33 | 1.88 |
| | 29 | 14/09/18 - 08/10/19 | 8528 | 26.62 | 41.23 | 18.43 | 3.90 | 8760 | 25.44 | 32.97 | 21.13 | 3.59 | 9432 | 25.16 | 36.07 | 20.38 | 1.91 |
| | 34 | 14/09/18 - 08/10/19 | 9197 | 26.96 | 38.16 | 19.47 | 3.72 | 8760 | 25.22 | 32.68 | 20.93 | 3.56 | 9432 | 25.20 | 36.42 | 20.43 | 1.94 |
| 4 | 22 | Failed/lost | * | * | * | * | * | 8760 | 25.66 | 33.25 | 21.33 | 3.62 | 9432 | 25.09 | 35.40 | 20.27 | 1.87 |
| | 27 | 02/10/18 - 07/10/19 | 8764 | 26.58 | 38.27 | 19.38 | 3.23 | 8760 | 25.37 | 32.87 | 21.08 | 3.57 | 9432 | 25.14 | 35.98 | 20.32 | 1.91 |
| | 32 | 10/02/18 - 07/10/19 | 5721 | 26.78 | 35.12 | 20.04 | 3.07 | 8760 | 25.13 | 32.56 | 20.87 | 3.54 | 9432 | 25.19 | 36.37 | 20.37 | 1.94 |
| 5 | 20 | 30/09/18 - 10/02/19 | 3186 | 25.26 | 31.98 | 20.52 | 2.31 | 8760 | 25.56 | 32.88 | 21.39 | 3.47 | 9432 | 25.06 | 35.22 | 20.22 | 1.86 |
| | 25 | 30/09/18 - 07/10/19 | 8852 | 26.14 | 36.40 | 18.43 | 2.92 | 8760 | 25.36 | 32.76 | 21.13 | 3.52 | 9432 | 25.13 | 35.88 | 20.27 | 1.90 |
| | 30 | 30/09/18 - 23/05/19 | 5604 | 26.01 | 35.86 | 18.43 | 2.92 | 8760 | 25.20 | 32.66 | 20.92 | 3.55 | 9432 | 25.18 | 36.30 | 20.33 | 1.94 |
| 6 | 24 | 14/09/18 - 06/10/19 | 9276 | 25.89 | 34.59 | 18.33 | 2.70 | 8760 | 25.66 | 33.27 | 21.33 | 3.62 | 9432 | 25.11 | 35.56 | 20.31 | 1.88 |
| | 29 | 14/09/18 - 06/10/19 | 9228 | 26.21 | 37.94 | 18.05 | 3.25 | 8760 | 25.40 | 32.92 | 21.10 | 3.58 | 9432 | 25.16 | 36.08 | 20.36 | 1.91 |
| | 34 | 14/09/18 - 06/10/19 | 9069 | 26.40 | 40.88 | 18.05 | 3.55 | 8760 | 25.18 | 32.63 | 20.90 | 3.55 | 9432 | 25.20 | 36.42 | 20.41 | 1.94 |
| 7 | 22 | 03/10/18 - 10/02/19 | 3021 | 26.03 | 36.19 | 20.71 | 3.23 | 8760 | 25.51 | 32.82 | 21.33 | 3.47 | 9432 | 25.09 | 35.40 | 20.27 | 1.87 |
| | 27 | 03/10/18 - 07/10/19 | 7885 | 26.32 | 44.09 | 19.00 | 3.53 | 8760 | 25.32 | 32.71 | 21.09 | 3.51 | 9432 | 25.14 | 35.98 | 20.32 | 1.91 |
| | 32 | 03/10/18 - 10/02/19 | 2436 | 25.30 | 36.51 | 20.90 | 2.65 | 8760 | 25.18 | 32.62 | 20.90 | 3.55 | 9432 | 25.19 | 36.37 | 20.37 | 1.94 |
| 8 | 25 | 30/09/18 - 07/10/19 | 8649 | 26.74 | 38.27 | 18.62 | 3.35 | 8760 | 25.42 | 32.73 | 21.24 | 3.47 | 9432 | 25.12 | 35.63 | 20.33 | 1.88 |
| | 30 | 30/09/18 - 07/10/19 | 3244 | 26.17 | 34.48 | 19.19 | 3.08 | 8760 | 25.26 | 32.64 | 21.04 | 3.50 | 9432 | 25.17 | 36.12 | 20.38 | 1.92 |
| | 35 | 30/09/18 - 07/10/19 | 7478 | 26.63 | 37.49 | 21.28 | 3.35 | 8760 | 25.13 | 32.55 | 20.86 | 3.53 | 9432 | 25.21 | 36.45 | 20.42 | 1.94 |
| 9 | 28 | 02/10/18 - 07/10/19 | 8857 | 25.27 | 35.44 | 18.14 | 2.16 | 8760 | 25.40 | 32.73 | 21.21 | 3.48 | 9432 | 25.15 | 35.81 | 20.39 | 1.89 |
| | 33 | 02/10/18 - 15/02/19 | 3233 | 25.32 | 36.95 | 18.24 | 2.44 | 8760 | 25.26 | 32.64 | 21.03 | 3.51 | 9432 | 25.19 | 36.23 | 20.43 | 1.92 |
| | 38 | 02/10/18 - 07/06/19 | 5799 | 26.02 | 39.05 | 18.05 | 3.20 | 8760 | 25.14 | 32.57 | 20.87 | 3.54 | 9432 | 25.23 | 36.52 | 20.48 | 1.95 |
| 10 | 23 | 01/10/18 - 06/10/19 | 8472 | 26.77 | 43.00 | 19.47 | 3.74 | 8760 | 25.36 | 32.62 | 21.21 | 3.44 | 9432 | 25.10 | 35.48 | 20.29 | 1.87 |
| | 28 | 01/10/18 - 30/07/19 | 6945 | 26.29 | 39.39 | 19.09 | 3.28 | 8760 | 25.18 | 32.51 | 20.98 | 3.48 | 9432 | 25.15 | 36.03 | 20.34 | 1.91 |
| | 33 | Failed/lost | * | * | * | * | * | 8760 | 25.04 | 32.42 | 20.80 | 3.51 | 9432 | 25.20 | 36.40 | 20.39 | 1.94 |
| 11 | 10 | 02/10/18 - 08/10/19 | 8833 | 25.90 | 35.22 | 18.24 | 2.61 | 8760 | 26.03 | 33.29 | 21.93 | 3.44 | 9432 | 24.88 | 34.24 | 20.00 | 1.77 |
| | 15 | 02/10/18 - 08/10/19 | 8686 | 26.55 | 38.27 | 17.95 | 3.57 | 8760 | 25.63 | 33.05 | 21.40 | 3.52 | 9432 | 25.00 | 35.85 | 20.09 | 1.85 |
| | 20 | 02/10/18 - 08/10/19 | 8053 | 26.78 | 42.64 | 17.86 | 4.26 | 8760 | 25.35 | 32.88 | 21.03 | 3.59 | 9432 | 25.09 | 36.74 | 20.17 | 1.91 |
| 12 | 15 | 01/10/18 - 06/10/19 | 8841 | 26.54 | 39.96 | 18.71 | 3.61 | 8760 | 25.60 | 32.83 | 21.48 | 3.43 | 9432 | 24.99 | 35.07 | 20.07 | 1.82 |
| | 20 | 01/10/18 - 06/07/19 | 4580 | 26.61 | 37.17 | 18.52 | 3.43 | 8760 | 25.33 | 32.67 | 21.13 | 3.49 | 9432 | 25.07 | 36.11 | 20.14 | 1.88 |
| | 25 | 01/10/18 - 06/10/19 | 8664 | 26.23 | 37.60 | 18.33 | 3.16 | 8760 | 25.12 | 32.55 | 20.86 | 3.53 | 9432 | 25.14 | 36.74 | 20.21 | 1.92 |
| 13 | 25 | 30/09/18 - 14/02/19 | 3283 | 25.35 | 33.12 | 18.33 | 2.39 | 8760 | 25.52 | 32.93 | 21.30 | 3.52 | 9432 | 25.12 | 35.63 | 20.33 | 1.88 |
| | 30 | 30/09/18 - 14/02/19 | 3236 | 25.71 | 34.16 | 18.33 | 2.80 | 8760 | 25.34 | 32.77 | 21.09 | 3.53 | 9432 | 25.17 | 36.12 | 20.38 | 1.92 |
| | 35 | 10/02/19 - 07/10/19 | 5734 | 26.49 | 34.59 | 18.52 | 3.00 | 8760 | 25.19 | 32.64 | 20.91 | 3.55 | 9432 | 25.21 | 36.45 | 20.42 | 1.94 |
| 14 | 24 | 14/09/18 - 12/02/19 | 3618 | 25.43 | 32.81 | 18.43 | 2.45 | 8760 | 25.65 | 33.06 | 21.42 | 3.52 | 9432 | 25.11 | 35.56 | 20.33 | 1.88 |
| | 29 | 14/09/18 - 12/02/19 | 3620 | 25.73 | 33.33 | 18.24 | 2.86 | 8760 | 25.48 | 32.96 | 21.21 | 3.56 | 9432 | 25.16 | 36.07 | 20.38 | 1.91 |
| | 34 | 14/09/18 - 12/02/19 | 3548 | 25.70 | 35.01 | 18.14 | 2.98 | 8760 | 25.34 | 32.87 | 21.02 | 3.59 | 9432 | 25.20 | 36.42 | 20.43 | 1.94 |
| 15 | 21 | 03/10/18 - 06/10/19 | 8636 | 26.51 | 37.06 | 18.14 | 3.53 | 8760 | 25.50 | 32.80 | 21.33 | 3.46 | 9432 | 25.08 | 35.32 | 20.24 | 1.86 |
| | 26 | 03/10/18 - 06/10/19 | 8465 | 26.63 | 37.06 | 18.43 | 3.63 | 8760 | 25.31 | 32.68 | 21.08 | 3.50 | 9432 | 25.14 | 35.93 | 20.29 | 1.90 |
| | 31 | 03/10/18 - 09/02/19 | 2998 | 26.27 | 36.30 | 20.42 | 3.48 | 8760 | 25.15 | 32.58 | 20.88 | 3.54 | 9432 | 25.18 | 36.34 | 20.35 | 1.94 |

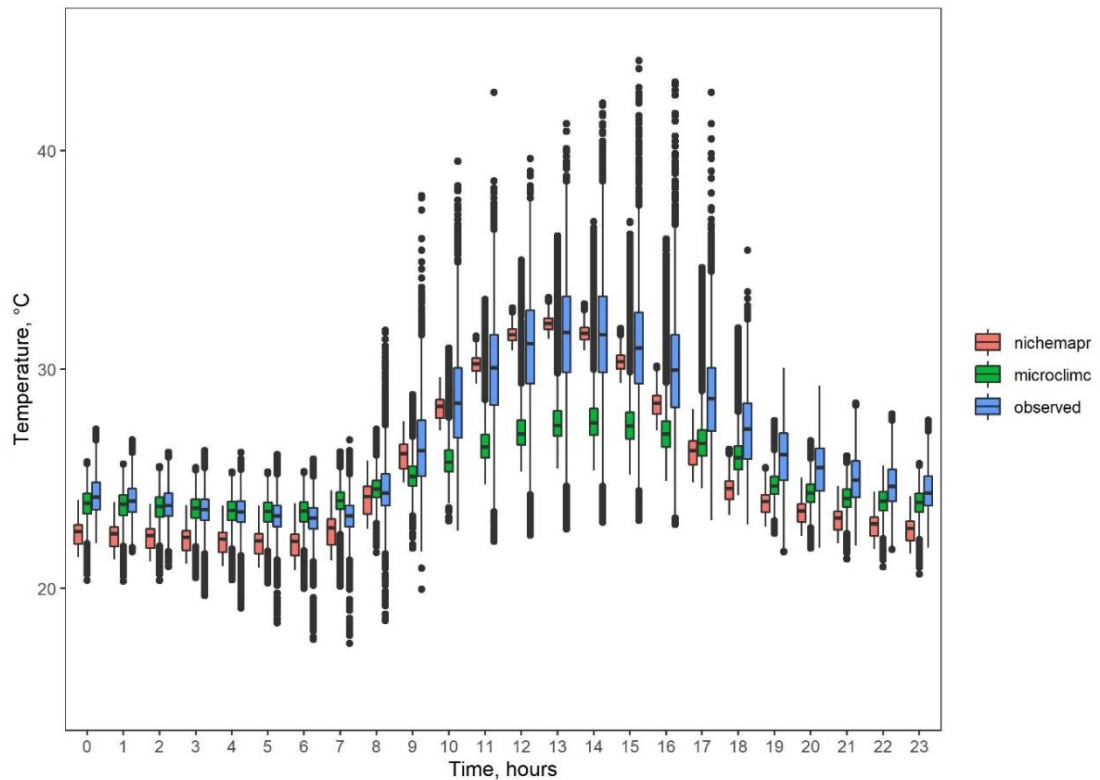


Figure 4.2: Hourly variation in ambient air temperatures, °C, observed from data loggers and predicted by NicheMapR and microclimc.

4.4.2.1 Model performance

There was a significant positive correlation between observed and predicted values for ambient temperature for both NicheMapR (Spearman's $Rho= 0.81$; $P<0.001$, $n = 267,466$; Figure 4.4a and b) and microclimc (Spearman's $Rho= 0.78$; $P<0.001$, $n = 267,466$; Figure 4.4c and d). Root mean square error, RMSE, and mean absolute error, MAE, were 2.25°C and 1.79°C , respectively for NicheMapR and 2.53°C and 1.79°C , respectively for microclimc. Predicted and observed temperatures at all individual locations and heights were significantly positively correlated ($P<0.01$) for both models, with correlation coefficients ranging from $0.69 - 0.86$ for NicheMapR, and $0.67-0.82$ for microclimc; RMSE and MAE were between $1.83^{\circ}\text{C} - 2.71^{\circ}\text{C}$ and $1.40^{\circ}\text{C} - 2.17^{\circ}\text{C}$ respectively for NicheMapR and $1.44 - 3.47^{\circ}\text{C}$ and $1.07 - 2.31^{\circ}\text{C}$ respectively for microclimc (see Table 4.2 for correlation coefficients, RMSE and MAE for both models at individual locations and heights).

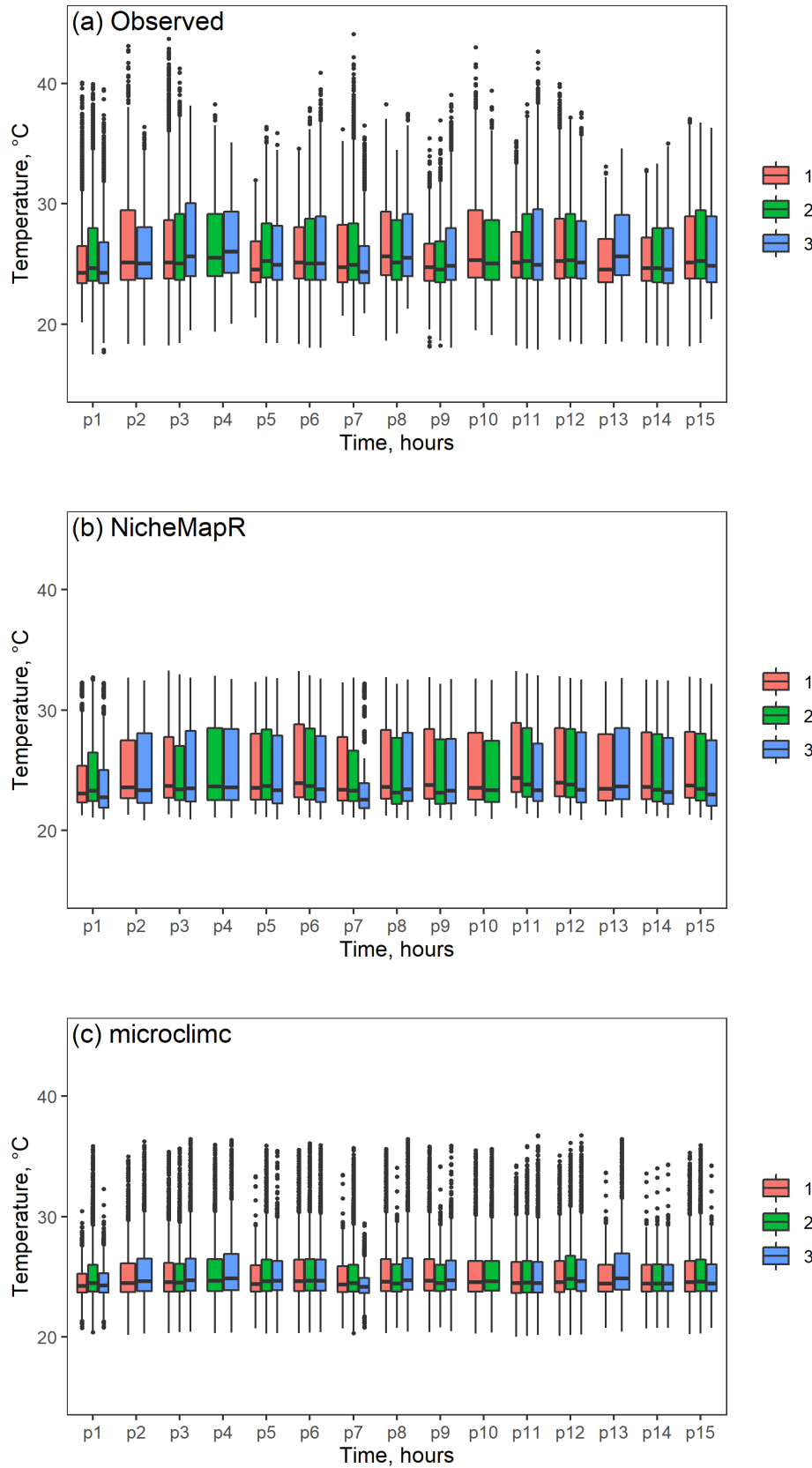


Figure 4.3: Range of temperatures for each location of a) observed values recorded from data loggers and b) values predicted by NicheMapR. Different heights are denoted by (1) bottom; (2) middle; and (3) top.

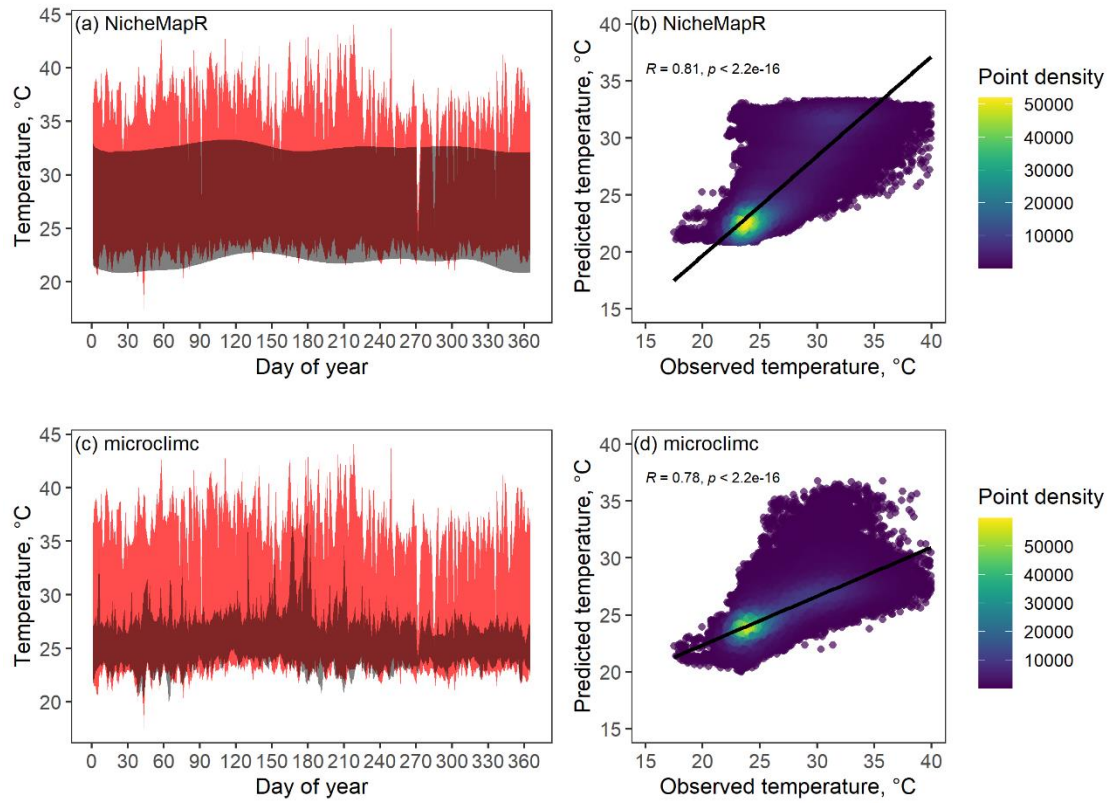


Figure 4.4: Observed and predicted values for ambient air temperature, °C, for all locations and heights at Sikundur (excluding points removed due to logger exposure to direct sunlight). (a) Observed (red) and NicheMapR predictions (black) of ambient temperature against day of year for the period October 2018 - October 2019; (b) Spearman's correlation of NicheMapR predictions against observed values for temperature; (c) Observed (red) and microclimc predictions (black) of ambient temperature against day of year for the period October 2018 - October 2019; and (d) Spearman's correlation of microclimc predictions against observed values for temperature.

Table 4.2: Spearman's correlation, root mean square error, RMSE, and mean absolute difference, MAD, between temperatures, °C, recorded from data loggers and temperatures, °C, predicted by NicheMapR at individual sampling locations and heights at Sikundur. *** $P < 0.001$ with Bonferroni adjustment.

| Location | Height, m | N | NicheMapR | | | microclimc | | |
|----------|-----------|------|----------------|------|------|----------------|------|------|
| | | | Spearman's rho | RMSE | MAE | Spearman's rho | RMSE | MAE |
| 1 | 25 | 2656 | 0.80*** | 2.00 | 1.55 | 0.79*** | 2.57 | 1.58 |
| | 30 | 7751 | 0.83*** | 2.16 | 1.72 | 0.79*** | 2.77 | 1.85 |
| | 35 | 2760 | 0.80*** | 2.31 | 1.91 | 0.78*** | 2.49 | 1.63 |
| 2 | 18 | 8156 | 0.83*** | 2.45 | 1.90 | 0.78*** | 3.30 | 2.30 |
| | 23 | * | - | - | - | - | - | - |
| | 28 | 8606 | 0.81*** | 2.15 | 1.77 | 0.79*** | 2.00 | 1.50 |
| 3 | 24 | 8274 | 0.82*** | 2.22 | 1.69 | 0.78*** | 2.93 | 2.02 |
| | 29 | 7987 | 0.83*** | 2.36 | 1.91 | 0.78*** | 3.18 | 2.22 |
| | 34 | 8656 | 0.83*** | 2.64 | 2.17 | 0.79*** | 3.08 | 2.28 |
| 4 | 22 | * | - | - | - | - | - | - |
| | 27 | 8607 | 0.81*** | 2.31 | 1.87 | 0.78*** | 2.54 | 1.93 |
| | 32 | 5561 | 0.78*** | 2.51 | 2.05 | 0.75*** | 2.48 | 1.95 |
| 5 | 20 | 3179 | 0.78*** | 2.05 | 1.59 | 0.80*** | 1.45 | 1.12 |
| | 25 | 8693 | 0.81*** | 2.10 | 1.69 | 0.79*** | 2.10 | 1.59 |
| | 30 | 5597 | 0.80*** | 2.20 | 1.78 | 0.80*** | 2.04 | 1.54 |
| 6 | 24 | 8756 | 0.80*** | 2.05 | 1.63 | 0.78*** | 1.87 | 1.45 |
| | 29 | 8709 | 0.82*** | 2.02 | 1.60 | 0.79*** | 2.35 | 1.75 |
| | 34 | 8549 | 0.83*** | 2.24 | 1.83 | 0.79*** | 2.70 | 1.94 |
| 7 | 22 | 3021 | 0.81*** | 2.05 | 1.62 | 0.80*** | 2.54 | 1.81 |
| | 27 | 7727 | 0.80*** | 2.46 | 1.95 | 0.75*** | 2.86 | 1.99 |
| | 32 | 2436 | 0.69*** | 2.57 | 2.15 | 0.67*** | 2.17 | 1.49 |
| 8 | 25 | 8487 | 0.81*** | 2.36 | 1.93 | 0.77*** | 2.74 | 2.06 |
| | 30 | 3237 | 0.80*** | 2.30 | 1.90 | 0.79*** | 2.42 | 1.79 |
| | 35 | 7316 | 0.80*** | 2.49 | 2.05 | 0.76*** | 2.62 | 1.96 |
| 9 | 28 | 8698 | 0.78*** | 2.19 | 1.77 | 0.77*** | 1.44 | 1.07 |
| | 33 | 3233 | 0.78*** | 2.13 | 1.74 | 0.8*** | 1.52 | 1.11 |
| | 38 | 5799 | 0.83*** | 2.20 | 1.76 | 0.81*** | 2.25 | 1.59 |
| 10 | 23 | 8348 | 0.82*** | 2.42 | 1.94 | 0.78*** | 3.08 | 2.21 |
| | 28 | 6945 | 0.81*** | 2.24 | 1.81 | 0.77*** | 2.49 | 1.83 |
| | 33 | * | - | - | - | - | - | - |
| 11 | 10 | 8651 | 0.83*** | 1.83 | 1.40 | 0.80*** | 1.90 | 1.41 |
| | 15 | 8502 | 0.86*** | 1.96 | 1.57 | 0.82*** | 2.84 | 1.99 |
| | 20 | 7890 | 0.85*** | 2.71 | 2.15 | 0.81*** | 3.47 | 2.31 |
| 12 | 15 | 8709 | 0.82*** | 2.19 | 1.69 | 0.79*** | 2.86 | 2.00 |
| | 20 | 4580 | 0.81*** | 2.19 | 1.71 | 0.78*** | 2.61 | 1.91 |
| | 25 | 8543 | 0.82*** | 2.17 | 1.77 | 0.79*** | 2.36 | 1.73 |
| 13 | 25 | 3276 | 0.79*** | 2.05 | 1.62 | 0.81*** | 1.49 | 1.15 |
| | 20 | 3229 | 0.81*** | 2.03 | 1.64 | 0.82*** | 1.94 | 1.42 |
| | 35 | 5575 | 0.80*** | 2.27 | 1.84 | 0.77*** | 2.23 | 1.73 |
| 14 | 24 | 3229 | 0.78*** | 2.05 | 1.61 | 0.80*** | 1.61 | 1.21 |
| | 29 | 3229 | 0.81*** | 1.99 | 1.56 | 0.81*** | 2.01 | 1.49 |
| | 34 | 3181 | 0.80*** | 2.07 | 1.64 | 0.81*** | 2.11 | 1.55 |
| 15 | 21 | 8505 | 0.84*** | 2.09 | 1.66 | 0.80*** | 2.73 | 1.94 |
| | 26 | 8332 | 0.84*** | 2.29 | 1.86 | 0.79*** | 2.83 | 2.05 |
| | 31 | 2998 | 0.82*** | 2.37 | 1.97 | 0.81*** | 2.77 | 1.94 |

4.4.3 Vegetation structure

A total of 223 trees were measured over the 15 plots. Total number of trees per plot ranged from 7 to 20. Tree height and bole height ranged from 5.9 – 56.7m and 0.5 – 44m, respectively. Crown depth ranged from 1 – 25.15m and crown area from 1.06 – 430.02m². DBH and basal area ranged from 10.19 – 220.59cm and 0.008 – 3.82m², respectively. Lorey's mean height of plots ranged from 18.44 – 47.75m. The summary variables used in the MEM for each location are shown in Table 4.3 and Figure 4.5. Overall, canopy height and DBH were generally low, with relatively few tall emergent trees. Total tree height, bole height and crown connectivity varied significantly between plots (Total height: Kruskal-Wallis $X^2 = 24.95$, $df = 14$, $P = 0.03$; Bole height, Kruskal-Wallis $X^2 = 25.14$, $df = 14$, $P = 0.03$; connectivity: Kruskal-Wallis $X^2 = 42.03$, $df = 14$, $P < 0.01$), while DBH, crown area and crown depth did not (DBH: Kruskal-Wallis $X^2 = 19.30$, $df = 14$, $P = 0.15$; crown area: Kruskal-Wallis $X^2 = 10.84$, $df = 14$, $P = 0.70$; crown depth: Kruskal-Wallis $X^2 = 18.56$, $df = 14$, $P = 0.18$).

4.4.4 Vegetation effects on observed microclimate and model performance

Lorey's mean height was found to be significantly correlated with unweighted mean height, maximum tree height, mean bole height, mean DBH, mean basal area and mean crown area ($r > 0.6$, $P < 0.05$). Therefore, only Lorey's mean height, number of trees, canopy connectivity and logger height were used as explanatory variables in the LMMs. After performing a dredge on the models, the only significant explanatory variable in all cases was logger height, which had a small, but statistically significant positive effect on recorded monthly mean temperature (estimate \pm SE: 0.01 ± 0.003 ; 95% CI: 0.01-0.02; $P < 0.01$; Table 4.4 and Figure 4.6), daily maximum temperature (estimate \pm SE: 0.06 ± 0.004 ; 95% CI: 0.06-0.07; $P < 0.01$; Table 4.5 and Figure 4.7), RMSE (estimate \pm SE; 0.02 ± 0.003 ; 95% CI; 0.01-0.02; $P < 0.01$, Table 4.6 and Figure 4.8), and MAE (estimate \pm SE: 0.02 ± 0.003 ; 95% CI: 0.02-0.03; $P < 0.01$; Table 4.7 and Figure 4.9).

Table 4.3: Summary of forest structure variables collected from vegetation plots at Sikundur.

| Location | Number of trees, n | Loreys mean height, m | Total height, m | | | | Bole height, m | | | | Diameter at breast height, cm | | | | Crown depth, m | | | | Crown area, m2 | | | | Crown connectivity, % | | | |
|----------|--------------------|-----------------------|-----------------|------|------|-------|----------------|------|-----|-------|-------------------------------|--------|-------|-------|----------------|-------|-----|------|----------------|--------|-------|--------|-----------------------|-----|-----|-------|
| | | | Mean | Max | Min | SD | Mean | Max | Min | SD | Mean | Max | Min | SD | Mean | Max | Min | SD | Mean | Max | Min | SD | Mean | Max | Min | SD |
| 1 | 18 | 36.30 | 16.98 | 42.9 | 9.3 | 8.19 | 10.41 | 20.6 | 6.1 | 3.92 | 30.66 | 168.7 | 10.19 | 35.58 | 6.57 | 22.3 | 1.2 | 5.35 | 50.9 | 430.02 | 1.29 | 95.42 | 40.56 | 80 | 5 | 22.94 |
| 2 | 17 | 21.70 | 18 | 31.9 | 9.9 | 6.95 | 11.13 | 24.2 | 1.6 | 5.85 | 32.52 | 57.93 | 11.46 | 14.83 | 6.87 | 21.2 | 2.2 | 5.25 | 33.63 | 113.47 | 7.88 | 27.27 | 36.47 | 70 | 10 | 18.09 |
| 3 | 6 | 38.08 | 21.85 | 42.1 | 14.7 | 10.39 | 10.9 | 22 | 6.5 | 5.58 | 40.11 | 121.28 | 16.55 | 40.25 | 10.95 | 20.1 | 5.1 | 5.49 | 62.29 | 178.37 | 22.16 | 58.98 | 19.17 | 30 | 0 | 10.21 |
| 4 | 19 | 34.64 | 22.43 | 42.4 | 12.8 | 9.14 | 13.68 | 22.9 | 7.4 | 4.64 | 27.41 | 80.53 | 11.78 | 20.93 | 8.75 | 22.2 | 2.6 | 5.57 | 35.02 | 101.44 | 6.97 | 28.45 | 50.53 | 80 | 20 | 18.4 |
| 5 | 17 | 23.30 | 19.25 | 35.1 | 5.9 | 7.93 | 9.57 | 18.9 | 0.5 | 4.54 | 26.64 | 51.88 | 10.5 | 13.81 | 9.68 | 22.7 | 1.7 | 6.03 | 36.9 | 86.24 | 4.14 | 25.84 | 49.12 | 85 | 5 | 22.1 |
| 6 | 13 | 24.14 | 17.92 | 41.9 | 7.2 | 8.59 | 9.62 | 19.2 | 5.5 | 4.31 | 22.23 | 47.75 | 10.82 | 13.05 | 8.29 | 22.7 | 1 | 5.37 | 28.29 | 76.18 | 5.06 | 22.52 | 58.46 | 95 | 5 | 21.35 |
| 7 | 15 | 29.61 | 21.54 | 39.9 | 9 | 7.76 | 12.49 | 20.8 | 5.9 | 4.29 | 28.2 | 77.35 | 11.46 | 17.59 | 9.05 | 19.1 | 2.1 | 4.55 | 30.44 | 103.18 | 9.05 | 26.4 | 34.67 | 70 | 5 | 19.5 |
| 8 | 14 | 30.44 | 20.82 | 43.1 | 8.7 | 9.03 | 12.84 | 27.8 | 4 | 6.68 | 27.22 | 73.21 | 10.5 | 19.69 | 7.99 | 15.3 | 3.9 | 3.49 | 39.68 | 132.54 | 14.93 | 36.88 | 47.86 | 100 | 0 | 27.01 |
| 9 | 16 | 47.75 | 24.22 | 56.7 | 14.5 | 12.2 | 16.38 | 44 | 3 | 10.36 | 46 | 220.59 | 10.5 | 63.03 | 7.84 | 25.15 | 1.7 | 5.82 | 65.98 | 419.8 | 7.26 | 114.93 | 30.31 | 60 | 5 | 15.76 |
| 10 | 13 | 30.84 | 22.65 | 37.4 | 12.1 | 7.11 | 14.15 | 23.2 | 5.5 | 4.48 | 25.44 | 75.12 | 10.82 | 18.33 | 8.49 | 18.2 | 3.6 | 3.85 | 41.84 | 163.04 | 5.7 | 44.04 | 27.31 | 50 | 10 | 13.79 |
| 11 | 14 | 18.43 | 15.86 | 24.3 | 7.8 | 5.12 | 8.36 | 15.4 | 0.9 | 4.53 | 27.24 | 66.53 | 11.46 | 16.7 | 7.49 | 13.8 | 2.5 | 4.2 | 36.08 | 163.76 | 7.98 | 40.59 | 37.5 | 60 | 15 | 14.77 |
| 12 | 12 | 31.42 | 20.73 | 41.6 | 11.8 | 8.74 | 12.74 | 24.6 | 2.1 | 6.15 | 44.7 | 117.46 | 17.83 | 35.81 | 7.98 | 17 | 2.2 | 4.22 | 52.24 | 168.28 | 8.2 | 50.12 | 52.92 | 95 | 15 | 23.4 |
| 13 | 18 | 26.51 | 19.92 | 38.5 | 12.2 | 6.75 | 12.04 | 18.8 | 4.5 | 4.73 | 28.45 | 88.49 | 11.46 | 23.15 | 7.87 | 19.9 | 1.5 | 4.53 | 37.09 | 165.78 | 1.06 | 39.84 | 43.06 | 80 | 15 | 19.03 |
| 14 | 12 | 32.05 | 26.03 | 38.3 | 11.9 | 7.29 | 14.13 | 19.8 | 7.8 | 4.89 | 41.14 | 120 | 17.19 | 28.59 | 11.89 | 20 | 1.7 | 5.81 | 62.36 | 278.16 | 5.9 | 73.26 | 49.58 | 75 | 25 | 14.69 |
| 15 | 19 | 31.50 | 20.48 | 39.8 | 8 | 9.33 | 13.71 | 29.3 | 3 | 7.99 | 43.63 | 157.56 | 11.78 | 41.41 | 6.77 | 12.5 | 3.4 | 2.64 | 54.67 | 209.72 | 2.14 | 61.16 | 39.74 | 70 | 0 | 20.91 |

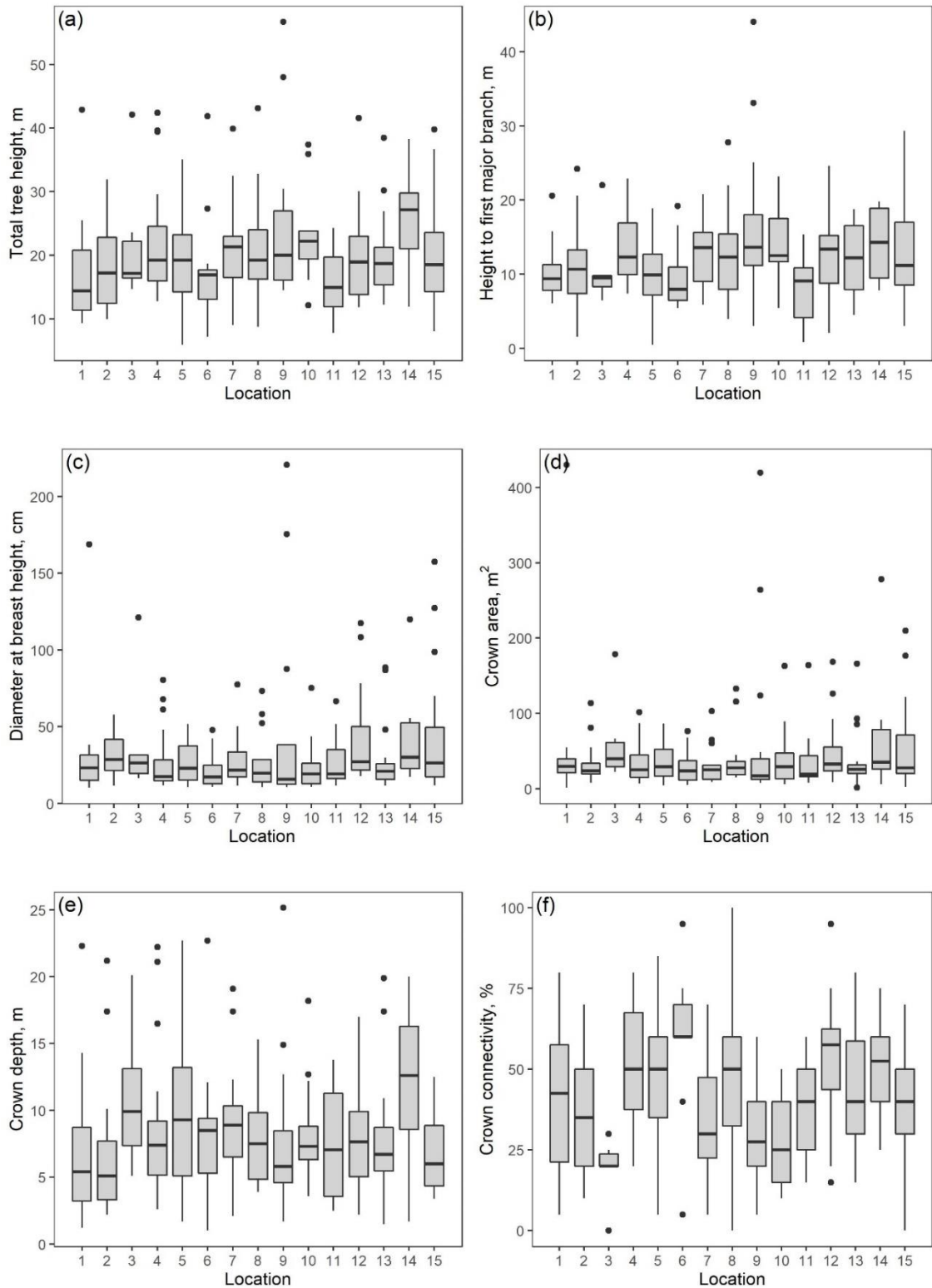


Figure 4.5: The range of values of forest structure variables collected from vegetation plots at Sikundur: (a) Total tree height, m; (b) bole height, m; (c) diameter at breast height, cm; (d) crown area, m²; (e) crown depth, m; and (f) crown connectivity, %.

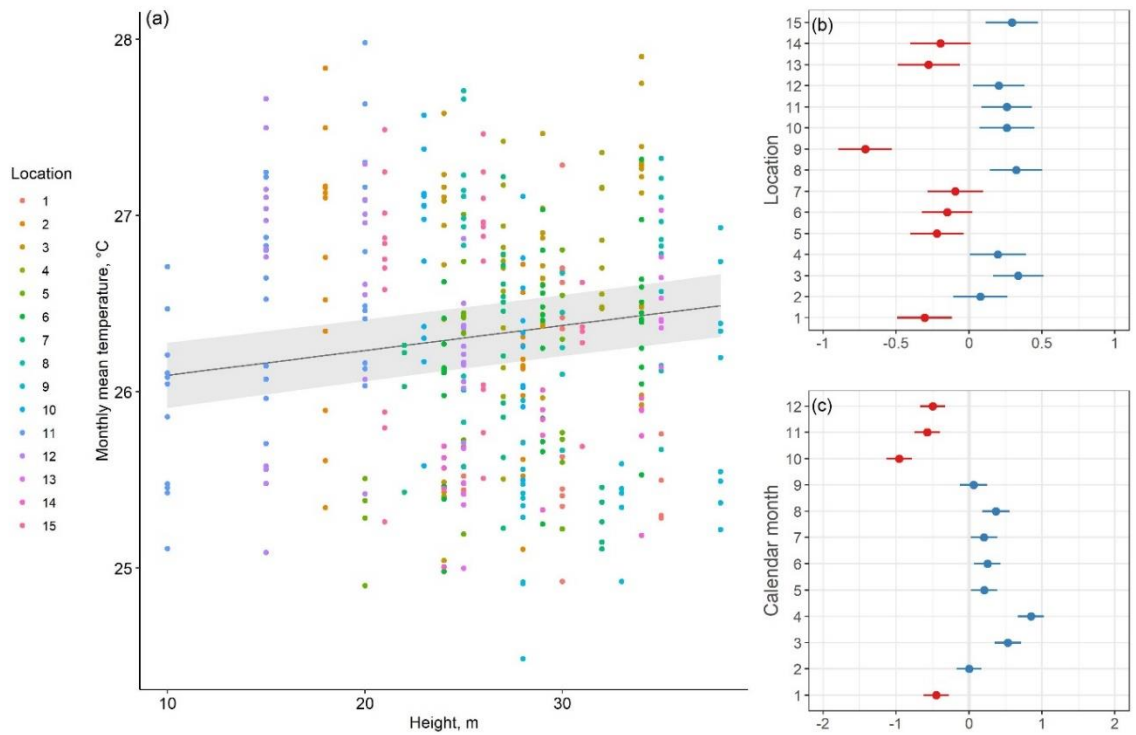


Figure 4.6: Linear mixed model predictions (line) with 95% confidence intervals (grey shading) and observed values (points) of monthly mean temperature against a) logger height, m; b) plot location; and c) calendar month on monthly mean temperatures recorded by data loggers at Sikundur.

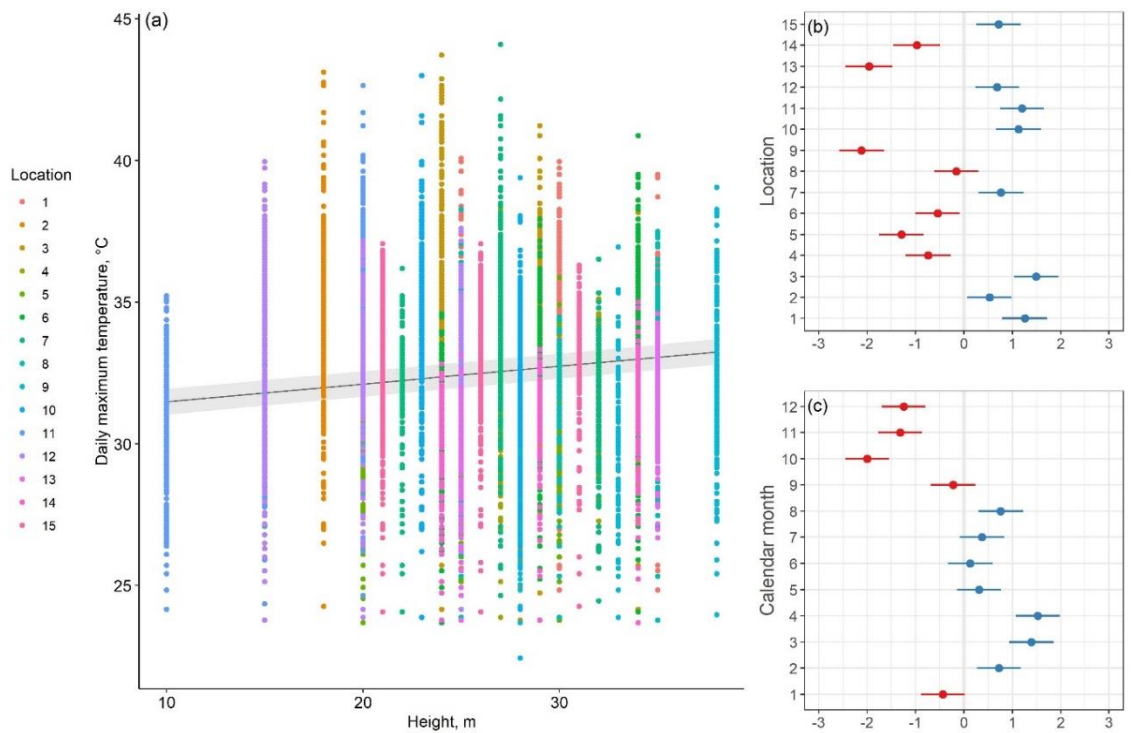


Figure 4.7: Linear mixed model predictions (line) with 95% confidence intervals (grey shading) and observed values (points) of daily maximum temperature against a) logger height, m; b) plot location; and c) calendar month on daily maximum temperatures recorded by data loggers at Sikundur.

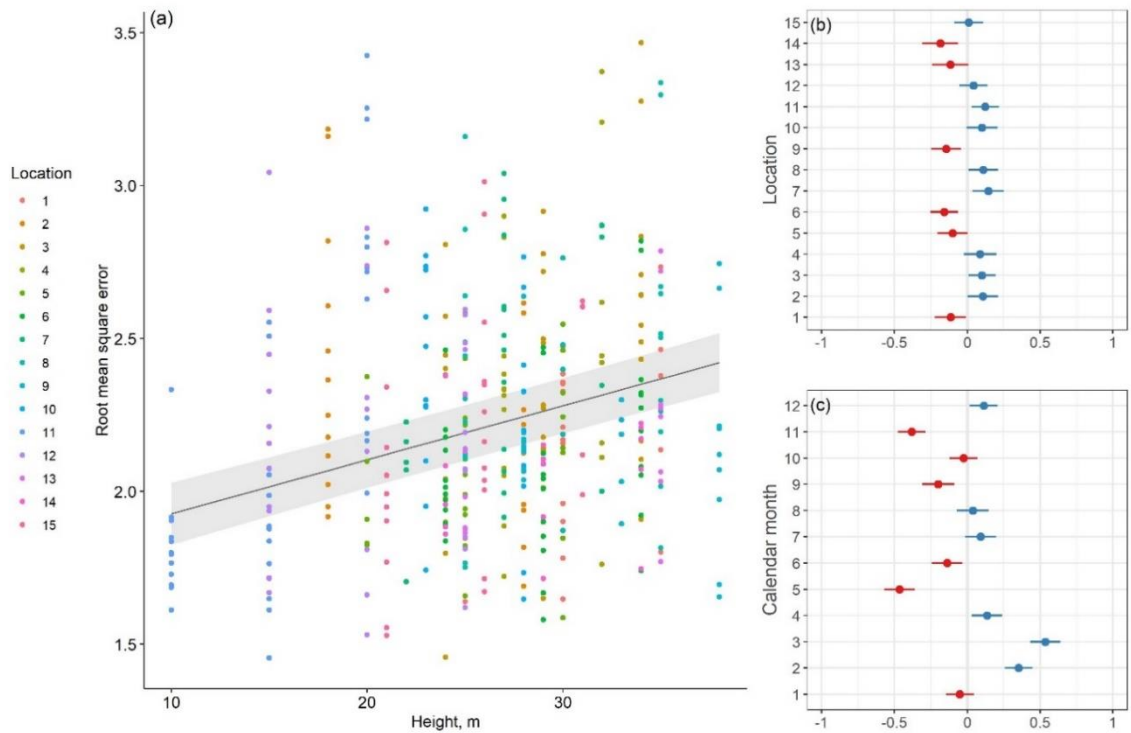


Figure 4.8: Linear mixed model predictions (line) with 95% confidence intervals (grey shading) and observed values (points) of root mean square error of NicheMapR temperature predictions against a) logger height, m; b) plot location; and c) calendar month on root mean square error of NicheMapR microclimate predictions at Sikundur.

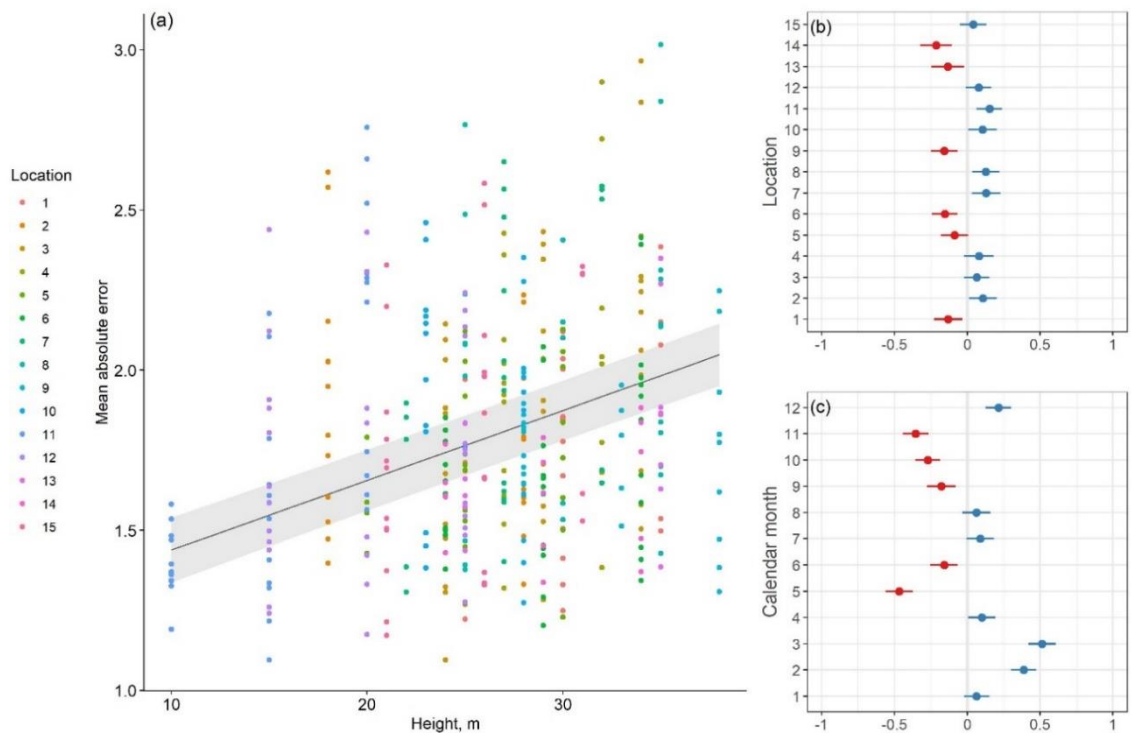


Figure 4.9: Linear mixed model predictions (line) with 95% confidence intervals (grey shading) and observed values (points) of mean absolute error of NicheMapR temperature predictions against a) logger height, m; b) plot location; and c) calendar month on mean absolute error of NicheMapR microclimate predictions at Sikundur.

Table 4.4: Results of the linear mixed model for effect of logger height (H) on monthly mean temperature recorded by data loggers at Sikundur, σ^2 denotes within group variance, while τ_{00} denotes between group variance of random effects.

| Monthly mean temperature | | | | |
|--|-----------|---------------|--------|---------|
| Predictors | Estimates | CI | t | p |
| (Intercept) | 25.95 | 25.56 – 26.35 | 128.11 | <0.001* |
| Height, m | 0.01 | 0.01 – 0.02 | 3.54 | <0.001* |
| Random Effects | | | | |
| σ^2 | 0.10 | | | |
| τ_{00} Location | 0.10 | | | |
| τ_{00} Month | 0.27 | | | |
| ICC | 0.79 | | | |
| N _{Location} | 15 | | | |
| N _{Month} | 12 | | | |
| Observations | 386 | | | |
| Marginal R ² / Conditional R ² | 0.016 / 0 | | | |

Table 4.5: Results of the linear mixed model for effect of logger height on daily maximum temperature recorded by data loggers at Sikundur, σ^2 denotes within group variance, while τ_{00} denotes between group variance of random effects.

| Daily maximum temperature | | | | |
|--|---------------|---------------|-------|---------|
| Predictors | Estimates | CI | t | p |
| (Intercept) | 30.87 | 29.97 – 31.76 | 67.67 | <0.001* |
| H | 0.06 | 0.06 – 0.07 | 16.85 | <0.001* |
| Random Effects | | | | |
| σ^2 | 2.47 | | | |
| τ_{00} date | 2.38 | | | |
| τ_{00} Location | 1.45 | | | |
| τ_{00} month | 1.14 | | | |
| ICC | 0.67 | | | |
| N _{Location} | 15 | | | |
| N _{month} | 12 | | | |
| N _{date} | 365 | | | |
| Observations | 11391 | | | |
| Marginal R ² / Conditional R ² | 0.020 / 0.674 | | | |

Table 4.6: Results of the linear mixed model for effect of logger height on root mean square error of microclimate predictions generated by NicheMapR for individual locations at Sikundur, σ^2 denotes within group variance, while τ_{00} denotes between group variance of random effects.

| Predictors | Root mean square error | | | |
|--|------------------------|-------------|-------|---------|
| | Estimates | CI | t | p |
| (Intercept) | 1.75 | 1.52 – 1.98 | 14.96 | <0.001* |
| Height, m | 0.02 | 0.01 – 0.02 | 6.27 | <0.001* |
| Random Effects | | | | |
| σ^2 | 0.06 | | | |
| τ_{00} Location | 0.02 | | | |
| τ_{00} Month | 0.08 | | | |
| ICC | 0.64 | | | |
| N _{Location} | 15 | | | |
| N _{Month} | 12 | | | |
| Observations | 386 | | | |
| Marginal R ² / Conditional R ² | 0.073 / 0.667 | | | |

Table 4.7: Results of the linear mixed model for effect of logger height on mean absolute error of microclimate predictions generated by NicheMapR for individual locations at Sikundur, σ^2 denotes within group variance, while τ_{00} denotes between group variance of random effects.

| Predictors | Mean absolute error | | | |
|--|---------------------|-------------|-------|---------|
| | Estimates | CI | t | p |
| (Intercept) | 1.22 | 1.00 – 1.44 | 10.89 | <0.001* |
| Height, m | 0.02 | 0.02 – 0.03 | 9.34 | <0.001* |
| Random Effects | | | | |
| σ^2 | 0.04 | | | |
| τ_{00} Location | 0.02 | | | |
| τ_{00} Month | 0.09 | | | |
| ICC | 0.75 | | | |
| N _{Location} | 15 | | | |
| N _{Month} | 12 | | | |
| Observations | 386 | | | |
| Marginal R ² / Conditional R ² | 0.115 / 0.776 | | | |

4.5 Discussion

The aim of this study was to determine the applicability of a mechanistic approach to predicting microclimate in heterogenous secondary tropical lowland forest and to compare two available modelling approaches, NicheMapR and microclimc. Both microclimate models generally performed well, producing relatively small RMSEs and MAEs (less than 3°C) across both the whole site and at individual sampling locations. This is despite the significant variation noted in some attributes of canopy structure and observed climate conditions between locations (Mean tree height ranged from 15.86 – 26.03m; Lorey's mean height ranged from 18.44 – 47.75m; mean bole height ranged from 8.36 – 16.38m; crown connectivity ranged from 19.17-58.46%; mean temperature ranged from 25.26-26.96°C; and maximum temperature ranged from 31.98-44.09°C). These results demonstrate that these mechanistic models can be applied in secondary tropical forest and provide reliable estimates of below canopy climate conditions. Global datasets of macroclimate and topography are now freely available for most terrestrial locations, and the microclimate models performed well using only those inputs, with limited data collected directly from the field.

4.5.1 Vegetation structure & microclimate conditions

Forest structure recorded at Sikundur is characterised by low canopy height, DBH and connectivity between crowns. There are very few large, emergent trees. This is consistent with results reported previously from Sikundur, and other areas of secondary tropical forest (e.g., Priatna et al. 2000; Hankinson et al. 2021). The vegetation structure is also different compared to that recorded in primary forests in Indonesia/Asia (e.g., Manduelli et al. 2012). Total tree height, bole height and crown connectivity were significantly different between plots, highlighting that there are considerable fine-scale variations in forest structure throughout the site. There are also significant fine-scale variations in temperature, which would not be accounted for in global climate datasets with coarser resolutions. Despite the extensive historical disturbance in the area, there are still a variety of microhabitats available for species to utilise, and the area is therefore an important haven for biodiversity.

Daily and monthly average temperatures throughout the site do not go above what would be considered a maximum threshold for most species, however, there are times (usually between 12:00 and 15:00pm) when daily maximums do reach extremes which

would be likely to result in physiological stress. This highlights the importance of considering both spatial and temporal variations at finer scales. Ignoring this could result in an under-estimation of species extinction risks by overlooking the effects of extreme temperature highs during the afternoon, such as those observed in this study. Repeated and prolonged exposure to sub-optimal high temperatures are likely to have a detrimental impact on endotherms, due to cumulative physiological stress and elevated metabolic costs of maintaining their body temperature during these periods (Rezende et al. 2014). Additionally, animals may be unable to carry out behaviours such as socialisation and foraging during times of extreme high temperatures, thereby affecting their activity budgets and potentially lowering fitness (Kearney 2013). Climatic conditions during the hottest parts of the day and year are likely to be a much stronger driver of species extinction risks from climate change than macroclimate averages (Rezende et al. 2014).

It is generally assumed that the buffering effect on microclimates will be lessened in secondary versus primary forests, however there is little empirical evidence to confirm this (Ewers and Banks-Leite 2013; Hardwick et al. 2015). Recent work has suggested that secondary forest microclimates are still cooler than macroclimate, and still offer valuable microclimate refuges for species (Blonder et al. 2018; Senior et al. 2018). The results here also suggest that temperatures in Sikundur are buffered compared with macroclimate temperatures. Canopy structure variables did not significantly affect temperatures, although there were no data from non-forested areas to compare against in this study, and so the effect of vegetation may not be apparent. There was a significant effect of height in the canopy on temperature, with cooler temperatures lower in the canopy. In particular, daily maximum temperatures were lower closer to the ground, and further from the top of the canopy. This effect was captured by both modelling approaches. This would suggest that fine-scale variations in vegetation structure do not significantly alter the microclimate processes under forest canopies. Arboreal species could minimise their thermoregulatory costs and risks of overheating by utilising the lower canopy during the hottest parts of the day, when temperatures in the higher strata may be sub-optimal.

4.5.2 Microclimate model performance

Both models performed generally well, producing errors which are comparable with other studies (e.g., Fitzpatrick et al. 2019; Bentley et al. 2020; Kearney 2020), however NicheMapR produced lower error values and predicted maximum temperatures better

compared with microclimc. The microclimc model is still under development and requires further testing and calibrating for tropical and secondary forest types. The current habitat classes included in the 'habitatvars' function are fairly broad, and there are limited data available for detailed forest structure in tropical forests, particularly secondary forests. Canopy height and connectivity recorded at Sikundur are lower than what is generally reported for primary forests in Sumatra (Knop 2004; Manduell et al. 2012), it is also likely that vegetation thickness and leaf area index differ, although there is not currently data available for this. Further work to obtain more detailed habitat structure variables, such as vegetation thickness profiles and leaf area index, for secondary forests would likely improve the model performance.

Both models tend to underestimate maximum temperatures, although NicheMapR generally performed better than microclimc at predicting midday temperatures. It is important to note that recorded temperatures could still be elevated due to the greenhouse effect of the logger housing, although steps have been taken to reduce the effects of this. It is, however, more likely that both models are not able to properly account for vertical gradients in forest canopies and perform less well higher up in the canopy. This is confirmed by the LMM results, which show that logger height has a significant effect on model errors, with increasing height leading to increasing error, although the observed effect is small. Very little is known about vertical microclimate variation in forest canopies, especially disturbed canopies (Marsh 2019). The lower canopy height and connectivity at the site most likely contributes to more pronounced gradients in temperature increase compared with less disturbed forest types. The majority of ecological studies which investigate microclimate or utilise microclimate models have focussed on ground-dwelling species (e.g., lizards: Kearney and Porter 2004; Strangas et al. 2019; insects: Gillingham et al. 2012; small mammals: Mathewson et al. 2017). There are far fewer studies which fully investigate vertical temperature variation in forests. Future work should focus on improving the available empirical data on the nature of vertical gradients in forest temperature and incorporating these into microclimate models to better predict conditions higher up in forest canopies. Studies which use these modelling approaches should focus on acquiring more detailed input data than what is currently available from global databases for their specific habitat type, especially those being conducted in secondary forests. This will be invaluable to microclimate studies for arboreal species, for whom vertical climate variations are the most relevant.

In general, the range of temperatures predicted by NicheMapR for mid-afternoon (i.e., the hottest parts of the day) were much closer to the observed temperatures than microclimate. In the tropics, it is maximum temperatures, rather than mean or minimum temperatures, which are most significant in limiting species fitness and survival. The predictions produced by NicheMapR are therefore more likely to produce realistic results about climate effects on animals. Other work has already shown that using the NicheMapR microclimate model to predict species responses highlights that climate change will negatively impact species through increased physiological stress and water loss during times of higher temperatures (Kearney et al. 2013). Utilising the NicheMapR microclimate model in combination with other mechanistic models of species responses to climate change will provide more insight into the potential impacts of climate change for organisms in secondary forests, and the capacity of these organisms to adapt, beyond simply looking at species range dynamics.

The results from this study demonstrate that mechanistic microclimate models can be applied in tropical secondary forest and produce predictions of forest microclimate conditions with high spatial and temporal resolutions with a reasonable accuracy. The increased availability of global high-resolution datasets of topography and elevation mean that these models are a promising tool which can be applied across wide areas at very low cost. With further development, and a focus on gathering data for a range of different forest types, mechanistic models have the potential to accurately compute high resolution microclimate datasets, even in locations where direct measurements from the field are limited. Accurate predictions and mapping of microclimate variation in forests are vital steps in understanding the underlying mechanisms behind species responses and vulnerability to climate change. Incorporating fine-scale microclimate variations into studies of species responses will improve the reliability of predictions of exposure and vulnerability to climate change, produce better predictions of species future ranges, and identify microclimate refuges which should be prioritised for protection.

Chapter 5

A biophysical modelling approach to investigating edge effects on arboreal mammals: a case study of the Sumatran orangutan, *Pongo abelii*

Abstract

Models of species-environment relationships can provide a useful empirical basis for conservation, but they must include information on the local-scale processes which drive population changes to provide meaningful information to conservation planners. Correlative modelling approaches, which are most commonly used, work well for species with large geographic ranges and comprehensive distribution data, however, they have more uncertainty for species which are rare, have limited ranges or do not have widespread population data. They also provide limited insight into the underlying mechanisms behind population declines and local scale threats. Biophysical models use a theoretical approach to determine an individual organism's response to climatic variations; this can then be scaled up to predict population level changes. Although they require more detailed inputs on species physiology than correlative approaches, they can be utilised with estimates derived from captive individuals, similar species, or expert opinions. This chapter uses a freely available biophysical model, the NicheMapR endotherm model, to predict orangutan energetics and water loss at a forest edge and 2km into the forest in North Sumatra, Indonesia. The NicheMapR model has been used for a number of small ground-dwelling terrestrial ectotherms, but applications in larger bodied terrestrial mammals are limited to a handful of species, and only two primates (sportive lemurs and vervet monkeys), both of which occur mainly in open, dry forests or savannah. This is the first use of this model for an ape species in disturbed tropical rainforest. The results suggest that orang-utans will begin to experience thermal stress at temperatures above 32°C and are already exposed to these temperatures at frequent intervals, although only for short periods of time. These potentially stressful periods occur more frequently at the forest boundary compared to the interior. This mechanism would be missed by models which only use macroclimate averages of temperature, potentially resulting in under-estimations of extinction risk from climate change. Metabolic rates and water loss were also higher at the edge, and these differences were more pronounced for an adult

male, which has a larger mass and higher basal metabolic rate than females and juveniles. These results suggest that the availability of cooler refuges during hotter parts of the day, and the ability to replenish lost water from canopy reservoirs or fruit will be important in facilitating orang-utan survival in fragmented forest following climate change. The study also showed that the relatively low basal metabolic rates typical of great apes, are helping orangutans survive in the canopies under these warm conditions.

5.1 Introduction

Research into species-environment relationships is needed to inform predictive models of species responses to change, which can provide conservation planners with empirical evidence to support decision making when prioritising species, locations and habitats for protection and restoration. Correlative species distribution models (SDMs) are most frequently used to predict species responses; however, they do not incorporate physiological mechanisms and fine-scale interactions which drive species-environment relationships (chapter 2). While they perform well for species with large geographic ranges and comprehensive distribution data, they are harder to apply for species with very small ranges or with limited data, as is often the case with rare or endangered species (Stalenberg 2019). Individual populations are influenced by their own unique combination of biotic and abiotic factors (e.g., species traits, climate, topography, competition, human activities; Bogoni et al. 2020) and there is no one-size-fits-all management solution which will be applicable to all species and/or populations. Therefore, SDMs are not always able to provide conservation planners with relevant information to manage the wider range of processes and threats for their site at the right scale. Instead, more informative models would be those that study species-environment relationships from the bottom up because changes at the population level are driven by behaviour and physical characteristics of the individuals that make up the population (Foden et al. 2018). Research into responses to climate change should therefore focus on more than simply projecting species potential geographical ranges, and instead work to identify the underlying mechanisms behind species responses and vulnerability to climate change (Serra-Diaz and Franklin 2019).

Our current understanding of mammal vulnerability to climate change is hindered by a lack of knowledge on the underlying mechanisms of mammal biogeography and demographics. Mammal-climate relationships remain poorly understood, with only a small proportion of current literature explicitly investigating mammal-climate interactions (Paniw et al. 2021). There is increasing recognition of the complexity of species-climate relationships and the limitations of simplistic correlative approaches to projecting responses to climate change (Norberg et al. 2019). A meta-analysis of climate change literature by Paniw et al. (2021) found that only 106 studies, covering 87 mammal species, have investigated responses of more than one demographic indicator (e.g., survival, growth, or reproduction) to climate; of these, very few were conducted in

biodiverse regions or on species which are currently considered to be vulnerable to climate change. Most study species included in this meta-analysis are not considered climate sensitive based on IUCN classifications, however many of the studies it was based on still reported negative impacts, such as population declines or lowered reproductive rates. This highlights an inadequacy in the way in which species vulnerability is currently assessed (Foden et al. 2019). Species' persistence is determined by multiple demographic variables, biotic and abiotic factors, which often interact with each other and may not respond to climate change in a uniform way (Pacifci et al. 2015). Future climate change research needs to incorporate a mechanistic understanding of how climate affects survival, development, and reproduction, in order to provide more reliable projections of species responses and a strong evidence base for long term conservation planning.

Staying cool and hydrated is the main challenge posed by climate change for tropical animals (Kearney, Shine & Porter 2009). Thermoregulation is critical for animals to survive when ambient temperatures are outside their thermal neutral zone, however, there is an upper limit to what they can tolerate, and regulatory strategies can be costly. In the tropics, species' thermal tolerances are expected to be lower, and many species are already living closer to their maximum temperature limit (Carvalho et al. 2019). Prolonged exposure to extreme high temperatures will result in increased heat stress and water loss, and reduced fitness from climate change for many organisms (Kearney et al. 2013). Animals can regulate their body temperature through evaporative cooling by wetting surfaces (e.g., licking, sweating, or panting), which leads to water loss; they can also alter their posture or lose heat through radiative transfer through contact with cooler surfaces (e.g., tree-hugging by koalas, Briscoe et al. 2014). Heterothermy (i.e., allowing core body temperature to increase or decrease in order to reduce metabolic costs) is another potential strategy which is understudied in large-bodied mammals which do not hibernate or go into torpor (Mitchell et al. 2002). Primates may also alter their social behaviour to aid in thermoregulation; for example, baboons are less selective about which partners they huddle with in colder conditions (MacLarnon et al., 2014). Finally, animals can avoid extremes by sheltering in cooler microhabitats. To date, there is little information on the energetic costs of thermoregulation for free-living mammals. Although thermoregulatory strategies will play a key role in mammal responses to climate change, the lack of ecophysiological data for most species means that thermoregulation is not accounted for in most models of species' responses to climate change.

Biophysical models use a theoretical approach to determine species' ecophysiology and can therefore be used to fill in the gaps when modelling species' responses to environmental change at smaller scales when field data are limited (Kearney, Porter & Murphy 2016). These models have been successfully applied for many terrestrial ectotherms, mostly lizards (e.g., Kearney et al. 2018; Malishev et al. 2018), as well as turtles (e.g., Cavallo et al. 2015; Mitchell et al. 2016), and amphibians (e.g., Kearney et al. 2008; Enriquez-Urzelai et al. 2019; Fitzpatrick et al. 2019). Implementations of biophysical models for terrestrial endotherms are fewer. Examples include the Australian night parrot (Kearney et al. 2010; 2016; Mathewson and Porter 2013; Mathewson et al. 2020), Australian marsupials (Kearney et al. 2010; Mathewson and Porter 2013; Stalenberg 2019), polar bears (Mathewson and Porter 2013), and primates (Stalenberg 2019; Mathewson et al. 2020). These models can be adapted to incorporate behavioural and physiological responses to climatic variations to predict the potential metabolic costs of climate change and thermoregulation at the individual level. These predictions can then be scaled up to determine climate change impacts on fitness and survival at population and species levels without the need for detailed and extensive distribution data (Mathewson et al. 2017). Although they have not yet been applied to apes, they have been tested and shown to work well for other wild primates, including sportive lemurs (Stalenberg 2019) and vervet monkeys (Mathewson et al. 2020).

Primates are particularly vulnerable to climate change and understanding their potential responses is now a major priority for ecologists and conservationists (Korstjens and Hillyer 2016; Carvalho et al. 2019; Bernard and Marshall 2020). Over two thirds of primate species are threatened with extinction (i.e., Vulnerable, Endangered or Critically Endangered) according to their IUCN status (Estrada et al. 2017). A large proportion of these are threatened even before incorporating climate change by threats such as habitat loss, fragmentation, and hunting (Estrada et al. 2017). These species are then particularly vulnerable to climate change due to small population sizes, low densities, limited geographic ranges, slow life histories and relatively high dependence on forest cover, which is dwindling fast (Bernard and Marshall 2020). Additionally, primate exposure to climate change is high compared to other taxa. Mean temperature increases in primate ranges are estimated to be 10% greater than the global average (Graham et al. 2016), while maximum temperatures are predicted to increase by as much as 7°C (Carvalho et al. 2019). Their location in the warm tropics means that primates already exist closer to their maximum tolerance thresholds than temperate species, and these increases are very

likely to push them beyond their physiological limits (Khaliq et al. 2014). Therefore, although many primates have relatively high plasticity in their behaviour and ecology, are able to exploit a wide range of food sources, and their phenology is rarely strongly linked to seasonal climatic changes, physiological stress may still limit their ability to persist in situ. To improve our ability to predict primate responses to climate change, it is thus essential to incorporate physiological constraints to studying their flexibility to adapt to changes.

Another limitation in predicting responses to change is the limited data available on microclimate variation within tropical forests, which approximately 90% of primate species are dependent on (IUCN 2008). The importance of microclimate to terrestrial mammals has been relatively overlooked; however, it is likely to play a key role in their responses to climate change. Primates within tropical forests experience high levels of climatic variations which are influenced by vegetation type and cover, presence and size of canopy gaps, forest edges, and distance from the ground (Vanwalleghem and Meentemeyer 2009; Marsh 2019). Dense forest canopies have lower radiation penetration and are sheltered from wind, air currents and precipitation, while gaps and forest edges have increased radiation penetration and are more exposed to wind and rain (Heithecker and Halpern 2007; Brammer et al. 2020). This means that dense, continuous forest canopies experience fewer temperature extremes or changes than more open forests, such as those found near the edges of forest patches (de Frenne et al. 2019). As habitat degradation and modification increases in forest environments, the physical landscape of forest canopies will be altered, and as such this will cause changes in microclimate variation. Fine-scale climate variations in forests are not captured by the macro-climate data typically used to predict species distributions, and this can result in inaccurate predictions. Incorporating microclimate and fine scale climate data is therefore necessary to accurately predict species responses to future climate change scenarios. It is also necessary to include the non-climate related impacts of anthropogenic land use, and habitat degradation/fragmentation, as this too will determine if a species can survive in a location.

The Sumatran orangutan, *Pongo abelii*, is a Critically Endangered arboreal great ape, which is endemic to Sumatra and found predominantly in tropical lowland dipterocarp forest. The most recent published population estimate is ~13,500 individuals in the wild in Sumatra (Wich et al. 2016). Deforestation and fragmentation are the biggest threats to orangutan populations, although human-wildlife conflict and the illegal wildlife trade

have also contributed to declines (Wich 2009; Singleton et al. 2017). Unlike other great apes, orangutans are mainly solitary, apart from females with infants, although larger parties do occur for short time periods (Wich et al. 2006; Roth et al. 2020). Orangutans have a lower metabolic rate compared to other mammals of their size and primates in general (Pontzer et al. 2010); this is possibly an adaptation to unpredictable food availability and relatively large size for a purely arboreal species. Despite being a relatively well-studied species, which receives a great deal of conservation attention, relatively little is known about orangutan biogeography beyond simple correlations between their current ranges, landscape data, and macroclimate data (e.g., Marshall et al. 2006; Husson et al. 2008; Carne et al. 2012; Gregory et al. 2012). No studies to date have utilised microclimate data or adopted a mechanistic approach to determine how climate change and human disturbance will impact orangutans.

5.2 Aim & objectives

This chapter will determine how distance to forest edge influences the energetic costs and water loss of thermoregulation in Sumatran orang-utans in secondary tropical forest at Sikundur in Sumatra, Indonesia. Understanding the impact of forest fragmentation and edge effects is important as the percentage of edge forest increases, potentially reducing availability of microclimate refuges, which are essential for animals to persist *in situ* within tropical forests following climate change.

1. Determine the relationship between ambient air temperature and body temperature, metabolic rate and water loss for juvenile, adult female, and adult male orangutans under typical conditions for Sikundur, based on an endotherm model.
2. Predict orangutan metabolic rate and water loss based on microclimate conditions for specific locations at Sikundur, using the NicheMapR endotherm model.
3. Determine the impact of edge-related microclimate variations on orangutan metabolism and water balance by comparing model outputs of metabolic rates and water loss between the forest edge and interior for each of the age-sex categories.

5.3 Methods

The study was conducted in the Sikundur region of North Sumatra, Indonesia, within the Gunung Leuser National Park (see chapter 1 for a full description of the site). Eight of the 20 sampling points used in chapter 3 were chosen: four at the boundary between the forest and adjacent smallholder orange farms, and four in the forest interior, 2km from the edge (locations are shown in figure 3.1 in chapter 3). For all of these points, ground measurements (~1.5m) of temperature, °C, and light intensity, lux, are available at hourly intervals for the period Aug – Oct 2019 using HOBO pendant data loggers, as well as data on canopy structure, including tree height, bole height, tree density and canopy connectivity from vegetation plots (see chapter 3 for full data collection methods). All data analyses were conducted using R version 4.0.0 (R Core Team 2020).

5.3.1 The endotherm model

The endotherm model is included as part of the ‘NicheMapR’ R-package (Kearney 2020). A full description of the endotherm model and its subroutines is provided by Kearney and Porter (n.d.; under review).

The model was used to simulate metabolic rate, body temperature and water loss for a typical adult male, adult female, and juvenile orangutan.

5.3.1.1 Input parameters

Orangutans were modelled as an ellipsoid, with parameter values for body mass, hair density, hair diameter, fur thickness, fur reflectivity, oxygen extraction efficiency and basal metabolic rates being defined for an adult male, adult female, and juvenile (~4 years old). Inputs were taken from published literature (Table 1). Where data for Sumatran orangutans were not available, parameters were either taken for phylogenetically similar species or estimated based on expert opinion.

Two measures of BMR were used (Table 5.1), the first was estimated based on the mouse-elephant curve using the equation (Smil 2004):

$$BMR (watts) = 3.4 \times M^{0.75}$$

Secondly, values for BMR were taken from observed resting metabolic rates (kcal/day) of captive orangutans reported by Pontzer et al. (2010).

Table 5.1: Input parameters and their sources used for the NicheMapR endotherm model for adult male, adult female and juvenile orangutans.

| Variable | Explanation | Adult male | Adult Female | Juvenile | References |
|---------------------|--|------------|--------------|----------|---|
| AMASS | Body mass (kg) | 116.00 | 55.00 | 25.50 | Pontzer et al 2010 |
| DHAIR | hair diameter (m) | 1.50E-04 | 1.50E-04 | 1.50E-04 | Chernova 2014 |
| LHAIRV | Hair length, ventral (m) | 0.05 | 0.05 | 0.05 | Amaral 2008, Schultz 1931 |
| LHAIRD | Hair length, dorsal (m) | 0.15 | 0.10 | 0.05 | Amaral 2008, Schultz 1931 |
| RHOD | Hair density, dorsal (hairs/m ²) | 1.76E+06 | 1.76E+06 | 1.76E+06 | Sandel 2013 |
| RHOV | Hair density, ventral (hairs/m ²) | 9.00E+05 | 9.00E+05 | 9.00E+05 | Schultz 1931 |
| REFL | Fur reflectivity (%) | 0.20 | 0.20 | 0.20 | Average for mammals: from Stalenberg 2019 |
| QBASAL ₁ | Basal heat generation (W) - observed | 77.39 | 63.77 | 49.96 | Pontzer et al 2010 |
| QBASAL ₂ | Basal heat generation (W) – estimated based on body mass from mouse-elephant curve | 120.18 | 68.67 | 38.58 | Smil 2004 |

5.3.1.2 Relationship between air temperature and metabolism

Simulations were run for a series of ambient temperatures from 0-50°C in 1° steps, with a wind speed of 1 m/s and a relative humidity of 90% (to reflect typical conditions at the site, based on an average of microclimate predictions generated by NicheMapR, since no other data were available). The upper critical temperature, UCT, was determined by the point at which the model can no longer find a solution (i.e., it is no longer possible for the animal to maintain their body temperature based on the current parameters).

5.3.1.3 Modelling energetics for specific locations

Hourly climate conditions at each location were modelled over 365 days for the year 2019 using the NicheMapR microclimate model. Full descriptions of the microclimate model and its required inputs are provided in chapter 4. The NicheMapR model generates hourly predictions at user-defined heights of air temperature, relative humidity, wind speed and solar radiation based on site-specific variables. Information on local topography and vegetation can either be user-defined, or, where data are not available, derived from remotely sensed global data, such as SRTM. Unlike in chapter 4, UAV data were not available for these locations, therefore inputs for canopy height and shading were estimated from plot measurements on the ground (taken in chapter 3), and values for elevation, slope and aspect were extracted from SRTM 1 Arc-second global digital elevation (NASA 2002) using ArcGIS Pro version 2.8.0 (ESRI 2010). The microclimate model was first validated at the eight locations by comparing temperatures predicted by NicheMapR, with a defined height of 1.5m, against observed temperatures from the data loggers for a two-month period from August – October 2019. A Spearman's rank correlation, the root mean square error, RMSE, and mean absolute error, MAE, for both the whole data set pooled and each individual location were used to evaluate the model performance. RMSE and MAE were calculated in R using the package 'metrics' (Hamner and Frasco 2018).

Following validation, the microclimate model was then used to generate hourly climate predictions for the estimated mid-point of the canopy (determined as the mid-point between the average bole height and average tree height in metres measured within the vegetation plots) for each of the eight locations. The number of days in which air temperature exceeded the UCT identified by the endotherm model and the total proportion of time when temperatures were above the UCT were calculated for each point

to enable comparisons of potential heat stress between edge and interior locations. Microclimate model outputs for wind speed, m/s, relative humidity, %, air temperature, °C (at mid canopy height), soil temperature, °C, and solar radiation, W/m², were extracted and used as climate inputs for the endotherm model for each age-sex class of orangutan.

A linear regression was used to determine and compare the relationship between predicted air temperature, °C, and predicted water loss, g/h, for each age-sex class. All modelled microclimate variables were found to be significantly correlated with each other ($R > 0.8$, $P < 0.01$), therefore only temperature was used in the regression analyses. The analyses were run using the base-R 'lm' function.

5.4 Results

5.4.1.1 Air temperature effects on body temperature, metabolism, and water loss

When BMR is estimated based on the mouse-elephant curve, the model is unable to find a solution (i.e., it is not possible for an animal to maintain their body temperature) at air temperatures at mid-canopy height of 12°C and above for an adult male, 30°C and above for an adult female, and 34°C and above for a juvenile (Figure 5.1). Male and female body temperature reaches the maximum allowed value (38°C) at modelled air temperatures of 1-2°C, while juvenile body temperature starts to increase at 16°C and reaches the maximum allowed temperature by 19°C. Water loss rates for males are already increasing rapidly at 0°C, while females start to lose water at faster rates at 4°C, and juveniles begin to rapidly lose water at 19°C. Metabolic rates remain constant with increasing air temperatures until the point where the model fails.

When using observed BMR, the model is no longer able to find a solution at air temperatures of 32°C and above for all age/sex classes (Figure 5.2). Body temperature starts to increase at 7°C for adult females, and reaches maximum allowed temperature at 9°C, while core temperature in adult males and juveniles begins to increase at 9°C, reaching maximum allowed temperature at 12°C. Metabolic rate remains relatively constant until the point where the model fails. Water loss rates start to increase rapidly for adult females roughly 2°C before adult males and juveniles (10°C for females, compared to 12°C for males and juveniles).

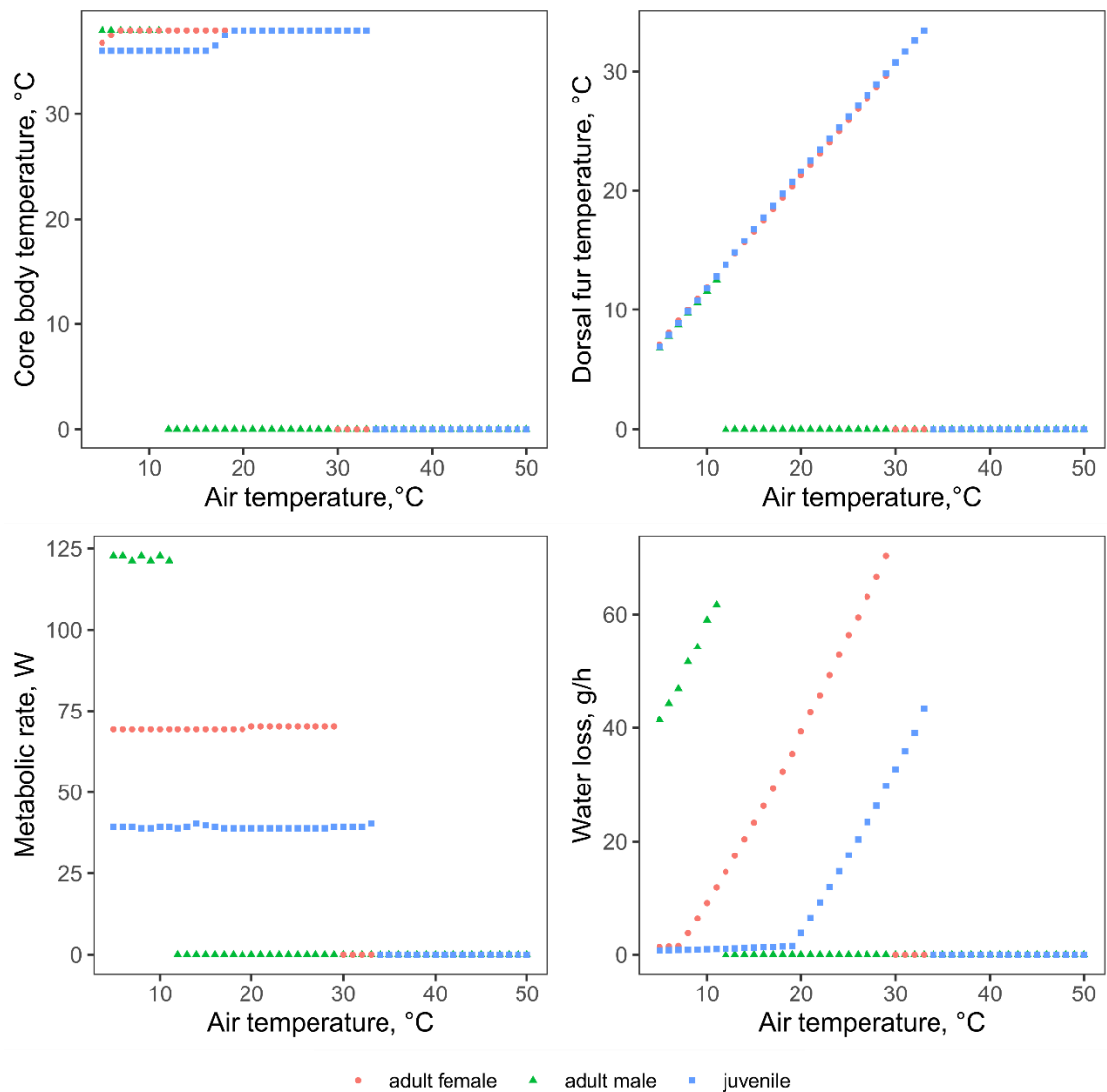


Figure 5.1: NicheMapR endotherm model predictions of core body temperature, dorsal fur temperature, metabolic rate, and water loss across a series of ambient temperatures for adult male, adult female, and juvenile orangutans when using estimates of basal metabolic rate based on the mouse-elephant curve of body mass against BMR. Zero values were produced when the endotherm model was unable to find a solution (i.e., it was not possible for the modelled organism to maintain their body temperature within the defined parameters for metabolic rate, panting and sweating).

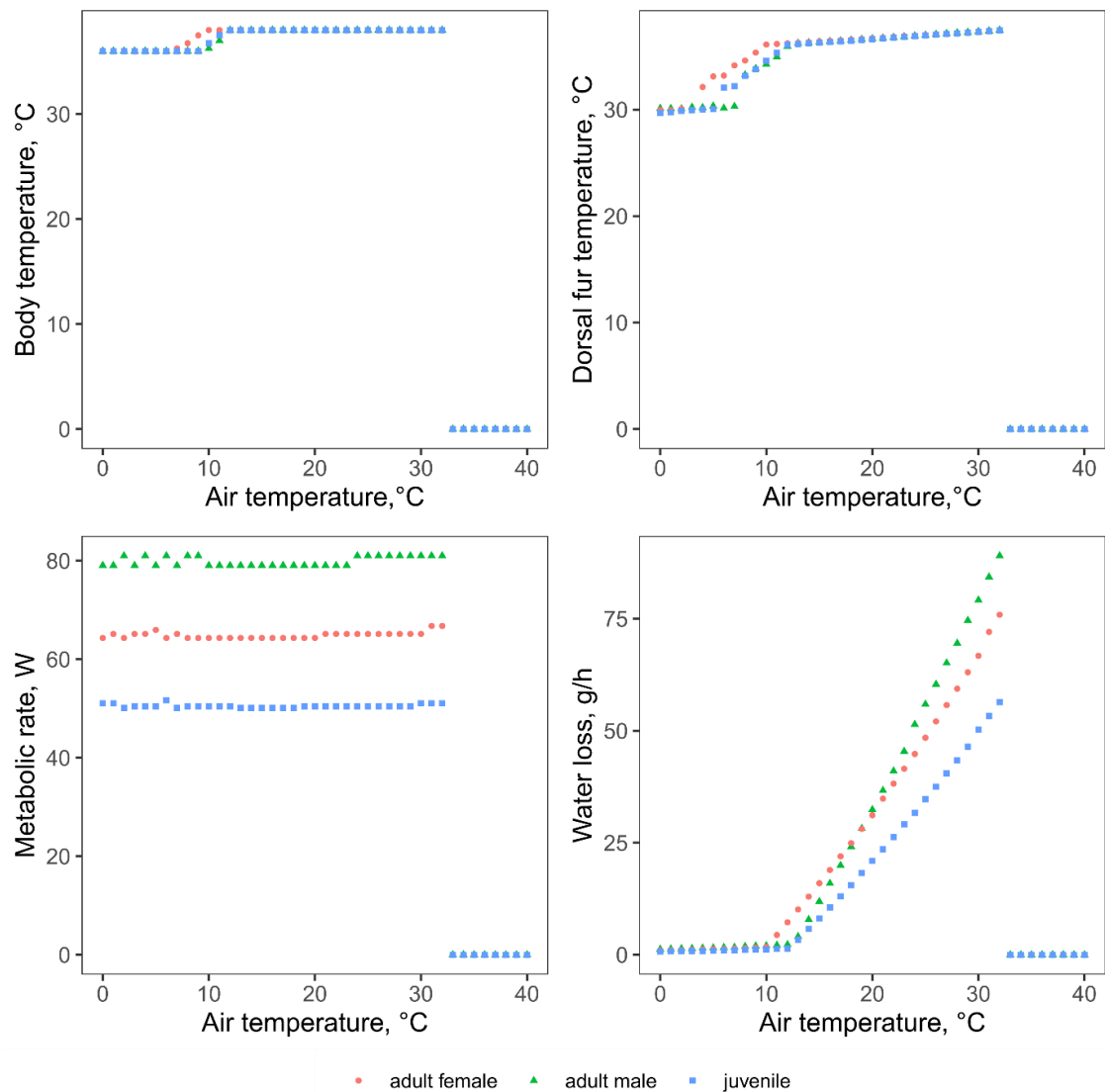


Figure 5.2: NicheMapR endotherm model predictions of core body temperature, dorsal fur temperature, metabolic rate, and water loss across a series of ambient temperatures for adult male, adult female, and juvenile orangutans when using observed basal metabolic rates from Pontzer et al (2010). Zero values were produced when the endotherm model was unable to find a solution (i.e., it was not possible for the modelled organism to maintain their body temperature within the defined parameters for metabolic rate, panting and sweating).

5.4.1.2 Microclimate predictions

Predicted temperatures at plot locations ranged between 20.84°C and 32.97°C. The mean predicted temperature during the study period across the whole site was 25.27°C. Mean predicted temperatures across the time period at individual locations ranged from 25.10°C to 25.41°C (Figure 5.3a). Maximum predicted temperatures at individual locations ranged between 32.51°C and 32.97°C, while minimum temperatures ranged from 20.84°C to 21.07°C. Observed temperatures ranged between 21.09°C and 37.50°C. The mean observed temperature across the whole site during the study period was

25.54°C. Mean observed temperatures across the study period at individual locations ranged from 24.97°C to 26.73°C (Figure 5.3a). Maximum observed temperatures at individual locations ranged between 29.35°C and 37.50°C, while minimum temperatures ranged from 21.09°C to 21.86°C. A full summary of observed and predicted temperatures is given in Table 5.2.

The microclimate model performed well in predicting temperatures at ~1.5m above the ground, with the root mean square error and mean absolute error for the whole dataset (n=8261) of 2.16°C and 1.74°C, respectively. Observed and predicted temperatures were significantly correlated with each other ($\rho = 0.82$; $P < 0.001$; Figure 5.3b). RMSE and MAE at individual locations ranged from 1.75 – 2.28°C and 1.41-1.87°C, respectively. Observed and predicted temperatures were significantly correlated at all locations (ρ : 0.78 – 0.88; $P < 0.001$). A summary of model errors and Spearman's correlation between observed and predicted values is given in Table 5.2.

Predicted temperatures at 1.5m exceeded the upper critical threshold of 32°C on more days per year and for higher proportions of time at edge locations compared with interior locations (Figure 5.4a & b). Temperatures exceeded 32°C on an average of 325.5 days and 0.07% of the time for edge locations, and an average of 224 days per year and for 0.04% of the time for interior locations.

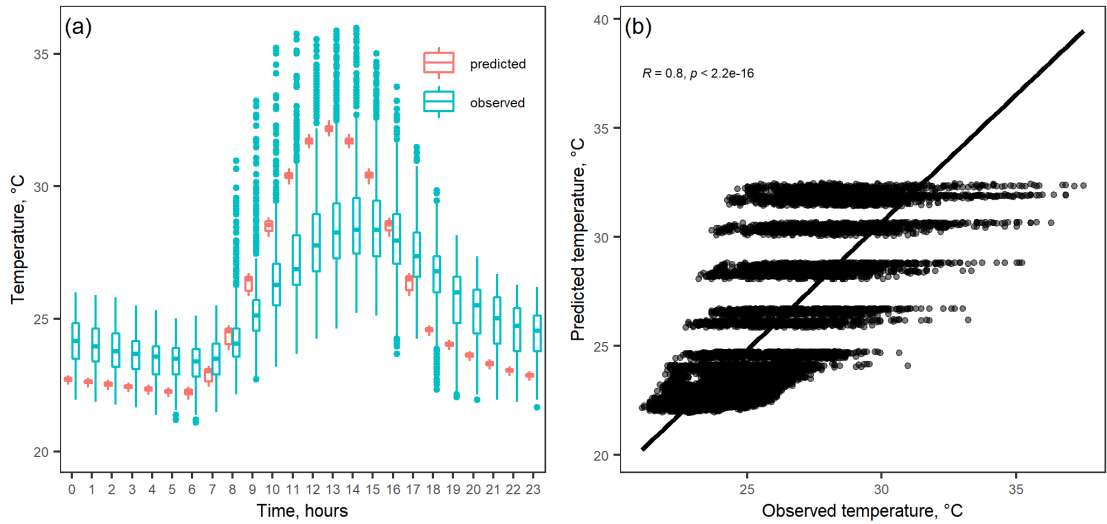


Figure 5.3: Air temperatures, °C, predicted by NicheMapR and recorded from data loggers at 1.5m from the ground for the time period August – October 2019: (a) The range of predicted and observed temperatures for each hour of the day; and (b) predicted temperatures against observed temperatures.

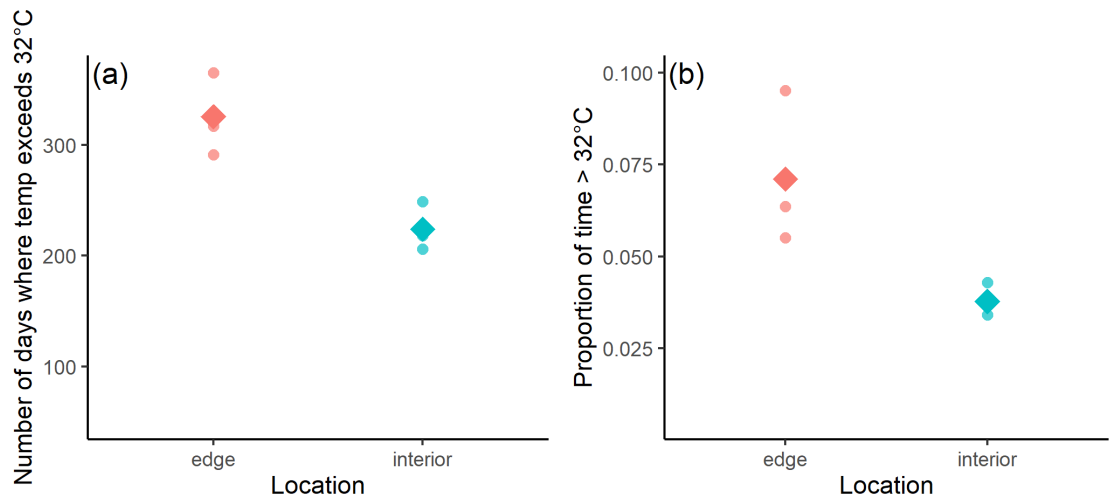


Figure 5.4: (a) The number of days per year where maximum temperature predicted by NicheMapR exceeds the upper critical temperature, UCT of 32°C at 4 locations at the edge and the interior; and (b) the proportion of total time where temperatures predicted by NicheMapR exceed the UCT at 4 edge and 4 interior locations. Circles represent actual values, while diamonds represent the group means.

Table 5.2: Summary of temperatures recorded by data loggers, temperatures predicted by NicheMapR, and model performance at individual locations at Sikundur.

| Location | Forest type | Observed temperatures, °C | | | | | Predicted temperatures, °C | | | | | MSE |
|----------|-------------|---------------------------|-------|------|-------|-------|----------------------------|-------|------|-------|-------|-----|
| | | n | mean | SD | max | min | n | mean | SD | max | min | |
| 1.1 | edge | 994 | 37.49 | 3.73 | 21.38 | 26.73 | 8760 | 32.97 | 3.60 | 21.07 | 25.41 | 9 |
| 1.5 | interior | 1058 | 31.78 | 2.19 | 21.86 | 25.58 | 8760 | 32.51 | 3.53 | 20.84 | 25.10 | 1 |
| 2.1 | edge | 894 | 35.54 | 3.07 | 21.09 | 25.71 | 8760 | 32.91 | 3.60 | 21.05 | 25.37 | 8 |
| 2.5 | interior | 1058 | 31.17 | 2.13 | 21.57 | 25.56 | 8760 | 32.63 | 3.55 | 20.90 | 25.18 | 1 |
| 3.1 | edge | 1040 | 33.85 | 2.78 | 21.38 | 26.08 | 8760 | 32.87 | 3.59 | 21.02 | 25.34 | 1 |
| 3.5 | interior | 1082 | 31.06 | 1.92 | 21.66 | 25.39 | 8760 | 32.66 | 3.55 | 20.92 | 25.20 | 1 |
| 4.1 | edge | 1077 | 32.09 | 2.20 | 21.76 | 25.73 | 8760 | 32.82 | 3.58 | 21.00 | 25.31 | 1 |
| 4.5 | interior | 1058 | 32.19 | 2.02 | 21.38 | 25.41 | 8760 | 32.68 | 3.56 | 20.93 | 25.21 | 1 |

5.4.1.3 Modelled energetics at Sikundur

When using an estimated input value for basal metabolic rate based on the mouse-elephant curve, the overall mean predicted metabolic rate was 145.05W for adult males, 82.38W for adult females and 45.77W for juveniles (Figure 5.5a). Core body temperature was 38°C for all three classes. Adult males had the highest water loss rates (ranging from 136.04 – 199.26g/h, with a mean of 156.60g/h), while juveniles had the lowest (ranging from 18.41 – 57.43g/h, with a mean of 30.35g/h). Female water loss rates ranged between 61.54 – 110.05g/h, with a mean of 77.22g/h (Figure 5.6a). Estimated dorsal fur temperatures ranged from 20.35 – 33.18°C, with mean of 25.06°C for males; 20.85 – 33.29°C, with mean of 25.33°C for females; and 21.59 – 33.42°C, with mean of 25.69°C for juveniles (Figure 5.7a).

NicheMapR predictions of metabolic rate and water loss rate were lower when using input BMR values taken from Pontzer et al. (2010) for males and females, although they were higher for juveniles (Figure 5.5 & Figure 5.6). The overall mean predicted BMR was 93.81W for adult males, 76.59W for adult females and 59.25W for juveniles (Figure 5.5b). Core temperature was 38°C (the maximum allowed value) for all three classes. Adult males had the highest water loss rates (ranging from 59.16 – 120.42g/h, with a mean of 79.04g/h), while juveniles had the lowest (ranging from 38.23 – 78.36g/h, with a mean of 50.59g/h; Figure 5.6b). Female water loss rates ranged between 52.82 – 101.09g/h, with a mean of 68.44g/h. Predicted fur temperature ranged from 20.42 – 33.18°C, with a mean of 25.08°C for males; 20.86 – 33.29°C, with mean of 25.33°C for females; and 21.55 – 33.42°C with a mean of 25.69°C for juveniles (Figure 7b).

Estimated metabolic rates are at their highest around midday (between 10am and 2pm) and are similar between edge and interior locations for adults, while juveniles have a higher estimated metabolic rate in the afternoon at edge locations (Table 5.3 & Figure 5.5). Mean estimated water loss rates and dorsal fur temperatures were higher at edge locations than interior locations with both BMR inputs for all age/sex classes (see Table 5.3 & Figure 5.56 - Figure 5.7). The model predicts a higher rate of increase in water loss with increasing temperature for males compared with females and juveniles (Figure 5.8). For every 1°C increase in air temperature, estimated water loss increases by 4.74g/h for males, 3.70g/h for females, and 2.94g/h for juveniles. Summaries of the endotherm model outputs at individual locations for each age/sex class are given in Table 5.3.

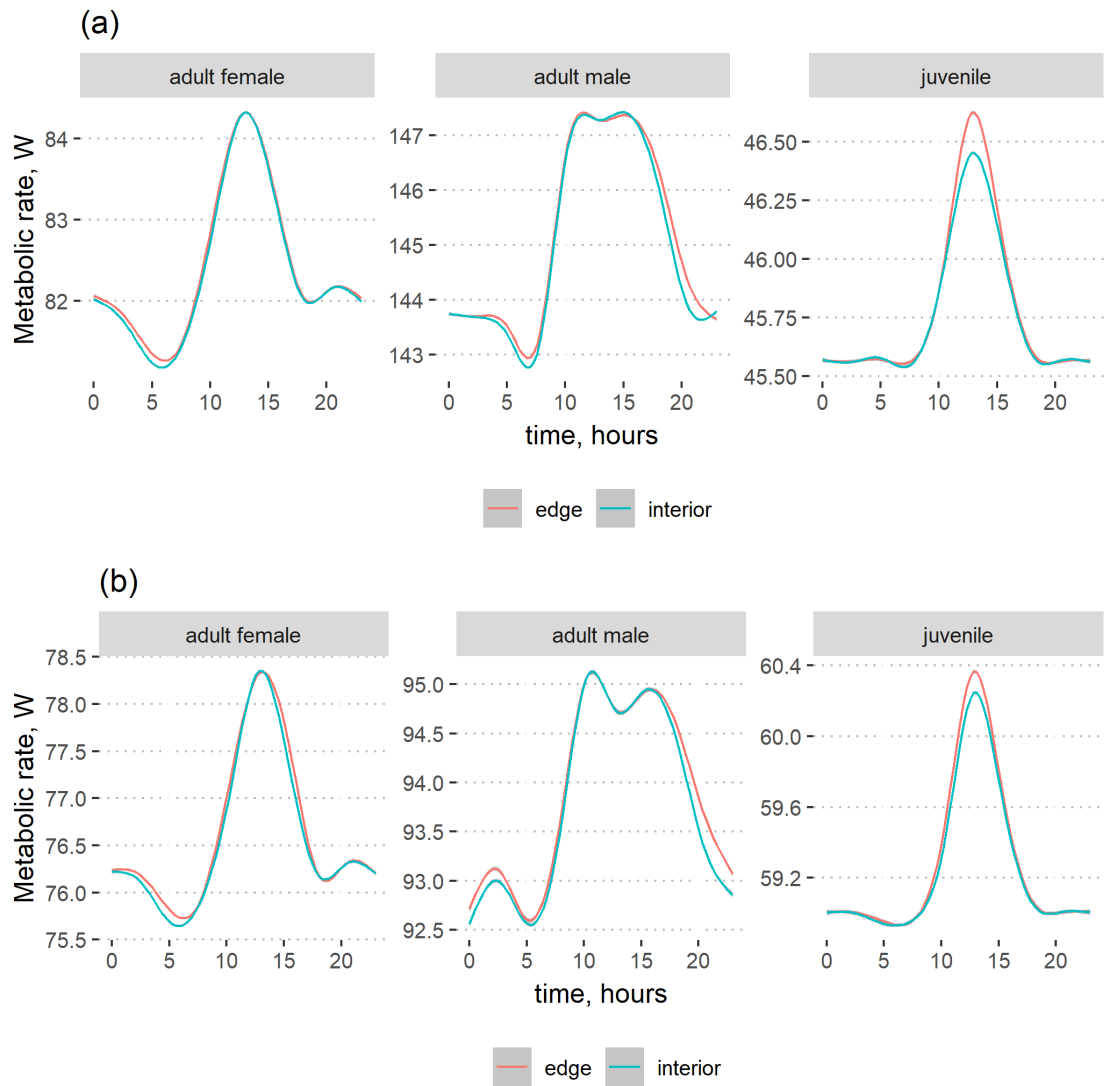


Figure 5.5: NicheMapR predictions of metabolic rate, W , for different age/sex classes of orangutans at edge and interior locations at Sikundur when using inputs of basal metabolic rate from (a) estimates based on the mouse-elephant curve; and (b) observed values from Pontzer et al 2010.

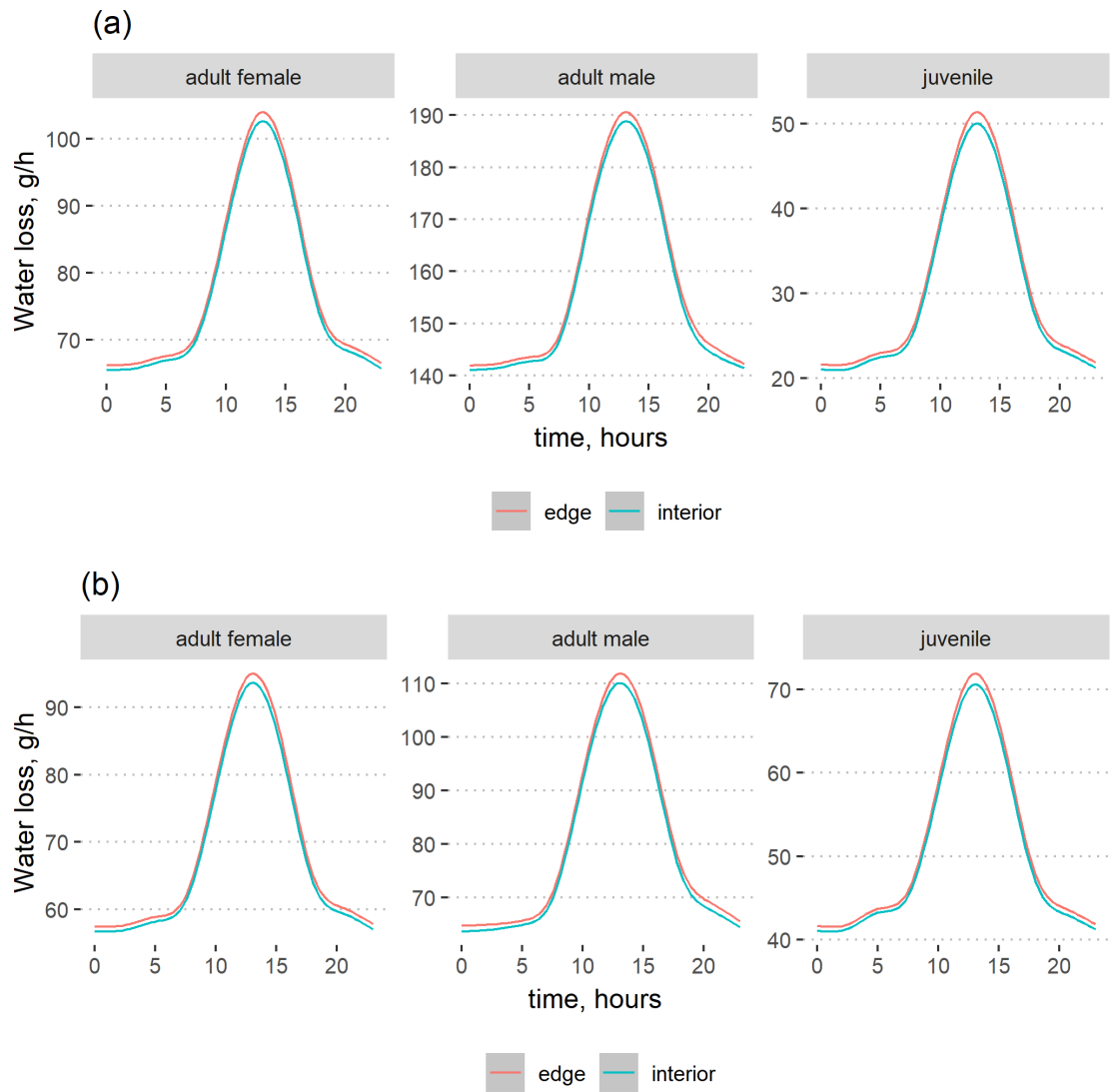


Figure 5.6: NicheMapR predictions of water loss rate, g/h, for different age/sex classes of orangutans at edge and interior locations at Sikundur when using inputs of basal metabolic rate from (a) estimates based on the mouse-elephant curve; and (b) observed values from Pontzer et al 2010.

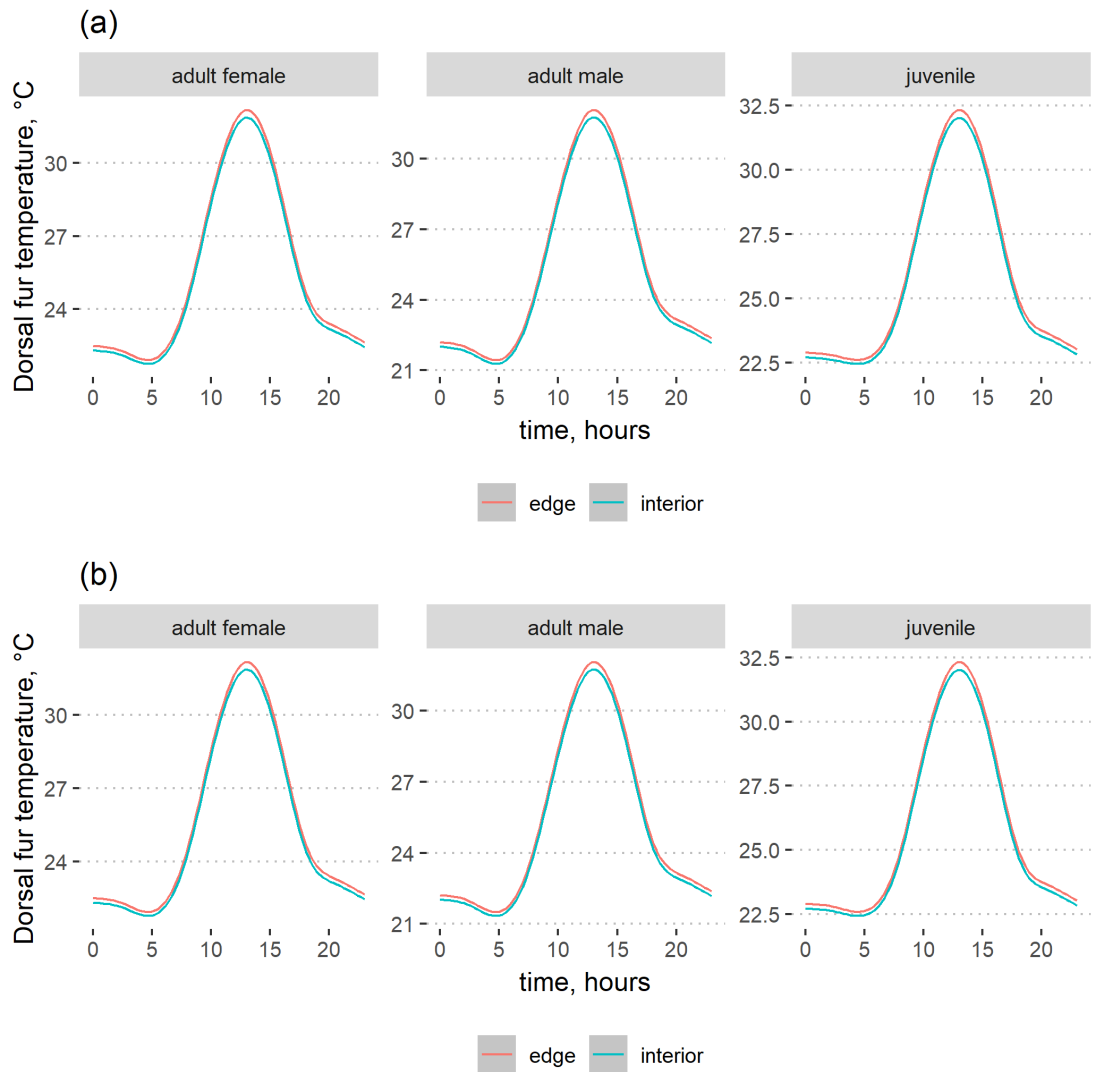


Figure 5.7: NicheMapR predictions of dorsal fur temperature, °C, for different age/sex classes of orangutans at edge and interior locations at Sikundur when using inputs of basal metabolic rate from (a) estimates based on the mouse-elephant curve; and (b) observed values from Pontzer et al 2010.

Table 5.3: NicheMapR endotherm model predictions for metabolic rate, *W*, water loss rate, *g/h*, and dorsal fur temperature, °C of adult male, female, and juvenile orangutans from individual sampling locations at Sikundur.

| Location | Forest type | Age/sex class | Basal metabolic rate input | Metabolic rate, <i>W</i> | | | Water loss rate, <i>g/h</i> | | | Dorsal fur temperature | | |
|----------|--------------|----------------------|----------------------------|--------------------------|--------|--------|-----------------------------|--------|--------|------------------------|-------|-------|
| | | | | min | max | mean | min | max | mean | min | max | mean |
| 1.1 | Edge | Adult male | Mouse-elephant curve | 141.94 | 147.30 | 145.09 | 137.69 | 193.96 | 156.81 | 20.67 | 32.62 | 25.16 |
| | | | Pontzer et al 2010 | 92.56 | 94.86 | 93.88 | 60.40 | 115.00 | 79.29 | 20.74 | 32.62 | 25.18 |
| | Adult female | Mouse-elephant curve | 81.11 | 84.17 | 82.38 | 62.40 | 106.14 | 77.36 | 21.16 | 32.73 | 25.42 | |
| | | Pontzer et al 2010 | 75.32 | 78.16 | 76.61 | 53.88 | 97.04 | 68.62 | 21.17 | 32.73 | 25.42 | |
| | Juvenile | Mouse-elephant curve | 45.57 | 47.29 | 45.77 | 19.18 | 54.11 | 30.49 | 21.89 | 32.87 | 25.79 | |
| | | Pontzer et al 2010 | 58.64 | 61.24 | 59.26 | 39.08 | 75.01 | 50.74 | 21.85 | 32.87 | 25.78 | |
| 1.5 | Interior | Adult male | Mouse-elephant curve | 141.94 | 147.30 | 145.02 | 137.01 | 196.60 | 157.18 | 20.35 | 32.73 | 25.03 |
| | | | Pontzer et al 2010 | 92.56 | 94.86 | 93.80 | 59.46 | 117.58 | 79.64 | 20.42 | 32.73 | 25.05 |
| | Adult female | Mouse-elephant curve | 81.11 | 84.17 | 82.40 | 61.75 | 107.97 | 77.69 | 20.85 | 32.84 | 25.30 | |
| | | Pontzer et al 2010 | 75.32 | 78.16 | 76.63 | 53.12 | 99.01 | 68.92 | 20.86 | 32.84 | 25.30 | |
| | Juvenile | Mouse-elephant curve | 45.57 | 47.29 | 45.78 | 18.52 | 55.58 | 30.69 | 21.59 | 32.97 | 25.67 | |
| | | Pontzer et al 2010 | 58.64 | 61.24 | 59.28 | 38.26 | 76.53 | 50.96 | 21.55 | 32.97 | 25.66 | |
| 2.1 | Edge | Adult male | Mouse-elephant curve | 141.94 | 147.30 | 145.12 | 137.78 | 193.72 | 156.83 | 20.67 | 32.58 | 25.15 |
| | | | Pontzer et al 2010 | 92.56 | 94.86 | 93.86 | 60.35 | 114.85 | 79.27 | 20.74 | 32.58 | 25.17 |
| | Adult female | Mouse-elephant curve | 81.11 | 84.17 | 82.38 | 62.47 | 105.97 | 77.36 | 21.16 | 32.70 | 25.41 | |
| | | Pontzer et al 2010 | 75.32 | 78.16 | 76.60 | 53.75 | 97.01 | 68.61 | 21.17 | 32.70 | 25.41 | |
| | Juvenile | Mouse-elephant curve | 45.57 | 47.29 | 45.77 | 19.22 | 53.94 | 30.49 | 21.89 | 32.84 | 25.78 | |
| | | Pontzer et al 2010 | 58.64 | 61.24 | 59.25 | 39.14 | 74.93 | 50.72 | 21.85 | 32.84 | 25.78 | |
| 2.5 | Interior | Adult male | Mouse-elephant curve | 141.94 | 147.30 | 144.96 | 136.04 | 192.09 | 155.38 | 20.46 | 32.27 | 24.88 |
| | | | Pontzer et al 2010 | 92.56 | 94.86 | 93.72 | 59.16 | 113.14 | 77.81 | 20.53 | 32.27 | 24.90 |
| | Adult female | Mouse-elephant curve | 81.11 | 84.17 | 82.33 | 61.64 | 104.67 | 76.30 | 20.95 | 32.38 | 25.14 | |
| | | Pontzer et al 2010 | 75.32 | 78.16 | 76.52 | 52.82 | 95.68 | 67.49 | 20.96 | 32.38 | 25.14 | |
| | Juvenile | Mouse-elephant curve | 45.57 | 47.29 | 45.74 | 18.44 | 52.82 | 29.58 | 21.67 | 32.52 | 25.51 | |
| | | Pontzer et al 2010 | 58.64 | 61.24 | 59.22 | 38.23 | 73.74 | 49.83 | 21.63 | 32.52 | 25.50 | |
| 3.1 | Edge | Adult male | Mouse-elephant curve | 141.94 | 147.30 | 145.09 | 137.51 | 193.52 | 156.58 | 20.64 | 32.53 | 25.11 |
| | | | Pontzer et al 2010 | 92.56 | 94.86 | 93.86 | 60.27 | 114.60 | 79.06 | 20.71 | 32.53 | 25.13 |
| | Adult female | Mouse-elephant curve | 81.11 | 84.17 | 82.38 | 62.29 | 105.77 | 77.20 | 21.13 | 32.65 | 25.37 | |
| | | Pontzer et al 2010 | 75.32 | 78.16 | 76.60 | 53.79 | 96.76 | 68.43 | 21.14 | 32.65 | 25.38 | |
| | Juvenile | Mouse-elephant curve | 45.57 | 47.29 | 45.76 | 19.12 | 53.85 | 30.35 | 21.86 | 32.79 | 25.74 | |
| | | Pontzer et al 2010 | 58.64 | 61.24 | 59.24 | 39.14 | 74.70 | 50.58 | 21.82 | 32.79 | 25.74 | |
| 3.5 | Interior | Adult male | Mouse-elephant curve | 141.94 | 147.30 | 145.00 | 137.14 | 192.44 | 155.92 | 20.52 | 32.32 | 24.95 |
| | | | Pontzer et al 2010 | 92.56 | 94.86 | 93.78 | 59.79 | 113.63 | 78.36 | 20.59 | 32.32 | 24.97 |
| | Adult female | Mouse-elephant curve | 81.11 | 84.17 | 82.35 | 61.97 | 105.06 | 76.70 | 21.01 | 32.44 | 25.21 | |
| | | Pontzer et al 2010 | 75.32 | 78.16 | 76.55 | 53.31 | 95.96 | 67.89 | 21.02 | 32.44 | 25.22 | |
| | Juvenile | Mouse-elephant curve | 45.57 | 47.29 | 45.75 | 18.78 | 53.12 | 29.92 | 21.74 | 32.58 | 25.58 | |
| | | Pontzer et al 2010 | 58.64 | 61.24 | 59.23 | 38.67 | 74.05 | 50.16 | 21.70 | 32.58 | 25.58 | |
| 4.1 | Edge | Adult male | Mouse-elephant curve | 141.94 | 147.30 | 145.13 | 137.53 | 199.26 | 158.72 | 20.49 | 33.18 | 25.30 |
| | | | Pontzer et al 2010 | 92.56 | 94.86 | 93.86 | 60.13 | 120.42 | 81.13 | 20.56 | 33.18 | 25.32 |
| | Adult female | Mouse-elephant curve | 81.11 | 84.17 | 82.47 | 62.36 | 110.05 | 78.85 | 20.98 | 33.29 | 25.56 | |
| | | Pontzer et al 2010 | 75.32 | 78.16 | 76.67 | 53.60 | 101.09 | 70.06 | 20.99 | 33.29 | 25.56 | |
| | Juvenile | Mouse-elephant curve | 45.57 | 47.29 | 45.82 | 19.07 | 57.43 | 31.65 | 21.72 | 33.42 | 25.92 | |
| | | Pontzer et al 2010 | 58.64 | 61.24 | 59.33 | 38.84 | 78.36 | 51.92 | 21.68 | 33.42 | 25.92 | |
| 4.5 | Interior | Adult male | Mouse-elephant curve | 141.94 | 147.30 | 145.00 | 136.62 | 192.32 | 155.38 | 20.50 | 32.32 | 24.93 |
| | | | Pontzer et al 2010 | 92.56 | 94.86 | 93.73 | 59.21 | 113.37 | 77.79 | 20.57 | 32.32 | 24.95 |
| | Adult female | Mouse-elephant curve | 81.11 | 84.17 | 82.32 | 61.54 | 104.90 | 76.28 | 20.99 | 32.43 | 25.19 | |
| | | Pontzer et al 2010 | 75.32 | 78.16 | 76.55 | 52.85 | 95.75 | 67.51 | 21.00 | 32.43 | 25.19 | |
| | Juvenile | Mouse-elephant curve | 45.57 | 47.29 | 45.74 | 18.41 | 52.96 | 29.60 | 21.72 | 32.58 | 25.56 | |
| | | Pontzer et al 2010 | 58.64 | 61.24 | 59.22 | 38.36 | 73.94 | 49.83 | 21.68 | 32.58 | 25.55 | |

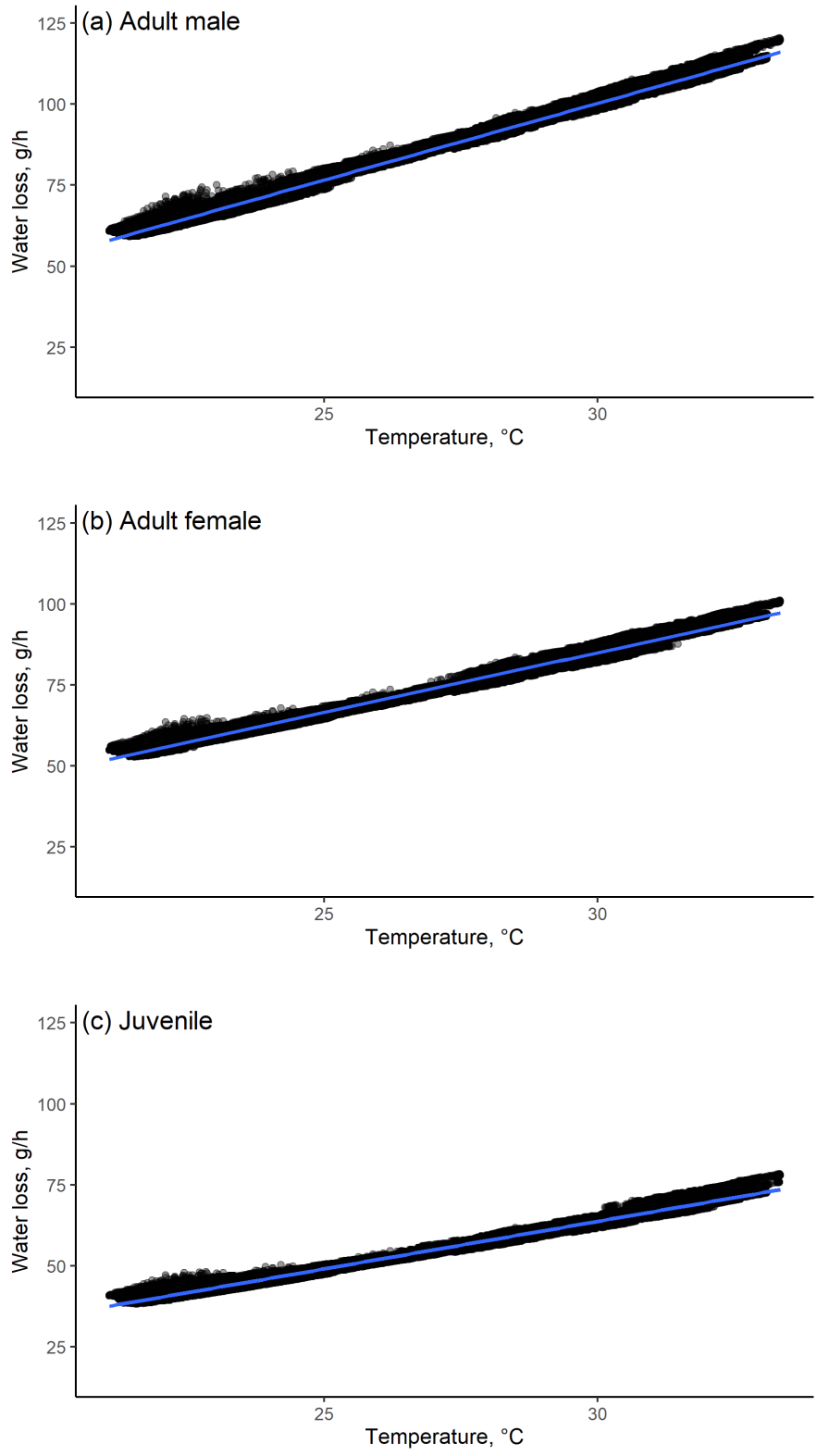


Figure 5.8: Water loss rate, g/h, estimated by NicheMapR using observed values of metabolic rate from Pontzer et al 2010, against predicted air temperature, mid canopy, in °C, for (a) adult male; (b) adult female; and (c) juvenile orangutans.

5.5 Discussion

This chapter tested how energetic costs and thermal stress in the Critically Endangered Sumatran orangutan differed at a forest edge compared with the interior using a biophysical model. Using the biophysical model, I have identified that thermal stress is higher at forest edges, and that water balance is an important mechanism which underlies orangutan relationships with climate. Fur temperatures and water loss rates were higher at the forest edge compared with the interior for all age-sex classes, while estimated metabolic rate was highest at the edge for juveniles only. Estimated differences in metabolic rate and water loss were more pronounced for an adult male compared with both adult female and juvenile orangutans (mean difference of 0.11W and 1.27 g/h for MR and water loss respectively in males, compared with 0.06W and 0.96 g/h in females and 0.03W and 0.8g/h in juveniles). This means that physiological stress is higher at the forest edge, and that adult males are more vulnerable to this thermal stress than females or juveniles and will therefore be disproportionately affected by climate change. This will have implications for reproductive success and population structure.

Using the model, I identified 32°C as the upper threshold air temperature above which orangutans were likely to be experiencing notable thermal stress. When temperatures exceed this threshold, animals cannot maintain their body temperature within the allowed ranges through physiological thermoregulation alone (i.e., through increased metabolism, sweating, or panting). Although the upper threshold is exceeded less in the forest interior compared with the edge, it is still exceeded on average 225 days per year, meaning that orangutans are exposed to potentially stressful conditions at least once on many days of the year. Based on these results, it appears that orangutans are currently tolerating extremely warm temperatures for short periods regularly, however it is unclear to what extent and for how long they can endure these conditions before they begin to suffer reduced individual fitness resulting in population declines. It is possible that they are already declining, but we do not currently have sufficient long-term climate and population data for the area to determine this. Answering this question will be instrumental in determining the impacts of climate change, which will result in the upper threshold being exceeded for a larger proportion of time and potentially for longer periods.

Orangutans are likely to avoid edges during hotter periods. Conditions were notably warmer at the forest edge and the upper threshold of 32°C was exceeded on more days and for longer periods of time per day compared with the interior. In addition, the canopy height at these edge forests was lower than in the interior. The higher canopy would provide a clearer negative vertical temperature gradient, allowing more cooler locations inside taller interior areas. In Chapter 4 I showed the positive effect of height in the canopy on temperature, meaning that lower areas within closed canopy forests may be a last refuge during the hottest time of day. It would be interesting to see whether orangutans would even come to the ground more regularly as temperatures increase. Availability of cool locations is an important consideration in forest management. Increased fragmentation and a higher prevalence of forest edges will decrease the amount of climatically suitable habitat available to orangutans. Additionally, forest corridors or remnant forests in plantations may not be able to support orangutans in the long-term if they do not sufficiently shelter them from temperature extremes. Changes in climate conditions brought on by edge effects can occur up to 2km into forests (Broadbent et al. 2008; also see chapter 3), therefore corridors and forest remnants would have to include a buffer larger than this in order to be useful for orangutan conservation, but few forest fragments will have a diameter of more than 4km.

Temporal, as well as spatial, variation in climate is important in determining climate change impacts. This has been overlooked in previous climate change work on orangutans, which has only incorporated mean annual temperatures from WorldClim data (Carne et al. 2012; Gregory et al. 2012; Condro et al. 2019). Average annual temperatures recorded in Sikundur are well below the upper threshold of 32°C (ranging from 24.97 – 27.52°C), however maximum temperatures frequently exceed it (Figure 5.4). These extremes are not captured by annual temperature averages, and previous models are therefore likely to underestimate orangutan exposure to the most severe effects of climate change and its resulting impacts. Microclimate models can be used to overcome this and incorporate temporal climate variation into predictive models. The NicheMapR microclimate model has already been validated for the site and shown to work well at predicting microclimate conditions (see chapter 4). Error values produced by the microclimate model in this chapter were still comparable with those which used more site-specific UAV data in chapter 4, despite only using field data on mean canopy height; all other input parameters were derived from satellite data which is freely available. It can therefore be used to generate climate data quickly and cheaply with high temporal and

spatial resolution for other locations in Sumatra, and potentially other tropical forests, for improved distribution modelling and local-scale climate change projections. Biophysical models can be combined with dynamic energy budget and time budget models to produce more dynamic and physiologically grounded predictions of extinction risk from disturbance and climate change.

Increased thermal stress in individuals results in reduced fitness by increasing enforced resting time, with knock-on effects for activity budgets. Increased enforced resting time will reduce the amount of time available for movement and foraging activities (Korstjens et al. 2010). This will have negative effects at the population level through reduced individual fitness. Conversely, orangutans will have to move and forage more to locate adequate resources and meet their energy requirements due to lower quality food resources in disturbed and fragmented forests and the increased costs of thermoregulation following climate change (Carne et al. 2012). This means that the combined effects of forest disturbance and climate change on orangutan energy budgets will limit their future ability to survive in Sikundur and other human-modified forests.

As well as maintaining their body temperature, organisms must maintain water balance, and this too will limit their activity budgets and ability to survive following climate change (Kearney et al. 2016). An understanding of water exchange is also necessary for making predictions of climate change responses which are physiologically grounded. Water loss is strongly affected by ambient temperature, and this effect is strongest for adult males with their larger body size and higher metabolic rate. Water loss is likely to be particularly problematic for orangutans, since they rely mostly on obtaining water from their food, or from canopy ‘reservoirs’ in epiphytes on mature trees (Sharma et al. 2016). This means that orangutans in disturbed forests will have fewer opportunities to replenish lost water. Hotter and drier conditions in disturbed forests and near forest edges will result in smaller canopy reservoirs, while the reduced density of mature trees in selectively logged forest will also mean that there are fewer epiphytes in the canopy (Parra-Sanchez and Banks-Leite 2020; Richards et al. 2020).

Adult orangutans have a lower metabolic rate than expected based on their body size (Pontzer et al. 2010), and the model results suggest that this helps them to maintain energy balance in the hot and humid conditions of Sumatran rainforests. When using estimates of metabolic rate calculated based on body size, simulated orangutans are unable to

maintain homeostasis in conditions which are typical of their habitat, however they perform much better when modelled with the lower metabolic rates observed by Pontzer et al. (2010), with the model predicting much lower rates of water loss. It has previously been suggested that reduced energy expenditure in orangutans is a physiological adaptation to minimise the risk of starvation during periods of low food availability, since fruit availability in Sumatra and Borneo is highly variable and unpredictable, and orangutans often undergo long periods of scarcity (Pontzer et al. 2010). This study suggests that lowered metabolic rates may also help orangutans to maintain their body temperature and energy balance in warmer temperatures.

Although it was not possible within the constraints of this study to fully validate the predictions of the model, it has been shown to perform well in other endotherms, including primates. The NicheMapR ellipsoid model predicted field metabolic rate with higher accuracy than more simplified models for *Lepilemur* species (root mean square error = 34.1 – 35.6 for the ellipsoid model, compared with 244.8 for an allometric model based on mass alone; Stalenberg 2019). Predictions of body temperature and metabolic rates have corresponded well with observed field measurements for both vervet monkeys (Mathewson et al 2020) and polar bears (Mathewson and Porter 2013). A mechanistic model of habitat loss for American Pika produced higher confidence intervals than correlative approaches (Mathewson et al 2017). Before the model can be more generally applied, it will be necessary to complete further validation and sensitivity testing to determine the model's accuracy in predicting orangutan energetics and to highlight which variables are most important in parameterising the model and determine potential sources of error.

The model used here does have several limitations. Firstly, it is a very simplified mechanistic model which currently does not incorporate activity costs of movement, feeding and reproduction, and also does not account for potential behavioural thermoregulatory strategies which may be employed by orangutans in the wild. The differences in results produced from different measures of metabolic rate highlights the importance of using the correct input parameters. Values for metabolic rate taken from Pontzer et al. (2010) were measured from three captive individuals which were hybrids of the two *Pongo* spp., *P. pygmaeus* and *P. abelii*. Actual values for metabolic rate are likely to vary between the two species, it would therefore be preferable to obtain values from a larger number of individuals from *P. abelii*. Here, only default values were used

for options allowing organisms to sweat and pant in order to cool down since no data on this were available for orangutans. Improving the quality of input data used to parameterise the model would improve the quality of predictions and the general applicability of the model to answer questions relating to the biophysical ecology of Sumatran orangutans.

Bioenergetics studies for other species have highlighted important mechanisms through which organisms respond and adapt to changing temperatures. For example, biophysical models were used to determine the importance of tree-hugging behaviours by koalas in maintaining their body temperature during periods of extreme heat in Tasmania (Briscoe et al 2016), while Stalenberg (2019) identified fur licking as an important thermoregulatory response to higher temperatures in *Lepilemur* species in Madagascar. Predictions of metabolic rates from the NicheMapper biophysical model (an earlier, more complex iteration of NicheMapR) were used to predict weight loss and mortality of polar bears during periods of low food availability in the ice-free season in Hudson Bay (Mathewson and Porter 2013). Similarly, the model used here could be expanded and applied to other apes in order to explore questions related to hominid evolution, adaptations to climate change, historical landscape use and thermoregulatory behaviours. Certain behaviours exhibited by apes are thought to have a thermoregulatory component (e.g., see Stelzner and Hausfater 1986; Stelzner 1988; Carvalho et al. 2015), and biophysical models could be used to test this. For example, the function of nest building by great apes is not well understood, with various theories invoking the role of comfort and sleep quality, protection from predators and parasites, and thermoregulation (Fruth 2017). Climate change may also have played a role in landscape use and terrestrial behaviour by early hominins (Takemoto 2017; van Leeuwen 2019). There is evidence that terrestrial behaviour by chimpanzees is linked to microclimate variation (Takemoto 2004), while morphological adaptations to bipedalism and increasing dietary breadth may have allowed early hominins to persist in more open savannah habitats, despite highly elevated costs of maintaining homeostasis compared to forests (van Leeuwen 2019). Empirical evidence for thermoregulatory behaviours exhibited by hominids is limited, however this could be provided using a combination of mechanistic models of microclimate and animal physiology.

The advantage of mechanistic models is that once the relevant input parameters have been obtained for a species they can be applied in any location, even where there are no

reliable distribution data. The most important next step for research is to collect data to validate the model outputs with observed physiological data. Collecting this data would be far easier and safer with captive individuals, where it would be possible to conduct metabolic chamber experiments, or collect samples, for example using labelled water methods to measure energy expenditure (as used by Pontzer et al. 2010). It was not possible to collect such data for this study since I did not have access to captive individuals, or the relevant permissions and resources required to collect and analyse biological samples in Indonesia. Once the model has been validated and shown to produce reliable predictions of orangutan energetics, it will be a powerful tool which can be used to identify individual physiological responses to climatic conditions, which can then be scaled up to determine population level effects of climate change.

This is the first test of a biophysical model of physiological responses to climate for an ape species. Although the model requires further validation to ensure it is producing accurate predictions, the results here highlight that biophysical models can provide useful insights into individual responses to forest disturbance and climate change by identifying the physiological drivers of population declines. Outputs from this model can be used to predict the fundamental niche of orangutans under different climate and land use scenarios. These models can be implemented with other spatial distribution models to provide more detailed understanding of future orangutan distributions and habitat requirements and highlight areas where conservation efforts should be focussed. This has been achieved for other primates; for example, Stalenberg (2019) used the NicheMapR model to identify the thermal neutral zone and predict water loss and physiological stress of sportive lemurs (*Lepilemur* spp.), these results were then used to create interactive, high-resolution maps of current and future extinction risk which can be utilised by conservation planners to identify priority areas for conservation. This enabled the identification of areas in the Northern part in Madagascar as important microclimate refuges, where higher rainfall and more moderate temperatures results in lowered water loss rates for individuals, thereby reducing climate-related mortality. As well as exploring questions relating to climate change responses, the model can also be used to highlight physiological responses to changes brought about by human disturbance, such as the physiological differences caused by forest edges identified here. Mechanistic and biophysical models can be used to simultaneously predict consequences of both climate change and human activities for wild populations. This is particularly important for orangutans, which are subject to both threats simultaneously (Gregory et al. 2012).

Chapter 6

General discussion

In this final chapter I will summarise and discuss the main findings and wider implications of my research within the context of existing literature on ecology and conservation of tropical forest mammals. Many key points have already been discussed in the relevant chapters, and so I will focus mainly on additional points which have not been previously covered in detail. Finally, I will conclude by providing recommendations for future research.

The aim of this thesis was to determine the long-term value of an area of regenerating selectively logged forest to conserve threatened mammals in Sumatra, Indonesia, and to identify its potential to provide microclimate refuges for these mammals to persist following climate change. The results indicate that this area is still an important habitat for many mammals, despite its history of disturbance and proximity to agricultural land. While the physical structure of the forest does differ from those typical of primary forest in the same region (i.e., lower canopy height and connectivity), the results indicate that there are still significant microclimate variations underneath the canopy and that conditions are cooler, and less variable compared with non-forested areas. This indicates that, although this area of forest is not considered ideal or ‘pristine’ habitat for most species, it will still be of fundamental importance in allowing forest-dependent mammals to persist in the long-term.

I also tested mechanistic approaches to modelling microclimates and mammal responses at small spatial and temporal scales. These models were developed and initially tested for microclimates in the USA and Australia and have rarely been applied in tropical forest environments. This is the first study to test these models for a disturbed forest location in Indonesia, and the first time that the biophysical models have been tested for a great ape species. The models all performed well, producing results which were congruent with observed or expected data. Differences from observed values for the microclimate models was fairly low, and comparable with published studies in other locations with different macroclimatic conditions. This was true both when model inputs for vegetation and topographical parameters were taken directly from photographs taken of the canopy using an Unmanned Aerial Vehicle (UAV) (as in chapter 4), and when data

were derived exclusively from global Shuttle Radar Topography Mission (SRTM) data, which are freely available elevation data for terrestrial areas +/- 60 degrees latitude, remotely sensed from space (as in chapter 5). This demonstrates that these models are appropriate for use in tropical and/or disturbed forests, even for locations which lack high-resolution data on local-scale topography and vegetation.

6.1 Structure and microclimate in secondary forests

Most studies have established that human-modified and secondary forests are, on average, warmer, drier, and brighter than primary forests, however, few studies to date have measured spatial and temporal variations in secondary forests at fine scales (Marsh 2019; Jucker et al. 2020). The reduction in canopy cover often leads to an increase in the density of understorey vegetation, and results in more spatially and temporally heterogeneous microclimate conditions. This could actually increase the availability of microclimate refuges for some species. There is evidence for this heterogeneity in secondary forests (e.g., Blonder et al. 2018; Senior et al. 2018), although it is still not known the extent to which these microclimates are decoupled from the macroclimate. My study, combined with previous research in the region, provides further evidence for fine-scale climate variations in secondary forests. Previous work at Sikundur noted differences of up to 14 °C between simultaneous recordings from different locations in the forest interior (Marsh 2019). Senior et al. (2018) found that conditions in tree holes, deadwood and leaf litter in selectively logged forests were equally buffered against macroclimate warming compared with those in primary forests, highlighting that secondary forests still maintain various microhabitats for organisms to utilise during extremely hot weather. On the other hand, Blonder et al. (2018) noted that, as well as increased variability in climate conditions, selectively logged forests had much higher extremes in temperature compared with primary forests, thereby increasing the exposure of organisms to potentially harmful extremes. My results from chapters 3 and 5 confirm this observation. It is currently unclear what the impact of increased spatial variation is on forest-dwelling or climate-sensitive species. Here, I did not compare conditions against primary forest but did still note significant spatial and temporal variations across Sikundur. Having validated NicheMapR for my study area and shown that it performs well, the model can be used to further explore this variation, and to identify the extent and direction in which conditions within disturbed forests are decoupled from macroclimate and buffered against climate warming.

Microclimate ecology research to date has been heavily biased towards conditions near the ground and this has limited applicability to arboreal organisms. Here, I provide further evidence of significant microclimate variations in the upper canopy and highlight the potential importance of these variations for behavioural thermoregulation and ultimate survival of arboreal species. There was some evidence of vertical temperature gradients in the forest, as was also found by Marsh (2019). Recorded mean temperatures were warmer in the higher parts of the canopy, although the noted effect was overshadowed by seasonal and daily temperature fluctuations (chapter 4). All of the plots measured in this study had relatively lower canopy heights than would normally be expected in tropical forests, and this may affect the steepness of the gradients. The lower canopy height in this region has potentially reduced microclimate variability in the upper canopy, which could result in a negative impact on the ability of arboreal animals to avoid extreme temperatures. As the forest regenerates and average canopy height increases, vertical temperature gradients may also become more pronounced, providing more opportunities for organisms to shelter from warmer conditions in lower parts of the canopy. This is an important consideration when managing stands of secondary forest in human-modified landscapes as a means to conserve arboreal species; areas with taller canopies are preferable, since they will have higher availability of cooler microclimates in the upper canopy.

6.2 Edge effects on forest conditions and mammals

Edge effects on abiotic forest conditions were evident at the site, as shown in chapters 3 and 5. Conditions were significantly warmer and brighter at locations up to 500m from the forest than those in the interior. Simultaneous temperature recordings taken at the same height differed as much as 8.83°C between locations at the edge and those 2km into the interior. Other research from tropical forests has highlighted that edge effects are evident between 500m-1km; the effect distance is thought to be greater in secondary forests, however few studies have implicitly tested this (Broadbent et al. 2008). To date there is little evidence of the extent to which abiotic edge effects impact forest-dwelling species, although it is generally assumed that these abiotic changes will have negative consequences. In chapter 3, I explored how different species have differing responses to forest edge effects and demonstrated that some species are less affected by negative effects of increased temperatures than others. This could be the result of those species being able to exploit increased foraging opportunities in farmland (e.g., pigs and

macaques are dietary generalists), while others may be excluded from locations closer to the edge, either due to conflict or specializations (e.g., lack of prey for carnivores). I also showed that higher temperatures resulted in decreased mammal occurrence, and this relationship was consistent across mammal orders. Accordingly, in chapter 5, I showed that orangutans have a higher exposure to potentially harmful climatic conditions at the forest edge, compared to locations 2km into the interior. Abiotic changes in forest conditions negatively impact species, although for many mammals it is unclear how these impacts will affect population dynamics in the long-term.

When designating areas for conservation, it is important to take the spatial extent of edge effects into consideration. For example, the establishment of conservation set asides within oil palm plantations are a requirement for plantations to be certified as sustainable by the Roundtable on Sustainable Palm Oil (RSPO). However, in a recent analysis, Morgans et al. (2019) showed that RSPO plantations were not more effective in supporting orangutans than non-RSPO plantations. For these set-asides to be effective, they must include a buffer which is large enough to protect the core from edge effects. The minimum size of this buffer will depend on the target organism and the quality of the forest patch in question. For example, based on results from chapter 3, large carnivores will need a buffer of 1-1.5km, whereas ungulates and small carnivores would only require around 500m. Wildlife corridors will also need to be wide enough that they will actually be utilised by their target species. Larger carnivores that avoid edge habitats would be unlikely to move through corridors which are less than 2km wide. If the aim is to maintain high levels of diversity within these patches, then they will need to be sufficiently large to accommodate this and provide suitable corridors and pathways to maintain patch connectivity and protect species long-term. However, RSPO plantations are typically smaller than this. In Borneo, the average high conservation area is 1.2km², with only 21% of these being forested (Scriven et al. 2019).

6.3 Microclimate modelling in secondary tropical forests

Both the NicheMapR and microclimc microclimate models performed well in predicting microclimate variation, with values for root mean square error and mean absolute difference being comparable with reported values from other published microclimate studies in temperate areas. NicheMapR outperformed microclimc, producing slightly lower error values. NicheMapR performed well, even for locations

where drone data were not available, and could therefore be used to model microclimate conditions in other tropical locations with limited field data. It is still preferable to collect *in situ* measurements to validate the model predictions at specific locations, however the sampling effort required for this is substantially less than relying on direct measurements alone. Model validation only needs to be carried out once; once the model has been shown to perform effectively it can be used without requiring further field data inputs. Mechanistic models therefore provide many advantages to studies in tropical forest ecology, since they can provide accurate and detailed climate data at more ecologically relevant scales than global climate datasets with coarser resolutions, with fairly minimal requirements for sampling effort and fieldwork costs.

6.4 Applications of mechanistic models in mammal ecology and conservation

Conservation is implemented at a local scale. Global or regional scale models do not provide detailed enough information to be of much use to practitioners outside of highlighting general areas, species or populations which should be prioritised for protection. Mechanistic models, i.e., models that predict habitat suitability and species responses based on understanding of the organisms' behavioural and physiological flexibility in response to ecological conditions, can be used to identify local-scale mechanisms which will shape species responses to climate change and future population trends. This is much more useful to conservationists since it can identify the underlying causes of population declines and signpost the most appropriate interventions (such as active restoration of forests through planting; assisted translocation into areas which are more climatically suitable; establishing connectivity between patches to maintain genetic diversity of metapopulations; facilitating range shifts etc).

As well as providing valuable information about species' ecology, biogeography, and evolution, mechanistic models can be used to provide valuable empirical evidence and justification for conservation planning and decision making. Gathering the appropriate and relevant input data for mechanistic models can be difficult for lesser-known species; however, it is also difficult to gather widespread population or abundance data that is required for correlative models to work effectively. As long as mechanistic models are used with caution, and users are aware of the limitations of their input data, they can be effectively applied, even for data-deficient species by using estimated values based on

similar species or expert opinions (Stalenberg 2019). While predictive models will never be able to replace field data, in practice many conservation projects do not have resources to conduct regular extensive field surveys. A great deal of conservation work and species assessments are based on expert assessments and assumptions with limited empirical backing. This is often due to the difficult nature of gathering data on rare or cryptic species in the wild. Most predictions about species' responses to climate change are based on correlative distribution models, which require detailed distribution and/or abundance data and tend to perform better for species with large geographic ranges that cover a variety of climate conditions (Stalenberg 2019). It is harder to infer species-climate relationships with this approach for rare and range-restricted species since they have limited data available, and often have not fully realised their fundamental climatic niche (i.e., all climatic conditions they can persist in). Mechanistic and biophysical approaches are advantageous for these species since they are based on an understanding of the underlying physiological and ecological processes involved in species biogeography, rather than relying on present distributions. They can be used in scenario testing enabling researchers and conservationists to simulate the outcomes of different management, land use and climate change scenarios (e.g., Kearney et al. 2016; Mathewson et al. 2017). This will be highly advantageous to conservation planning, helping to ensure that resources are allocated in the most effective and efficient way and ensure the best possible conservation outcomes.

Many primates are generalist species which are able to exist in a wide variety of habitats, and their fundamental thermal niche (i.e., the range of climatic conditions in which they could theoretically survive) is most likely wider than their current realized niche (i.e., the actual conditions in which they currently exist). This can make it difficult to infer relationships based on their current distributions alone. Despite this limitation, there have been very few attempts to apply mechanistic models to primates. Biophysical models have only been applied to a small number of primate species (vervet monkeys, Mathewson et al. 2020; and sportive lemurs, Stalenberg 2019). The majority of published models that predict future orangutan distributions have focussed on the effects of habitat loss and land use change, which are currently the most important drivers of population declines (Husson et al. 2008; Wich et al. 2016; Milne et al. 2021). Those studies that have investigated climate change predict a negative impact and potential range reductions of up to 15% (Carne et al. 2012; Condro et al. 2019), and conclude that climate change mitigation, as well as habitat restoration and protection will be important for orangutan

conservation in the near future (Gregory et al. 2012). Applications of mechanistic models to orangutan distributions have been limited to time-budget models of their potential responses to climate and land use change (Carne et al. 2012). This study is the first attempt to apply biophysical models to orangutans and great apes in general. In chapter 5, I identified water loss as being an important limiting factor and demonstrated that orangutans are already likely to be experiencing physiological stress due to hotter conditions for at least a short period of time on many days of the year (ranging from 110-283 days), with this period of stress being longer at forest edges compared to the interior. Therefore, it will be important to focus on protecting forest patches which contain large trees with epiphytes that can act as canopy reservoirs to provide drinking water and reduce dehydration. This effect would not be captured using a correlative approach which ignores temporal and spatial climate variation. These results highlight the potential value of mechanistic modelling approaches to provide more detailed information regarding animal responses to changing climates at finer scales. They can also signpost potential conservation actions.

Additionally, mechanistic models can be used to project future population trends and accurately determine population viability in the long-term. A common critique of existing conservation strategies is that they are primarily ‘reactionary’, meaning that most interventions take place only once populations have already become dangerously low. Most vulnerability assessments (e.g., the IUCN red list) rely on using past population data and trends to determine which species are currently threatened (Rodrigues et al. 2006). This means that threatened species are not identified as such until major population declines have already occurred. Areas which have been identified as hotspots of extinction debt do not correlate well with areas which have been highlighted as high extinction-risk based on IUCN classifications (Chen and Peng 2017). Relying solely on current conditions and species status is therefore inadequate for long-term conservation planning. Combining mechanistic population modelling with traditional methods of monitoring and research will enable us to identify population threats before they result in serious declines.

6.5 Conclusions & recommendations for future research

The structure of the forest at Sikundur is characteristic of heavily disturbed forest and, being close to the national park boundary and adjacent to agricultural lands, is subject

to extensive edge effects up to 500m – 1 km away from the boundary. Despite this, the area is still important habitat which supports a wide range of mammals, including several Critically Endangered species. Conditions in the forest interior are still buffered against temperature extremes, having lower maximum temperatures than the forest edge. The site is also highly heterogenous, with significant spatial and temporal variation in microclimate and physical vegetation structure. This spatial heterogeneity helps to support a diverse range of different mammal species, ranging from generalist and disturbance-tolerant species, such as macaques and pigs, to more specialised large carnivores, such as sun bears and tigers, which are more sensitive to human activities. The microclimatic variation exhibited across the site provides opportunities for animals to avoid prolonged exposure to sub-optimal extremes and thereby reduce the potential fitness costs of climate change. These results highlight the importance of considering fine-scale variation in ecological research at smaller scales. The variations observed across Sikundur would be missed by coarser resolution global models of climate and topography. This variation impacts the physiology of forest-dwelling organisms and will have subsequent implications for population-level dynamics.

Finally, these results add to the growing body of existing evidence that secondary and disturbed forests are valuable conservation areas which should be prioritised for protection and restoration, along with preservation of primary forest (Barlow et al. 2007; Meijaard 2017; Senior et al. 2018). That being said, it will still be necessary to focus efforts on restoring and regenerating forests to increase the extent of forest cover, and the overall habitat quality of forested areas. Knowledge of the abiotic conditions which are most important to threatened species can guide these efforts by highlighting which characteristics (e.g., canopy height, canopy cover, connectedness, forest patch size, distance between patches) should be focussed on. Secondary forests, as well as primary forests, will be highly valuable in providing mammals with microclimate refuges which will allow them to persist following climate change.

6.5.1 Future work

6.5.1.1 Improving model performance

Microclimate models require further testing and validation in a wider variety of habitats. To date, the NicheMapR microclimate model has mainly been applied in relatively simple terrains, such as arid grasslands and scrublands in Australia (Kearney et

al. 2020). This is the first test of the model for tropical lowland forest in Indonesia. Although they perform well enough to capture most horizontal variations in climate, the model does not appear to perform as well in capturing vertical gradients in forest canopies, since the error of the model increased with height above ground. Both models could be further improved by collecting further data on below canopy processes in tropical forests. Microclimc currently has the option to generate habitat structure variables based on habitat type, which was utilised in this study since the required parameters were unknown for the site, however the options for this remain very broad. More detailed habitat data to characterise different forest types, including secondary forest and tropical lowland forest, would help to further improve the model performance and make it easier to tailor it for specific locations. Further work to validate and improve the performance of these models will make their use in forest ecology and conservation planning far more accessible. Another current limitation in microclimate modelling is the steep learning curve involved in the implementation of the models, which can make their use intimidating and overly-complex for those without background knowledge of mechanistic models and microclimate ecology. Gathering a database of standardised input parameters for different habitat types and developing a more user-friendly interface would enable practitioners who are not familiar with R or Python programming languages to implement these models for their specific sites. This has been done for sportive lemurs in Madagascar (Stalenberg 2019) and can provide a useful tool for conservation planners to incorporate into their decision-making process.

A major barrier to more widespread use of mechanistic modelling approaches is their complex requirements for input parameters in order to work effectively. The ellipsoid model of NicheMapR has been developed partly in responses to this. This is a simplified version of the earlier NicheMapper endotherm model which only requires inputs on animal mass, body temperature ranges, fur properties, basal metabolic rate, and respiratory rate. These inputs can be extrapolated from phylogenetically similar species if there are no data available. Care should be taken when using estimates instead of direct measurements, however, as demonstrated by the substantial differences between predictions that were produced by NicheMapR when using estimates of basal metabolic rate (BMR) derived from the mouse-elephant curve compared with direct measurements of BMR from captive orangutans in chapter 5. The ability to integrate microclimate predictions using the microclimate module also means that it can be applied for any location. Further work on testing the sensitivity of these models to uncertainties in their

inputs and efforts to fill on knowledge gaps for species physiology will help to improve the accessibility and general applicability of biophysical models. Although they do require a number of detailed inputs for their initial setup, once they have been tested and validated, mechanistic models are powerful tools which can provide detailed data to support conservation.

6.5.1.2 Utilising models to understand climate change impacts

The forest at Sikundur is thermally buffered, with lower maximum temperatures compared to the edge, however it remains unclear to what extent this effect will persist with macroclimate warming. An important next step in determining if the area will serve as a microclimate refuge in the future is to predict the microclimate using macroclimate predictions from different climate change scenarios. This would help to identify how many degrees of warming in the macroclimate can be tolerated before the conditions underneath the forest canopy will be affected beyond what the species living there can cope with. Given the buffering effect of dense forest cover, it is likely that climate warming and subsequent exposure of forest mammals to warmer temperatures will be less severe than predicted in this region. Now that the microclimate models have been validated and shown to perform well, they can be used for scenario testing to determine how climate change might impact the microclimate conditions in the forest.

Scenario testing of the endotherm model can also be used to better understand the potential implications of climate change for orangutan bioenergetics. I identified that orangutans are likely to be experiencing some degree of thermal stress even under current conditions. It is likely that they are able to tolerate this stress since it is short-lived (less than 0.05% of the time). Running the endotherm model for a variety of different climate scenarios will help to identify the maximum thresholds of local warming that orangutans are able to tolerate, and also the maximum amount of time outside of their 'comfort zone' they are able to endure. Further data is also needed on orangutan thermoregulatory strategies, such as sweating and panting. Currently, the default values were used as inputs for these since there were no other data available for orangutans. Including these will provide more accurate predictions of metabolic rate and water loss.

Further information is also needed for different types of behavioural thermoregulation which may be employed by mammals. Investigating this is challenging with wild and unhabituated animals. It may be possible to test this in captive settings,

where animals have access to a range of different microclimates, by tracking animal movement and activity patterns in relation to temperature. It would also be possible to utilise thermal imaging to non-invasively monitor mammal habitat use in relation to climate (Cilulko et al. 2013), however, currently the technology required for this is costly and challenging to implement in humid, dense forest canopies, with animals that are often 10-30 meters away from the observer and obscured by vegetation.

Outputs from biophysical models can be fed into other modelling approaches, such as time budget models or individual based models, to predict potential species responses to climate change. NicheMapR has already been used to predict water and energy budgets and map potential distributions for a variety of species, including reptiles (e.g., Mitchell et al. 2013; Malishev et al. 2018), birds (e.g., Kearney et al. 2016) and mammals (Mathewson and Porter 2013; Stalenberg 2019). In many cases, the use of biophysical models improved the performance of distribution models, and identified important mechanisms for species declines, such as dehydration/desiccation, which would otherwise have been missed. When modelling climate change responses, particularly for species which are already threatened, it is vital to consider climate change together with other threats, such as habitat loss or hunting. Biophysical models are valuable tools which can be used to complement and improve predictions from traditional approaches, such as correlative SDMs, however they do not provide enough information to identify population threats or predict climate change responses on their own.

6.5.1.3 Biodiversity responses to edges and human disturbance

This study has focussed on conspicuous, larger bodied mammals; however, the forest at Sikundur is important habitat for many other taxa, for which camera trap surveys are not effective. Other monitoring techniques, such as acoustic monitoring, can be used to sample a wider range of species and providing better estimates of biodiversity for the region. Acoustic monitoring has already been utilised to monitor habitat use by forest elephants, and to carry out rapid biodiversity assessments in forest (Sueur et al. 2008; Wrege et al. 2017). Acoustic recorders cover a wider area than camera traps, which can only detect animals directly in front of them, and it is now possible to obtain recorders that can record a wide range of frequencies with battery power that can last from days to months depending on the settings used (Sugai et al. 2019). As the technology is further developed, equipment costs are decreasing, making it more accessible to conservationists.

There are now several open-source software's available for analysing recordings and identifying species (e.g., Arbimon, Rainforest Connection 2021; Audacity, Audacity Team 2021; and Raven, The Cornell Lab 2021) and as more data are collected and analysed, the performance of these algorithms will be improved as more species sounds are identified and added to their databases. This method can be used to identify changes in biodiversity levels and community composition along the gradient moving from the edge to interior, providing more in-depth information about the ecological consequences of forest edge effects.

Forest edges are likely to be linked to other forms of anthropogenic disturbance. During this study evidence was found of people entering the forest for resource extraction, including fishing, hunting of birds and mammals, and removal of tree sap. Almost all of this was observed less than one km from the forest boundary, or close to the larger old logging trails. All instances of non-researchers being recorded on camera traps were either at the edge or at 500m. This demonstrates that the impacts of edge effects on mammals are numerous, complex, and interlinked. Further work on human disturbances within the protected forest at Sikundur is needed to quantify the levels of hunting within the area, identify which species are being harvested and at what levels, and determine what the effect of this is on populations in the area.

References

- Abdullah, A., Sayuti, A., Hasanuddin, H., Affan, M., and Wilson, G., 2019. People's perceptions of elephant conservation and the human-elephant conflict in Aceh Jaya, Sumatra, Indonesia. *European Journal of Wildlife Research*, 65 (5), 69.
- Abram, N. K., Meijaard, E., Wells, J. A., Ancrenaz, M., Pellier, A.-S., Runting, R. K., Gaveau, D., Wich, S., Nardiyono, Tjiu, A., Nurcahyo, A., and Mengersen, K., 2015. Mapping perceptions of species' threats and population trends to inform conservation efforts: the Bornean orangutan case study. *Diversity and Distributions*, 21 (5), 487–499.
- Ahumada, J. A., Hurtado, J., and Lizcano, D., 2013. Monitoring the Status and Trends of Tropical Forest Terrestrial Vertebrate Communities from Camera Trap Data: A Tool for Conservation. *PLoS ONE*, 8 (9), e73707.
- Allan, J. R., Watson, J. E. M., di Marco, M., O'Bryan, C. J., Possingham, H. P., Atkinson, S. C., and Venter, O., 2019. Hotspots of human impact on threatened terrestrial vertebrates. *PLoS Biology*, 17 (3).
- Allen, M. L., Sibarani, M. C., & Krofel, M. (2021). Predicting preferred prey of Sumatran tigers *Panthera tigris sumatrae* via spatio-temporal overlap. *Oryx*, 55(2), 197–203. <https://doi.org/10.1017/S0030605319000577>
- Ancrenaz, M., Oram, F., Ambu, L., Lackman, I., Ahmad, E., Elahan, H., Kler, H., Abram, N. K., and Meijaard, E., 2015. Of Pongo, palms and perceptions: a multidisciplinary assessment of Bornean orangutans *Pongo pygmaeus* in an oil palm context. *Oryx*, 49 (03), 465–472.
- Antón Fernández, C., 2019. sitreeE: Sitree Extensions. [online]. Available from: <https://CRAN.R-project.org/package=sitreeE>.
- Arroyo-Rodríguez, V., Saldaña-Vázquez, R. A., Fahrig, L., and Santos, B. A., 2017. Does forest fragmentation cause an increase in forest temperature? *Ecological Research*, 32 (1), 81–88.

- Ashcroft, M. B., 2010. Identifying refugia from climate change. *Journal of Biogeography*, 37 (8), 1407–1413.
- Ashcroft, M. B., Chisholm, L. A., & French, K. O. (2008). The effect of exposure on landscape scale soil surface temperatures and species distribution models. *Landscape Ecology*, 23(2), 211–225. <https://doi.org/10.1007/s10980-007-9181-8>
- Ashcroft, M. B. and Gollan, J. R., 2011. Fine-resolution (25 m) topoclimatic grids of near-surface (5 cm) extreme temperatures and humidities across various habitats in a large (200 × 300 km) and diverse region. *International Journal of Climatology*, 32 (14), 2134–2148.
- Ashcroft, M. B., Gollan, J. R., Warton, D. I., and Ramp, D., 2012. A novel approach to quantify and locate potential microrefugia using topoclimate, climate stability, and isolation from the matrix. *Global Change Biology* [online], 18 (6), 1866–1879. Available from: <https://onlinelibrary.wiley.com/doi/full/10.1111/j.1365-2486.2012.02661.x> [Accessed 8 Jul 2020].
- Asner, G. P., Loarie, S. R., and Heyder, U., 2010. Combined effects of climate and land-use change on the future of humid tropical forests. *Conservation Letters*, 3, 395–403.
- Astuti, R. and McGregor, A., 2015. Governing carbon, transforming forest politics: A case study of Indonesia’s REDD+ Task Force. *Asia Pacific Viewpoint*, 56 (1), 21–36.
- Audacity Team, 2021. Audacity(R): Free Audio Editor and Recorder. [online]. Available from: <https://www.audacityteam.org/> [Accessed 25 May 2021].
- Azhar, B., Saadun, N., Puan, C. L., Kamarudin, N., Aziz, N., Nurhidayu, S., and Fischer, J., 2015. Promoting landscape heterogeneity to improve the biodiversity benefits of certified palm oil production: Evidence from Peninsular Malaysia. *Global Ecology and Conservation*, 3, 553–561.

- Barlow, J., Gardner, T. A., Araujo, I. S., Ávila-Pires, T. C., Bonaldo, A. B., Costa, J. E., Esposito, M. C., Ferreira, L. v., Hawes, J., Hernandez, M. I. M., Hoogmoed, M. S., Leite, R. N., Lo-Man-Hung, N. F., Malcolm, J. R., Martins, M. B., Mestre, L. A. M., Miranda-Santos, R., Nunes-Gutjahr, A. L., Overal, W. L., Parry, L., Peters, S. L., Ribeiro, M. A., da Silva, M. N. F., da Silva Motta, C., and Peres, C. A., 2007. Quantifying the biodiversity value of tropical primary, secondary, and plantation forests. *Proceedings of the National Academy of Sciences of the United States of America*, 104 (47), 18555–18560.
- Barlow, J., Lennox, G. D., Ferreira, J., Berenguer, E., Lees, A. C., Nally, R. mac, Thomson, J. R., Ferraz, S. F. D. B., Louzada, J., Oliveira, V. H. F., Parry, L., Ribeiro De Castro Solar, R., Vieira, I. C. G., Aragaõ, L. E. O. C., Begotti, R. A., Braga, R. F., Cardoso, T. M., Jr, R. C. D. O., Souza, C. M., Moura, N. G., Nunes, S. S., Siqueira, J. V., Pardini, R., Silveira, J. M., Vaz-De-Mello, F. Z., Veiga, R. C. S., Venturieri, A., and Gardner, T. A., 2016. Anthropogenic disturbance in tropical forests can double biodiversity loss from deforestation. *Nature*.
- Barton, K., 2020. MuMIn: Multi-Model Inference. [online]. Available from: <https://CRAN.R-project.org/package=MuMIn>.
- Bentley, B. P., Kearney, M. R., Whiting, S. D., and Mitchell, N. J., 2020. Microclimate modelling of beach sand temperatures reveals high spatial and temporal variation at sea turtle rookeries. *Journal of Thermal Biology*, 88, 102522.
- Bernard, A. B. and Marshall, A. J., 2020. Assessing the state of knowledge of contemporary climate change and primates. *Evolutionary Anthropology: Issues, News, and Reviews*, 29 (6), 317–331.
- Bisi, F., Gagliardi, A., Cremonesi, G., Colombo, R., Mazzamuto, M. V., Wauters, L. A., Preatoni, D. G., and Martinoli, A., 2019. Distribution of Wildlife and Illegal Human Activities in the Lampi Marine National Park (Myanmar). *Environmental Conservation*, 46 (2), 163–170.
- Blonder, B., Both, S., Coomes, D. A., Elias, D., Jucker, T., Kvasnica, J., Majalap, N., Malhi, Y. S., Milodowski, D., Riutta, T., and Svátek, M., 2018. Extreme and Highly

Heterogeneous Microclimates in Selectively Logged Tropical Forests. *Frontiers in Forests and Global Change*, 1, 5.

Bogoni, J. A., Peres, C. A., and Ferraz, K. M. P. M. B., 2020. Extent, intensity and drivers of mammal defaunation: a continental-scale analysis across the Neotropics. *Scientific Reports*, 10 (1), 14750.

Bolt, L. M., Schreier, A. L., Voss, K. A., Sheehan, E. A., Barrickman, N. L., Pryor, N. P., and Barton, M. C., 2018. The influence of anthropogenic edge effects on primate populations and their habitat in a fragmented rainforest in Costa Rica. *Primates*, 59 (3), 301–311.

Bonebrake, T. C., Brown, C. J., Bell, J. D., Blanchard, J. L., Chauvenet, A., Champion, C., Chen, I.-C., Clark, T. D., Colwell, R. K., Danielsen, F., Dell, A. I., Donelson, J. M., Evengård, B., Ferrier, S., Frusher, S., Garcia, R. A., Griffis, R. B., Hobday, A. J., Jarzyna, M. A., Lee, E., Lenoir, J., Linnetved, H., Martin, V. Y., McCormack, P. C., McDonald, J., McDonald-Madden, E., Mitchell, N., Mustonen, T., Pandolfi, J. M., Pettorelli, N., Possingham, H., Pulsifer, P., Reynolds, M., Scheffers, B. R., Sorte, C. J. B., Strugnell, J. M., Tuanmu, M.-N., Twiname, S., Vergés, A., Villanueva, C., Wapstra, E., Wernberg, T., and Pecl, G. T., 2018. Managing consequences of climate-driven species redistribution requires integration of ecology, conservation and social science. *Biological Reviews*, 93 (1), 284–305.

Boutin, S. and Lane, J. E., 2014. Climate change and mammals: evolutionary versus plastic responses. *Evolutionary Applications*, 7 (1), 29–41.

Bradshaw, C. J., Sodhi, N. S., and Brook, B. W., 2009. Tropical turmoil: a biodiversity tragedy in progress. *Frontiers in Ecology and the Environment*, 7 (2), 79–87.

Braidwood, D. W., Taggart, M. A., Smith, M., and Andersen, R., 2018. Translocations, conservation, and climate change: use of restoration sites as protorefuges and protorefugia. *Restoration Ecology*, 26 (1), 20–28.

Bramer, I., Anderson, B., Bennie, J., Bladon, A., Frenne, P. de, Hemming, D., Hill, R. A., Kearney, M. R., Korner, C., Korstjens, A. H., Lenoir, J., Marsh, C. D., Morecroft,

- M. D., Slater, H. D., Suggitt, A. J., Zellweger, F., and Gillingham, P. K., 2018. Advances in Monitoring and Modelling Climate at Ecologically Relevant Scales. *Advances in Ecological Research*, 58, 101–161.
- Bramer, I., Newton, A., Korstjens, A. H., and Gillingham, P. K., 2020. A global meta-analysis of forest microclimatic edge-effects. (under review). *Agricultural and Forest Meteorology*.
- Branton, M. and Richardson, J. S., 2011. Assessing the Value of the Umbrella-Species Concept for Conservation Planning with Meta-Analysis. *Conservation Biology*, 25 (1), 9–20.
- Briscoe, N. J., Handasyde, K. A., Griffiths, S. R., Porter, W. P., Krockenberger, A., and Kearney, M. R., 2014. Tree-hugging koalas demonstrate a novel thermoregulatory mechanism for arboreal mammals. *Biology letters*, 10 (20140235).
- Briscoe, N. J., Kearney, M. R., Taylor, C. A., and Wintle, B. A., 2016. Unpacking the mechanisms captured by a correlative species distribution model to improve predictions of climate refugia. *Global Change Biology*, 22 (7), 2425–2439.
- Broadbent, E. N., Asner, G. P., Keller, M., Knapp, D. E., Oliveira, P. J. C., and Silva, J. N., 2008. Forest fragmentation and edge effects from deforestation and selective logging in the Brazilian Amazon. *Biological Conservation*, 141 (7), 1745–1757.
- Brodie, J. F., 2016. Synergistic effects of climate change and agricultural land use on mammals. *Frontiers in Ecology and the Environment*, 14 (1), 20–26.
- Brodie, J. F., Giordano, A. J., and Ambu, L., 2015. Differential responses of large mammals to logging and edge effects. *Mammalian Biology*, 80, 7–13.
- Brooks, M. E., Kristensen, K., van Benthem, K. J., Magnusson, A., Berg, C. W., Nielsen, A., Skaug, H. J., Maechler, M., and Bolker, B. M., 2017. glmmTMB balances speed and flexibility among packages for zero-inflated Generalized Linear Mixed Modelling. *The R journal*, 9 (2), 378–400.

- Brozovic, R., Abrams, J. F., Mohamed, A., Wong, S. T., Niedballa, J., Bhagwat, T., Sollmann, R., Mannan, S., Kissing, J., and Wilting, A., 2018. Effects of forest degradation on the moonrat *Echinosorex gymnura* in Sabah, Malaysian Borneo. *Mammalian Biology*, 93, 135–143.
- Bruner, A. G., Gullison, R. E., and Balmford, A., 2004. *Financial Costs and Shortfalls of Managing and Expanding Protected-Area Systems in Developing Countries*. BioScience. Oxford Academic.
- Bryson, J. J., Ando, Y., and Lehmann, H., 2007. Agent-based modelling as scientific method: A case study analysing primate social behaviour. *Philosophical Transactions of the Royal Society B: Biological Sciences*, 362 (1485), 1685–1698.
- Burivalova, Z., Miteva, D., Salafsky, N., Butler, R. A., and Wilcove, D. S., 2019. Evidence Types and Trends in Tropical Forest Conservation Literature. *Trends in Ecology & Evolution*, 34 (7), 669–679.
- Burkett-Cadena, N. D. and Vittor, A. Y., 2017. Deforestation and vector-borne disease: Forest conversion favors important mosquito vectors of human pathogens. *Basic and Applied Ecology*.
- Camargo-Sanabria, A. A., Mendoza, E., Guevara, R., Martinez-Ramos, M., and Dirzo, R., 2014. Experimental defaunation of terrestrial mammalian herbivores alters tropical rainforest understorey diversity. *Proceedings of the Royal Society B: Biological Sciences*, 282 (1800), 20142580–20142580.
- Campbell, M. J., Edwards, W., Magrath, A., Laurance, S. G., Alamgir, M., Porolak, G., and Laurance, W. F., 2017. Forest edge disturbance increases rattan abundance in tropical rain forest fragments. *Scientific Reports*, 7 (6071).
- Campbell-Smith, G., Sembiring, R., and Linkie, M., 2012. Evaluating the effectiveness of human-orangutan conflict mitigation strategies in Sumatra. *Journal of Applied Ecology*, 49 (2), 367–375.

- Campos-Arceiz, A. and Blake, S., 2011. Megagardeners of the forest – the role of elephants in seed dispersal. *Acta Oecologica*, 37 (6), 542–553.
- Caravaggi, A., Banks, P. B., Burton, A. C., Finlay, C. M. V., Haswell, P. M., Hayward, M. W., Rowcliffe, M. J., and Wood, M. D., 2017. A review of camera trapping for conservation behaviour research. *Remote Sensing in Ecology and Conservation*.
- Carne, C., Semple, S., and Lehmann, J., 2012. The Effects of Climate Change on Orangutans: A Time Budget Model. In: Druyan, L., ed. *Climate Models*. InTech, 314–336.
- Carvalho, J. S., Graham, B., Rebelo, H., Bocksberger, G., Meyer, C. F. J., Wich, S., and Kühl, H. S., 2019. A global risk assessment of primates under climate and land use/cover scenarios. *Global Change Biology*, 25 (9), 3163–3178.
- Carvalho, J. S., Meyer, C. F. J., Vicente, L., and Marques, T. A., 2015. Where to nest? Ecological determinants of chimpanzee nest abundance and distribution at the habitat and tree species scale. *American Journal of Primatology* [online], 77 (2), 186–199. Available from: <http://doi.wiley.com/10.1002/ajp.22321> [Accessed 22 Sep 2017].
- Castillo-Contreras, R., Carvalho, J., Serrano, E., Mentaberre, G., Fernández-Aguilar, X., Colom, A., González-Crespo, C., Lavín, S., and López-Olvera, J. R., 2018. Urban wild boars prefer fragmented areas with food resources near natural corridors. *Science of the Total Environment*, 615, 282–288.
- Cavaleri, M. A., Reed, S. C., Smith, W. K., and Wood, T. E., 2015. Urgent need for warming experiments in tropical forests. *Global Change Biology*, 21 (6), 2111–2121.
- Cavallo, C., Dempster, T., Kearney, M. R., Kelly, E., Booth, D., Hadden, K. M., and Jessop, T. S., 2015. Predicting climate warming effects on green turtle hatchling viability and dispersal performance. *Functional Ecology*, 29 (6), 768–778.

- Chen, I.-C., Hill, J. K., Ohlemüller, R., Roy, D. B., and Thomas, C. D., 2011. Rapid range shifts of species associated with high levels of climate warming. *Science*, 333 (6045), 1024–6.
- Chen, Y. and Peng, S., 2017. Evidence and mapping of extinction debts for global forest-dwelling reptiles, amphibians and mammals. *Scientific Reports*, 7 (1), 1–10.
- Choi, F., Gouhier, T., Lima, F., Rilov, G., Seabra, R., and Helmuth, B., 2019. Mapping physiology: Biophysical mechanisms define scales of climate change impacts. *Conservation Physiology*, 7 (1), 1–18.
- Cilulko, J., Janiszewski, P., Bogdaszewski, M., and Szczygielska, E., 2013. Infrared thermal imaging in studies of wild animals. *European Journal of Wildlife Research*.
- Clark, N. J., Seddon, J. M., Šlapeta, J., and Wells, K., 2018. Parasite spread at the domestic animal - wildlife interface: anthropogenic habitat use, phylogeny and body mass drive risk of cat and dog flea (*Ctenocephalides* spp.) infestation in wild mammals. *Parasites & Vectors*, 11 (1), 8.
- Collins, N. J., 2018. Sumatran elephant *Elephas maximus sumatranus* density and habitat use in relation to forest characteristics in the Leuser Ecosystem, North Sumatra. [online]. Available from: <http://eprints.bournemouth.ac.uk/31522/> [Accessed 3 Mar 2020].
- Condro, A. A., Prasetyo, L. B., and Rushayati, S. B., 2019. Short-term projection of Bornean orangutan spatial distribution based on climate and land cover change scenario. In: *Sixth International Symposium on LAPAN-IPB Satellite*. SPIE-Intl Soc Optical Eng, 113721B-undefined.
- Conrad, O., Bechtel, B., Bock, M., Dietrich, H., Fischer, E., Gerlitz, L., Wehberg, J., Wichmann, V., and Böhner, J., 2015. System for Automated Geoscientific Analyses (SAGA) v. 2.1.4. *Geoscientific Model Development*, 8 (7), 1991–2007.
- Costantini, D., Edwards, D. P., and Simons, M. J. P., 2016. Life after logging in tropical forests of Borneo: A meta-analysis. *Biological Conservation*, 196, 182–188.

- Cristoffer, C. and Peres, C. A., 2003. Elephants versus butterflies: the ecological role of large herbivores in the evolutionary history of two tropical worlds. *Journal of Biogeography*, 30, 1357–1380.
- Crooks, K. R., 2002. Relative sensitivities of mammalian carnivores to habitat fragmentation. *Conservation Biology*, 16 (2), 488–502.
- Crooks, K. R., Burdett, C. L., Theobald, D. M., King, S. R. B., Di Marco, M., Rondinini, C., and Boitani, L., 2017. Quantification of habitat fragmentation reveals extinction risk in terrestrial mammals. *Proceedings of the National Academy of Sciences of the United States of America*, 114 (29), 7635–7640.
- Curtis, P. G., Slay, C. M., Harris, N. L., Tyukavina, A., and Hansen, M. C., 2018. Classifying drivers of global forest loss. *Science*, 361 (6407), 1108–1111.
- Daily, G. C., Polasky, S., Goldstein, J., Kareiva, P. M., Mooney, H. A., Pejchar, L., Ricketts, T. H., Salzman, J., and Shallenberger, R., 2009. Ecosystem services in decision making: time to deliver. *Frontiers in Ecology and the Environment*, 7 (1), 21–28.
- Daly, C., 2006. Guidelines for assessing the suitability of spatial climate data sets. *International Journal of Climatology*, 26 (6), 707–721.
- Davidson, A. D., Shoemaker, K. T., Weinstein, B., Costa, G. C., Brooks, T. M., Ceballos, G., Radeloff, V. C., Rondinini, C., and Graham, C. H., 2017. Geography of current and future global mammal extinction risk. *PLOS ONE*, 12 (11), e0186934.
- Davies, A. B., Ancrenaz, M., Oram, F., and Asner, G. P., 2017. Canopy structure drives orangutan habitat selection in disturbed Bornean forests. *Proceedings of the National Academy of Sciences of the United States of America* [online], 114 (31), 8307–8312. Available from: <http://www.ncbi.nlm.nih.gov/pubmed/28720703> [Accessed 6 Feb 2018].

- Davis, K. T., Dobrowski, S. Z., Holden, Z. A., Higuera, P. E., and Abatzoglou, J. T., 2019. Microclimatic buffering in forests of the future: the role of local water balance. *Ecography*, 42, 1–11.
- Dawson, T. P., Jackson, S. T., House, J. I., Prentice, I. C., and Mace, G. M., 2011. Beyond predictions: Biodiversity conservation in a changing climate. *Science*, 332 (6025), 53–58.
- Dent, D. H. and Wright, S. J., 2009. The future of tropical species in secondary forests: A quantitative review. *Biological Conservation*.
- Deutsch, C. A., Tewksbury, J. J., Huey, R. B., Sheldon, K. S., Ghalambor, C. K., Haak, D. C., and Martin, P. R., 2008. Impacts of climate warming on terrestrial ectotherms across latitude. *Proceedings of the National Academy of Sciences of the United States of America*, 105 (18), 6668–6672.
- digiKam, 2021. *digiKam* [online]. Available from: <https://www.digikam.org/> [Accessed 25 May 2021].
- Dillon, M. E., Wang, G., and Huey, R. B., 2010. Global metabolic impacts of recent climate warming. *Nature*, 467 (7316), 704–706.
- Dingman, J. R., Sweet, L. C., McCullough, I., Davis, F. W., Flint, A., Franklin, J., and Flint, L. E., 2013. Cross-scale modeling of surface temperature and tree seedling establishment in mountain landscapes. *Ecological Processes*, 2 (1), 30.
- Dobrowski, S. Z., Abatzoglou, J. T., Greenberg, J. A., and Schladow, S. G., 2009. How much influence does landscape-scale physiography have on air temperature in a mountain environment? *Agricultural and Forest Meteorology*, 149 (10), 1751–1758.
- Dunn, R. R., 2004. Recovery of Faunal Communities During Tropical Forest Regeneration. *Conservation Biology*, 18 (2), 302–309.
- Ehrlén, J. and Morris, W. F., 2015. Predicting changes in the distribution and abundance of species under environmental change. *Ecology Letters*, 18 (3), 303–314.

- Elith, J. and Leathwick, J. R., 2009. Species Distribution Models: Ecological Explanation and Prediction Across Space and Time. *Annual Review of Ecology, Evolution, and Systematics*, 40 (1), 677–697.
- Englhart, S., Jubanski, J., and Siegert, F., 2013. Quantifying Dynamics in Tropical Peat Swamp Forest Biomass with Multi-Temporal LiDAR Datasets. *Remote Sensing* [online], 5 (5), 2368–2388. Available from: <http://www.mdpi.com/2072-4292/5/5/2368/> [Accessed 9 Jan 2018].
- Enriquez-Urzelai, U., Kearney, M. R., Nicieza, A. G., and Tingley, R., 2019. Integrating mechanistic and correlative niche models to unravel range-limiting processes in a temperate amphibian. *Global Change Biology*, 25 (8), 2633–2647.
- Enriquez-Urzelai, U., Tingley, R., Kearney, M. R., Sacco, M., Palacio, A. S., Tejedo, M., and Nicieza, A. G., 2020. The roles of acclimation and behaviour in buffering climate change impacts along elevational gradients. *Journal of Animal Ecology*, 89 (7), 1722–1734.
- Eppley, T. M., Donati, G., and Ganzhorn, J. U., 2016. Unusual sleeping site selection by southern bamboo lemurs. *Primates* [online], 57, 167–173. Available from: <https://link.springer.com/content/pdf/10.1007%2Fs10329-016-0516-4.pdf> [Accessed 12 Oct 2017].
- ESRI, 2010. ArcGIS Pro | 2D, 3D & 4D GIS Mapping Software. [online]. Available from: <https://www.esri.com/en-us/arcgis/products/arcgis-pro/overview> [Accessed 25 May 2021].
- Estrada, A., Garber, P. A., Rylands, A. B., Roos, C., Fernandez-Duque, E., di Fiore, A., Nekaris, K. A.-I., Nijman, V., Heymann, E. W., Lambert, J. E., Rovero, F., Barelli, C., Setchell, J. M., Gillespie, T. R., Mittermeier, R. A., Arregoitia, L. V., de Guinea, M., Gouveia, S., Dobrovolski, R., Shanee, S., Shanee, N., Boyle, S. A., Fuentes, A., MacKinnon, K. C., Amato, K. R., Meyer, A. L. S., Wich, S., Sussman, R. W., Pan, R., Kone, I., and Li, B., 2017. Impending extinction crisis of the world's primates: Why primates matter. *Science Advances* [online], 3 (1), e1600946. Available from: <https://advances.sciencemag.org/lookup/doi/10.1126/sciadv.1600946>.

- Estrada, A., Morales-Castilla, I., Caplat, P., and Early, R., 2016. Usefulness of Species Traits in Predicting Range Shifts. *Trends in Ecology & Evolution* [online], 31 (3), 190–203. Available from: <https://linkinghub.elsevier.com/retrieve/pii/S0169534715003262> [Accessed 24 Jun 2019].
- Evans, L. N., 2009. Roosting behaviour of urban microbats: the influence of ectoparasites, roost microclimate and sociality. [online]. Available from: <https://minerva-access.unimelb.edu.au/handle/11343/35319> [Accessed 30 Jan 2018].
- Ewers, R. M. and Banks-Leite, C., 2013. Fragmentation Impairs the Microclimate Buffering Effect of Tropical Forests. *PLoS ONE*, 8 (3), e58093.
- Farris, Z. J., Gerber, B. D., Valenta, K., Rafaliarison, R., Razafimahaimodison, J. C., Larney, E., Rajaonarivelo, T., Randriana, Z., Wright, P. C., and Chapman, C. A., 2017. Threats to a rainforest carnivore community: A multi-year assessment of occupancy and co-occurrence in Madagascar. *Biological Conservation*, 210, 116–124.
- Faye, E., Herrera, M., Bellomo, L., Silvain, J.-F., and Dangles, O., 2014. Strong Discrepancies between Local Temperature Mapping and Interpolated Climatic Grids in Tropical Mountainous Agricultural Landscapes. *PLoS ONE*, 9 (8), e105541.
- Feeley, K. J., Stroud, J. T., and Perez, T. M., 2017. Most ‘global’ reviews of species’ responses to climate change are not truly global. *Diversity and Distributions*, 23 (3), 231–234.
- Fitzpatrick, M. J., Zuckerberg, B., Pauli, J. N., Kearney, M. R., Thompson, K. L., Werner, L. C., and Porter, W. P., 2019. Modeling the distribution of niche space and risk for a freeze-tolerant ectotherm, *Lithobates sylvaticus*. *Ecosphere*, 10 (7).
- Flint, L. E. and Flint, A. L., 2012. Downscaling future climate scenarios to fine scales for hydrologic and ecological modeling and analysis. *Ecological Processes*, 1 (1), 1–15.

- Foden, W. B., Young, B. E., Akçakaya, H. R., Garcia, R. A., Hoffmann, A. A., Stein, B. A., Thomas, C. D., Wheatley, C. J., Bickford, D., Carr, J. A., Hole, D. G., Martin, T. G., Pacifici, M., Pearce-Higgins, J. W., Platts, P. J., Visconti, P., Watson, J. E. M., and Huntley, B., 2019. Climate change vulnerability assessment of species. *Wiley Interdisciplinary Reviews: Climate Change*, 10 (1), e551.
- de Frenne, P., Zellweger, F., Rodríguez-Sánchez, F., Scheffers, B. R., Hylander, K., Luoto, M., Vellend, M., Verheyen, K., and Lenoir, J., 2019. Global buffering of temperatures under forest canopies. *Nature Ecology & Evolution*, 3 (5), 744–749.
- Frey, S. J. K., Hadley, A. S., and Betts, M. G., 2016. Microclimate predicts within-season distribution dynamics of montane forest birds. *Diversity and Distributions*, 22 (9), 944–959.
- Frey, S. J. K., Hadley, A. S., Johnson, S. L., Schulze, M., Jones, J. A., and Betts, M. G., 2016a. Spatial models reveal the microclimatic buffering capacity of old-growth forests. *Science Advances*, 2 (4), e1501392.
- Frey, S. J. K., Hadley, A. S., Johnson, S. L., Schulze, M., Jones, J. A., and Betts, M. G., 2016b. Spatial models reveal the microclimatic buffering capacity of old-growth forests. *Science Advances*, 2 (4), e1501392.
- Fridley, J. D., 2009. Downscaling Climate over Complex Terrain: High Finescale (<1000 m) Spatial Variation of Near-Ground Temperatures in a Montane Forested Landscape (Great Smoky Mountains)*. *Journal of Applied Meteorology and Climatology*, 48 (5), 1033–1049.
- Fruth, B. I., 2017. Great Ape Nest-Building. In: *The International Encyclopedia of Primatology* [online]. Hoboken, NJ, USA: John Wiley & Sons, Inc., 1–3. Available from: <http://doi.wiley.com/10.1002/9781119179313.wbprim0294> [Accessed 6 Feb 2018].
- Fuller, A., Dawson, T., Helmuth, B., Hetem, R. S., Mitchell, D., and Maloney, S. K., 2010. Physiological mechanisms in coping with climate change. *Physiological and Biochemical Zoology*, 83 (5), 713–720.

- Fung, E., Imbach, P., Corrales, L., Vilchez, S., Zamora, N., Argotty, F., Hannah, L., and Ramos, Z., 2017. Mapping conservation priorities and connectivity pathways under climate change for tropical ecosystems. *Climatic Change*, 141 (1), 77–92.
- Galetti, M. and Dirzo, R., 2013. Ecological and evolutionary consequences of living in a defaunated world. *Biological Conservation*, 163, 1–6.
- Gardner, A. S., Maclean, I. M. D., and Gaston, K. J., 2019. Climatic predictors of species distributions neglect biophysiological meaningful variables. *Diversity and Distributions*, 25 (8), 1318–1333.
- Gardner, T. A., Barlow, J., Chazdon, R., Ewers, R. M., Harvey, C. A., Peres, C. A., and Sodhi, N. S., 2009a. Prospects for tropical forest biodiversity in a human-modified world. *Ecology Letters* [online], 12 (6), 561–582. Available from: <http://doi.wiley.com/10.1111/j.1461-0248.2009.01294.x> [Accessed 2 Mar 2021].
- Gardner, T. A., Barlow, J., Chazdon, R., Ewers, R. M., Harvey, C. A., Peres, C. A., and Sodhi, N. S., 2009b. Prospects for tropical forest biodiversity in a human-modified world. *Ecology Letters*, 12 (6), 561–582.
- Gaston, K. J., 2000. Global patterns in biodiversity. *Nature*, 405, 220–227.
- Gaudio, N., Gendre, X., Saudreau, M., Seigner, V., and Balandier, P., 2017. Impact of tree canopy on thermal and radiative microclimates in a mixed temperate forest: A new statistical method to analyse hourly temporal dynamics. *Agricultural and Forest Meteorology*, 237–238, 71–79.
- Geiger, R., 1971. *The Climate Near the Ground*. Harvard University Press.
- Gerber, B. D., Karpanty, S. M., and Randrianantenaina, J., 2012. The impact of forest logging and fragmentation on carnivore species composition, density and occupancy in Madagascar's rainforests. *ORYX*, 46 (3), 414–422.
- Gibson, L., Lee, T. M., Koh, L. P., Brook, B. W., Gardner, T. A., Barlow, J., Peres, C. A., Bradshaw, C. J. A. A., Laurance, W. F., Lovejoy, T. E., and Sodhi, N. S., 2011.

Primary forests are irreplaceable for sustaining tropical biodiversity. *Nature*, 478 (7369), 378–381.

Gillingham, P. K., Huntley, B., Kunin, W. E., and Thomas, C. D., 2012. The effect of spatial resolution on projected responses to climate warming. *Diversity and Distributions*, 18 (10), 990–1000.

Global Forest Watch, 2018. *Tree cover loss in Indonesia* [online]. Available from: <https://www.globalforestwatch.org/> [Accessed 1 Jul 2019].

Graham, T. L., Matthews, H. D., and Turner, S. E., 2016. A Global-Scale Evaluation of Primate Exposure and Vulnerability to Climate Change. *International Journal of Primatology*.

Gregory, S. D., Brook, B. W., Goossens, B., Ancrenaz, M., Alfred, R., Ambu, L. N., and Fordham, D. A., 2012. Long-Term Field Data and Climate-Habitat Models Show That Orangutan Persistence Depends on Effective Forest Management and Greenhouse Gas Mitigation. *PLoS ONE*, 7 (9), e43846.

Guisan, A., Tingley, R., Baumgartner, J. B., Naujokaitis-Lewis, I., Sutcliffe, P. R., Tulloch, A. I. T., Regan, T. J., Brotons, L., McDonald-Madden, E., Mantyka-Pringle, C., Martin, T. G., Rhodes, J. R., Maggini, R., Setterfield, S. A., Elith, J., Schwartz, M. W., Wintle, B. A., Broennimann, O., Austin, M., Ferrier, S., Kearney, M. R., Possingham, H. P., and Buckley, Y. M., 2013. Predicting species distributions for conservation decisions. *Ecology Letters*, 16 (12), 1424–1435.

Haddad, N. M., Brudvig, L. A., Clobert, J., Davies, K. F., Gonzalez, A., Holt, R. D., Lovejoy, T. E., Sexton, J. O., Austin, M. P., Collins, C. D., Cook, W. M., Damschen, E. I., Ewers, R. M., Foster, B. L., Jenkins, C. N., King, A. J., Laurance, W. F., Levey, D. J., Margules, C. R., Melbourne, B. A., Nicholls, A. O., Orrock, J. L., Song, D.-X., and Townshend, J. R., 2015. Habitat fragmentation and its lasting impact on Earth's ecosystems. *Science Advances*, 1 (2), e1500052.

- Haider, N., Kirkeby, C., Kristensen, B., Kjær, L. J., Sørensen, J. H., and Bødker, R., 2017. Microclimatic temperatures increase the potential for vector-borne disease transmission in the Scandinavian climate. *Scientific Reports*, 7 (1), 8175.
- Hamard, M., Cheyne, S. M., and Nijman, V., 2010. Vegetation correlates of gibbon density in the peat-swamp forest of the Sabangau catchment, Central Kalimantan, Indonesia. *American journal of primatology*, 72 (7), 607–16.
- Hamner, B. and Frasco, M., 2018. Metrics: Evaluation Metrics for Machine Learning. R package version 0.1.4. [online]. Available from: <https://CRAN.R-project.org/package=Metrics>.
- Hankinson, E. L., Hill, R. A., Marsh, C. D., Nowak, M. G., Abdullah, A., Pasaribu, N., Supriadi, Nijman, V., Cheyne, S. M., and Korstjens, A. H., 2021. Influences of Forest Structure on the Density and Habitat Preference of Two Sympatric Gibbons (*Symphalangus syndactylus* and *Hylobates lar*). *International Journal of Primatology*, 42 (2), 237–261.
- Hannah, L. and Lovejoy, T., 2007. Conservation, climate change, and tropical forests. In: Bush, M., Flenley, J., and Gosling, W., eds. *Tropical Rainforest Responses to Climatic Change*. Springer Berlin Heidelberg, 367–378.
- Hardwick, S. R., Toumi, R., Pfeifer, M., Turner, E. C., Nilus, R., and Ewers, R. M., 2015. The relationship between leaf area index and microclimate in tropical forest and oil palm plantation: Forest disturbance drives changes in microclimate. *Agricultural and Forest Meteorology*, 201, 187–195.
- Harrison, S. and Noss, R., 2017. Endemism hotspots are linked to stable climatic refugia. *Annals of Botany*, 119 (2), 207–214.
- Harrison, X. A., Donaldson, L., Correa-Cano, M. E., Evans, J., Fisher, D. N., Goodwin, C. E. D., Robinson, B. S., Hodgson, D. J., and Inger, R., 2018. A brief introduction to mixed effects modelling and multi-model inference in ecology. *PeerJ*, 6 (5), e4794.

- Hedges, S., Tyson, M. J., Sitompul, A. F., Kinnaird, M. F., and Gunaryadi, D., 2005. Distribution, status, and conservation needs of Asian elephants (*Elephas maximus*) in Lampung Province, Sumatra, Indonesia. *Biological Conservation*, 124, 35–48.
- Heim, N. A., 2011. Complex Effects of Human-Impacted Landscapes on the Spatial Patterns of Mammalian Carnivores.
- Heithecker, T. D. and Halpern, C. B., 2007. Edge-related gradients in microclimate in forest aggregates following structural retention harvests in western Washington. *Forest Ecology and Management*, 248, 163–173.
- Hellmann, J. J., Prior, K. M., and Pelini, S. L., 2012. The influence of species interactions on geographic range change under climate change. *Annals of the New York Academy of Sciences*, 1249 (1), 18–28.
- Hetem, R. S., Strauss, W. M., Fick, L. G., Maloney, S. K., Meyer, L. C. R., Fuller, A., Shobrak, M., and Mitchell, D., 2012. Selective brain cooling in Arabian oryx (*Oryx Leucoryx*): A physiological mechanism for coping with aridity? *Journal of Experimental Biology*, 215 (22), 3907–3924.
- Hijmans, R. J., Cameron, S., and Parra, J., 2015. *WorldClim* [online]. Berkley, University of California. Available from: <http://worldclim.org/>.
- Hill, C. M., 2017. Primate Crop Feeding Behavior, Crop Protection, and Conservation. *International Journal of Primatology*, 38, 385–400.
- Hodgson, J. A., Thomas, C. D., Wintle, B. A., and Moilanen, A., 2009. Climate change, connectivity and conservation decision making: back to basics. *Journal of Applied Ecology*, 46 (5), 964–969.
- Husson, S. J., Wich, S. A., Marshall, A. J., Dennis, R. D., Ancrenaz, M., Brassey, R., Gumal, M., Hearn, A. J., Meijaard, E., Simorangkir, T., and Singleton, I., 2008. Orangutan distribution, density, abundance and impacts of disturbance. *In: Orangutans*. 77–96.

- Hylander, K., Ehrlén, J., Luoto, M., and Meineri, E., 2015. Microrefugia: Not for everyone. *AMBIO*, 44 (S1), 60–68.
- IPBES, 2019. *Global assessment report on biodiversity and ecosystem services of the Intergovernmental Science-Policy Platform on Biodiversity and Ecosystem Services*. Bonn, Germany.
- IPCC, 2007. *Climate Change 2007: The Physical Science Basis*. Cambridge: Cambridge University Press.
- ITIS, 2021. *Integrated Taxonomic Information System* [online]. Available from: <https://www.itis.gov/> [Accessed 25 May 2021].
- IUCN, 2008. *Extinction threat growing for mankind's closest relatives* [online]. Available from: <http://www.iucn.org/?1391/1/Extinction-threat-growing-for-mankinds-closest-relatives>.
- IUCN, 2014. *Table 4a: red list category summary for all animal classes and orders* [online]. The IUCN Red List of Threatened Species. Available from: http://www.iucnredlist.org/about/summary-statistics#Tables_3_4.
- IUCN, 2021. *Mapping Standards and Data Quality for IUCN Red List Spatial Data* [online]. Available from: <https://www.iucnredlist.org/resources/mappingstandards> [Accessed 21 May 2021].
- Iwamura, T., Guisan, A., Wilson, K. A., and Possingham, H. P., 2013. How robust are global conservation priorities to climate change? *Global Environmental Change*, 23 (5), 1277–1284.
- Jones, K. E. and Safi, K., 2011. Ecology and evolution of mammalian biodiversity. *Philosophical Transactions of the Royal Society B: Biological Sciences*, 366 (1577), 2451–2461.
- Jones, K. R., Watson, J. E. M., Possingham, H. P., and Klein, C. J., 2016. Incorporating climate change into spatial conservation prioritisation: A review. *Biological Conservation*, 194, 121–130.

- Jucker, T., Hardwick, S. R., Both, S., Elias, D. M. O., Ewers, R. M., Milodowski, D. T., Swinfield, T., and Coomes, D. A., 2018. Canopy structure and topography jointly constrain the microclimate of human-modified tropical landscapes. *Global Change Biology*, 24 (11), 5243–5258.
- Jucker, T., Jackson, T. D., Zellweger, F., Swinfield, T., Gregory, N., Williamson, J., Slade, E. M., Phillips, J. W., Bittencourt, P. R. L., Blonder, B., Boyle, M. J. W., Ellwood, M. D. F., Hemprich-Bennett, D., Lewis, O. T., Matula, R., Senior, R. A., Shenkin, A., Svátek, M., and Coomes, D. A., 2020. A Research Agenda for Microclimate Ecology in Human-Modified Tropical Forests. *Frontiers in Forests and Global Change*, 2, 92.
- Kakati, K., Raghavan, R., Chellam, R., Qureshi, Q., and Chivers, D. J., 2009. Status of Western Hoolock Gibbon (*Hoolock hoolock*) Populations in Fragmented Forests of Eastern Assam. *Primate Conservation*, 24 (1), 127–137.
- Kearney, M., 2020. NicheMapR: R implementation of Niche Mapper software for biophysical modelling.
- Kearney, M., Phillips, B. L., Tracy, C. R., Christian, K. A., Betts, G., and Porter, W. P., 2008. Modelling species distributions without using species distributions: The cane toad in Australia under current and future climates. *Ecography*, 31 (4), 423–434.
- Kearney, M. and Porter, W., 2009. Mechanistic niche modelling: combining physiological and spatial data to predict species' ranges. *Ecology Letters*, 12 (4), 334–350.
- Kearney, M. and Porter, W., n.d. *NicheMapR-an R package for biophysical modelling: the endotherm model*.
- Kearney, M. and Porter, W. P., 2004. Mapping the fundamental niche: Physiology, climate, and the distribution of a nocturnal lizard. *Ecology*, 85 (11), 3119–3131.
- Kearney, M. R., 2013. Activity restriction and the mechanistic basis for extinctions under climate warming. *Ecology Letters*, 16 (12), 1470–1479.

- Kearney, M. R., 2019. MicroclimOz – A microclimate data set for Australia, with example applications. *Austral Ecology*, 44 (3), 534–544.
- Kearney, M. R., Gillingham, P. K., Bramer, I., Duffy, J. P., and Maclean, I. M. D., 2020. A method for computing hourly, historical, terrain-corrected microclimate anywhere on earth. *Methods in Ecology and Evolution*, 11 (1), 38–43.
- Kearney, M. R., Isaac, A. P., and Porter, W. P., 2014. Microclim: Global estimates of hourly microclimate based on long-term monthly climate averages. *Scientific Data*, 1 (1), 1–9.
- Kearney, M. R., Munns, S. L., Moore, D., Malishev, M., and Bull, C. M., 2018. Field tests of a general ectotherm niche model show how water can limit lizard activity and distribution. *Ecological Monographs*, 88 (4), 672–693.
- Kearney, M. R. and Porter, W. P., 2017. NicheMapR - an R package for biophysical modelling: the microclimate model. *Ecography*, 40 (5), 664–674.
- Kearney, M. R., Porter, W. P., and Murphy, S. A., 2016. An estimate of the water budget for the endangered night parrot of Australia under recent and future climates. *Climate Change Responses*, 3 (1), 1–17.
- Kearney, M. R., Shamakhy, A., Tingley, R., Karoly, D. J., Hoffmann, A. A., Briggs, P. R., and Porter, W. P., 2014. Microclimate modelling at macro scales: A test of a general microclimate model integrated with gridded continental-scale soil and weather data. *Methods in Ecology and Evolution*, 5 (3), 273–286.
- Kearney, M. R., Simpson, S. J., Raubenheimer, D., and Kooijman, S. A. L. M., 2013. Balancing heat, water and nutrients under environmental change: a thermodynamic niche framework. *Functional Ecology*, 27 (4), 950–966.
- Kearney, M. R., Wintle, B. A., and Porter, W. P., 2010. Correlative and mechanistic models of species distribution provide congruent forecasts under climate change. *Conservation Letters*, 3 (3), 203–213.

- Keinath, D. A., Doak, D. F., Hodges, K. E., Prugh, L. R., Fagan, W., Sekercioglu, C. H., Buchar, S. H. M., and Kauffman, M., 2017. A global analysis of traits predicting species sensitivity to habitat fragmentation. *Global Ecology and Biogeography*, 26 (1), 115–127.
- Kelley, E. A., Jablonski, N. G., Chaplin, G., Sussman, R. W., and Kamilar, J. M., 2016. Behavioral thermoregulation in *Lemur catta*: The significance of sunning and huddling behaviors. *American Journal of Primatology*, 78 (7), 745–754.
- Khaliq, I., Hof, C., Prinzinger, R., Böhning-Gaese, K., and Pfenninger, M., 2014. Global variation in thermal tolerances and vulnerability of endotherms to climate change. *Proceedings of the Royal Society B: Biological Sciences*, 281 (1789), 20141097.
- Kinnaird, M. F., Sanderson, E. W., O'Brien, T. G., Wibisono, H. T., and Woolmer, G., 2003. Deforestation Trends in a Tropical Landscape and Implications for Endangered Large Mammals. *Conservation Biology*, 17 (1), 245–257.
- Knop, E., 2004. A comparison of orang-utan density in a logged and unlogged forest on Sumatra. *Biological Conservation*, 120 (2), 183–188.
- Koh, L. P. and Wich, S. A., 2012. Dawn of drone ecology : low-cost autonomous aerial vehicles for conservation. *Tropical Conservation Science*, 5 (2), 121–132.
- Korstjens, A. H. and Hillyer, A. P., 2016. Primates and climate change: a review of current knowledge. In: *An Introduction to Primate Conservation*. Oxford: Oxford University Press, 175–192.
- Korstjens, A. H., Lehmann, J., and Dunbar, R. I. M., 2010. Resting time as an ecological constraint on primate biogeography. *Animal Behaviour*, 79 (2), 361–374.
- Korstjens, A. H., Lehmann, J., and Dunbar, R. I. M., 2018. Time Constraints Do Not Limit Group Size in Arboreal Guenons but Do Explain Community Size and Distribution Patterns. *International Journal of Primatology*, 39 (4), 511–531.

- Laurance, W. F., 2004. Forest-climate interactions in fragmented tropical landscapes. *In: Philosophical Transactions of the Royal Society B: Biological Sciences*. Royal Society, 345–352.
- Laurance, W. F., Sayer, J., and Cassman, K. G., 2014. Agricultural expansion and its impacts on tropical nature. *Trends in Ecology & Evolution*, 29 (2), 107–116.
- van Leeuwen, K. L., 2019. Landscapes of the apes: Modelling landscape use of chimpanzees and early hominins across an environmental gradient. [online]. Available from: <http://eprints.bournemouth.ac.uk/32589/> [Accessed 27 May 2021].
- Lehmann, J., Korstjens, A. H., and Dunbar, R. I. M., 2008. Time and distribution : a model of ape biogeography. *Ethology Ecology & Evolution*, 20, 337–359.
- Lembrechts, J. J., Aalto, J., Ashcroft, M. B., de Frenne, P., Kopecký, M., Lenoir, J., Luoto, M., Maclean, I. M. D., Roupsard, O., Fuentes-Lillo, E., García, R. A., Pellissier, L., Pitteloud, C., Alatalo, J. M., Smith, S. W., Björk, R. G., Muffler, L., Ratier Backes, A., Cesarz, S., Gottschall, F., Okello, J., Urban, J., Plichta, R., Svátek, M., Phartyal, S. S., Wipf, S., Eisenhauer, N., Puşcaş, M., Turtureanu, P. D., Varlagin, A., Dimarco, R. D., Jump, A. S., Randall, K., Dorrepaal, E., Larson, K., Walz, J., Vitale, L., Svoboda, M., Finger Higgens, R., Halbritter, A. H., Curasi, S. R., Klupar, I., Koontz, A., Pearse, W. D., Simpson, E., Stemkovski, M., Jessen Graae, B., Vedel Sørensen, M., Høye, T. T., Fernández Calzado, M. R., Lorite, J., Carbognani, M., Tomaselli, M., Forte, T. G. W., Petraglia, A., Haesen, S., Somers, B., van Meerbeek, K., Björkman, M. P., Hylander, K., Merinero, S., Gharun, M., Buchmann, N., Dolezal, J., Matula, R., Thomas, A. D., Bailey, J. J., Ghosn, D., Kazakis, G., de Pablo, M. A., Kempainen, J., Niittynen, P., Rew, L., Seipel, T., Larson, C., Speed, J. D. M., Ardö, J., Cannone, N., Guglielmin, M., Malfasi, F., Bader, M. Y., Canessa, R., Stanisci, A., Kreyling, J., Schmeddes, J., Teuber, L., Aschero, V., Čiliak, M., Máliš, F., de Smedt, P., Govaert, S., Meeussen, C., Vangansbeke, P., Gigauri, K., Lamprecht, A., Pauli, H., Steinbauer, K., Winkler, M., Ueyama, M., Nuñez, M. A., Ursu, T. M., Haider, S., Wedegärtner, R. E. M., Smiljanic, M., Trouillier, M., Wilmking, M., Altman, J., Brúna, J., Hederová, L., Macek, M., Man, M., Wild, J., Vittoz, P., Pärtel, M., Barančok, P., Kanka, R., Kollár, J., Palaj, A., Barros, A., Mazzolari, A. C., Bauters, M., Boeckx, P., Benito Alonso, J. L., Zong, S., di Cecco,

V., Sitková, Z., Tielbörger, K., van den Brink, L., Weigel, R., Homeier, J., Dahlberg, C. J., Medinets, S., Medinets, V., de Boeck, H. J., Portillo-Estrada, M., Verryckt, L. T., Milbau, A., Daskalova, G. N., Thomas, H. J. D., Myers-Smith, I. H., Blonder, B., Stephan, J. G., Descombes, P., Zellweger, F., Frei, E. R., Heinesch, B., Andrews, C., Dick, J., Siebicke, L., Rocha, A., Senior, R. A., Rixen, C., Jimenez, J. J., Boike, J., Pauchard, A., Scholten, T., Scheffers, B., Klinges, D., Basham, E. W., Zhang, J., Zhang, Z., Géron, C., Fazlioglu, F., Candan, O., Sallo Bravo, J., Hrbacek, F., Laska, K., Cremonese, E., Haase, P., Moyano, F. E., Rossi, C., and Nijs, I., 2020. SoilTemp: A global database of near-surface temperature. *Global Change Biology*, 26 (11), 6616–6629.

Lembrechts, J. J., Lenoir, J., Roth, N., Hattab, T., Milbau, A., Haider, S., Pellissier, L., Pauchard, A., Ratier Backes, A., Dimarco, R. D., Nuñez, M. A., Aalto, J., and Nijs, I., 2019. Comparing temperature data sources for use in species distribution models: From in-situ logging to remote sensing. *Global Ecology and Biogeography*, 28 (11), 1578–1596.

Lenoir, J. and Svenning, J.-C., 2015. Climate-related range shifts - a global multidimensional synthesis and new research directions. *Ecography*, 38 (1), 15–28.

Levy, O., Dayan, T., Porter, W. P., and Kronfeld-Schor, N., 2019. Time and ecological resilience: can diurnal animals compensate for climate change by shifting to nocturnal activity? *Ecological Monographs*, 89 (1), e01334.

Linkie, M., Dinata, Y., Nofrianto, A., and Leader-Williams, N., 2007. Patterns and perceptions of wildlife crop raiding in and around Kerinci Seblat National Park, Sumatra. *Animal Conservation*, 10 (1), 127–135.

Lister, A. M. and Stuart, A. J., 2008. The impact of climate change on large mammal distribution and extinction: Evidence from the last glacial/interglacial transition. *Comptes Rendus Geoscience*, 340 (9–10), 615–620.

de los Ríos, C., Watson, J. E. M., and Butt, N., 2018. Persistence of methodological, taxonomical, and geographical bias in assessments of species' vulnerability to climate change: A review. *Global Ecology and Conservation*, 15, e00412.

- Love, K., Kurz, D. J., Vaughan, I. P., Ke, A., Evans, L. J., and Goossens, B., 2017. Bearded pig (*Sus barbatus*) utilisation of a fragmented forest–oil palm landscape in Sabah, Malaysian Borneo. *Wildlife Research*, 44 (8), 603.
- Lv, S., Zhang, Y., Steinmann, P., Yang, G., Yang, K., Zhou, X., and Utzinger, J., 2011. The emergence of angiostrongyliasis in the People’s Republic of China: the interplay between invasive snails, climate change and transmission dynamics. *Freshwater Biology*, 56 (4), 717–734.
- Mace, G. M., Reyers, B., Alkemade, R., Biggs, R., Chapin, F. S., Cornell, S. E., Díaz, S., Jennings, S., Leadley, P., Mumby, P. J., Purvis, A., Scholes, R. J., Seddon, A. W. R., Solan, M., Steffen, W., and Woodward, G., 2014. Approaches to defining a planetary boundary for biodiversity. *Global Environmental Change*, 28 (1), 289–297.
- Mace, G., Masundire, H., Baillie, J., Ricketts, T., Brooks, T., Hoffmann, M., Stuart, S., Balmford, A., Purvis, A., Reyers, B., Wang, J., Revenga, C., Kennedy, E., Naeem, S., Alkemade, R., Allnutt, T., Bakarr, M., Bond, W., Chanson, J., Cox, N., Fonseca, G., Hilton-Taylor, C., Loucks, C., Rodrigues, A., Sechrest, W., Stattersfield, A., Janse van Rensburg, B., and Whiteman, C., 2005. Biodiversity. *In: Hassan, R., Scholes, R., and Ash, N., eds. Ecosystems and Human Well-Being: Current State and Trends*. Island Press, 77–122.
- MacLarnon, A. M., Sommer, V., Goffe, A. S., Higham, J. P., Lodge, E., Tkaczynski, P., and Ross, C., 2015. Assessing adaptability and reactive scope: Introducing a new measure and illustrating its use through a case study of environmental stress in forest-living baboons. *General and Comparative Endocrinology*, 215, 10–24.
- Maclean, I. M. D., Hopkins, J. J., Bennie, J., Lawson, C. R., and Wilson, R. J., 2015. Microclimates buffer the responses of plant communities to climate change. *Global Ecology and Biogeography*, 24 (11), 1340–1350.
- Maclean, I. M. D. and Klinges, D., 2021. microclimc: Below or above canopy microclimate modelling with R. [online]. Available from: <https://github.com/ilyamaclean/microclimc> [Accessed 12 Apr 2021].

- Maclean, I. M. D., Mosedale, J. R., and Bennie, J. J., 2019. Microclima: An R package for modelling meso- and microclimate. *Methods in Ecology and Evolution*, 10 (2), 280–290.
- Maclean, I. M. D., Suggitt, A. J., Wilson, R. J., Duffy, J. P., and Bennie, J. J., 2017. Fine-scale climate change: modelling spatial variation in biologically meaningful rates of warming. *Global Change Biology*, 23 (1), 256–268.
- Malcom, J. R., LIU, C., NEILSON, R. P., HANSEN, L., and HANNAH, L., 2006. Global Warming and Extinctions of Endemic Species from Biodiversity Hotspots. *Conservation Biology* [online], 20 (2), 538–548. Available from: <http://doi.wiley.com/10.1111/j.1523-1739.2006.00364.x> [Accessed 2 Feb 2018].
- Malishev, M., Bull, C. M., and Kearney, M. R., 2018. An individual-based model of ectotherm movement integrating metabolic and microclimatic constraints. *Methods in Ecology and Evolution*, 9 (3), 472–489.
- Manduell, K. L., Harrison, M. E., and Thorpe, S. K. S., 2012. Forest structure and support availability influence orangutan locomotion in Sumatra and Borneo. *American Journal of Primatology*, 74 (12), 1128–42.
- Marsh, C. D., 2019. The effects of forest degradation on arboreal apes within Sikundur, the Gunung Leuser Ecosystem, Northern Sumatra. [online]. Available from: <http://eprints.bournemouth.ac.uk/33153/> [Accessed 27 May 2021].
- Marshall, A. J., Nardiyono, Engström, L. M., Pamungkas, B., Palapa, J., Meijaard, E., and Stanley, S. A., 2006. The blowgun is mightier than the chainsaw in determining population density of Bornean orangutans (*Pongo pygmaeus morio*) in the forests of East Kalimantan. *Biological Conservation*, 129 (4), 566–578.
- Martin, E. H., Cavada, N., Ndibalema, V. G., and Rovero, F., 2015. Modelling fine-scale habitat associations of medium-to-large forest mammals in the Udzungwa Mountains of Tanzania using camera trapping. *Tropical Zoology*, 28 (4), 137–151.

- Mathewson, P. D., Moyer-Horner, L., Beever, E. A., Briscoe, N. J., Kearney, M., Yahn, J. M., and Porter, W. P., 2017. Mechanistic variables can enhance predictive models of endotherm distributions: the American pika under current, past, and future climates. *Global Change Biology*, 23 (3), 1048–1064.
- Mathewson, P. D. and Porter, W. P., 2013. Simulating Polar Bear Energetics during a Seasonal Fast Using a Mechanistic Model. *PLoS ONE*, 8 (9), 72863.
- Mathewson, P. D., Porter, W. P., Barrett, L., Fuller, A., Henzi, S. P., Hetem, R. S., Young, C., and McFarland, R., 2020. Field data confirm the ability of a biophysical model to predict wild primate body temperature. *Journal of Thermal Biology*, 94, 102754.
- Matos, F. A. R., Magnago, L. F. S., Aquila Chan Miranda, C., de Menezes, L. F. T., Gastauer, M., Safar, N. V. H., Schaefer, C. E. G. R., da Silva, M. P., Simonelli, M., Edwards, F. A., Martins, S. v., Meira-Neto, J. A. A., and Edwards, D. P., 2020. Secondary forest fragments offer important carbon and biodiversity cobenefits. *Global Change Biology*, 26 (2), 509–522.
- McCullough, I. M., Davis, F. W., Dingman, J. R., Flint, L. E., Flint, A. L., Serra-Diaz, J. M., Syphard, A. D., Moritz, M. A., Hannah, L., and Franklin, J., 2016. High and dry: high elevations disproportionately exposed to regional climate change in Mediterranean-climate landscapes. *Landscape Ecology*, 31 (5), 1063–1075.
- McFarland, R., Fuller, A., Hetem, R. S., Mitchell, D., Maloney, S. K., Henzi, S. P., and Barrett, L., 2015. Social integration confers thermal benefits in a gregarious primate. *Journal of Animal Ecology*, 84 (3), 871–878.
- McGregor, R. A., Stokes, V. L., and Craig, M. D., 2014. Does forest restoration in fragmented landscapes provide habitat for a wide-ranging carnivore? *Animal Conservation*, 17 (5), 467–475.
- Meijaard, E., 2017. How a mistaken ecological narrative could be undermining orangutan conservation. In: *Effective Conservation Science: Data Not Dogma*. Oxford University Press, 90–97.

- Meijaard, E. and Wich, S., 2007. Putting orang-utan population trends into perspective. *Current Biology*, 17 (14), R540.
- Meijaard, E., Wich, S., Ancrenaz, M., and Marshall, A. J., 2012. Not by science alone: why orangutan conservationists must think outside the box. *Annals of the New York Academy of Sciences*, 1249 (1), 29–44.
- Meineri, E. and Hylander, K., 2017. Fine-grain, large-domain climate models based on climate station and comprehensive topographic information improve microrefugia detection. *Ecography*, 40 (8), 1003–1013.
- Michalski, F. and Peres, C. A., 2005. Anthropogenic determinants of primate and carnivore local extinctions in a fragmented forest landscape of southern Amazonia. *Biological Conservation*, 124, 383–396.
- Milling, C. R., Rachlow, J. L., Olsoy, P. J., Chappell, M. A., Johnson, T. R., Forbey, J. S., Shipley, L. A., and Thornton, D. H., 2018. Habitat structure modifies microclimate: An approach for mapping fine-scale thermal refuge. *Methods in Ecology and Evolution*, 9 (6), 1648–1657.
- Milne, S., Martin, J. G. A., Reynolds, G., Vairappan, C. S., Slade, E. M., Brodie, J. F., Wich, S. A., Williamson, N., and Burslem, D. F. R. P., 2021. Drivers of Bornean Orangutan Distribution across a Multiple-Use Tropical Landscape. *Remote Sensing*, 13 (3), 458.
- Mitchell, D., Maloney, S. K., Jessen, C., Laburn, H. P., Kamerman, P. R., Mitchell, G., and Fuller, A., 2002. Adaptive heterothermy and selective brain cooling in arid-zone mammals. *Comparative Biochemistry and Physiology*, 131, 571–585.
- Mitchell, N., Hipsey, M. R., Arnall, S., McGrath, G., Tareque, H. bin, Kuchling, G., Vogwill, R., Sivapalan, M., Porter, W. P., and Kearney, M. R., 2013. Linking eco-energetics and eco-hydrology to select sites for the assisted colonization of Australia's rarest reptile. *Biology*, 2 (1), 1–25.

- Mitchell, N. J., Rodriguez, N., Kuchling, G., Arnall, S. G., and Kearney, M. R., 2016. Reptile embryos and climate change: Modelling limits of viability to inform translocation decisions. *Biological Conservation*, 204, 134–147.
- Mittermeier, R. A., Turner, W. R., Larsen, F. W., Brooks, T. M., and Gascon, C., 2011. Global Biodiversity Conservation: The Critical Role of Hotspots. *In: Zachos, F. E. and Habel, J. C., eds. Biodiversity Hotspots*. Berlin, Heidelberg: Springer Berlin Heidelberg, 3–22.
- Morelli, T. L., Daly, C., Dobrowski, S. Z., Dulen, D. M., Ebersole, J. L., Jackson, S. T., Lundquist, J. D., Millar, C. I., Maher, S. P., Monahan, W. B., Nydick, K. R., Redmond, K. T., Sawyer, S. C., Stock, S., and Beissinger, S. R., 2016. Managing Climate Change Refugia for Climate Adaptation. *PLoS ONE*, 11 (8), e0159909.
- Morgans, C. L., Santika, T., Meijaard, E., Ancrenaz, M., and Wilson, K. A., 2019. Cost-benefit based prioritisation of orangutan conservation actions in Indonesian Borneo. *Biological Conservation*, 238, 108236.
- Mugasha, W. A., Bollandsås, O. M., and Eid, T., 2013. Relationships between diameter and height of trees in natural tropical forest in Tanzania. *Southern Forests*, 75 (4), 221–237.
- Muñoz, M. C., Schaefer, H. M., Böhning-Gaese, K., and Schleuning, M., 2017. Positive relationship between fruit removal by animals and seedling recruitment in a tropical forest. *Basic and Applied Ecology*, 20, 31–39.
- Myers, N., Mittermeier, R. A., Mittermeier, C. G., Fonseca, G. A. B., and Kent, J., 2000. Biodiversity hotspots for conservation priorities. *Nature*, 403, 853–858.
- Mynářová, A., Foitová, I., Kváč, M., Květoňová, D., Rost, M., Morrogh-Bernard, H., Nurcahyo, W., Nguyen, C., Supriyadi, S., and Sak, B., 2016. Prevalence of *Cryptosporidium* spp., *Enterocytozoon bieneusi*, *Encephalitozoon* spp. and *Giardia intestinalis* in Wild, Semi-Wild and Captive Orangutans (*Pongo abelii* and *Pongo pygmaeus*) on Sumatra and Borneo, Indonesia. *PLOS ONE*, 11 (3), e0152771.

- Nadkarni, N. M. and Solano, R., 2002. Potential effects of climate change on canopy communities in a tropical cloud forest: an experimental approach. *Oecologia*, 131 (4), 580–586.
- Nakamura, A., Kitching, R. L., Cao, M., Creedy, T. J., Fayle, T. M., Freiberg, M., Hewitt, C. N., Itioka, T., Koh, L. P., Ma, K., Malhi, Y., Mitchell, A., Novotny, V., Ozanne, C. M. P., Song, L., Wang, H., and Ashton, L. A., 2017. Forests and Their Canopies: Achievements and Horizons in Canopy Science. *Trends in Ecology & Evolution*, 32 (6), 438–451.
- NASA, 2002. *Shuttle Radar Topography Mission (SRTM) Elevation Dataset* [online]. USGS EROS. Available from: <https://earthexplorer.usgs.gov/> [Accessed 25 May 2021].
- Niedballa, J., Sollmann, R., Courtiol, A., and Wilting, A., 2016. camtrapR: an R package for efficient camera trap data management. *Methods in Ecology and Evolution*, 7 (12), 1457–1462.
- NOAA Physical Sciences Laboratory, 2021. *NCEP/NCAR Reanalysis 1: NOAA Physical Sciences Laboratory* [online]. Available from: <https://psl.noaa.gov/data/gridded/data.ncep.reanalysis.html> [Accessed 25 May 2021].
- Nogués-Bravo, D., Rodríguez-Sánchez, F., Orsini, L., de Boer, E., Jansson, R., Morlon, H., Fordham, D. A., and Jackson, S. T., 2018. Cracking the Code of Biodiversity Responses to Past Climate Change. *Trends in Ecology & Evolution*, 33 (10), 765–776.
- Norberg, A., Abrego, N., Blanchet, F. G., Adler, F. R., Anderson, B. J., Anttila, J., Araújo, M. B., Dallas, T., Dunson, D., Elith, J., Foster, S. D., Fox, R., Franklin, J., Godsoe, W., Guisan, A., O’Hara, B., Hill, N. A., Holt, R. D., Hui, F. K. C., Husby, M., Kålås, J. A., Lehtikoinen, A., Luoto, M., Mod, H. K., Newell, G., Renner, I., Roslin, T., Soininen, J., Thuiller, W., Vanhatalo, J., Warton, D., White, M., Zimmermann, N. E., Gravel, D., and Ovaskainen, O., 2019. A comprehensive evaluation of predictive

- performance of 33 species distribution models at species and community levels. *Ecological Monographs*, 89 (3), 1370.
- Norris, K., Asase, A., Collen, B., Gockowksi, J., Mason, J., Phalan, B., and Wade, A., 2010. Biodiversity in a forest-agriculture mosaic – The changing face of West African rainforests. *Biological Conservation*, 143 (10), 2341–2350.
- Noss, R. F., 2001. Beyond Kyoto: Forest Management in a Time of Rapid Climate Change. *Conservation Biology*, 15 (3), 578–590.
- Nummelin, M., 1990. Relative habitat use of duikers, bush pigs, and elephants in virgin and selectively logged areas of the Kibale Forest, Uganda. *Tropical Zoology*, 3 (2), 111–120.
- Nyhus, P. J. and Tilson, R., 2004a. Characterizing human-tiger conflict in Sumatra, Indonesia: implications for conservation. *Oryx*, 38 (01).
- Nyhus, P. and Tilson, R., 2004b. Agroforestry, elephants, and tigers: balancing conservation theory and practice in human-dominated landscapes of Southeast Asia. *Agriculture, Ecosystems & Environment*, 104 (1), 87–97.
- O’Grady, A. P., Tissue, D. T., and Beadle, C. L., 2011. Canopy processes in a changing climate. *Tree Physiology*, 31 (9), 887–892.
- Oke, T. R., 1987. *Boundary Layer Climates*. 2nd edition. Routledge.
- Oksanen, J., Blanchet, F. G., Friendly, M., Kindt, R., Legendre, P., McGlinn, D., Minchin, P. R., O’Hara, R. B., Simpson, G. L., Solymos, P., Stevens, M. H. H., Szoecs, E., and Wagner, H., 2019. Vegan: community ecology package.
- Oliver, T. H., Smithers, R. J., Beale, C. M., and Watts, K., 2016. Are existing biodiversity conservation strategies appropriate in a changing climate? *Biological Conservation*, 193, 17–26.

- Osborne, T. M., Lawrence, A. D. M., Slingo, A. J. M., Challinor, A. J., and Wheeler, A. T. R., 2004. Influence of vegetation on the local climate and hydrology in the tropics: sensitivity to soil parameters. *Climate Dynamics*, 23, 45–61.
- Pacifici, M., Foden, W. B., Visconti, P., Watson, J. E. M., Butchart, S. H. M., Kovacs, K. M., Scheffers, B. R., Hole, D. G., Martin, T. G., Akçakaya, H. R., Corlett, R. T., Huntley, B., Bickford, D., Carr, J. A., Hoffmann, A. A., Midgley, G. F., Pearce-Kelly, P., Pearson, R. G., Williams, S. E., Willis, S. G., Young, B., and Rondinini, C., 2015. Assessing species vulnerability to climate change. *Nature Climate Change*, 5 (3), 215–224.
- Pacifici, M., Visconti, P., Butchart, S. H. M., Watson, J. E. M., Cassola, F. M., and Rondinini, C., 2017. Species' traits influenced their response to recent climate change. *Nature Climate Change* [online], 7 (3), 205–208. Available from: <http://www.nature.com/articles/nclimate3223> [Accessed 11 Jul 2019].
- Paniw, M., James, T. D., Ruth Archer, C., Römer, G., Levin, S., Compagnoni, A., Castellano, J., Bennett, J. M., Mooney, A., Childs, D. Z., Ozgul, A., Jones, O. R., Burns, J. H., Beckerman, A. P., Patwary, A., Sanchez-Gassen, N., Knight, T. M., and Salguero-Gómez, R., 2021. The myriad of complex demographic responses of terrestrial mammals to climate change and gaps of knowledge: A global analysis. *Journal of Animal Ecology*, 00, 1365-2656.13467.
- Parra-Sanchez, E. and Banks-Leite, C., 2020. The magnitude and extent of edge effects on vascular epiphytes across the Brazilian Atlantic Forest. *Scientific Reports*, 10 (1), 1–11.
- Pecl, G. T., Araújo, M. B., Bell, J. D., Blanchard, J., Bonebrake, T. C., Chen, I.-C., Clark, T. D., Colwell, R. K., Danielsen, F., Evengård, B., Falconi, L., Ferrier, S., Frusher, S., Garcia, R. A., Griffis, R. B., Hobday, A. J., Janion-Scheepers, C., Jarzyna, M. A., Jennings, S., Lenoir, J., Linnetved, H. I., Martin, V. Y., McCormack, P. C., McDonald, J., Mitchell, N. J., Mustonen, T., Pandolfi, J. M., Pettorelli, N., Popova, E., Robinson, S. A., Scheffers, B. R., Shaw, J. D., Sorte, C. J. B., Strugnell, J. M., Sunday, J. M., Tuanmu, M.-N., Vergés, A., Villanueva, C., Wernberg, T., Wapstra,

- E., and Williams, S. E., 2017. Biodiversity redistribution under climate change: Impacts on ecosystems and human well-being. *Science*, 355 (6332), eaai9214.
- Pereira, H. M., Leadley, P. W., Proença, V., Alkemade, R., Scharlemann, J. P. W., Fernandez-Manjarrés, J. F., Araújo, M. B., Balvanera, P., Biggs, R., Cheung, W. W. L., Chini, L., Cooper, H. D., Gilman, E. L., Guénette, S., Hurtt, G. C., Huntington, H. P., Mace, G. M., Oberdorff, T., Revenga, C., Rodrigues, P., Scholes, R. J., Sumaila, U. R., and Walpole, M., 2010. Scenarios for global biodiversity in the 21st century. *Science*, 330 (6010), 1496–1501.
- Pfeifer, M., Lefebvre, V., Peres, C., Banks-Leite, C., Wearn, O., Marsh, C., Butchart, S., Arroyo-Rodríguez, V., Barlow, J., Cerezo, A., and Cisneros, L., 2017. Creation of forest edges has a global impact on forest vertebrates. *Nature*, 17, 187–191.
- Pimm, S. L., Jenkins, C. N., Abell, R., Brooks, T. M., Gittleman, J. L., Joppa, L. N., Raven, P. H., Roberts, C. M., and Sexton, J. O., 2014. The biodiversity of species and their rates of extinction, distribution, and protection. *Science*, 344 (6187), 1246752–1246752.
- Pincebourde, S., Murdock, C. C., Vickers, M., and Sears, M. W., 2016. Fine-scale microclimatic variation can shape the responses of organisms to global change in both natural and urban environments. *In: Integrative and Comparative Biology*. Oxford University Press, 45–61.
- Pohlman, C. L., Turton, S. M., and Goosem, M., 2007. Edge Effects of Linear Canopy Openings on Tropical Rain Forest Understory Microclimate. *Biotropica*, 39 (1), 62–71.
- Pontzer, H., Raichlen, D. A., Shumaker, R. W., Ocobock, C., and Wich, S. A., 2010. Metabolic adaptation for low energy throughput in orangutans. *Proceedings of the National Academy of Sciences*, 107 (32), 14048–14052.
- Poor, E. E., Frimpong, E., Imron, M. A., and Kelly, M. J., 2019. Protected area effectiveness in a sea of palm oil: A Sumatran case study. *Biological Conservation*, 234, 123–130.

- Poor, E. E., Jati, V. I. M., Imron, M. A., and Kelly, M. J., 2019. The road to deforestation: Edge effects in an endemic ecosystem in Sumatra, Indonesia. *PLoS ONE*, 14 (7).
- Poor, E. E., Shao, Y., and Kelly, M. J., 2019. Mapping and predicting forest loss in a Sumatran tiger landscape from 2002 to 2050. *Journal of Environmental Management*, 231, 397–404.
- Porter, W. P. and Kearney, M., 2009. Size, shape, and the thermal niche of endotherms. *Proceedings of the National Academy of Sciences of the United States of America*, 106 (SUPPL. 2), 19666–19672.
- Porter, W. P., Ostrowski, S., and Williams, J. B., 2010. Modeling animal landscapes. *Physiological and Biochemical Zoology*, 83 (5), 705–712.
- Posa, M. R. C., Wijedasa, L. S., and Corlett, R. T., 2011. Biodiversity and Conservation of Tropical Peat Swamp Forests. *BioScience*, 61 (1), 49–57.
- Pourrahmati, M. R., Baghdadi, N., Darvishsefat, A. A., Namiranian, M., Gond, V., Bailly, J.-S., and Zargham, N., 2018. Mapping Lorey's height over Hyrcanian forests of Iran using synergy of ICESat/GLAS and optical images. *European Journal of Remote Sensing*, 51 (1), 100–115.
- Priatna, D., Kartaminata, K., and Abdulhadi, R., 2000. Recovery of a lowland dipterocarp forest twenty two years after selective logging at Sekundur, Gunung Leuser National Park, North Sumatra, Indonesia. *Reinwardtia*, 12 (1), 237–255.
- Pringle, R. M., 2017. Upgrading protected areas to conserve wild biodiversity. *Nature*, 546 (7656), 91–99.
- Pyke, G. H. and Szabo, J. K., 2018. Conservation and the 4 Rs, which are rescue, rehabilitation, release, and research. *Conservation Biology*, 32 (1), 50–59.
- R Core Team, 2020. R: A language and environment for statistical computing. [online]. Available from: <https://www.r-project.org/>.

- Rainforest Connection, n.d. RFCx Arbimon. 2020 [online]. Available from: <https://arbimon.rfcx.org/> [Accessed 25 May 2021].
- Reiners, A. W. A., Bouwman, A. F., Parsons, W. F. J., and Keller, M., 2015. Tropical Rain Forest Conversion to Pasture: Changes in Vegetation and Soil Properties. *Ecological Applications*, 4 (2), 363–377.
- Reside, A. E., Butt, N., and Adams, V. M., 2018. Adapting systematic conservation planning for climate change. *Biodiversity and Conservation*, 27 (1), 1–29.
- Rezende, E. L. and Bozinovic, F., 2019. Thermal performance across levels of biological organization. *Philosophical Transactions of the Royal Society of Biology*, 374, 20180549.
- Rezende, E. L., Casta ñ Neda, L. E., and Santos, M., 2014. Tolerance landscapes in thermal ecology. *Functional Ecology*, 28, 799–809.
- Richards, J. H., Torrez Luna, I. M., and Waller, D. M., 2020. Tree longevity drives conservation value of shade coffee farms for vascular epiphytes. *Agriculture, Ecosystems and Environment*, 301, 107025.
- Ries, L., Fletcher, R. J., Battin, J., and Sisk, T. D., 2004. Ecological Responses to Habitat Edges: Mechanisms, Models, and Variability Explained. *Annual Review of Ecology, Evolution, and Systematics*, 35 (1), 491–522.
- Ripple, W. J. and Beschta, R. L., 2012. Trophic cascades in Yellowstone: The first 15years after wolf reintroduction. *Biological Conservation*, 145 (1), 205–213.
- Rockström, J., Steffen, W., Noone, K., Persson, Å., Chapin, F. S., Lambin, E. F., Lenton, T. M., Scheffer, M., Folke, C., Schellnhuber, H. J., Nykvist, B., de Wit, C. A., Hughes, T., van der Leeuw, S., Rodhe, H., Sörlin, S., Snyder, P. K., Costanza, R., Svedin, U., Falkenmark, M., Karlberg, L., Corell, R. W., Fabry, V. J., Hansen, J., Walker, B., Liverman, D., Richardson, K., Crutzen, P., and Foley, J. A., 2009. A safe operating space for humanity. *Nature*, 461 (7263), 472–475.

- Rodrigues, A. S. L., Pilgrim, J. D., Lamoreux, J. F., Hoffmann, M., and Brooks, T. M., 2006. The value of the IUCN Red List for conservation. *Trends in Ecology and Evolution*, 21 (2), 71–76.
- Rood, E., Ganie, A. A., and Nijman, V., 2010. Using presence-only modelling to predict Asian elephant habitat use in a tropical forest landscape: implications for conservation. *Diversity and Distributions*, 16 (6), 975–984.
- Roth, T. S., Rianti, P., Fredriksson, G. M., Wich, S. A., and Nowak, M. G., 2020. Grouping behavior of Sumatran orangutans (*Pongo abelii*) and Tapanuli orangutans (*Pongo tapanuliensis*) living in forest with low fruit abundance. *American Journal of Primatology*, 82 (5), e23123.
- Rovero, F., Owen, N., Jones, T., Canteri, E., Iemma, A., and Tattoni, C., 2017. Camera trapping surveys of forest mammal communities in the Eastern Arc Mountains reveal generalized habitat and human disturbance responses. *Biodiversity and Conservation*, 26 (5), 1103–1119.
- Ruppert, N., Holzner, A., See, K. W., Gisbrecht, A., and Beck, A., 2018. Activity Budgets and Habitat Use of Wild Southern Pig-Tailed Macaques (*Macaca nemestrina*) in Oil Palm Plantation and Forest. *International Journal of Primatology*, 39 (2), 237–251.
- Russon, A. E., 2002. Return of the Native: Cognition and Site-Specific Expertise in Orangutan Rehabilitation. *International Journal of Primatology*, 23 (3), 461–478.
- Russon, A. E., 2009. Orangutan rehabilitation and reintroduction. In: *Orangutans: Geographic Variation in Behavioral Ecology and Conservation*. Oxford University Press, 327–350.
- Saiful, I. and Latiff, A., 2019. Canopy gap dynamics and effects of selective logging: A study in a primary hill dipterocarp forest in Malaysia. *Journal of Tropical Forest Science*, 31 (2), 175–188.
- Santini, L., Cornulier, T., Bullock, J. M., Palmer, S. C. F., White, S. M., Hodgson, J. A., Bocedi, G., and Travis, J. M. J., 2016. A trait-based approach for predicting species

responses to environmental change from sparse data: how well might terrestrial mammals track climate change? *Global Change Biology*, 22 (7), 2415–2424.

Saura, S., Bertzky, B., Bastin, L., Battistella, L., Mandrici, A., and Dubois, G., 2018. Protected area connectivity: Shortfalls in global targets and country-level priorities. *Biological Conservation*, 219, 53–67.

Scheffers, B. R., Evans, T. A., Williams, S. E., and Edwards, D. P., 2014. Microhabitats in the tropics buffer temperature in a globally coherent manner. *Biology Letters*, 10 (12), 20140819.

Scheffers, B. R., Phillips, B. L., Laurance, W. F., Sodhi, N. S., Diesmos, A., and Williams, S. E., 2013. Increasing arboreality with altitude: a novel biogeographic dimension. *Proceedings of the Royal Society of Biology* [online], 280. Available from: <http://dx.doi.org/10.1098/rspb.2013.1581>.

Schino, G. and Troisi, A., 1990. Behavioral thermoregulation in long-tailed macaques: Effect on social preference. *Physiology & Behavior*, 47 (6), 1125–1128.

Schloss, C. A., Nunez, T. A., and Lawler, J. J., 2012. Dispersal will limit ability of mammals to track climate change in the Western Hemisphere. *Proceedings of the National Academy of Sciences*, 109 (22), 8606–8611.

Scott, D. M., Brown, D., Mahood, S., Denton, B., Silburn, A., and Rakotondrapary, F., 2005. The impacts of forest clearance on lizard, small mammal and bird communities in the arid spiny forest, southern Madagascar. *Biological Conservation*, 7, 72–87.

Scriven, S. A., Carlson, K. M., Hodgson, J. A., McClean, C. J., Heilmayr, R., Lucey, J. M., and Hill, J. K., 2019. Testing the benefits of conservation set-asides for improved habitat connectivity in tropical agricultural landscapes. *Journal of Applied Ecology*, 56 (10), 2274–2285.

- Segan, D. B., Murray, K. A., and Watson, J. E. M., 2016. A global assessment of current and future biodiversity vulnerability to habitat loss–climate change interactions. *Global Ecology and Conservation*, 5, 12–21.
- Senior, R. A., 2020. Hot and bothered: The role of behaviour and microclimates in buffering species from rising temperatures. *Journal of Animal Ecology*, 89 (11), 2392–2396.
- Senior, R. A., Hill, J. K., Benedick, S., and Edwards, D. P., 2018. Tropical forests are thermally buffered despite intensive selective logging. *Global Change Biology* [online], 24 (3), 1267–1278. Available from: <https://onlinelibrary.wiley.com/doi/abs/10.1111/gcb.13914> [Accessed 6 Jun 2019].
- Senior, R. A., Hill, J. K., and Edwards, D. P., 2019. Global loss of climate connectivity in tropical forests. *Nature Climate Change*, 9 (8), 623–626.
- Serra-Diaz, J. M. and Franklin, J., 2019. What’s hot in conservation biogeography in changing climate? Going beyond species range dynamics. *Diversity and Distributions*, 25 (4), 492–498.
- Sharma, N., Huffman, M. A., Gupta, S., Nautiyal, H., Mendonça, R., Morino, L., and Sinha, A., 2016. Watering holes: The use of arboreal sources of drinking water by Old World monkeys and apes. *Behavioural Processes*, 129, 18–26.
- Sheil, D., 2001. Conservation and Biodiversity Monitoring in the Tropics: Realities, Priorities, and Distractions. *Conservation Biology*, 15 (4), 1179–1182.
- Da Silva, L. G., Ribeiro, M. C., Hasui, É., Da Costa, C. A., and Da Cunha, R. G. T., 2015. Patch size, functional isolation, visibility and matrix permeability influences neotropical primate occurrence within highly fragmented landscapes. *PLoS ONE*, 10 (2), e0114025.
- Singleton, I., Wich, S. A., Nowak, M., Usher, G., and Utami-Atmoko, S. S., 2017. *Pongo abelii* (Sumatran Orangutan) [online]. The IUCN Red List of Threatened Species .

Available from: <https://www.iucnredlist.org/species/121097935/123797627>
[Accessed 25 May 2021].

- Slavich, E., Warton, D. I., Ashcroft, M. B., Gollan, J. R., and Ramp, D., 2014. Topoclimate versus macroclimate: how does climate mapping methodology affect species distribution models and climate change projections? *Diversity and Distributions*, 20 (8), 952–963.
- Smil, V., 2004. Conversion of Energy: People and Animals. *In: Encyclopedia of Energy*. Elsevier, 697–705.
- Sodhi, N. S., Koh, L. P., Clements, R., Wanger, T. C., Hill, J. K., Hamer, K. C., Clough, Y., Tscharntke, T., Posa, M. R. C., and Lee, T. M., 2010. Conserving Southeast Asian forest biodiversity in human-modified landscapes. *Biological Conservation*, 143 (10), 2375–2384.
- Stalenberg, E. M., 2019. Biophysical ecology of the white-footed sportive lemur (*Lepilemur leucopus*) of Southern Madagascar.
- Steenweg, R., Hebblewhite, M., Kays, R., Ahumada, J., Fisher, J. T., Burton, C., Townsend, S. E., Carbone, C., Rowcliffe, J. M., Whittington, J., Brodie, J., Royle, J. A., Switalski, A., Clevenger, A. P., Heim, N., and Rich, L. N., 2017. Scaling-up camera traps: monitoring the planet’s biodiversity with networks of remote sensors. *Frontiers in Ecology and the Environment*.
- Stelzner, J. K., 1988. Thermal effects on movement patterns of yellow baboons. *Primates*, 29 (1), 91–105.
- Stelzner, J. K. and Hausfater, G., 1986. Posture, microclimate, and thermoregulation in yellow baboons. *Primates*, 27 (4), 449–463.
- Stephenson, P., 2019. Integrating Remote Sensing into Wildlife Monitoring for Conservation. *Environmental Conservation*, 46 (3), 181–183.

- Stevens, J. T., Safford, H. D., Harrison, S., and Latimer, A. M., 2015. Forest disturbance accelerates thermophilization of understory plant communities. *Journal of Ecology*, 103 (5), 1253–1263.
- Stewart, F. E. C., Heim, N. A., Clevenger, A. P., Paczkowski, J., Volpe, J. P., & Fisher, J. T. (2016). Wolverine behavior varies spatially with anthropogenic footprint: implications for conservation and inferences about declines. *Ecology and Evolution*, 6(5), 1493–1503. <https://doi.org/10.1002/ECE3.1921>
- Still, C., Powell, R., Aubrecht, D., Kim, Y., Helliker, B., Roberts, D., Richardson, A. D., and Goulden, M., 2019. Thermal imaging in plant and ecosystem ecology: applications and challenges. *Ecosphere*, 10 (6), e02768.
- Strangas, M. L., Navas, C. A., Rodrigues, M. T., and Carnaval, A. C., 2019. Thermophysiology, microclimates, and species distributions of lizards in the mountains of the Brazilian Atlantic Forest. *Ecography*, 42 (2), 354–364.
- Struebig, M. J., Wilting, A., Gaveau, D. L. A., Meijaard, E., Smith, R. J., Fischer, M., Metcalfe, K., Kramer-Schadt, S., Abdullah, T., Abram, N., Alfred, R., Ancrenaz, M., Augeri, D. M., Belant, J. L., Bernard, H., Bezuijen, M., Boonman, A., Boonratana, R., Boorsma, T., Breitenmoser-Würsten, C., Brodie, J., Cheyne, S. M., Devens, C., Duckworth, J. W., Duplaix, N., Eaton, J., Francis, C., Fredriksson, G., Giordano, A. J., Gonner, C., Hall, J., Harrison, M. E., Hearn, A. J., Heckmann, I., Heydon, M., Hofer, H., Hon, J., Husson, S., Anwarali Khan, F. A., Kingston, T., Krebs, D., Lammertink, M., Lane, D., Lasmana, F., Liat, L. B., Lim, N. T.-L., Lindenborn, J., Loken, B., Macdonald, D. W., Marshall, A. J., Maryanto, I., Mathai, J., McShea, W. J., Mohamed, A., Nakabayashi, M., Nakashima, Y., Niedballa, J., Noerfahmy, S., Persey, S., Peter, A., Pieterse, S., Pilgrim, J. D., Pollard, E., Purnama, S., Rafiastanto, A., Reinfelder, V., Reusch, C., Robson, C., Ross, J., Rustam, R., Sadikin, L., Samejima, H., Santosa, E., Sapari, I., Sasaki, H., Scharf, A. K., Semiadi, G., Shepherd, C. R., Sykes, R., van Berkel, T., Wells, K., Wielstra, B., and Wong, A., 2015. Targeted Conservation to Safeguard a Biodiversity Hotspot from Climate and Land-Cover Change. *Current Biology*, 25 (3), 372–378.

- Sueur, J., Pavoine, S., Hamerlynck, O., and Duvail, S., 2008. Rapid Acoustic Survey for Biodiversity Appraisal. *PLoS ONE*, 3 (12), e4065.
- Sugai, L. S. M., Silva, T. S. F., Ribeiro, J. W., and Llusia, D., 2019. Terrestrial Passive Acoustic Monitoring: Review and Perspectives. *BioScience*, 69 (1), 5–11.
- Suggitt, A. J., Gillingham, P. K., Hill, J. K., Huntley, B., Kunin, W. E., Roy, D. B., and Thomas, C. D., 2011. Habitat microclimates drive fine-scale variation in extreme temperatures. *Oikos*, 120 (1), 1–8.
- Suggitt, A. J., Wilson, R. J., Isaac, N. J. B., Beale, C. M., Auffret, A. G., August, T., Bennie, J. J., Crick, H. Q. P., Duffield, S., Fox, R., Hopkins, J. J., Macgregor, N. A., Morecroft, M. D., Walker, K. J., and Maclean, I. M. D., 2018. Extinction risk from climate change is reduced by microclimatic buffering. *Nature Climate Change*, 8 (8), 713–717.
- Sumida, A., Miyaura, T., and Torii, H., 2013. Relationships of tree height and diameter at breast height revisited: analyses of stem growth using 20-year data of an even-aged *Chamaecyparis obtusa* stand. *Tree Physiology*, 33 (1), 106–118.
- Sutherland, W. J., Butchart, S. H. M., Connor, B., Culshaw, C., Dicks, L. v., Dinsdale, J., Doran, H., Entwistle, A. C., Fleishman, E., Gibbons, D. W., Jiang, Z., Keim, B., Roux, X. le, Lickorish, F. A., Markillie, P., Monk, K. A., Mortimer, D., Pearce-Higgins, J. W., Peck, L. S., Pretty, J., Seymour, C. L., Spalding, M. D., Tonneijck, F. H., and Gleave, R. A., 2018. A 2018 Horizon Scan of Emerging Issues for Global Conservation and Biological Diversity. *Trends in Ecology & Evolution*, 33 (1), 47–58.
- Takemoto, H., 2004. Seasonal Change in Terrestriality of Chimpanzees in Relation to Microclimate in the Tropical Forest. *American Journal of Physical Anthropology*, 124, 81–92.
- Takemoto, H., 2017. Acquisition of terrestrial life by human ancestors influenced by forest microclimate. *Scientific Reports*, 7 (1), 5741.

- The Cornell Lab, 2021. RAVEN - Interactive Sound Analysis Software. [online]. Available from: <https://ravensoundsoftware.com/> [Accessed 25 May 2021].
- Thomas, C. D. and Gillingham, P. K., 2015. The performance of protected areas for biodiversity under climate change. *Biological Journal of the Linnean Society*, 115 (3), 718–730.
- Thomas, C. D. and Lennon, J. J., 1999. Birds extend their ranges northwards. *Nature*, 399 (6733), 213–213.
- Tilman, D., Clark, M., Williams, D. R., Kimmel, K., Polasky, S., and Packer, C., 2017. Future threats to biodiversity and pathways to their prevention. *Nature*, 546 (7656), 73–81.
- Trew, B. T. and Maclean, I. M. D., 2021. Vulnerability of global biodiversity hotspots to climate change. *Global Ecology and Biogeography*, 30 (4), 768–783.
- Trisurat, Y., Kanchanasaka, B., and Kreft, H., 2014. Assessing potential effects of land use and climate change on mammal distributions in northern Thailand. *Wildlife Research* [online], 41 (6), 522. Available from: <http://www.publish.csiro.au/?paper=WR14171> [Accessed 16 Jul 2019].
- Tucker, M. A., Böhning-Gaese, K., Fagan, W. F., Fryxell, J. M., van Moorter, B., Alberts, S. C., Ali, A. H., Allen, A. M., Attias, N., Avgar, T., Bartlam-Brooks, H., Bayarbaatar, B., Belant, J. L., Bertassoni, A., Beyer, D., Bidner, L., van Beest, F. M., Blake, S., Blaum, N., Bracis, C., Brown, D., de Bruyn, P. J. N., Cagnacci, F., Calabrese, J. M., Camilo-Alves, C., Chamaillé-Jammes, S., Chiaradia, A., Davidson, S. C., Dennis, T., DeStefano, S., Diefenbach, D., Douglas-Hamilton, I., Fennessy, J., Fichtel, C., Fiedler, W., Fischer, C., Fischhoff, I., Fleming, C. H., Ford, A. T., Fritz, S. A., Gehr, B., Goheen, J. R., Gurarie, E., Hebblewhite, M., Heurich, M., Hewison, A. J. M., Hof, C., Hurme, E., Isbell, L. A., Janssen, R., Jeltsch, F., Kaczensky, P., Kane, A., Kappeler, P. M., Kauffman, M., Kays, R., Kimuyu, D., Koch, F., Kranstauber, B., LaPoint, S., Leimgruber, P., Linnell, J. D. C., López-López, P., Markham, A. C., Mattisson, J., Medici, E. P., Mellone, U., Merrill, E., de Miranda Mourão, G., Morato, R. G., Morellet, N., Morrison, T. A., Díaz-Muñoz, S.

- L., Myserud, A., Nandintsetseg, D., Nathan, R., Niamir, A., Odden, J., O'Hara, R. B., Oliveira-Santos, L. G. R., Olson, K. A., Patterson, B. D., Cunha de Paula, R., Pedrotti, L., Reineking, B., Rimmler, M., Rogers, T. L., Rolandsen, C. M., Rosenberry, C. S., Rubenstein, D. I., Safi, K., Saïd, S., Sapir, N., Sawyer, H., Schmidt, N. M., Selva, N., Sergiel, A., Shiilegdamba, E., Silva, J. P., Singh, N., Solberg, E. J., Spiegel, O., Strand, O., Sundaresan, S., Ullmann, W., Voigt, U., Wall, J., Wattles, D., Wikelski, M., Wilmers, C. C., Wilson, J. W., Wittemyer, G., Zięba, F., Zwijacz-Kozica, T., and Mueller, T., 2018. Moving in the Anthropocene: Global reductions in terrestrial mammalian movements. *Science*, 359 (6374), 466–469.
- Tulloch, A. I. T., Sutcliffe, P., Naujokaitis-Lewis, I., Tingley, R., Brotons, L., Ferraz, K. M. P. M. B., Possingham, H., Guisan, A., and Rhodes, J. R., 2016. Conservation planners tend to ignore improved accuracy of modelled species distributions to focus on multiple threats and ecological processes. *Biological Conservation*, 199, 157–171.
- Turner, J. M., 2020. Facultative hyperthermia during a heatwave delays injurious dehydration of an arboreal marsupial. *Journal of Experimental Biology*, 223 (4).
- Urban, M. C., 2015. Accelerating extinction risk from climate change. *Science*, 348 (6234), 571–573.
- Urban, M. C., Tewksbury, J. J., and Sheldon, K. S., 2012. On a collision course: competition and dispersal differences create no-analogue communities and cause extinctions during climate change. *Proceedings of the Royal Society B: Biological Sciences*, 279 (1735), 2072–2080.
- Valencia, B. G., Matthews-Bird, F., Urrego, D. H., Williams, J. J., Gosling, W. D., and Bush, M., 2016. Andean microrefugia: testing the Holocene to predict the Anthropocene. *New Phytologist*, 212 (2), 510–522.
- Vanwallegem, T. and Meentemeyer, R. K., 2009. Predicting Forest Microclimate in Heterogeneous Landscapes. *Ecosystems*, 12 (7), 1158–1172.

- Venables, W. N. and Ripley, D. B., 2002. *Modern applied statistics with S*. 4th ed. New York: Springer.
- Venter, O., Fuller, R. A., Segan, D. B., Carwardine, J., and Brooks, T., 2014. Targeting Global Protected Area Expansion for Imperiled Biodiversity. *PLoS Biol*, 12 (6), 1001891.
- Wall, J., Wittemyer, G., Klinkenberg, B., and Douglas-Hamilton, I., 2014. Novel opportunities for wildlife conservation and research with real-time monitoring. *Ecological Applications*, 24 (4), 593–601.
- Waller, N. L., Gynther, I. C., Freeman, A. B., Lavery, T. H., and Leung, L. K.-P., 2017. The Bramble Cay melomys *Melomys rubicola* (Rodentia: Muridae): a first mammalian extinction caused by human-induced climate change? *Wildlife Research*, 44 (1), 9.
- Walsh, P. D., White, L. J. T., Mbina, C., Idiata, D., Mihindou, Y., Maisels, F., and Thibault, M., 2001. Estimates of forest elephant abundance: Projecting the relationship between precision and effort. *Journal of Applied Ecology*, 38 (1), 217–228.
- Wearn, O. R., Rowcliffe, J. M., Carbone, C., Pfeifer, M., Bernard, H., and Ewers, R. M., 2017. Mammalian species abundance across a gradient of tropical land-use intensity: A hierarchical multi-species modelling approach. *Biological Conservation*, 212, 162–171.
- Wich, S. A., 2009. *Orangutans: geographic variation in behavioral ecology and conservation*. Oxford University Press.
- Wich, S. A., Geurts, M. L., Setia, T. M., and Utami-Atmoko, S. S., 2006. Influence of fruit availability on Sumatran orangutan sociality and reproduction. In: Hohmann, G., Robbins, M. M., and Boesch, C., eds. *Feeding Ecology in Apes and Other Primates*. Cambridge University Press, 337–358.

- Wich, S. A., Singleton, I., Nowak, M. G., Utami Atmoko, S. S., Nisam, G., Arif, S. Mhd., Putra, R. H., Ardi, R., Fredriksson, G., Usher, G., Gaveau, D. L. A., and Kühl, H. S., 2016. Land-cover changes predict steep declines for the Sumatran orangutan (*Pongo abelii*). *Science Advances*, 2 (3), e1500789.
- Wiens, J. A., Seavy, N. E., and Jongsomjit, D., 2011. Protected areas in climate space: What will the future bring? *Biological Conservation*, 144 (8), 2119–2125.
- Wiens, J. J., 2016. Climate-Related Local Extinctions Are Already Widespread among Plant and Animal Species. *PLoS Biology*, 14 (12), e2001104.
- Wilson, H. B., Meijaard, E., Venter, O., Ancrenaz, M., and Possingham, H. P., 2014. Conservation Strategies for Orangutans: Reintroduction versus Habitat Preservation and the Benefits of Sustainably Logged Forest. *PLoS ONE*, 9 (7), e102174.
- Wittmann, M. E., Barnes, M. A., Jerde, C. L., Jones, L. A., and Lodge, D. M., 2016. Confronting species distribution model predictions with species functional traits. *Ecology and Evolution*, 6, 873–879.
- World Meteorological Organization, 2020. *Observing Systems Capability Analysis and Review Tool (OSCAR)* [online]. Available from: <https://oscar.wmo.int/surface/index.html#/> [Accessed 9 Dec 2020].
- Wrege, P. H., Rowland, E. D., Keen, S., and Shiu, Y., 2017. Acoustic monitoring for conservation in tropical forests: examples from forest elephants. *Methods in Ecology and Evolution* [online], 8 (10), 1292–1301. Available from: <http://doi.wiley.com/10.1111/2041-210X.12730> [Accessed 26 Nov 2019].
- WWF, 2018. *Living Planet Report - 2018: Aiming higher*. Gland, Switzerland: WWF.
- Wynn-Grant, R., Ginsberg, J. R., Lackey, C. W., Sterling, E. J., and Beckmann, J. P., 2018. Risky business: Modeling mortality risk near the urban-wildland interface for a large carnivore. *Global Ecology and Conservation*, 16, e00443.
- Yeager, C. P., 1997. Orangutan Rehabilitation in Tanjung Puting National Park, Indonesia. *Conservation Biology*, 11 (3), 802–805.

- YOSL-OIC, 2009. The Gunung Leuser National Park. *In: Guidebook to The Gunung Leuser National Park*. Medan: Orangutan Information Centre.
- Yuliani, E. L., Adnan, H., Achdiawan, R., Bakara, D., Heri, V., Sammy, J., Salim, M. A., and Sunderland, T., 2018. The roles of traditional knowledge systems in orang-utan *Pongo* spp. and forest conservation: a case study of Danau Sentarum, West Kalimantan, Indonesia. *Oryx*, 52 (1), 156–165.
- Zellweger, F., de Frenne, P., Lenoir, J., Rocchini, D., and Coomes, D., 2019. Advances in Microclimate Ecology Arising from Remote Sensing. *Trends in Ecology and Evolution*.
- Zurita, G., Pe'er, G., Bellocq, M. I., and Hansbauer, M. M., 2012. Edge effects and their influence on habitat suitability calculations: a continuous approach applied to birds of the Atlantic forest. *Journal of Applied Ecology*, 49 (2), 503–512.

Appendix 3.1

R scripts to run generalized linear models and generalized linear mixed models of microclimate and forest structure effects on mammals

This document includes the R code required to run generalized linear model and generalized linear mixed models to test the effects of microclimate and habitat characteristics on mammal occurrence at Sikundur, Sumatra.

```
library(dplyr)
library(car)
library(MASS)
library(ggplot2)
library(ggfortify)
library(lme4)
library(glmmTMB)
library(sjPlot)
library(sjmisc)
library(ggsci)
library(parameters)
library(sjstats)
library(jtools)
library(egg)
library(lemon)
library(modEvA)
library(colorspace)
library(ggeffects)
library(corrplot)
library(Hmisc)
library(sitreeE)
library(MuMIn)

#Load data
transect <- read.csv("transects.csv")
camtraps <- read.csv("detectionsbyorder.csv")
```

1) GLM of total mammal occurrence

```
poisson <- glm(data = transect,
               detections_total ~ dist + Tmax + Tmin +
                 Theightmean + no_trees + CA_mean + DBH_mean + conn_mean,
               family = "poisson", na.action=na.fail)
dredge(poisson)

## Global model call: glm(formula = detections_total ~ dist + Tmax + Tmin + Theightmean +
##   no_trees + CA_mean + DBH_mean + conn_mean, family = "poisson",
##   data = transect, na.action = na.fail)
## ---
```

```

## Model selection table
##          (Int)      CA_men   cnn_men DBH_men      dst      no_trs
Thg
## 229 27.470000          0.18030          -0
.106600
## 237 35.090000          0.20820  0.224100          -0
.116500
## 101  2.176000          0.16200          -0
.113900
## 230 27.660000  1.023e-02          0.17110          -0
.112800
## 231 27.390000          -0.0032440  0.18140          -0
.101600
## 102  2.345000  1.028e-02          0.15140          -0
.119300
## 245 27.660000          0.17990          -0.0009018 -0
.105900
## 117  2.192000          0.17450          0.0242600 -0
.130000
## 103  2.260000          -0.0035770  0.16310          -0
.107800
## 109  1.772000          0.17180  0.084660          -0
.119100
## 238 34.500000  8.650e-03          0.19750  0.207800          -0
.120100
## 253 32.280000          0.22260  0.263500  0.0206700 -0
.133200
## 119  2.445000          -0.0096900  0.19380          0.0536400 -0
.133800
## 239 34.880000          -0.0005340  0.20770  0.219000          -0
.115400
## 118  2.388000  1.205e-02          0.16670          0.0306300 -0
.141600
## 125  1.382000          0.20250  0.170000  0.0396600 -0
.150600
## 232 27.630000  9.507e-03 -0.0020940  0.17230          -0
.108800
## 246 26.510000  1.055e-02          0.17330          0.0056020 -0
.117200
## 110  1.997000  9.822e-03          0.15970  0.071280          -0
.122900
## 104  2.385000  9.388e-03 -0.0023740  0.15270          -0
.114400
## 247 22.880000          -0.0056970  0.19100          0.0212100 -0
.113200
## 127  1.554000          -0.0102900  0.22670  0.191600  0.0744000 -0
.158100
## 111  1.932000          -0.0028350  0.17030  0.065480          -0
.113000
## 120  2.570000  1.027e-02 -0.0086040  0.18470          0.0556000 -0
.142600
## 126  1.567000  1.214e-02          0.19450  0.170800  0.0464500 -0
.161800
## 254 30.810000  1.001e-02          0.21500  0.257400  0.0267100 -0
.142700

```

| | | | | | | | | |
|--------|-----------|-----------|------------|------------|-----------|------------|-----------|----|
| ## 255 | 27.620000 | | | -0.0050740 | 0.23210 | 0.257900 | 0.0406800 | -0 |
| | .139800 | | | | | | | |
| ## 240 | 34.660000 | 8.791e-03 | 0.0004559 | 0.19780 | 0.211900 | | | -0 |
| | .121100 | | | | | | | |
| ## 112 | 2.080000 | 9.236e-03 | -0.0016970 | 0.15930 | 0.060250 | | | -0 |
| | .118900 | | | | | | | |
| ## 248 | 22.760000 | 9.903e-03 | -0.0047420 | 0.18270 | | 0.0234200 | | -0 |
| | .122000 | | | | | | | |
| ## 128 | 1.682000 | 1.012e-02 | -0.0091830 | 0.21710 | 0.188800 | 0.0760700 | | -0 |
| | .165800 | | | | | | | |
| ## 213 | 46.040000 | | | 0.09881 | | -0.0664900 | | |
| ## 37 | 0.632900 | | | 0.10030 | | | | -0 |
| | .068800 | | | | | | | |
| ## 45 | -0.040160 | | | 0.12460 | 0.173900 | | | -0 |
| | .084290 | | | | | | | |
| ## 256 | 27.190000 | 9.452e-03 | -0.0042000 | 0.22330 | 0.253400 | 0.0428100 | | -0 |
| | .147300 | | | | | | | |
| ## 165 | -8.645000 | | | 0.11040 | | | | -0 |
| | .083970 | | | | | | | |
| ## 53 | 0.762700 | | | 0.09988 | | -0.0242300 | | -0 |
| | .061430 | | | | | | | |
| ## 221 | 44.750000 | | | 0.09671 | -0.040350 | -0.0680700 | | |
| ## 214 | 46.170000 | 2.190e-03 | | 0.09528 | | -0.0670700 | | |
| ## 215 | 46.880000 | | 0.0011690 | 0.09806 | | -0.0701300 | | |
| ## 38 | 0.665000 | 2.079e-03 | | 0.09669 | | | | -0 |
| | .069180 | | | | | | | |
| ## 39 | 0.634900 | | -0.0001641 | 0.10020 | | | | -0 |
| | .068470 | | | | | | | |
| ## 173 | -5.784000 | | | 0.12620 | 0.136500 | | | -0 |
| | .090510 | | | | | | | |
| ## 61 | 0.127300 | | | 0.12040 | 0.144900 | -0.0105000 | | -0 |
| | .078470 | | | | | | | |
| ## 46 | -0.007054 | 2.198e-03 | | 0.12070 | 0.174300 | | | -0 |
| | .084530 | | | | | | | |
| ## 47 | -0.074100 | | 0.0011150 | 0.12570 | 0.178600 | | | -0 |
| | .086990 | | | | | | | |
| ## 197 | 34.350000 | | | 0.08525 | | | | |
| ## 199 | 32.610000 | | -0.0084300 | 0.09386 | | | | |
| ## 166 | -9.328000 | 4.393e-03 | | 0.10370 | | | | -0 |
| | .085960 | | | | | | | |
| ## 181 | -5.997000 | | | 0.10720 | | -0.0124200 | | -0 |
| | .075780 | | | | | | | |
| ## 167 | -8.953000 | | -0.0012480 | 0.11040 | | | | -0 |
| | .081890 | | | | | | | |
| ## 55 | 0.761400 | | 0.0024400 | 0.10040 | | -0.0287100 | | -0 |
| | .064990 | | | | | | | |
| ## 54 | 0.802500 | 2.572e-03 | | 0.09542 | | -0.0245500 | | -0 |
| | .061720 | | | | | | | |
| ## 40 | 0.664300 | 2.116e-03 | 0.0001019 | 0.09665 | | | | -0 |
| | .069400 | | | | | | | |
| ## 222 | 44.710000 | 2.662e-03 | | 0.09210 | -0.047190 | -0.0690600 | | |
| ## 216 | 47.210000 | 2.445e-03 | 0.0014300 | 0.09395 | | -0.0716000 | | |
| ## 223 | 45.370000 | | 0.0007119 | 0.09644 | -0.036500 | -0.0701200 | | |
| ## 174 | -6.431000 | 3.622e-03 | | 0.12000 | 0.132000 | | | -0 |
| | .091680 | | | | | | | |

| | | | | | | | |
|--------|-----------|------------|------------|---------|-----------|------------|----|
| ## 205 | 35.650000 | | | 0.08713 | 0.031350 | | |
| ## 198 | 34.340000 | -7.827e-04 | | 0.08658 | | | |
| ## 189 | -5.357000 | | | 0.12510 | 0.132600 | -0.0024090 | -0 |
| | .088740 | | | | | | |
| ## 175 | -5.699000 | | 0.0002068 | 0.12640 | 0.138000 | | -0 |
| | .090920 | | | | | | |
| ## 63 | 0.130900 | | 0.0023460 | 0.12070 | 0.142700 | -0.0153000 | -0 |
| | .081590 | | | | | | |
| ## 62 | 0.166900 | 2.320e-03 | | 0.11610 | 0.144200 | -0.0107700 | -0 |
| | .078550 | | | | | | |
| ## 48 | -0.044070 | 2.809e-03 | 0.0014900 | 0.12110 | 0.180700 | | -0 |
| | .088250 | | | | | | |
| ## 21 | 1.333000 | | | 0.05388 | | -0.0472100 | |
| ## 182 | -6.889000 | 4.010e-03 | | 0.10150 | | -0.0111200 | -0 |
| | .078360 | | | | | | |
| ## 207 | 31.200000 | | -0.0088360 | 0.09237 | -0.034020 | | |
| ## 200 | 32.590000 | -1.018e-03 | -0.0084350 | 0.09561 | | | |
| ## 168 | -9.465000 | 4.125e-03 | -0.0007651 | 0.10410 | | | -0 |
| | .084510 | | | | | | |
| ## 183 | -5.598000 | | 0.0003893 | 0.10690 | | -0.0138400 | -0 |
| | .075500 | | | | | | |
| ## 149 | 12.540000 | | | 0.05985 | | -0.0575200 | |
| ## 56 | 0.817600 | 3.794e-03 | 0.0030810 | 0.09403 | | -0.0303300 | -0 |
| | .066460 | | | | | | |
| ## 71 | 2.241000 | | -0.0100300 | 0.06670 | | | |
| ## 29 | 1.726000 | | | 0.04839 | -0.129700 | -0.0550300 | |
| ## 85 | 1.938000 | | | 0.05767 | | -0.0430500 | |
| ## 79 | 3.009000 | | -0.0114800 | 0.06402 | -0.171900 | | |
| ## 93 | 2.791000 | | | 0.05157 | -0.192300 | -0.0523400 | |
| ## 5 | 1.087000 | | | 0.04604 | | | |
| ## 69 | 1.830000 | | | 0.05274 | | | |
| ## 7 | 1.128000 | | -0.0067680 | 0.05337 | | | |
| ## 23 | 1.303000 | | -0.0026040 | 0.05600 | | -0.0407900 | |
| ## 22 | 1.343000 | 5.924e-04 | | 0.05282 | | -0.0474000 | |
| ## 206 | 35.700000 | -9.924e-04 | | 0.08891 | 0.032750 | | |
| ## 87 | 2.168000 | | -0.0070200 | 0.06556 | | -0.0235600 | |
| ## 151 | 15.590000 | | 0.0035860 | 0.05843 | | -0.0690400 | |
| ## 98 | 3.817000 | 2.509e-02 | | | | | -0 |
| | .048350 | | | | | | |
| ## 157 | 10.840000 | | | 0.05654 | -0.058390 | -0.0595200 | |
| ## 150 | 12.550000 | -3.165e-04 | | 0.06044 | | -0.0574500 | |
| ## 176 | -6.215000 | 3.834e-03 | 0.0006406 | 0.12020 | 0.136300 | | -0 |
| | .093060 | | | | | | |
| ## 190 | -6.173000 | 3.582e-03 | | 0.11950 | 0.129700 | -0.0014140 | -0 |
| | .090620 | | | | | | |
| ## 77 | 2.358000 | | | 0.04895 | -0.128100 | | |
| ## 133 | 6.869000 | | | 0.04823 | | | |
| ## 64 | 0.189600 | 3.558e-03 | 0.0029540 | 0.11450 | 0.141400 | -0.0168800 | -0 |
| | .082650 | | | | | | |
| ## 191 | -4.494000 | | 0.0008219 | 0.12450 | 0.133700 | -0.0053710 | -0 |
| | .088210 | | | | | | |
| ## 72 | 2.220000 | -1.046e-03 | -0.0100400 | 0.06857 | | | |
| ## 95 | 3.058000 | | -0.0075400 | 0.06090 | -0.200500 | -0.0326500 | |
| ## 224 | 45.530000 | 2.780e-03 | 0.0009381 | 0.09153 | -0.042460 | -0.0718200 | |
| ## 13 | 1.229000 | | | 0.04339 | -0.054590 | | |

| | | | | | | | |
|---------|-----------|------------|------------|---------|-----------|------------|----|
| ## 184 | -5.963000 | 4.225e-03 | 0.0009663 | 0.10030 | | -0.0145500 | -0 |
| .077860 | | | | | | | |
| ## 6 | 1.055000 | -1.948e-03 | | 0.04970 | | | |
| ## 31 | 1.688000 | | -0.0016890 | 0.05012 | -0.124300 | -0.0506800 | |
| ## 208 | 31.240000 | -7.917e-04 | -0.0088240 | 0.09377 | -0.032710 | | |
| ## 30 | 1.754000 | 1.371e-03 | | 0.04588 | -0.131400 | -0.0555900 | |
| ## 86 | 1.967000 | 1.411e-03 | | 0.05523 | | -0.0434800 | |
| ## 106 | 4.357000 | 2.366e-02 | | | -0.150800 | | -0 |
| .047730 | | | | | | | |
| ## 210 | 27.810000 | 1.991e-02 | | | | -0.0494300 | |
| ## 34 | 2.396000 | 1.908e-02 | | | | | -0 |
| .034710 | | | | | | | |
| ## 15 | 1.260000 | | -0.0067490 | 0.05088 | -0.050620 | | |
| ## 135 | 3.761000 | | -0.0061200 | 0.05359 | | | |
| ## 8 | 1.081000 | -2.766e-03 | -0.0068450 | 0.05870 | | | |
| ## 70 | 1.816000 | -6.747e-04 | | 0.05393 | | | |
| ## 26 | 2.803000 | 1.225e-02 | | | -0.188600 | -0.0539700 | |
| ## 18 | 2.408000 | 1.366e-02 | | | | -0.0407800 | |
| ## 80 | 3.011000 | 7.344e-05 | -0.0114800 | 0.06389 | -0.172100 | | |
| ## 94 | 2.883000 | 3.164e-03 | | 0.04600 | -0.199000 | -0.0537100 | |
| ## 90 | 3.963000 | 1.351e-02 | | | -0.258800 | -0.0534400 | |
| ## 226 | 12.990000 | 2.523e-02 | | | | | -0 |
| .042210 | | | | | | | |
| ## 24 | 1.301000 | -8.202e-05 | -0.0026120 | 0.05615 | | -0.0407400 | |
| ## 218 | 23.660000 | 1.829e-02 | | | -0.207700 | -0.0605200 | |
| ## 50 | 2.516000 | 1.905e-02 | | | | -0.0279800 | -0 |
| .025400 | | | | | | | |
| ## 114 | 3.732000 | 2.427e-02 | | | | -0.0133500 | -0 |
| .041980 | | | | | | | |
| ## 25 | 3.262000 | | | | -0.217600 | -0.0433300 | |
| ## 100 | 3.826000 | 2.505e-02 | -0.0004667 | | | | -0 |
| .047350 | | | | | | | |
| ## 134 | 7.032000 | -2.702e-03 | | 0.05341 | | | |
| ## 2 | 2.118000 | 1.046e-02 | | | | | |
| ## 141 | 6.721000 | | | 0.04796 | -0.004327 | | |
| ## 159 | 13.850000 | | 0.0031250 | 0.05595 | -0.046210 | -0.0690900 | |
| ## 146 | 10.140000 | 1.470e-02 | | | | -0.0464700 | |
| ## 88 | 2.171000 | 1.651e-04 | -0.0070080 | 0.06526 | | -0.0236500 | |
| ## 152 | 15.620000 | 4.348e-04 | 0.0036390 | 0.05760 | | -0.0693100 | |
| ## 78 | 2.358000 | 8.247e-06 | | 0.04893 | -0.128100 | | |
| ## 14 | 1.197000 | -1.882e-03 | | 0.04693 | -0.054170 | | |
| ## 158 | 10.820000 | 1.827e-04 | | 0.05618 | -0.058750 | -0.0595800 | |
| ## 122 | 4.376000 | 2.117e-02 | | | -0.210900 | -0.0309400 | -0 |
| .032780 | | | | | | | |
| ## 194 | 20.500000 | 1.538e-02 | | | | | |
| ## 82 | 2.977000 | 1.445e-02 | | | | -0.0380400 | |
| ## 89 | 4.310000 | | | | -0.273700 | -0.0425900 | |
| ## 162 | -2.529000 | 2.038e-02 | | | | | -0 |
| .041270 | | | | | | | |
| ## 42 | 2.463000 | 1.791e-02 | | | -0.049140 | | -0 |
| .032880 | | | | | | | |
| ## 1 | 2.581000 | | | | | | |
| ## 66 | 2.832000 | 1.185e-02 | | | | | |
| ## 212 | 33.560000 | 1.937e-02 | 0.0064090 | | | -0.0708100 | |
| ## 36 | 2.391000 | 1.920e-02 | 0.0007672 | | | | -0 |

| | | | | | | | | |
|---------|-----------|------------|------------|---------|-----------|------------|----|--|
| .036410 | | | | | | | | |
| ## 58 | 2.792000 | 1.567e-02 | | | -0.150500 | -0.0435400 | -0 | |
| .015290 | | | | | | | | |
| ## 9 | 2.717000 | | | | -0.132700 | | | |
| ## 242 | 21.690000 | 2.334e-02 | | | | -0.0342600 | -0 | |
| .020610 | | | | | | | | |
| ## 17 | 2.855000 | | | | | -0.0259100 | | |
| ## 74 | 3.443000 | 1.076e-02 | | | -0.171500 | | | |
| ## 10 | 2.274000 | 9.234e-03 | | | -0.099730 | | | |
| ## 20 | 2.405000 | 1.355e-02 | 0.0006501 | | | -0.0425500 | | |
| ## 16 | 1.212000 | -2.694e-03 | -0.0068260 | 0.05609 | -0.050020 | | | |
| ## 4 | 2.222000 | 1.189e-02 | -0.0040550 | | | | | |
| ## 136 | 3.915000 | -3.063e-03 | -0.0061600 | 0.05952 | | | | |
| ## 143 | 2.105000 | | -0.0065380 | 0.05133 | -0.042930 | | | |
| ## 73 | 3.796000 | | | | -0.192900 | | | |
| ## 154 | 5.618000 | 1.277e-02 | | | -0.169900 | -0.0549200 | | |
| ## 28 | 2.801000 | 1.193e-02 | 0.0017450 | | -0.192700 | -0.0588300 | | |
| ## 32 | 1.709000 | 9.242e-04 | -0.0015900 | 0.04832 | -0.125700 | -0.0513100 | | |
| ## 108 | 4.458000 | 2.328e-02 | -0.0024730 | | -0.165500 | | -0 | |
| .042350 | | | | | | | | |
| ## 234 | 8.821000 | 2.393e-02 | | | -0.132700 | | -0 | |
| .044710 | | | | | | | | |
| ## 96 | 3.112000 | 2.037e-03 | -0.0073950 | 0.05715 | -0.204700 | -0.0338700 | | |
| ## 76 | 4.108000 | 1.393e-02 | -0.0079890 | | -0.212200 | | | |
| ## 68 | 3.222000 | 1.448e-02 | -0.0060780 | | | | | |
| ## 52 | 2.528000 | 1.972e-02 | 0.0044840 | | | -0.0366000 | -0 | |
| .032460 | | | | | | | | |
| ## 130 | 5.708000 | 1.073e-02 | | | | | | |
| ## 27 | 3.235000 | | 0.0032010 | | -0.222700 | -0.0527500 | | |
| ## 57 | 3.184000 | | | | -0.233700 | -0.0512100 | 0 | |
| .009370 | | | | | | | | |
| ## 192 | -4.844000 | 3.890e-03 | 0.0013520 | 0.11800 | 0.131300 | -0.0061670 | -0 | |
| .089980 | | | | | | | | |
| ## 65 | 3.141000 | | | | | | | |
| ## 148 | 16.190000 | 1.431e-02 | 0.0067970 | | | -0.0694300 | | |
| ## 153 | 2.128000 | | | | -0.224000 | -0.0431200 | | |
| ## 92 | 4.117000 | 1.416e-02 | -0.0024890 | | -0.263800 | -0.0467400 | | |
| ## 178 | 3.998000 | 1.869e-02 | | | | -0.0304400 | -0 | |
| .022730 | | | | | | | | |
| ## 33 | 2.714000 | | | | | | -0 | |
| .007020 | | | | | | | | |
| ## 196 | 18.770000 | 1.697e-02 | -0.0045150 | | | | | |
| ## 228 | 12.970000 | 2.520e-02 | -0.0002892 | | | | -0 | |
| .041620 | | | | | | | | |
| ## 202 | 16.940000 | 1.396e-02 | | | -0.112400 | | | |
| ## 3 | 2.648000 | | -0.0016240 | | | | | |
| ## 129 | 4.999000 | | | | | | | |
| ## 142 | 6.989000 | -2.695e-03 | | 0.05332 | -0.001232 | | | |
| ## 170 | -6.191000 | 1.890e-02 | | | -0.107900 | | -0 | |
| .042750 | | | | | | | | |
| ## 217 | 11.770000 | | | | -0.256500 | -0.0440100 | | |
| ## 116 | 3.684000 | 2.422e-02 | 0.0014250 | | | -0.0166700 | -0 | |
| .043480 | | | | | | | | |
| ## 75 | 4.260000 | | -0.0046610 | | -0.221500 | | | |
| ## 12 | 2.390000 | 1.061e-02 | -0.0042270 | | -0.102700 | | | |

| | | | | | | | | | |
|--------|-----------|------------|--|------------|------------|--|--|--|-------------------------|
| ## 81 | 3.279000 | | | | | | | | -0.0239300 |
| ## 145 | 7.514000 | | | | | | | | -0.0283900 |
| ## 11 | 2.817000 | | | | -0.0022960 | | | | -0.138500 |
| ## 220 | 27.640000 | 1.810e-02 | | 0.0041170 | | | | | -0.187800 -0.0730300 |
| ## 41 | 2.838000 | | | | | | | | -0.130500 -0 |
| | .006506 | | | | | | | | |
| ## 250 | 19.540000 | 2.072e-02 | | | | | | | -0.194800 -0.0486400 -0 |
| | .014730 | | | | | | | | |
| ## 19 | 2.833000 | | | | 0.0022820 | | | | -0.0326800 |
| ## 137 | 0.226800 | | | | | | | | -0.149900 |
| ## 193 | 13.250000 | | | | | | | | |
| ## 84 | 3.070000 | 1.487e-02 | | -0.0017570 | | | | | -0.0328700 |
| ## 121 | 4.224000 | | | | | | | | -0.278200 -0.0461500 0 |
| | .004292 | | | | | | | | |
| ## 91 | 4.278000 | | | | 0.0004468 | | | | -0.272700 -0.0438800 |
| ## 49 | 2.840000 | | | | | | | | -0.0268700 0 |
| | .001348 | | | | | | | | |
| ## 105 | 4.119000 | | | | | | | | -0.195900 -0 |
| | .010980 | | | | | | | | |
| ## 164 | -2.465000 | 2.043e-02 | | 0.0003922 | | | | | -0 |
| | .042070 | | | | | | | | |
| ## 44 | 2.459000 | 1.800e-02 | | 0.0003456 | | | | | -0.047830 -0 |
| | .033690 | | | | | | | | |
| ## 201 | 8.901000 | | | | | | | | -0.174200 |
| ## 138 | 2.435000 | 9.261e-03 | | | | | | | -0.098430 |
| ## 132 | 3.710000 | 1.187e-02 | | -0.0036940 | | | | | |
| ## 97 | 3.408000 | | | | | | | | -0 |
| | .009406 | | | | | | | | |
| ## 60 | 2.792000 | 1.648e-02 | | 0.0042880 | | | | | -0.145600 -0.0507600 -0 |
| | .022700 | | | | | | | | |
| ## 67 | 3.335000 | | | | -0.0024920 | | | | |
| ## 209 | 15.740000 | | | | | | | | -0.0273000 |
| ## 160 | 13.850000 | 7.448e-04 | | 0.0032050 | 0.05448 | | | | -0.047390 -0.0695700 |
| ## 156 | 10.660000 | 1.274e-02 | | 0.0050910 | | | | | -0.149100 -0.0709400 |
| ## 244 | 27.490000 | 2.265e-02 | | 0.0062640 | | | | | -0.0557200 -0 |
| | .019910 | | | | | | | | |
| ## 147 | 14.650000 | | | | 0.0074870 | | | | -0.0544700 |
| ## 124 | 4.363000 | 2.117e-02 | | 0.0003035 | | | | | -0.210000 -0.0315100 -0 |
| | .033160 | | | | | | | | |
| ## 186 | 1.160000 | 1.598e-02 | | | | | | | -0.155100 -0.0411500 -0 |
| | .018020 | | | | | | | | |
| ## 204 | 12.920000 | 1.558e-02 | | -0.0066810 | | | | | -0.167800 |
| ## 144 | 2.379000 | -2.837e-03 | | -0.0065390 | 0.05700 | | | | -0.039420 |
| ## 155 | 7.175000 | | | 0.0048990 | | | | | -0.203600 -0.0585500 |
| ## 35 | 2.717000 | | | -0.0006395 | | | | | -0 |
| | .005809 | | | | | | | | |
| ## 161 | 3.599000 | | | | | | | | -0 |
| | .006162 | | | | | | | | |
| ## 59 | 3.191000 | | | | 0.0023710 | | | | -0.231200 -0.0552800 0 |
| | .005990 | | | | | | | | |
| ## 131 | 4.233000 | | | | -0.0012570 | | | | |
| ## 185 | 6.270000 | | | | | | | | -0.223800 -0.0553900 0 |
| | .013570 | | | | | | | | |
| ## 180 | 10.080000 | 1.820e-02 | | 0.0067370 | | | | | -0.0534300 -0 |
| | .022440 | | | | | | | | |

| | | | | | | |
|--------|-----------|-----------|------------|--|------------|---------------|
| ## 177 | 11.770000 | | | | -0.0405400 | 0 |
| | .013680 | | | | | |
| ## 139 | -3.114000 | | -0.0039720 | | -0.183800 | |
| ## 169 | -3.071000 | | | | -0.169500 | -0 |
| | .012440 | | | | | |
| ## 249 | 20.330000 | | | | -0.262500 | -0.0645100 0 |
| | .022270 | | | | | |
| ## 236 | 8.265000 | 2.357e-02 | -0.0021930 | | -0.148500 | -0 |
| | .040430 | | | | | |
| ## 83 | 3.206000 | | 0.0012220 | | -0.0278300 | |
| ## 113 | 3.315000 | | | | -0.0227800 | -0 |
| | .001511 | | | | | |
| ## 43 | 2.852000 | | -0.0017470 | | -0.136000 | -0 |
| | .003180 | | | | | |
| ## 140 | -1.595000 | 1.026e-02 | -0.0053040 | | -0.136300 | |
| ## 51 | 2.852000 | | 0.0025480 | | -0.0321200 | -0 |
| | .001912 | | | | | |
| ## 211 | 23.220000 | | 0.0075120 | | -0.0533900 | |
| ## 195 | 12.520000 | | -0.0011560 | | | |
| ## 225 | 12.400000 | | | | | -0 |
| | .002895 | | | | | |
| ## 107 | 4.307000 | | -0.0040050 | | -0.218600 | -0 |
| | .003766 | | | | | |
| ## 219 | 16.240000 | | 0.0043590 | | -0.235900 | -0.0575100 |
| ## 203 | 5.423000 | | -0.0044310 | | -0.215900 | |
| ## 241 | 23.650000 | | | | -0.0449900 | 0 |
| | .020050 | | | | | |
| ## 172 | -6.548000 | 1.868e-02 | -0.0009796 | | -0.114200 | -0 |
| | .040810 | | | | | |
| ## 233 | 5.950000 | | | | -0.188800 | -0 |
| | .009507 | | | | | |
| ## 99 | 3.443000 | | -0.0013350 | | | -0 |
| | .006944 | | | | | |
| ## 123 | 4.230000 | | -0.0001357 | | -0.278600 | -0.0459000 0 |
| | .004457 | | | | | |
| ## 179 | 18.810000 | | 0.0074290 | | -0.0664100 | 0 |
| | .013800 | | | | | |
| ## 163 | 3.460000 | | -0.0005652 | | | -0 |
| | .005232 | | | | | |
| ## 252 | 23.480000 | 2.059e-02 | 0.0042570 | | -0.175100 | -0.0612700 -0 |
| | .015280 | | | | | |
| ## 187 | 11.100000 | | 0.0047850 | | -0.202900 | -0.0700600 0 |
| | .013290 | | | | | |
| ## 188 | 6.172000 | 1.605e-02 | 0.0053000 | | -0.134600 | -0.0573800 -0 |
| | .018820 | | | | | |
| ## 171 | -4.424000 | | -0.0029500 | | -0.188000 | -0 |
| | .008100 | | | | | |
| ## 243 | 31.280000 | | 0.0074980 | | -0.0713400 | 0 |
| | .020580 | | | | | |
| ## 115 | 3.258000 | | 0.0016050 | | -0.0266300 | -0 |
| | .003173 | | | | | |
| ## 227 | 12.260000 | | -0.0009938 | | | -0 |
| | .001228 | | | | | |
| ## 251 | 24.460000 | | 0.0041370 | | -0.241000 | -0.0767700 0 |
| | .021940 | | | | | |

| ## | Tmx | Tmn | df | logLik | AICc | delta | weight |
|---------|----------|-----------|----|------------|-------|-----------|--------|
| ## 235 | 4.669000 | | | -0.0039720 | | -0.217000 | -0 |
| .003539 | | | | | | | |
| ## 229 | -0.12890 | -1.143000 | 5 | -81.214 | 177.0 | 0.00 | 0.303 |
| ## 237 | -0.13560 | -1.532000 | 6 | -79.581 | 178.2 | 1.12 | 0.173 |
| ## 101 | -0.08382 | | 4 | -84.042 | 178.9 | 1.90 | 0.117 |
| ## 230 | -0.13510 | -1.145000 | 6 | -80.367 | 179.7 | 2.69 | 0.079 |
| ## 231 | -0.13140 | -1.136000 | 6 | -80.958 | 180.9 | 3.87 | 0.044 |
| ## 102 | -0.08939 | | 5 | -83.195 | 181.0 | 3.96 | 0.042 |
| ## 245 | -0.12880 | -1.152000 | 6 | -81.213 | 181.4 | 4.38 | 0.034 |
| ## 117 | -0.09555 | | 5 | -83.516 | 181.6 | 4.60 | 0.030 |
| ## 103 | -0.08659 | | 5 | -83.730 | 182.1 | 5.03 | 0.024 |
| ## 109 | -0.08081 | | 5 | -83.763 | 182.1 | 5.10 | 0.024 |
| ## 238 | -0.13960 | -1.496000 | 7 | -78.997 | 182.2 | 5.13 | 0.023 |
| ## 253 | -0.13980 | -1.414000 | 7 | -79.290 | 182.8 | 5.72 | 0.017 |
| ## 119 | -0.11800 | | 6 | -82.035 | 183.1 | 6.03 | 0.015 |
| ## 239 | -0.13580 | -1.521000 | 7 | -79.575 | 183.3 | 6.29 | 0.013 |
| ## 118 | -0.10570 | | 6 | -82.403 | 183.8 | 6.76 | 0.010 |
| ## 125 | -0.09697 | | 6 | -82.579 | 184.2 | 7.11 | 0.009 |
| ## 232 | -0.13610 | -1.142000 | 7 | -80.267 | 184.7 | 7.67 | 0.007 |
| ## 246 | -0.13600 | -1.093000 | 7 | -80.346 | 184.9 | 7.83 | 0.006 |
| ## 110 | -0.08644 | | 6 | -83.001 | 185.0 | 7.96 | 0.006 |
| ## 104 | -0.09059 | | 6 | -83.067 | 185.1 | 8.09 | 0.005 |
| ## 247 | -0.13590 | -0.929200 | 7 | -80.779 | 185.7 | 8.70 | 0.004 |
| ## 127 | -0.12150 | | 7 | -80.905 | 186.0 | 8.95 | 0.003 |
| ## 111 | -0.08363 | | 6 | -83.577 | 186.2 | 9.11 | 0.003 |
| ## 120 | -0.12380 | | 7 | -81.292 | 186.8 | 9.72 | 0.002 |
| ## 126 | -0.10710 | | 7 | -81.482 | 187.1 | 10.10 | 0.002 |
| ## 254 | -0.14590 | -1.340000 | 8 | -78.543 | 187.5 | 10.44 | 0.002 |
| ## 255 | -0.14570 | -1.197000 | 8 | -78.950 | 188.3 | 11.26 | 0.001 |
| ## 240 | -0.13950 | -1.505000 | 8 | -78.992 | 188.4 | 11.34 | 0.001 |
| ## 112 | -0.08772 | | 7 | -82.940 | 190.1 | 13.02 | 0.000 |
| ## 248 | -0.14150 | -0.918400 | 8 | -80.054 | 190.5 | 13.46 | 0.000 |
| ## 128 | -0.12700 | | 8 | -80.214 | 190.8 | 13.79 | 0.000 |
| ## 213 | -0.10220 | -1.985000 | 5 | -88.692 | 192.0 | 14.96 | 0.000 |
| ## 37 | | | 3 | -93.004 | 193.6 | 16.57 | 0.000 |
| ## 45 | | | 4 | -91.798 | 194.5 | 17.41 | 0.000 |
| ## 256 | -0.15050 | -1.172000 | 9 | -78.315 | 194.6 | 17.59 | 0.000 |
| ## 165 | | 0.429600 | 4 | -92.141 | 195.1 | 18.10 | 0.000 |
| ## 53 | | | 4 | -92.307 | 195.5 | 18.43 | 0.000 |
| ## 221 | -0.10190 | -1.920000 | 6 | -88.635 | 196.3 | 19.23 | 0.000 |
| ## 214 | -0.10280 | -1.989000 | 6 | -88.652 | 196.3 | 19.26 | 0.000 |
| ## 215 | -0.10150 | -2.024000 | 6 | -88.671 | 196.3 | 19.30 | 0.000 |
| ## 38 | | | 4 | -92.971 | 196.8 | 19.76 | 0.000 |
| ## 39 | | | 4 | -93.004 | 196.9 | 19.82 | 0.000 |
| ## 173 | | 0.272000 | 5 | -91.513 | 197.6 | 20.60 | 0.000 |
| ## 61 | | | 5 | -91.697 | 198.0 | 20.97 | 0.000 |
| ## 46 | | | 5 | -91.762 | 198.1 | 21.10 | 0.000 |
| ## 47 | | | 5 | -91.768 | 198.2 | 21.11 | 0.000 |
| ## 197 | -0.09134 | -1.470000 | 4 | -93.697 | 198.3 | 21.21 | 0.000 |
| ## 199 | -0.09918 | -1.374000 | 5 | -91.973 | 198.6 | 21.52 | 0.000 |
| ## 166 | | 0.464100 | 5 | -91.997 | 198.6 | 21.57 | 0.000 |
| ## 181 | | 0.310100 | 5 | -92.026 | 198.7 | 21.62 | 0.000 |
| ## 167 | | 0.444500 | 5 | -92.105 | 198.8 | 21.78 | 0.000 |
| ## 55 | | | 5 | -92.190 | 199.0 | 21.95 | 0.000 |

| | | | | | | | |
|--------|----------|-----------|---|----------|-------|-------|-------|
| ## 54 | | | 5 | -92.256 | 199.1 | 22.08 | 0.000 |
| ## 40 | | | 5 | -92.971 | 200.6 | 23.51 | 0.000 |
| ## 222 | -0.10260 | -1.915000 | 7 | -88.577 | 201.3 | 24.29 | 0.000 |
| ## 216 | -0.10200 | -2.038000 | 7 | -88.622 | 201.4 | 24.38 | 0.000 |
| ## 223 | -0.10150 | -1.950000 | 7 | -88.628 | 201.4 | 24.40 | 0.000 |
| ## 174 | | 0.305100 | 6 | -91.418 | 201.8 | 24.79 | 0.000 |
| ## 205 | -0.09188 | -1.534000 | 5 | -93.662 | 201.9 | 24.90 | 0.000 |
| ## 198 | -0.09117 | -1.470000 | 5 | -93.692 | 202.0 | 24.96 | 0.000 |
| ## 189 | | 0.253600 | 6 | -91.509 | 202.0 | 24.98 | 0.000 |
| ## 175 | | 0.267700 | 6 | -91.512 | 202.0 | 24.98 | 0.000 |
| ## 63 | | | 6 | -91.587 | 202.2 | 25.13 | 0.000 |
| ## 62 | | | 6 | -91.656 | 202.3 | 25.27 | 0.000 |
| ## 48 | | | 6 | -91.712 | 202.4 | 25.38 | 0.000 |
| ## 21 | | | 3 | -97.582 | 202.8 | 25.72 | 0.000 |
| ## 182 | | 0.353700 | 6 | -91.906 | 202.8 | 25.77 | 0.000 |
| ## 207 | -0.09919 | -1.304000 | 6 | -91.934 | 202.9 | 25.83 | 0.000 |
| ## 200 | -0.09897 | -1.374000 | 6 | -91.965 | 202.9 | 25.89 | 0.000 |
| ## 168 | | 0.470700 | 6 | -91.984 | 203.0 | 25.92 | 0.000 |
| ## 183 | | 0.291800 | 6 | -92.024 | 203.0 | 26.00 | 0.000 |
| ## 149 | | -0.525000 | 4 | -96.109 | 203.1 | 26.03 | 0.000 |
| ## 56 | | | 6 | -92.083 | 203.2 | 26.12 | 0.000 |
| ## 71 | -0.04398 | | 4 | -96.364 | 203.6 | 26.54 | 0.000 |
| ## 29 | | | 4 | -96.762 | 204.4 | 27.34 | 0.000 |
| ## 85 | -0.02409 | | 4 | -96.765 | 204.4 | 27.34 | 0.000 |
| ## 79 | -0.05790 | | 5 | -95.038 | 204.7 | 27.65 | 0.000 |
| ## 93 | -0.03529 | | 5 | -95.144 | 204.9 | 27.86 | 0.000 |
| ## 5 | | | 2 | -100.230 | 205.2 | 28.17 | 0.000 |
| ## 69 | -0.02994 | | 3 | -98.915 | 205.4 | 28.39 | 0.000 |
| ## 7 | | | 3 | -98.966 | 205.5 | 28.49 | 0.000 |
| ## 23 | | | 4 | -97.435 | 205.7 | 28.68 | 0.000 |
| ## 22 | | | 4 | -97.580 | 206.0 | 28.97 | 0.000 |
| ## 206 | -0.09170 | -1.537000 | 6 | -93.654 | 206.3 | 29.26 | 0.000 |
| ## 87 | -0.03666 | | 5 | -95.922 | 206.5 | 29.42 | 0.000 |
| ## 151 | | -0.666200 | 5 | -95.928 | 206.5 | 29.43 | 0.000 |
| ## 98 | -0.04453 | | 4 | -97.828 | 206.5 | 29.47 | 0.000 |
| ## 157 | | -0.437300 | 5 | -95.987 | 206.6 | 29.55 | 0.000 |
| ## 150 | | -0.526000 | 5 | -96.108 | 206.8 | 29.79 | 0.000 |
| ## 176 | | 0.294100 | 7 | -91.409 | 207.0 | 29.96 | 0.000 |
| ## 190 | | 0.294000 | 7 | -91.417 | 207.0 | 29.97 | 0.000 |
| ## 77 | -0.03850 | | 4 | -98.132 | 207.1 | 30.08 | 0.000 |
| ## 133 | | -0.272200 | 3 | -99.781 | 207.2 | 30.12 | 0.000 |
| ## 64 | | | 7 | -91.496 | 207.2 | 30.13 | 0.000 |
| ## 191 | | 0.213800 | 7 | -91.501 | 207.2 | 30.14 | 0.000 |
| ## 72 | -0.04378 | | 5 | -96.356 | 207.3 | 30.28 | 0.000 |
| ## 95 | -0.04965 | | 6 | -94.198 | 207.4 | 30.35 | 0.000 |
| ## 224 | -0.10210 | -1.953000 | 8 | -88.565 | 207.5 | 30.49 | 0.000 |
| ## 13 | | | 3 | -100.066 | 207.7 | 30.69 | 0.000 |
| ## 184 | | 0.311300 | 7 | -91.894 | 208.0 | 30.93 | 0.000 |
| ## 6 | | | 3 | -100.200 | 208.0 | 30.96 | 0.000 |
| ## 31 | | | 5 | -96.701 | 208.0 | 30.97 | 0.000 |
| ## 208 | -0.09902 | -1.307000 | 7 | -91.929 | 208.0 | 31.00 | 0.000 |
| ## 30 | | | 5 | -96.747 | 208.1 | 31.07 | 0.000 |
| ## 86 | -0.02434 | | 5 | -96.749 | 208.1 | 31.07 | 0.000 |
| ## 106 | -0.05496 | | 5 | -96.827 | 208.3 | 31.23 | 0.000 |
| ## 210 | -0.06104 | -1.099000 | 5 | -96.879 | 208.4 | 31.33 | 0.000 |

| | | | | | | | |
|--------|-----------|-----------|---|----------|-------|-------|-------|
| ## 34 | | | 3 | -100.425 | 208.4 | 31.41 | 0.000 |
| ## 15 | | | 4 | -98.825 | 208.5 | 31.46 | 0.000 |
| ## 135 | -0.124000 | | 4 | -98.883 | 208.6 | 31.58 | 0.000 |
| ## 8 | | | 4 | -98.908 | 208.7 | 31.63 | 0.000 |
| ## 70 | -0.02980 | | 4 | -98.912 | 208.7 | 31.64 | 0.000 |
| ## 26 | | | 4 | -98.947 | 208.8 | 31.71 | 0.000 |
| ## 18 | | | 3 | -100.641 | 208.9 | 31.84 | 0.000 |
| ## 80 | -0.05792 | | 6 | -95.038 | 209.1 | 32.03 | 0.000 |
| ## 94 | -0.03624 | | 6 | -95.061 | 209.1 | 32.08 | 0.000 |
| ## 90 | -0.03584 | | 5 | -97.320 | 209.3 | 32.21 | 0.000 |
| ## 226 | -0.05822 | -0.411900 | 5 | -97.387 | 209.4 | 32.35 | 0.000 |
| ## 24 | | | 5 | -97.435 | 209.5 | 32.44 | 0.000 |
| ## 218 | -0.06550 | -0.880600 | 6 | -95.374 | 209.7 | 32.71 | 0.000 |
| ## 50 | | | 4 | -99.485 | 209.8 | 32.78 | 0.000 |
| ## 114 | -0.04011 | | 5 | -97.636 | 209.9 | 32.84 | 0.000 |
| ## 25 | | | 3 | -101.291 | 210.2 | 33.14 | 0.000 |
| ## 100 | -0.04474 | | 5 | -97.823 | 210.3 | 33.22 | 0.000 |
| ## 134 | | -0.282100 | 4 | -99.724 | 210.3 | 33.26 | 0.000 |
| ## 2 | | | 2 | -102.802 | 210.4 | 33.31 | 0.000 |
| ## 141 | | -0.264700 | 4 | -99.780 | 210.4 | 33.37 | 0.000 |
| ## 159 | | -0.578200 | 6 | -95.855 | 210.7 | 33.67 | 0.000 |
| ## 146 | | -0.358900 | 4 | -99.958 | 210.8 | 33.73 | 0.000 |
| ## 88 | -0.03666 | | 6 | -95.922 | 210.8 | 33.80 | 0.000 |
| ## 152 | | -0.666900 | 6 | -95.927 | 210.9 | 33.81 | 0.000 |
| ## 78 | -0.03850 | | 5 | -98.132 | 210.9 | 33.84 | 0.000 |
| ## 14 | | | 4 | -100.038 | 210.9 | 33.89 | 0.000 |
| ## 158 | | -0.436200 | 6 | -95.986 | 211.0 | 33.93 | 0.000 |
| ## 122 | -0.04883 | | 6 | -95.989 | 211.0 | 33.93 | 0.000 |
| ## 194 | -0.05479 | -0.783500 | 4 | -100.086 | 211.0 | 33.99 | 0.000 |
| ## 82 | -0.01971 | | 4 | -100.106 | 211.1 | 34.03 | 0.000 |
| ## 89 | -0.03112 | | 4 | -100.121 | 211.1 | 34.06 | 0.000 |
| ## 162 | | 0.232200 | 4 | -100.190 | 211.2 | 34.19 | 0.000 |
| ## 42 | | | 4 | -100.302 | 211.5 | 34.42 | 0.000 |
| ## 1 | | | 1 | -104.643 | 211.5 | 34.48 | 0.000 |
| ## 66 | -0.02417 | | 3 | -101.970 | 211.5 | 34.50 | 0.000 |
| ## 212 | -0.06008 | -1.368000 | 6 | -96.314 | 211.6 | 34.59 | 0.000 |
| ## 36 | | | 4 | -100.412 | 211.7 | 34.64 | 0.000 |
| ## 58 | | | 5 | -98.605 | 211.8 | 34.78 | 0.000 |
| ## 9 | | | 2 | -103.600 | 211.9 | 34.91 | 0.000 |
| ## 242 | -0.06035 | -0.811600 | 6 | -96.475 | 212.0 | 34.91 | 0.000 |
| ## 17 | | | 2 | -103.632 | 212.0 | 34.97 | 0.000 |
| ## 74 | -0.03625 | | 4 | -100.589 | 212.0 | 34.99 | 0.000 |
| ## 10 | | | 3 | -102.253 | 212.1 | 35.06 | 0.000 |
| ## 20 | | | 4 | -100.632 | 212.1 | 35.08 | 0.000 |
| ## 16 | | | 5 | -98.770 | 212.2 | 35.11 | 0.000 |
| ## 4 | | | 3 | -102.313 | 212.2 | 35.18 | 0.000 |
| ## 136 | | -0.133800 | 5 | -98.813 | 212.2 | 35.20 | 0.000 |
| ## 143 | | -0.040750 | 5 | -98.819 | 212.3 | 35.21 | 0.000 |
| ## 73 | -0.03172 | | 3 | -102.366 | 212.3 | 35.29 | 0.000 |
| ## 154 | | -0.132400 | 5 | -98.870 | 212.4 | 35.31 | 0.000 |
| ## 28 | | | 5 | -98.879 | 212.4 | 35.33 | 0.000 |
| ## 32 | | | 6 | -96.694 | 212.4 | 35.35 | 0.000 |
| ## 108 | -0.05712 | | 6 | -96.710 | 212.4 | 35.38 | 0.000 |
| ## 234 | -0.06043 | -0.203500 | 6 | -96.732 | 212.5 | 35.42 | 0.000 |
| ## 96 | -0.04998 | | 7 | -94.166 | 212.5 | 35.47 | 0.000 |

| | | | | | | | |
|--------|-----------|-----------|---|----------|-------|-------|-------|
| ## 76 | -0.04982 | | 5 | -98.994 | 212.6 | 35.56 | 0.000 |
| ## 68 | -0.03217 | | 4 | -100.947 | 212.8 | 35.71 | 0.000 |
| ## 52 | | | 5 | -99.126 | 212.9 | 35.82 | 0.000 |
| ## 130 | -0.167500 | | 3 | -102.637 | 212.9 | 35.83 | 0.000 |
| ## 27 | | | 4 | -101.047 | 213.0 | 35.91 | 0.000 |
| ## 57 | | | 4 | -101.089 | 213.0 | 35.99 | 0.000 |
| ## 192 | 0.232800 | | 8 | -91.394 | 213.2 | 36.14 | 0.000 |
| ## 65 | -0.01745 | | 2 | -104.232 | 213.2 | 36.17 | 0.000 |
| ## 148 | -0.641100 | | 5 | -99.335 | 213.3 | 36.24 | 0.000 |
| ## 153 | 0.052930 | | 4 | -101.279 | 213.4 | 36.37 | 0.000 |
| ## 92 | -0.04040 | | 6 | -97.208 | 213.4 | 36.37 | 0.000 |
| ## 178 | -0.069290 | | 5 | -99.472 | 213.6 | 36.52 | 0.000 |
| ## 33 | | | 2 | -104.488 | 213.7 | 36.68 | 0.000 |
| ## 196 | -0.05731 | -0.693800 | 5 | -99.557 | 213.7 | 36.69 | 0.000 |
| ## 228 | -0.05832 | -0.410900 | 6 | -97.385 | 213.8 | 36.73 | 0.000 |
| ## 202 | -0.05579 | -0.607800 | 5 | -99.608 | 213.8 | 36.79 | 0.000 |
| ## 3 | | | 2 | -104.552 | 213.9 | 36.81 | 0.000 |
| ## 129 | -0.112500 | | 2 | -104.572 | 213.9 | 36.85 | 0.000 |
| ## 142 | -0.279900 | | 5 | -99.724 | 214.1 | 37.02 | 0.000 |
| ## 170 | 0.411900 | | 5 | -99.730 | 214.1 | 37.03 | 0.000 |
| ## 217 | -0.04176 | -0.331100 | 5 | -99.780 | 214.2 | 37.13 | 0.000 |
| ## 116 | -0.03836 | | 6 | -97.603 | 214.2 | 37.16 | 0.000 |
| ## 75 | -0.03931 | | 4 | -101.732 | 214.3 | 37.28 | 0.000 |
| ## 12 | | | 4 | -101.735 | 214.3 | 37.28 | 0.000 |
| ## 81 | -0.01386 | | 3 | -103.386 | 214.4 | 37.33 | 0.000 |
| ## 145 | -0.215400 | | 3 | -103.390 | 214.4 | 37.34 | 0.000 |
| ## 11 | | | 3 | -103.430 | 214.5 | 37.42 | 0.000 |
| ## 220 | -0.06419 | -1.070000 | 7 | -95.153 | 214.5 | 37.44 | 0.000 |
| ## 41 | | | 3 | -103.477 | 214.6 | 37.51 | 0.000 |
| ## 250 | -0.06476 | -0.688300 | 7 | -95.188 | 214.6 | 37.52 | 0.000 |
| ## 19 | | | 3 | -103.509 | 214.6 | 37.57 | 0.000 |
| ## 137 | 0.116600 | | 3 | -103.538 | 214.7 | 37.63 | 0.000 |
| ## 193 | -0.03391 | -0.445700 | 3 | -103.548 | 214.7 | 37.65 | 0.000 |
| ## 84 | -0.02264 | | 5 | -100.050 | 214.7 | 37.67 | 0.000 |
| ## 121 | -0.02967 | | 5 | -100.081 | 214.8 | 37.73 | 0.000 |
| ## 91 | -0.03032 | | 5 | -100.117 | 214.8 | 37.81 | 0.000 |
| ## 49 | | | 3 | -103.627 | 214.9 | 37.81 | 0.000 |
| ## 105 | -0.03522 | | 4 | -102.033 | 214.9 | 37.88 | 0.000 |
| ## 164 | 0.229000 | | 5 | -100.186 | 215.0 | 37.94 | 0.000 |
| ## 44 | | | 5 | -100.299 | 215.2 | 38.17 | 0.000 |
| ## 201 | -0.03867 | -0.228000 | 4 | -102.201 | 215.3 | 38.22 | 0.000 |
| ## 138 | -0.007612 | | 4 | -102.253 | 215.4 | 38.32 | 0.000 |
| ## 132 | -0.069870 | | 4 | -102.288 | 215.4 | 38.39 | 0.000 |
| ## 97 | -0.02022 | | 3 | -103.961 | 215.5 | 38.48 | 0.000 |
| ## 60 | | | 6 | -98.278 | 215.6 | 38.51 | 0.000 |
| ## 67 | -0.02032 | | 3 | -104.025 | 215.6 | 38.61 | 0.000 |
| ## 209 | -0.03365 | -0.548400 | 4 | -102.412 | 215.7 | 38.64 | 0.000 |
| ## 160 | -0.577300 | | 7 | -95.851 | 215.9 | 38.84 | 0.000 |
| ## 156 | -0.369700 | | 6 | -98.534 | 216.1 | 39.02 | 0.000 |
| ## 244 | -0.05931 | -1.083000 | 7 | -95.949 | 216.1 | 39.04 | 0.000 |
| ## 147 | -0.548800 | | 4 | -102.618 | 216.1 | 39.05 | 0.000 |
| ## 124 | -0.04843 | | 7 | -95.987 | 216.2 | 39.11 | 0.000 |
| ## 186 | 0.076730 | | 6 | -98.590 | 216.2 | 39.14 | 0.000 |
| ## 204 | -0.06062 | -0.401700 | 6 | -98.605 | 216.2 | 39.17 | 0.000 |
| ## 144 | -0.056380 | | 6 | -98.759 | 216.5 | 39.47 | 0.000 |

```

## 155      -0.184600    5 -100.962 216.5 39.50 0.000
## 35      -0.000000    3 -104.479 216.6 39.51 0.000
## 161     -0.041890    3 -104.481 216.6 39.52 0.000
## 59      -0.000000    5 -100.982 216.6 39.54 0.000
## 131     -0.074410    3 -104.525 216.7 39.61 0.000
## 185     -0.145700    5 -101.033 216.7 39.64 0.000
## 180     -0.353000    6  -98.875 216.7 39.71 0.000
## 177     -0.419700    4 -103.112 217.1 40.04 0.000
## 139      0.281200    4 -103.157 217.2 40.13 0.000
## 169      0.281900    4 -103.217 217.3 40.25 0.000
## 249 -0.04715 -0.730700    6  -99.166 217.3 40.29 0.000
## 236 -0.06158 -0.174100    7  -96.641 217.5 40.42 0.000
## 83  -0.01185      4 -103.356 217.6 40.53 0.000
## 113 -0.01447      4 -103.381 217.6 40.58 0.000
## 43      0.000000    4 -103.410 217.7 40.63 0.000
## 140      0.189700    5 -101.610 217.8 40.79 0.000
## 51      0.000000    4 -103.501 217.9 40.82 0.000
## 211 -0.03361 -0.897800    5 -101.624 217.9 40.82 0.000
## 195 -0.03393 -0.409500    4 -103.508 217.9 40.83 0.000
## 225 -0.03326 -0.404500    4 -103.529 217.9 40.87 0.000
## 107 -0.03948      5 -101.704 218.0 40.98 0.000
## 219 -0.04066 -0.543700    6  -99.527 218.1 41.01 0.000
## 203 -0.04057 -0.052930    5 -101.725 218.1 41.02 0.000
## 241 -0.03869 -0.917500    5 -101.843 218.3 41.26 0.000
## 172      0.429400    6  -99.711 218.4 41.38 0.000
## 233 -0.03732 -0.083660    5 -102.016 218.6 41.60 0.000
## 99  -0.02105      4 -103.919 218.7 41.65 0.000
## 123 -0.02986      6 -100.081 219.2 42.12 0.000
## 179     -0.748500    5 -102.342 219.3 42.26 0.000
## 163     -0.035200    4 -104.473 219.8 42.76 0.000
## 252 -0.06337 -0.875900    8  -94.954 220.3 43.27 0.000
## 187     -0.372900    6 -100.729 220.5 43.41 0.000
## 188     -0.158900    7  -98.232 220.6 43.60 0.000
## 171      0.347500    5 -103.042 220.7 43.66 0.000
## 243 -0.03890 -1.274000    6 -101.042 221.1 44.04 0.000
## 115 -0.01249      5 -103.335 221.3 44.24 0.000
## 227 -0.03365 -0.396900    5 -103.505 221.6 44.58 0.000
## 251 -0.04605 -0.926800    7  -98.935 222.1 45.01 0.000
## 235 -0.03986 -0.016630    6 -101.703 222.4 45.36 0.000
## Models ranked by AICc(x)

poisson2 <- glm(data = transect,
               detections_total ~ Tmax + Tmin +
               Theightmean + DBH_mean,
               family = "poisson",na.action=na.fail)
summary(poisson2)

##
## Call:
## glm(formula = detections_total ~ Tmax + Tmin + Theightmean +
##     DBH_mean, family = "poisson", data = transect, na.action = na.f
## ail)
##
## Deviance Residuals:
##      Min       1Q   Median       3Q      Max
## -3.8094  -1.8068   0.2687   0.9008   3.5766

```

```

##
## Coefficients:
##           Estimate Std. Error z value Pr(>|z|)
## (Intercept) 27.47080   10.72075   2.562  0.0104 *
## Tmax        -0.12895    0.02852  -4.522 6.14e-06 ***
## Tmin        -1.14335    0.48416  -2.362  0.0182 *
## Theightmean -0.10656    0.02084  -5.113 3.16e-07 ***
## DBH_mean     0.18028    0.02867   6.288 3.22e-10 ***
## ---
## Signif. codes:  0 '***' 0.001 '**' 0.01 '*' 0.05 '.' 0.1 ' ' 1
##
## (Dispersion parameter for poisson family taken to be 1)
##
## Null deviance: 134.116 on 18 degrees of freedom
## Residual deviance: 87.258 on 14 degrees of freedom
## AIC: 172.43
##
## Number of Fisher Scoring iterations: 5

autoplot(poisson2)

##Summarise model outputs

summ(poisson2)

## MODEL INFO:
## Observations: 19
## Dependent Variable: detections_total
## Type: Generalized linear model
## Family: poisson
## Link function: log
##
## MODEL FIT:
## <math>\chi^2(4) = 46.86, p = 0.00</math>
## Pseudo-R2 (Cragg-Uhler) = 0.92
## Pseudo-R2 (McFadden) = 0.22
## AIC = 172.43, BIC = 177.15
##
## Standard errors: MLE
## -----
##           Est.      S.E.    z val.      p
## -----
## (Intercept)    27.47    10.72     2.56    0.01
## Tmax           -0.13     0.03    -4.52    0.00
## Tmin           -1.14     0.48    -2.36    0.02
## Theightmean   -0.11     0.02    -5.11    0.00
## DBH_mean       0.18     0.03     6.29    0.00
## -----

#export_summs(poisson2, to.file = "docx", file.name = "GLMall.docx",ex
p=TRUE)
#Dsquared(poisson2)

tmax <- effect_plot(poisson2, pred = Tmax, interval = TRUE, plot.point
s = TRUE, x.label = "Maximum temperature, °C", y.label = "Total mamma

```

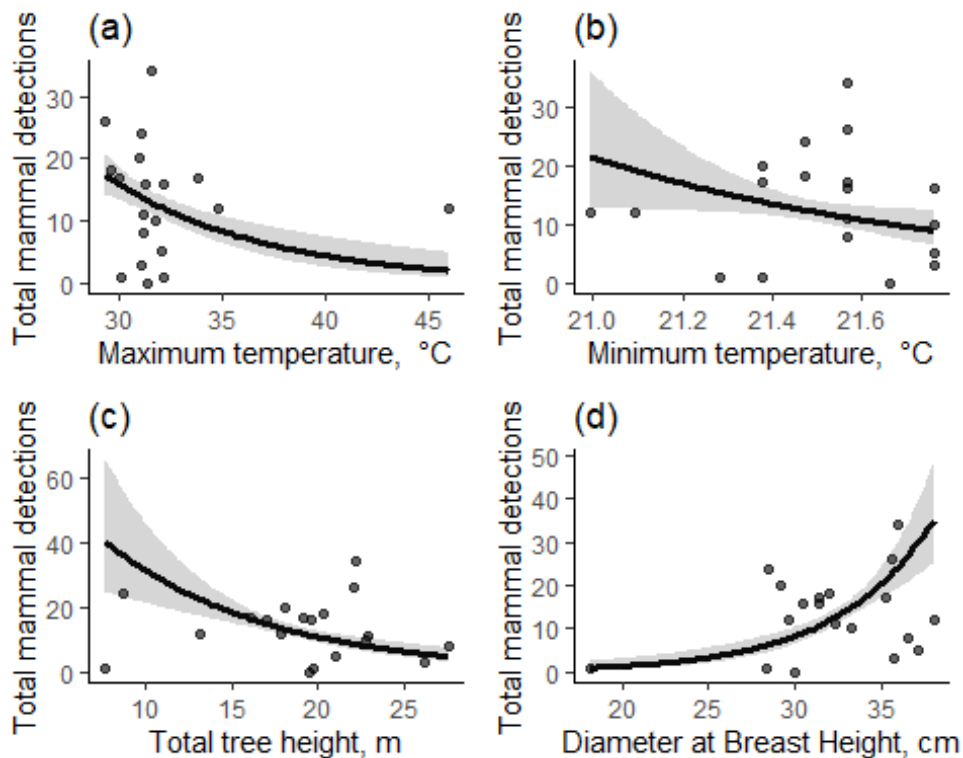
```

l detections")
tmin <- effect_plot(poisson2, pred = Tmin, interval = TRUE, plot.points = TRUE, x.label = "Minimum temperature, °C", y.label = "Total mammal detections")
height <- effect_plot(poisson2, pred = Theightmean, interval = TRUE, plot.points = TRUE, x.label = "Total tree height, m", y.label = "Total mammal detections")
dbh <- effect_plot(poisson2, pred = DBH_mean, interval = TRUE, plot.points = TRUE, x.label = "Diameter at Breast Height, cm", y.label = "Total mammal detections")

tmax <- tmax + theme_classic() + ggtitle("(a)")
tmin <- tmin + theme_classic() + ggtitle("(b)")
height <- height + theme_classic() + ggtitle("(c)")
dbh <- dbh + theme_classic() + ggtitle("(d)")

plots <- grid.arrange(tmax, tmin, height, dbh, ncol = 2)

```



```

#ggsave("GLMs.jpg", plot = plots, height = 200, width = 176, units = "mm")

```

2) GLMM of mammal occurrence, with Order included as a random factor

```

mem <- glmmTMB(detections ~
  Tmax+height+dbh+crown+conn+n+
  (1|order),
  data = camtraps, family=nbinom2, na.action="na.fail")
summary(mem)

```

```

## Family: nbinom2 ( log )
## Formula:
## detections ~ Tmax + height + dbh + crown + conn + n + (1 | order)
## Data: camtraps
##
##      AIC      BIC    logLik deviance df.resid
##    433.6    458.2   -207.8    415.6     105
##
## Random effects:
##
## Conditional model:
## Groups Name      Variance Std.Dev.
## order (Intercept) 0.9792   0.9895
## Number of obs: 114, groups: order, 6
##
## Overdispersion parameter for nbinom2 family (:): 0.686
##
## Conditional model:
##      Estimate Std. Error z value Pr(>|z|)
## (Intercept) -0.161818   1.886360  -0.086 0.931639
## Tmax        -0.181397   0.062508  -2.902 0.003708 **
## height      -0.207831   0.063883  -3.253 0.001141 **
## dbh         0.268027   0.078328   3.422 0.000622 ***
## crown       0.026142   0.017650   1.481 0.138573
## conn       -0.002326   0.012918  -0.180 0.857097
## n          0.062564   0.068749   0.910 0.362807
## ---
## Signif. codes:  0 '***' 0.001 '**' 0.01 '*' 0.05 '.' 0.1 ' ' 1

dredge(mem)

## Global model call: glmmTMB(formula = detections ~ Tmax + height + d
bh + crown +
##      conn + n + (1 | order), data = camtraps, family = nbinom2,
##      na.action = "na.fail", ziformula = ~0, dispformula = ~1)
## ---
## Model selection table
##      cnd((Int)) dsp((Int))    cnd(cnn) cnd(crw) cnd(dbh)  cnd(hgh)
cnd(n)
## 45  -0.59310          +                0.26760 -0.158000
## 47  -0.04987          +                0.02522 0.24010 -0.180600
## 61  -0.72080          +                0.29160 -0.184100 0.
049210
## 63  -0.24620          +                0.02630 0.26560 -0.208200 0.
055360
## 46  -0.75770          + 0.0036770                0.26960 -0.164600
## 48  -0.26770          + 0.0045410 0.02574 0.24150 -0.188100
## 62  -0.61020          + -0.0030660                0.29440 -0.183400 0.
058660
## 64  -0.16180          + -0.0023260 0.02614 0.26800 -0.207800 0.
062560
## 13  -3.86000          +                0.19050 -0.092440
## 15  -3.72000          +                0.01969 0.16660 -0.106000
## 5   -2.65800          +                0.09937
## 37  -0.91360          +                0.10820
## 14  -4.06200          + 0.0072330                0.19700 -0.108800

```

| | | | | | | | |
|--------|----------|---|------------|---------|---------|-----------|-----|
| ## 29 | -3.71900 | + | | | 0.18690 | -0.087860 | -0. |
| 010610 | | | | | | | |
| ## 21 | -2.39100 | + | | | 0.10560 | | -0. |
| 044340 | | | | | | | |
| ## 16 | -3.95100 | + | 0.0083820 | 0.02129 | 0.17180 | -0.125000 | |
| ## 3 | -0.67860 | + | | 0.02784 | | | |
| ## 7 | -2.48300 | + | | 0.01189 | 0.07739 | | |
| ## 38 | -0.62070 | + | -0.0081170 | | 0.12250 | | |
| ## 31 | -3.62600 | + | | 0.01953 | 0.16440 | -0.103100 | -0. |
| 006781 | | | | | | | |
| ## 53 | -0.88550 | + | | | 0.11260 | | -0. |
| 034940 | | | | | | | |
| ## 6 | -2.68800 | + | -0.0030360 | | 0.10420 | | |
| ## 39 | -0.71360 | + | | 0.01189 | 0.08582 | | |
| ## 30 | -3.68400 | + | 0.0111800 | | 0.18840 | -0.101600 | -0. |
| 037670 | | | | | | | |
| ## 35 | 0.97190 | + | | 0.02990 | | | |
| ## 23 | -2.20300 | + | | 0.01161 | 0.08353 | | -0. |
| 044210 | | | | | | | |
| ## 1 | 0.59370 | + | | | | | |
| ## 19 | -0.30560 | + | | 0.02862 | | | -0. |
| 038570 | | | | | | | |
| ## 32 | -3.56000 | + | 0.0120500 | 0.02112 | 0.16310 | -0.118000 | -0. |
| 036360 | | | | | | | |
| ## 43 | 2.00400 | + | | 0.04211 | | -0.050070 | |
| ## 11 | -0.43410 | + | | 0.03440 | | -0.028300 | |
| ## 22 | -2.29900 | + | 0.0039850 | | 0.10130 | | -0. |
| 055570 | | | | | | | |
| ## 4 | -0.71980 | + | 0.0012530 | 0.02760 | | | |
| ## 40 | -0.43680 | + | -0.0077920 | 0.01106 | 0.10080 | | |
| ## 55 | -0.68130 | + | | 0.01161 | 0.09029 | | -0. |
| 034660 | | | | | | | |
| ## 8 | -2.51300 | + | -0.0027670 | 0.01161 | 0.08223 | | |
| ## 54 | -0.70190 | + | -0.0053540 | | 0.11980 | | -0. |
| 018020 | | | | | | | |
| ## 51 | 1.07600 | + | | 0.03033 | | | -0. |
| 028670 | | | | | | | |
| ## 33 | 1.86500 | + | | | | | |
| ## 36 | 1.11800 | + | -0.0019450 | 0.03038 | | | |
| ## 17 | 0.93520 | + | | | | | -0. |
| 032240 | | | | | | | |
| ## 20 | -0.35580 | + | 0.0080960 | 0.02759 | | | -0. |
| 061350 | | | | | | | |
| ## 9 | 0.30950 | + | | | | 0.014800 | |
| ## 2 | 0.44230 | + | 0.0036400 | | | | |
| ## 27 | -0.19810 | + | | 0.03314 | | -0.020250 | -0. |
| 031440 | | | | | | | |
| ## 24 | -2.10100 | + | 0.0041880 | 0.01188 | 0.07847 | | -0. |
| 055980 | | | | | | | |
| ## 12 | -0.53130 | + | 0.0060950 | 0.03628 | | -0.040950 | |
| ## 44 | 1.85300 | + | 0.0037480 | 0.04292 | | -0.056640 | |
| ## 59 | 1.98500 | + | | 0.04164 | | -0.047660 | -0. |
| 008013 | | | | | | | |
| ## 56 | -0.51790 | + | -0.0048780 | 0.01124 | 0.09751 | | -0. |
| 019270 | | | | | | | |

| | | | | | | | | | |
|--------|----------|----|---|-----------|---------|-------|--------|--|---------------|
| ## 18 | 0.80730 | | + | 0.0104100 | | | | | -0. |
| 061130 | | | | | | | | | |
| ## 49 | 1.96500 | | + | | | | | | -0. |
| 023490 | | | | | | | | | |
| ## 28 | -0.18810 | | + | 0.0119600 | 0.03574 | | | | -0.037770 -0. |
| 058920 | | | | | | | | | |
| ## 52 | 0.87560 | | + | 0.0031340 | 0.02972 | | | | -0. |
| 038790 | | | | | | | | | |
| ## 25 | 0.56110 | | + | | | | | | 0.025570 -0. |
| 043320 | | | | | | | | | |
| ## 41 | 1.61600 | | + | | | | | | 0.009198 |
| ## 34 | 1.74300 | | + | 0.0015380 | | | | | |
| ## 10 | 0.29650 | | + | 0.0020660 | | | | | 0.011000 |
| ## 60 | 1.66700 | | + | 0.0067310 | 0.04195 | | | | -0.053570 -0. |
| 027010 | | | | | | | | | |
| ## 50 | 1.44200 | | + | 0.0078910 | | | | | -0. |
| 049040 | | | | | | | | | |
| ## 26 | 0.61260 | | + | 0.0085900 | | | | | 0.014910 -0. |
| 062640 | | | | | | | | | |
| ## 57 | 1.49600 | | + | | | | | | 0.018630 -0. |
| 033380 | | | | | | | | | |
| ## 42 | 1.60300 | | + | 0.0003773 | | | | | 0.008559 |
| ## 58 | 1.19900 | | + | 0.0066050 | | | | | 0.012910 -0. |
| 051790 | | | | | | | | | |
| ## | cnd(Tmx) | df | | logLik | AICc | delta | weight | | |
| ## 45 | -0.14190 | 6 | | -209.303 | 431.4 | 0.00 | 0.223 | | |
| ## 47 | -0.15330 | 7 | | -208.297 | 431.7 | 0.26 | 0.195 | | |
| ## 61 | -0.16330 | 7 | | -208.909 | 432.9 | 1.48 | 0.106 | | |
| ## 63 | -0.17690 | 8 | | -207.801 | 433.0 | 1.58 | 0.101 | | |
| ## 46 | -0.13960 | 7 | | -209.244 | 433.5 | 2.15 | 0.076 | | |
| ## 48 | -0.15020 | 8 | | -208.204 | 433.8 | 2.39 | 0.067 | | |
| ## 62 | -0.16910 | 8 | | -208.882 | 435.1 | 3.75 | 0.034 | | |
| ## 64 | -0.18140 | 9 | | -207.785 | 435.3 | 3.91 | 0.032 | | |
| ## 13 | | 5 | | -212.696 | 435.9 | 4.56 | 0.023 | | |
| ## 15 | | 6 | | -212.107 | 437.0 | 5.61 | 0.013 | | |
| ## 5 | | 4 | | -214.468 | 437.3 | 5.91 | 0.012 | | |
| ## 37 | -0.06371 | 5 | | -213.544 | 437.6 | 6.25 | 0.010 | | |
| ## 14 | | 6 | | -212.473 | 437.7 | 6.34 | 0.009 | | |
| ## 29 | | 6 | | -212.675 | 438.1 | 6.75 | 0.008 | | |
| ## 21 | | 5 | | -213.998 | 438.6 | 7.16 | 0.006 | | |
| ## 16 | | 7 | | -211.797 | 438.6 | 7.26 | 0.006 | | |
| ## 3 | | 4 | | -215.274 | 438.9 | 7.52 | 0.005 | | |
| ## 7 | | 5 | | -214.254 | 439.1 | 7.67 | 0.005 | | |
| ## 38 | -0.07685 | 6 | | -213.219 | 439.2 | 7.83 | 0.004 | | |
| ## 31 | | 7 | | -212.098 | 439.3 | 7.86 | 0.004 | | |
| ## 53 | -0.05749 | 6 | | -213.253 | 439.3 | 7.90 | 0.004 | | |
| ## 6 | | 5 | | -214.418 | 439.4 | 8.00 | 0.004 | | |
| ## 39 | -0.06408 | 6 | | -213.330 | 439.4 | 8.05 | 0.004 | | |
| ## 30 | | 7 | | -212.275 | 439.6 | 8.22 | 0.004 | | |
| ## 35 | -0.05461 | 5 | | -214.582 | 439.7 | 8.33 | 0.003 | | |
| ## 23 | | 6 | | -213.790 | 440.4 | 8.97 | 0.003 | | |
| ## 1 | | 3 | | -217.079 | 440.4 | 8.99 | 0.002 | | |
| ## 19 | | 5 | | -214.954 | 440.5 | 9.07 | 0.002 | | |
| ## 32 | | 8 | | -211.613 | 440.6 | 9.21 | 0.002 | | |
| ## 43 | -0.07420 | 6 | | -213.909 | 440.6 | 9.21 | 0.002 | | |

```

## 11      5 -215.029 440.6  9.22  0.002
## 22      6 -213.942 440.7  9.28  0.002
## 4       5 -215.265 441.1  9.69  0.002
## 40 -0.07670 7 -213.029 441.1  9.72  0.002
## 55 -0.05777 7 -213.045 441.1  9.76  0.002
## 8       6 -214.212 441.2  9.82  0.002
## 54 -0.06916 7 -213.180 441.4 10.03 0.001
## 51 -0.04897 6 -214.409 441.6 10.21 0.001
## 33 -0.03981 4 -216.676 441.7 10.33 0.001
## 36 -0.05732 6 -214.562 441.9 10.52 0.001
## 17      4 -216.874 442.1 10.72 0.001
## 20      6 -214.696 442.2 10.79 0.001
## 9       4 -216.985 442.3 10.95 0.001
## 2       4 -217.007 442.4 10.99 0.001
## 27      6 -214.845 442.5 11.09 0.001
## 24      7 -213.727 442.5 11.12 0.001
## 12      6 -214.867 442.5 11.13 0.001
## 44 -0.07160 7 -213.848 442.8 11.36 0.001
## 59 -0.07174 7 -213.898 442.9 11.46 0.001
## 56 -0.06847 8 -212.984 443.3 11.95 0.001
## 18      5 -216.473 443.5 12.11 0.001
## 49 -0.03514 5 -216.571 443.7 12.31 0.000
## 28      7 -214.361 443.8 12.39 0.000
## 52 -0.04259 7 -214.379 443.8 12.42 0.000
## 25      5 -216.634 443.8 12.43 0.000
## 41 -0.03753 5 -216.641 443.8 12.45 0.000
## 34 -0.03800 5 -216.664 443.9 12.49 0.000
## 10      5 -216.967 444.5 13.10 0.000
## 60 -0.06115 8 -213.763 444.9 13.51 0.000
## 50 -0.02058 6 -216.392 445.6 14.18 0.000
## 26      6 -216.400 445.6 14.20 0.000
## 57 -0.02839 6 -216.453 445.7 14.30 0.000
## 42 -0.03724 6 -216.640 446.1 14.68 0.000
## 58 -0.01817 7 -216.339 447.7 16.34 0.000
## Models ranked by AICc(x)
## Random terms (all models):
## 'cond(1 | order)'

mem2 <- glmmTMB(detections ~
               Tmax+height+dbh+
               (1|order),
               data = camtraps,family=nbinom2,na.action="na.fail")

##Plot model effects

temp <- plot_model(mem2, type = "pred", terms = c("Tmax", "order"),
                  pred.type="re",show.data = TRUE, title = "(a)")
height <- plot_model(mem2, type = "pred", terms = c("height", "order")
                    ,
                    pred.type="re",show.data = TRUE, title = "(b)")
dbh <- plot_model(mem2, type = "pred", terms = c("dbh", "order"),
                 pred.type="re",show.data = TRUE, title = "(c)")

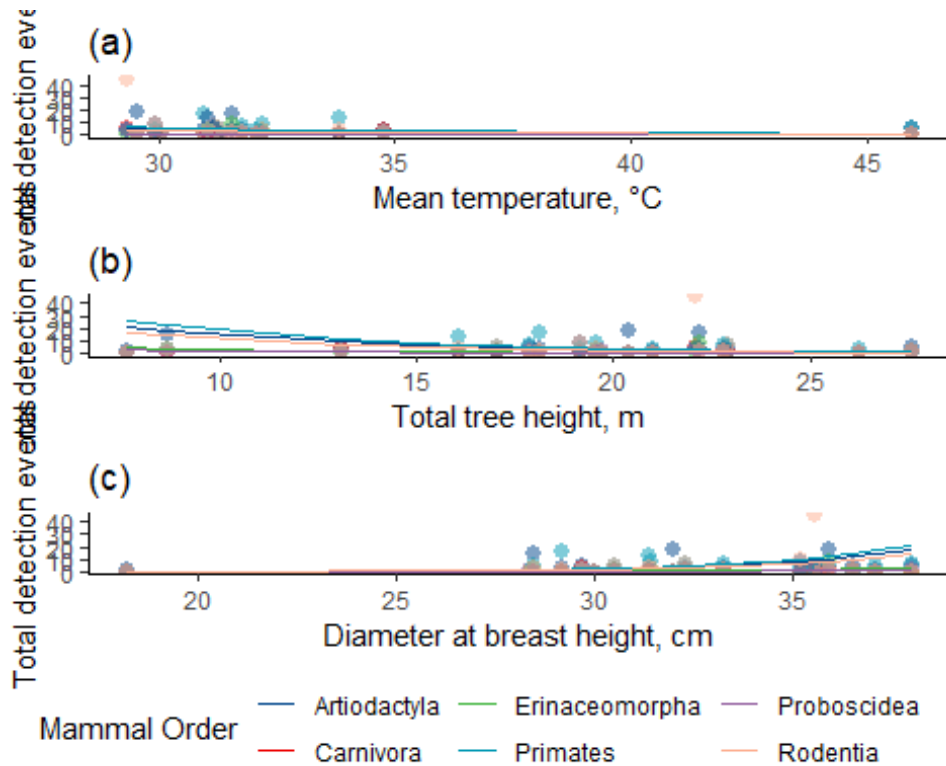
```

```

temp <- temp + theme_classic() + scale_color_lancet(name= "Mammal Order") +
  theme(legend.background = element_blank()) + geom_line(alpha = 1) +
  xlab("Mean temperature, °C") + ylab("Total detection events")
height <- height + theme_classic() + scale_color_lancet(name= "Mammal Order") +
  theme(legend.background = element_blank()) + geom_line(alpha = 1) +
  xlab("Total tree height, m") + ylab("Total detection events")
dbh <- dbh + theme_classic() + scale_color_lancet(name= "Mammal Order") +
  theme(legend.background = element_blank()) + geom_line(alpha = 1) +
  xlab("Diameter at breast height, cm") + ylab("Total detection events")

plots <- grid_arrange_shared_legend(temp, height, dbh,
  ncol = 1, nrow = 3, position = c("
bottom"))

```



```

#ggsave("memplots.jpg", plot = plots, height = 220, width = 130, units = "mm")

```

```

tab_model(mem2)

```

detections
Predictors
Incidence Rate Ratios
CI
p
(Intercept)

0.55
0.02 – 17.79
0.738
Tmax
0.87
0.78 – 0.96
0.006
height
0.85
0.77 – 0.95
0.004
dbh
1.31
1.14 – 1.50
<0.001
Random Effects
 σ^2
1.13
 τ_{00} order
0.94
ICC
0.45
N order
6
Observations
114
Marginal R2 / Conditional R2
0.194 / 0.560

Appendix 4.1

R scripts to run the NicheMapR microclimate model

Overview

This document includes the R code, required inputs and model outputs of the NicheMapR microclimate model for the Sikundur site in North Sumatra, Indonesia, and compares the model output with observed temperatures taken from data loggers for the period October 2018 - October 2019.

Setup for the model

First load the required packages and set the working directory.

```
library(NicheMapR)
library(ggplot2)
library(dplyr)
library(reshape2)
library(lubridate)
library(ggpubr)
library(gridExtra)
library(Metrics)
library(ggfortify)
library(ggforce)
library(ggeffects)
library(sjPlot)
library(corrplot)
library(MuMIn)
library(lme4)
library(Hmisc)
library(tidyverse)
library(sitreeE)
library(ggpointdensity)
library(viridis)

# setwd("~/PhD/Data/NicheMapR/")

# Next, download the global climate data set and unzip into working di
rectory, so that it can be called by NicheMapR(this only needs to be d
one once)
# get.global.climate(folder = "~/PhD/Data/NicheMapR/globalClimate")

# Load in site data containing parameters to be included in the model.
Slope, aspect and elevation are taken from global SRTM data, percentag
e shade was calculated from a DSM generated by UAVs in 2017 using Pote
ntial Incoming Solar Radiation (PISR) in SAGA-GIS.
control <- read.csv("control.csv")
```

Run the microclimate model

```
# Create empty data frames where models outputs will be stored.

M <- vector("list", length = nrow(control))
shadmet <- data.frame()
metout <- data.frame()

# Run the model using data from the control data frame as parameters.
Also, add columns to outputs for both max shade (shadmet) and no shade
(metout) for height, date, month and hour. The loop will run the model
for each row in the control data frame, and automatically add the outp
ut to the dataframes created in the previous step.

for(l in 1:nrow(control)) {
  M[[l]] <- micro_global(loc = c(control$long[l],control$lat[l]
), runmoist = 0, runshade = 1, minshade = 0, maxshade = control$shade1
[l], timeinterval = 365, REFL = 0.10, elev = control$SRTM_elev[l], slo
pe = control$SRTM_slope[l], ZH= control$ZH, aspect = control$SRTM_aspe
c[l], writescv = 1, message = 0, Refhyt = control$refhyt[l], Usrhyt =
control$usrhyt[l])
  shad <- data.frame(M[[l]][["shadmet"]])
  shad['LocID'] = control$LocID[l]
  shad['height'] = control$height[l]
  shad['H'] = control$usrhyt[l]
  shad['date'] <- if_else(shad$DOY > 273, as.Date(shad$DOY, orig
in = "2017-12-31"), as.Date(shad$DOY, origin = "2018-12-31"))
  shad['month'] = month(shad$date)
  shad['hour'] = shad$TIME/60
  shadmet <- rbind(shadmet,shad)
  met <- data.frame(M[[l]][["metout"]])
  met['LocID'] = control$LocID[l]
  met['height'] = control$height[l]
  met['H'] = control$usrhyt[l]
  met['date'] <- if_else(met$DOY > 273, as.Date(met$DOY, format
= "%j", origin = "2017-12-31"), as.Date(met$DOY, format = "%j", origin
= "2018-12-31"))
  met['month'] = month(met$date)
  met['hour'] = met$TIME/60
  metout <- rbind(metout,met)
}

# Reorder output dataframes to put Loc and height and date columns fir
st
metout <- metout[, c(20:25,1:19)]
shadmet <- shadmet[, c(20:25,1:19)]

# Write output files to .csv in source directory
write.csv(metout, "metout_SRTM.csv")
write.csv(shadmet, "shadmet_SRTM.csv")
```

Create a summary of the model outputs and observed values

Generate summary statistics for the air temperature output from the maximum shade model, and create a boxplot showing the range of predicted temperatures for each hour.

```
# Create datetime column in POSIXct format
model <- shadmet
dates <- as.character(model$date)
times <- as.character(model$hour)
datetime <- paste(dates, times)
datetime <- parse_date_time(datetime, "ymd H")
model <- cbind(model, datetime)
# Summarise model outputs for all data pooled
max(model$TALOC)

## [1] 33.27852

min(model$TALOC)

## [1] 20.7976

median(model$TALOC)

## [1] 23.68269

mean(model$TALOC)

## [1] 25.35264

# Read in logger data, and clean by removing rows of data where Lux >3
2,000, or where temp increased by >5, plus the following two data points
(to remove obs where logger was exposed to direct sunlight resulting
in high temp recordings). Records to remove are highlighted in the csv
with the value FALSE in the 'keep' column (value is generated using
'IF(AND())' rules in MS Excel).

loggers <- read.csv("log_hourly.csv")
loggers <- filter(loggers, keep != "FALSE")
# Create datetime column in POSIXct format and remove duplicate columns
dates <- as.character(loggers$date)
times <- as.character(loggers$time)
datetime <- paste(dates, times)
datetime <- parse_date_time(datetime, "dmy HMS")
loggers <- cbind(loggers,datetime)
loggers$LocID <- factor(loggers$LocID, levels = c("1","2","3","4","5",
"6","7","8",
"9","10","11","12",
"13","14","15"))
loggers$height <- factor(loggers$height, levels = c("1","2","3"))
model$LocID <- factor(model$LocID, levels = c("1","2","3","4","5","6",
"7","8",
"9","10","11","12",
"13","14","15"))
```

```

model$height <- factor(model$height, levels = c("1","2","3"))

#Summarise logger data
max(loggers$temp)

## [1] 44.089

min(loggers$temp)

## [1] 17.475

median(loggers$temp)

## [1] 25.028

mean(loggers$temp)

## [1] 26.26837

# Summary table of predictions for each loc and height
npred <- model %>% count(LocID,height)
modsum <- model %>%
  group_by(LocID, height) %>%
  summarise (Tmax=max(TALOC), Tmin=min(TALOC), Tmean=mean(TALOC), sdtemp=sd(TALOC))

## `summarise()` has grouped output by 'LocID'. You can override using
the `.groups` argument.

modsum <- merge (npred,modsum)
#write.csv(modsum, "model_tempsummaries.csv")

# Summary table of observed data for each location and height
nlog <- loggers %>% count(LocID,height)
logsum <- loggers %>%
  group_by(LocID, height) %>%
  summarise (Tmax=max(temp), Tmin=min(temp), Tmean=mean(temp), sdtemp=sd(temp))

## `summarise()` has grouped output by 'LocID'. You can override using
the `.groups` argument.

logsum <- merge(logsum, nlog)
#write.csv(logsum, "locsummary.csv")

# Clean model data by removing unnecessary columns
model <- select(model, LocID, height, H, DOY, datetime, month, hour, T
ALOC)

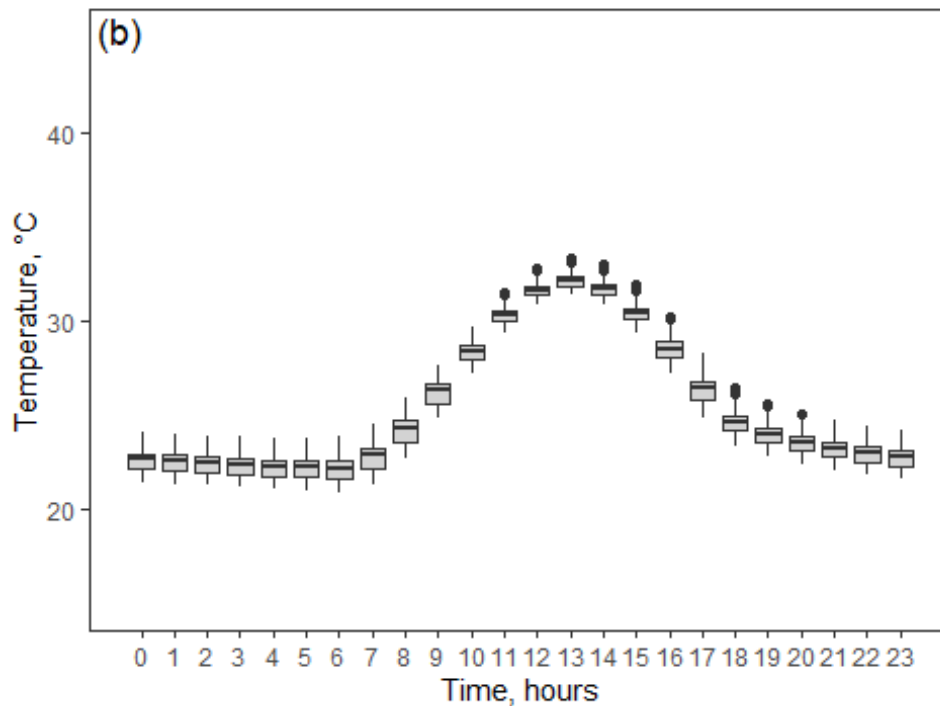
# Create boxplots for all predicted and observed temps by hour as two
plots with parts a) and b).
# Model boxplot
(boxplot2 <- ggplot(model, aes(group=hour, x=hour, y=TALOC)) +
  geom_boxplot(fill = 'lightgrey') +
  xlab('Time, hours') +
  ylab('Temperature, °C') +
  scale_x_continuous(breaks=seq(0,23,1)) +
  scale_y_continuous(limits = c(15,45)) +

```

```

theme_bw() +
theme(panel.grid = element_blank()) +
theme(legend.title = element_blank()) +
ggtitle("(b)") +
theme(plot.title = element_text(hjust = 0.01, vjust = - 6)))

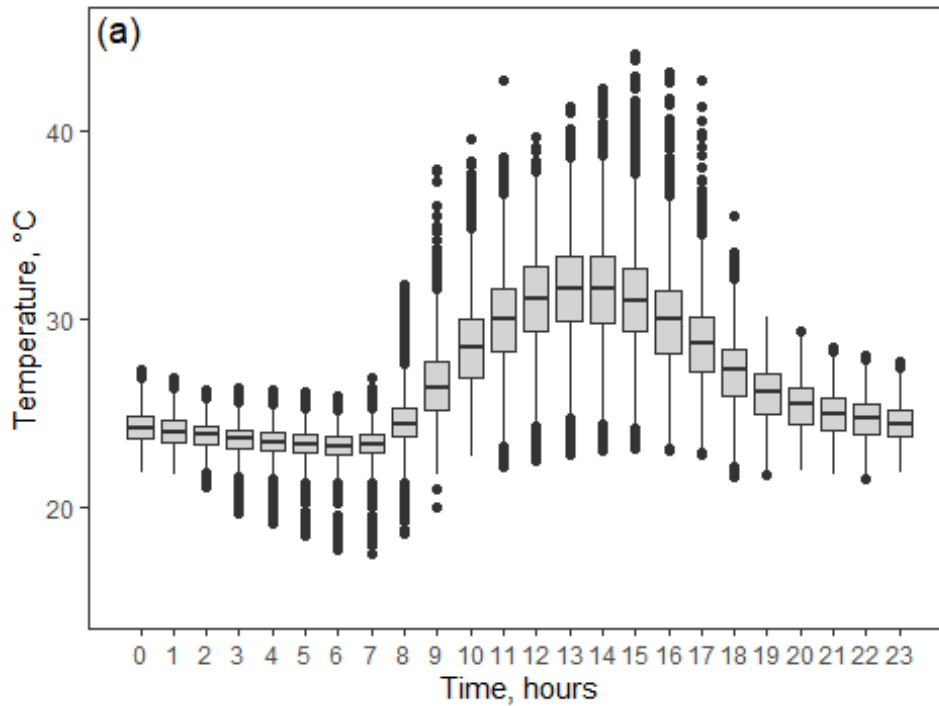
```



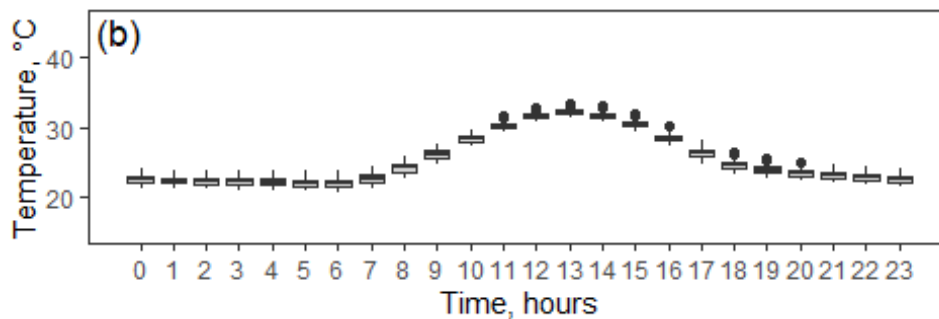
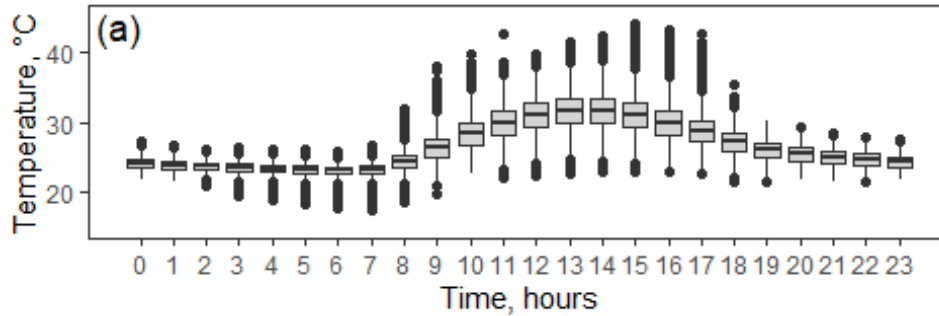
```

# Boxplot of observed values
(boxplot1 <- ggplot(loggers, aes(group=hour, x=hour, y=temp)) +
  geom_boxplot(fill = 'lightgrey') +
  xlab('Time, hours') +
  ylab('Temperature, °C') +
  scale_x_continuous(breaks=seq(0,23,1)) +
  scale_y_continuous(limits = c(15,45)) +
  theme_bw() +
  theme(panel.grid = element_blank()) +
  theme(legend.title = element_blank()) +
  ggtitle("(a)") +
  theme(plot.title = element_text(hjust = 0.01, vjust = - 6)))

```



```
#Combine into one plot with parts a) and b) and save as .jpg file
(boxplots <- grid.arrange(boxplot1,boxplot2, nrow=2))
```



```
## TableGrob (2 x 1) "arrange": 2 grobs
##   z      cells  name      grob
## 1 1 (1-1,1-1) arrange gtable[layout]
## 2 2 (2-2,1-1) arrange gtable[layout]
```

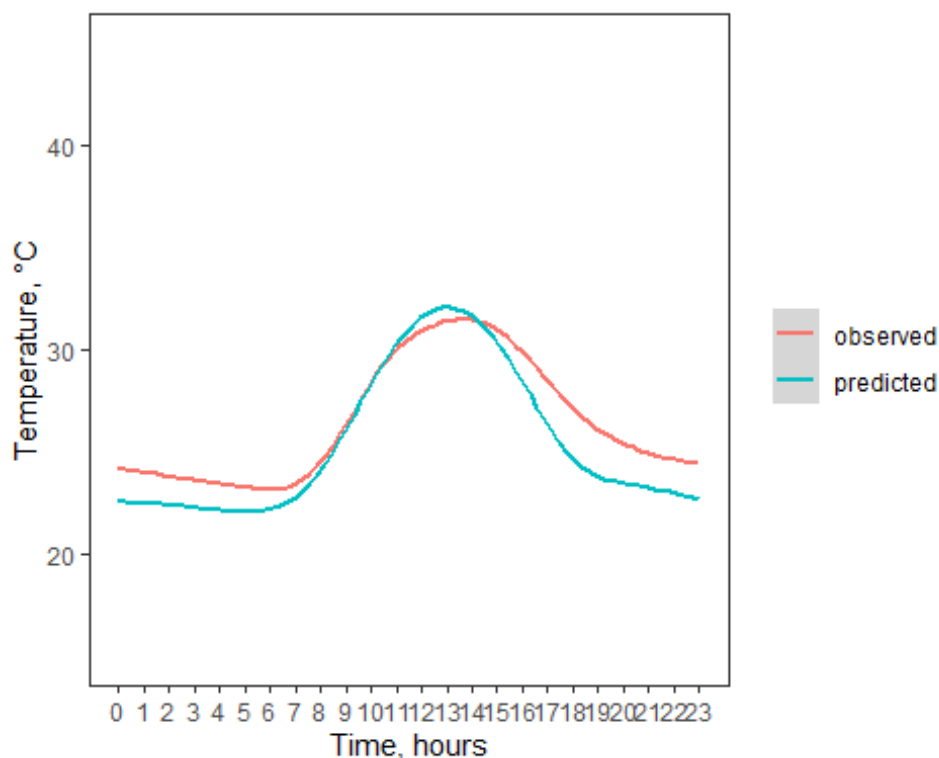
```

#ggsave("obs_pred_boxplots.jpg", plot = boxplots, height = 297, width
= 210, units = "mm")

# Plots daily obs and pred values as lines with SE on one plot
dayobs <- select(loggers, LocID, height, hour, temp)
daypred <- select(model, LocID, height, hour, TALOC)
daypred <- rename(daypred, "temp"=TALOC)
dayobs['type']="observed"
daypred['type']="predicted"
days <- rbind(dayobs,daypred)

(dayline <- ggplot(days, aes(group= type, x=hour, y=temp, color=type))
+
  geom_smooth(se=TRUE,level=0.5) +
  xlab('Time, hours') +
  ylab('Temperature, °C') +
  scale_x_continuous(breaks=seq(0,23,1)) +
  scale_y_continuous(limits = c(15,45)) +
  theme_bw() +
  theme(panel.grid = element_blank()) +
  theme(legend.title = element_blank())
)
## `geom_smooth()` using method = 'gam' and formula 'y ~ s(x, bs = "cs
")'

```



Test for differences between points

```

# Create variables in original dataframes with explicit nesting for Lo
cations and heights

```

```

loggers <- within(loggers, logID <- factor(LocID:height))
model <- within(model, logID <- factor(LocID:height))

##Test for differences between locations and heights
kruskal.test(temp ~ logID, data = loggers)

##
## Kruskal-Wallis rank sum test
##
## data: temp by logID
## Kruskal-Wallis chi-squared = 3660.4, df = 41, p-value < 2.2e-16

kruskal.test(TALOC ~ logID, data = model)

##
## Kruskal-Wallis rank sum test
##
## data: TALOC by logID
## Kruskal-Wallis chi-squared = 3280.5, df = 44, p-value < 2.2e-16

##Daily min, max and mean
obs <- loggers %>%
  group_by(logID,month) %>%
  summarise (meanObs = mean(temp), maxObs = max(temp), minObs = min(temp))

## `summarise()` has grouped output by 'logID'. You can override using
the `.groups` argument.

pred <- model %>%
  group_by(logID,month) %>%
  summarise (meanPred = mean(TALOC), maxPred = max(TALOC), minPred = min(TALOC))

## `summarise()` has grouped output by 'logID'. You can override using
the `.groups` argument.

kruskal.test(minPred ~ logID, data=pred)

##
## Kruskal-Wallis rank sum test
##
## data: minPred by logID
## Kruskal-Wallis chi-squared = 76.14, df = 44, p-value = 0.001878

kruskal.test(maxPred~logID,data=pred)

##
## Kruskal-Wallis rank sum test
##
## data: maxPred by logID
## Kruskal-Wallis chi-squared = 167.6, df = 44, p-value = 2.561e-16

kruskal.test(meanPred~logID,data=pred)

##
## Kruskal-Wallis rank sum test
##

```

```

## data: meanPred by logID
## Kruskal-Wallis chi-squared = 79.771, df = 44, p-value = 0.000777

kruskal.test(minObs~logID,data=obs)

##
## Kruskal-Wallis rank sum test
##
## data: minObs by logID
## Kruskal-Wallis chi-squared = 20.172, df = 41, p-value = 0.9974

kruskal.test(maxObs~logID,data=obs)

##
## Kruskal-Wallis rank sum test
##
## data: maxObs by logID
## Kruskal-Wallis chi-squared = 259.43, df = 41, p-value < 2.2e-16

kruskal.test(meanObs~logID,data=obs)

##
## Kruskal-Wallis rank sum test
##
## data: meanObs by logID
## Kruskal-Wallis chi-squared = 172.52, df = 41, p-value < 2.2e-16

```

Compare model outputs to logger data

Calculate and summarise model residuals (i.e. the difference between observed and expected values)

```

# Merge into on data frame and add column for observed - expected
all <- merge(loggers, model)
all <- select(all, LocID, height, H, DOY, datetime, month, hour, temp, TALOC)
all['diff'] = all$temp - all$TALOC

# write.csv(all, "diff.csv")

# Calculate root mean square error (RMSE), average absolute difference
(MAD), and Spearman's rho correlation
rms <- rmse(all$temp, all$TALOC)
mad <- mae(all$temp, all$TALOC)
corr <- cor.test(all$temp, all$TALOC, method = "spearman")
rho <- corr$estimate
stat <- cbind(rho,rms,mad)
stat

##           rho           rms           mad
## rho 0.8073995 2.253268 1.801031

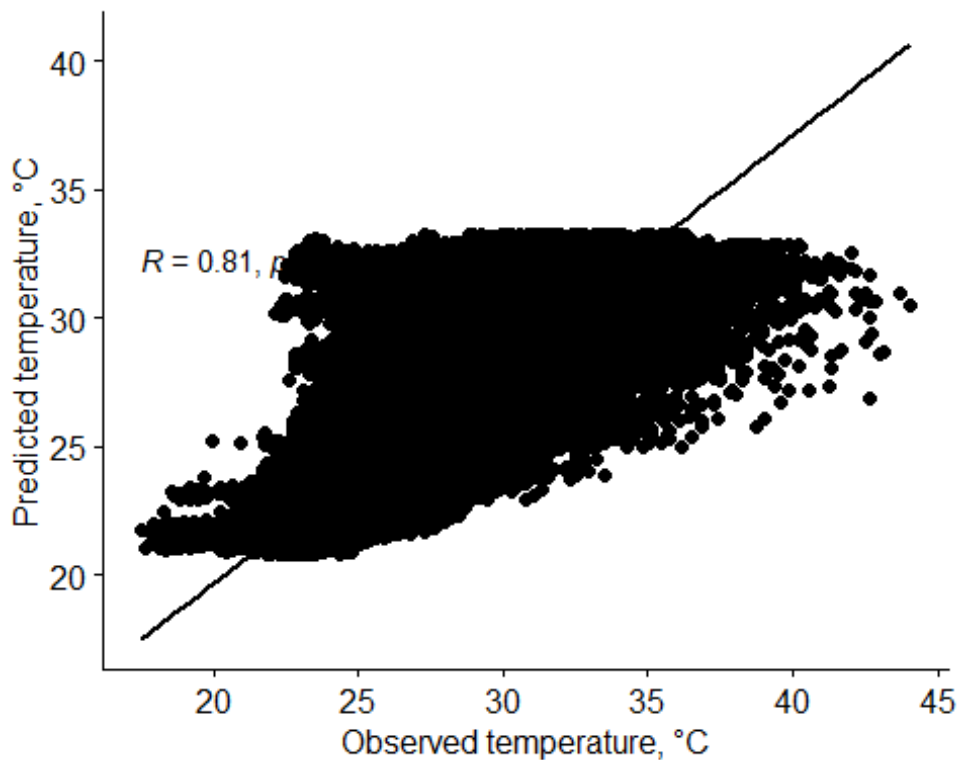
## Plot data
ggscatter(all, x = "temp", y = "TALOC",
          add = "reg.line", conf.int = TRUE,
          cor.coef = TRUE, cor.method = "spearman",

```

```

      xlab = "Observed temperature, °C", ylab = "Predicted temperature, °C")
## `geom_smooth()` using formula 'y ~ x'

```



Next, create ribbon plots of the range of both predicted and observed values for each day of the year (part a), and combine with scatter plot of predicted ~ observed values (part b).

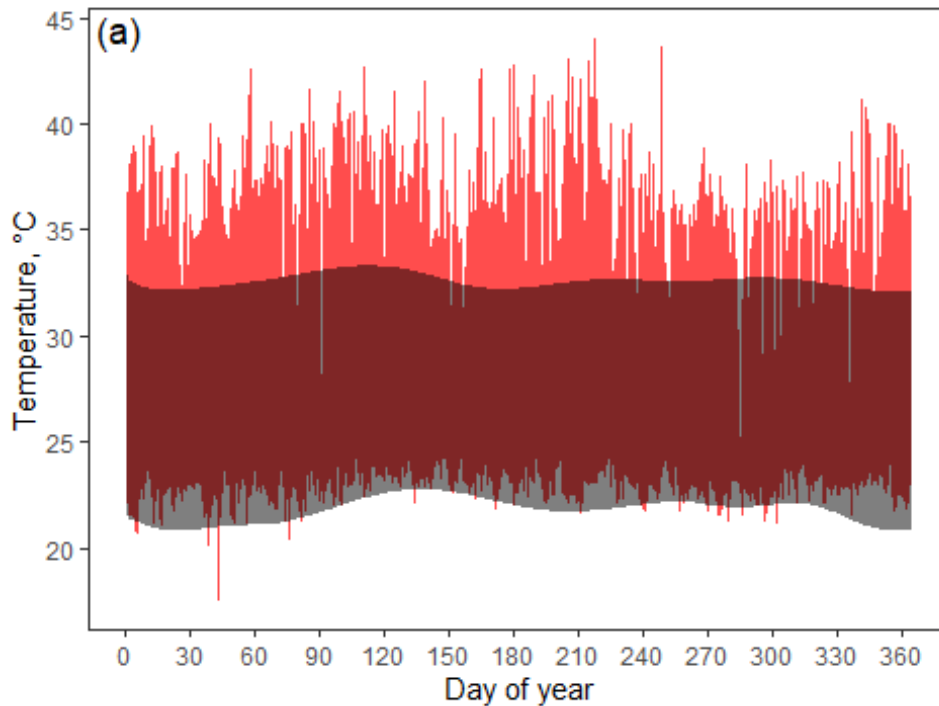
```

# Generate daily summaries and combine into one data frame
pred <- model %>%
  group_by(DOY) %>%
  summarise(TmaxPred = max(TALOC), TminPred = min(TALOC), TmeanPred =
mean(TALOC))
obs <- loggers %>%
  group_by(DOY) %>%
  summarise(TmaxObs = max(temp), TminObs = min(temp), TmeanObs = mean(
temp))
daily <- merge(obs,pred)

### ribbon plots of ranges of observed vs predicted values for each DO
Y.
(modplot <- ggplot(daily, aes(x=DOY)) +
  geom_ribbon(aes(ymin = TminObs, ymax = TmaxObs), fill = 'red', alpha
= 0.7) +
  geom_ribbon (aes(ymin= TminPred, ymax = TmaxPred), fill = 'black', a
lpha = 0.5) +
  xlab('Day of year') +
  ylab('Temperature, °C') +
  scale_x_continuous(breaks=seq(0,365,30)) +
  theme_bw() +
  theme(panel.grid = element_blank()) +

```

```
ggtitle("(a)") +
theme(plot.title = element_text(hjust = 0.01, vjust = - 6)))
```

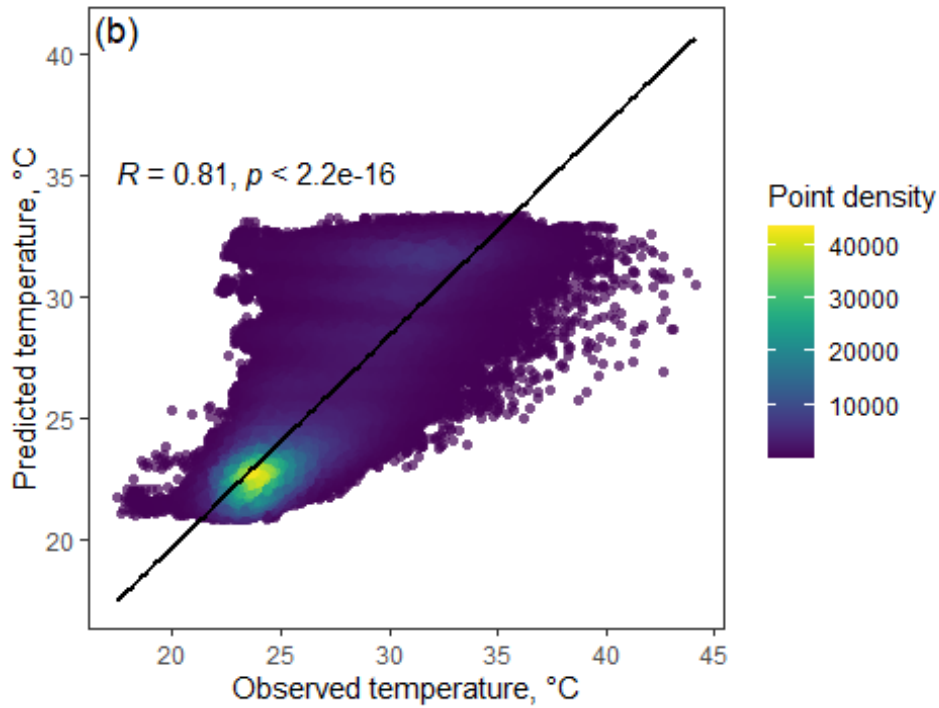


##Scatter plot (with points coloured by density) of predicted ~ observed values

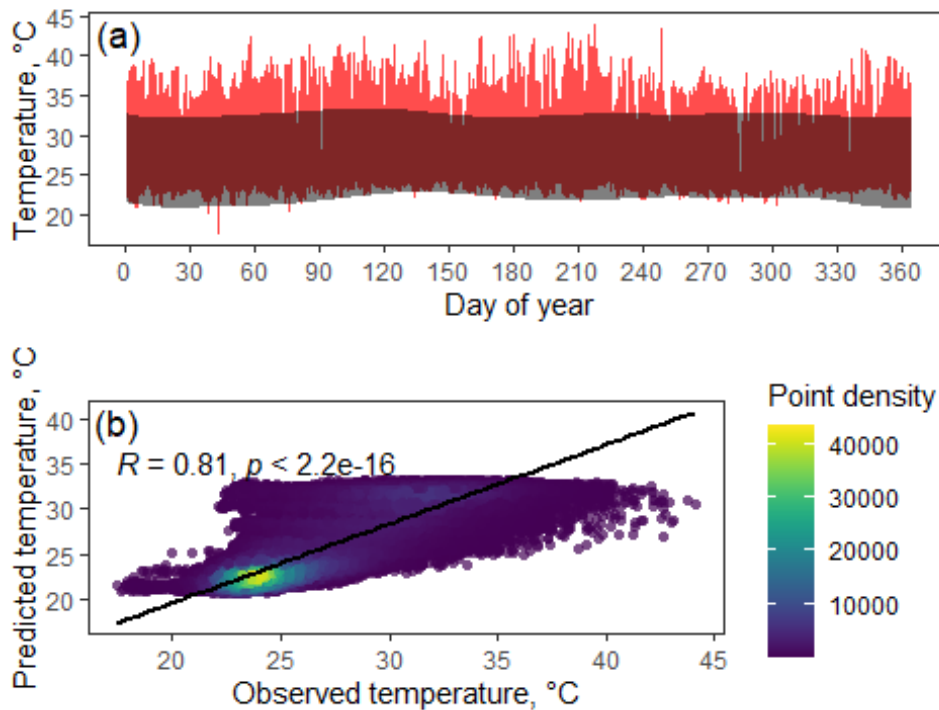
```
dat <- merge(loggers, model)
dat <- select(dat, temp, TALOC)

(densplot <- ggplot(dat, aes(x=temp,y=TALOC))+
  geom_pointdensity(alpha=0.7,shape=16) +
  scale_color_viridis("Point density") +
  geom_smooth(aes(x=temp,y=TALOC),method="lm",se=TRUE,colour="black"
) +
  stat_cor(method="spearman",label.y=35) +
  xlab("Observed temperature, °C") +
  ylab("Predicted temperature, °C") +
  ggtitle("(b)") +
  theme_bw() +
  theme(plot.title = element_text(hjust = 0.01, vjust = - 6))+
  theme(panel.grid = element_blank()) )

## `geom_smooth()` using formula 'y ~ x'
```



```
(plots <- grid.arrange(modplot, densplot, nrow = 2))
## `geom_smooth()` using formula 'y ~ x'
```



```
## TableGrob (2 x 1) "arrange": 2 grobs
##   z      cells  name      grob
## 1 1 (1-1,1-1) arrange gtable[layout]
## 2 2 (2-2,1-1) arrange gtable[layout]
```

```
#ggsave("modelcorrelation.jpg", plot = plots, height = 297, width = 210, units = "mm")
```

Calculate residuals for each individual location and height separately (multiple loops are used due to missing data in some locations)

```
# Empty data frame to store outputs in
stats <- data.frame(loc=vector(),h=vector(),rho=vector(),rms=vector(),
mad=vector())
# vectors for Loc and height IDs
l <- c(1,3,5,6,7,8,9,11,12,13,14,15)
ht <- c(1,2,3)
for (i in l) {
  log <- filter(loggers, LocID == i)
  mod <- filter(model, LocID == i)
  loc <- i
  for (h in ht) {
    obs <- filter(log, height == h)
    pred <- filter(mod, height == h)
    height <- h
    H <- obs$H[h]
    data <- merge(obs,pred, by="datetime")
    data <- rename(data, 'obs' = temp, 'pred' = TALOC)
    data <- select(data, obs, pred)
    n <- count(data)
    rms <- round(rmse(data$obs, data$pred),2)
    mad <- round(mae(data$obs, data$pred),2)
    corr <- cor.test(data$obs, data$pred, method = "spearman")
    rho <- round(corr$estimate,2)
    P <- round(p.adjust(corr$p.value,"bonferroni"),3)
    stats <- rbind(stats, cbind (loc,height,H,n,rho,rms,mad,P))
  } }

ht <- c(1,3)
loc <- 2
log <- filter(loggers, LocID == loc)
mod <- filter(model, LocID == loc)
for (h in ht) {
  obs <- filter(log, height == h)
  pred <- filter(mod, height == h)
  height <- h
  H <- obs$H[h]
  data <- merge(obs,pred, by="datetime")
  data <- rename(data, 'obs' = temp, 'pred' = TALOC)
  data <- select(data, obs, pred)
  n <- count(data)
  rms <- round(rmse(data$obs, data$pred),2)
  mad <- round(mae(data$obs, data$pred),2)
  corr <- cor.test(data$obs, data$pred, method = "spearman")
  rho <- round(corr$estimate,2)
  P <- round(p.adjust(corr$p.value,"bonferroni"),3)
  stats <- rbind(stats, cbind (loc,height,H,n,rho,rms,mad,P))
}

ht <- c(2,3)
```

```

loc <- 4
log <- filter(loggers, LocID == loc)
mod <- filter(model, LocID == loc)
for (h in ht) {
  obs <- filter(log, height == h)
  pred <- filter(mod, height == h)
  height <- h
  H <- obs$H[h]
  data <- merge(obs,pred, by="datetime")
  data <- rename(data, 'obs'= temp, 'pred' = TALOC)
  data <- select(data, obs, pred)
  n <- count(data)
  rms <- round(rmse(data$obs, data$pred),2)
  mad <- round(mae(data$obs, data$pred),2)
  corr <- cor.test(data$obs, data$pred, method = "spearman")
  rho <- round(corr$estimate,2)
  P <- round(p.adjust(corr$p.value,"bonferroni"),3)
  stats <- rbind(stats, cbind (loc,height,H,n,rho,rms, mad,P))
}

ht <- c(1,2)
loc <- 10
log <- filter(loggers, LocID == loc)
mod <- filter(model, LocID == loc)
for (h in ht) {
  obs <- filter(log, height == h)
  pred <- filter(mod, height == h)
  height <- h
  H <- obs$H[h]
  data <- merge(obs,pred, by="datetime")
  data <- rename(data, 'obs'= temp, 'pred' = TALOC)
  data <- select(data, obs, pred)
  n <- count(data)
  rms <- round(rmse(data$obs, data$pred),2)
  mad <- round(mae(data$obs, data$pred),2)
  corr <- cor.test(data$obs, data$pred, method = "spearman")
  rho <- round(corr$estimate,2)
  P <- round(p.adjust(corr$p.value,"bonferroni"),3)
  stats <- rbind(stats, cbind (loc,height,H,n,rho,rms, mad,P))
}
#write.csv(stats, "residuals.csv")

## Summary of residuals for individual sampling points
# Spearmans rho
max(stats$rho)

## [1] 0.86

min(stats$rho)

## [1] 0.69

# Root mean sqaure error
max(stats$rms)

## [1] 2.71

```

```

min(stats$rms)
## [1] 1.84
# Mean absolute error
max(stats$mad)
## [1] 2.17
min(stats$mad)
## [1] 1.41

```

Test for effects of vegetation on model performance

```

# Load in plot vegetation data, and create a data frame of summary variables for each plot.
rawveg <- read.csv("veg.csv")
# Calculate basal area for all indivl trees
basal.area.fn <- function(x){ (pi*(x)^2)/40000 } # calculate basal area in m^2
rawveg["ba"] = basal.area.fn(rawveg$dbh)
# Calculate Lorey's mean height for each plot (mean tree height weighted by basal area)
loreys <- lorey.height(rawveg$ba,rawveg$height,group.id=rawveg$LocID)
loreys <- rename(loreys, "LocID" = group.id, "lorey" = lorey.height)
# Count number of trees per plot
n <- rawveg %>% count(LocID)
# Calculate mean, max and min for tree variables
veg <- rawveg %>%
  group_by(LocID) %>%
  summarise(meanDbh = mean(dbh), meanheight = mean(height), maxheight = max(height),
            meanbole = mean(bole), meandepth = mean(depth), meanCA = mean(CA), meanconn = mean(conn))
# Combine data into one data frame
veg <- merge(veg,n)
veg <- merge(veg,loreys)

# Check for correlations between vegetation variables.
veg.cor <- cor(veg, method = c("pearson"))
round(veg.cor, 2)

##           LocID meanDbh meanheight maxheight meanbole meandepth meanCA
## LocID      1.00    0.36    0.34    -0.07    0.39    0.06
## meanDbh    0.36    1.00    0.48    0.43    0.53    0.12
## meanheight 0.34    0.48    1.00    0.54    0.84    0.62
## maxheight -0.07    0.43    0.54    1.00    0.66    0.03
## meanbole   0.39    0.53    0.84    0.66    1.00    0.10

```

```

## meandepth  0.06   0.12   0.62   0.03   0.10   1.00
0.28
## meanCA     0.26   0.87   0.55   0.50   0.51   0.28
1.00
## meanconn   0.15  -0.24  -0.15  -0.06  -0.16  -0.04  -
0.36
## n          0.00  -0.20  -0.25   0.00   0.11  -0.61  -
0.33
## lorey     -0.06   0.59   0.63   0.88   0.71   0.14
0.74
##          meanconn    n lorey
## LocID          0.15  0.00 -0.06
## meanDbh        -0.24 -0.20  0.59
## meanheight     -0.15 -0.25  0.63
## maxheight     -0.06  0.00  0.88
## meanbole      -0.16  0.11  0.71
## meandepth     -0.04 -0.61  0.14
## meanCA        -0.36 -0.33  0.74
## meanconn       1.00  0.31 -0.36
## n              0.31  1.00 -0.11
## lorey         -0.36 -0.11  1.00

veg.cor

##          LocID    meanDbh meanheight    maxheight    meanb
ole
## LocID      1.000000000  0.3581285  0.3399996 -0.067683019  0.39022
123
## meanDbh    0.358128483  1.0000000  0.4784851  0.426097522  0.52769
019
## meanheight 0.339999623  0.4784851  1.0000000  0.537621494  0.84032
876
## maxheight  -0.067683019  0.4260975  0.5376215  1.000000000  0.66075
217
## meanbole   0.390221227  0.5276902  0.8403288  0.660752171  1.00000
000
## meandepth  0.060906206  0.1167054  0.6227871  0.033208018  0.09922
945
## meanCA     0.258131116  0.8677214  0.5516407  0.502263809  0.50541
028
## meanconn   0.150944623  -0.2372800  -0.1525567  -0.056740642  -0.16498
367
## n          0.004614358  -0.1984556  -0.2457070  -0.004347349  0.11045
939
## lorey     -0.055515786  0.5928437  0.6332287  0.882982694  0.70766
636
##          meandepth    meanCA    meanconn          n          lo
rey
## LocID      0.06090621  0.2581311  0.15094462  0.004614358 -0.05551
579
## meanDbh    0.11670543  0.8677214  -0.23727998  -0.198455633  0.59284
369
## meanheight 0.62278707  0.5516407  -0.15255673  -0.245707004  0.63322
874
## maxheight  0.03320802  0.5022638  -0.05674064  -0.004347349  0.88298
269

```

```

## meanbole 0.09922945 0.5054103 -0.16498367 0.110459386 0.70766
636
## meandepth 1.00000000 0.2831507 -0.04191655 -0.610460787 0.14099
735
## meanCA 0.28315071 1.0000000 -0.35912708 -0.333290445 0.74211
953
## meanconn -0.04191655 -0.3591271 1.00000000 0.308307216 -0.35541
085
## n -0.61046079 -0.3332904 0.30830722 1.000000000 -0.11439
050
## lorey 0.14099735 0.7421195 -0.35541085 -0.114390496 1.00000
000

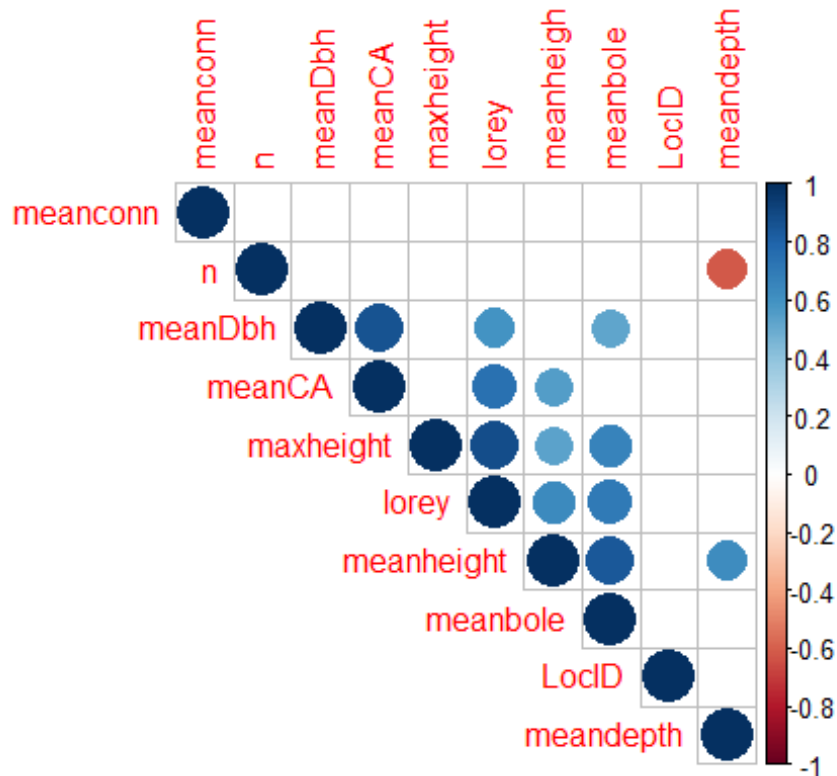
cor2 <- rcorr(as.matrix(veg))
cor2$P

##          LocID      meanDbh  meanheight  maxheight  mea
nbole
## LocID          NA 1.899644e-01 2.150022e-01 8.105879e-01 1.50445
2e-01
## meanDbh 0.1899644          NA 7.118908e-02 1.132632e-01 4.32089
7e-02
## meanheight 0.2150022 7.118908e-02          NA 3.873604e-02 8.78157
4e-05
## maxheight 0.8105879 1.132632e-01 3.873604e-02          NA 7.32601
3e-03
## meanbole 0.1504452 4.320897e-02 8.781574e-05 7.326013e-03
NA
## meandepth 0.8292814 6.787234e-01 1.314224e-02 9.064738e-01 7.24955
8e-01
## meanCA 0.3529488 2.769282e-05 3.302148e-02 5.639677e-02 5.46228
4e-02
## meanconn 0.5912799 3.944834e-01 5.872776e-01 8.408149e-01 5.56804
0e-01
## n 0.9869785 4.783020e-01 3.773948e-01 9.877319e-01 6.95134
9e-01
## lorey 0.8442120 1.984993e-02 1.127345e-02 1.296959e-05 3.16298
7e-03
##          meandepth      meanCA  meanconn          n      lore
y
## LocID 0.82928141 3.529488e-01 0.5912799 0.98697846 8.442120e-0
1
## meanDbh 0.67872335 2.769282e-05 0.3944834 0.47830197 1.984993e-0
2
## meanheight 0.01314224 3.302148e-02 0.5872776 0.37739480 1.127345e-0
2
## maxheight 0.90647377 5.639677e-02 0.8408149 0.98773189 1.296959e-0
5
## meanbole 0.72495582 5.462284e-02 0.5568040 0.69513492 3.162987e-0
3
## meandepth          NA 3.064852e-01 0.8820886 0.01564781 6.162150e-0
1
## meanCA 0.30648523          NA 0.1886428 0.22477305 1.534853e-0
3
## meanconn 0.88208861 1.886428e-01          NA 0.26357149 1.935915e-0
1

```

```
## n          0.01564781 2.247731e-01 0.2635715          NA 6.847907e-0
1
## lorey     0.61621496 1.534853e-03 0.1935915 0.68479071          N
A
```

```
corrplot(cor2$r, type="upper", order="hclust",
          p.mat = cor2$P, sig.level = 0.05, insig = "blank")
```



```
# Rename model error data, remove unnecessary columns and then merge w
ith vegetation data.
```

```
rawmod <- select(all, -height)
```

```
# Calculate monthly mean, max and min temp and rmse and mae per month
per point
```

```
mod <- rawmod%>%
```

```
  group_by(LocID,H,month)%>%
```

```
  summarise(rms=rmse(temp,TALOC), mad=mae(temp,TALOC),
```

```
            meandiff=mean(diff),maxdiff=max(diff),mindiff=min(diff),
```

```
            Tmean=mean(temp),Tmax=max(temp),Tmin=min(temp),
```

```
            TALOCmean=mean(TALOC),maxTALOC=max(TALOC),minTALOC=min(TAL
```

```
OC))
```

```
## `summarise()` has grouped output by 'LocID', 'H'. You can override
using the `.groups` argument.
```

```
# Tidy data to remove unnecessary columns, set location and month as f
actors and then merge with vegetation data
```

```
vars <- merge(mod, veg)
```

```
vars$LocID_f <- factor(vars$LocID, levels = c("1","2","3","4","5","6",
"7","8","9","10",
```

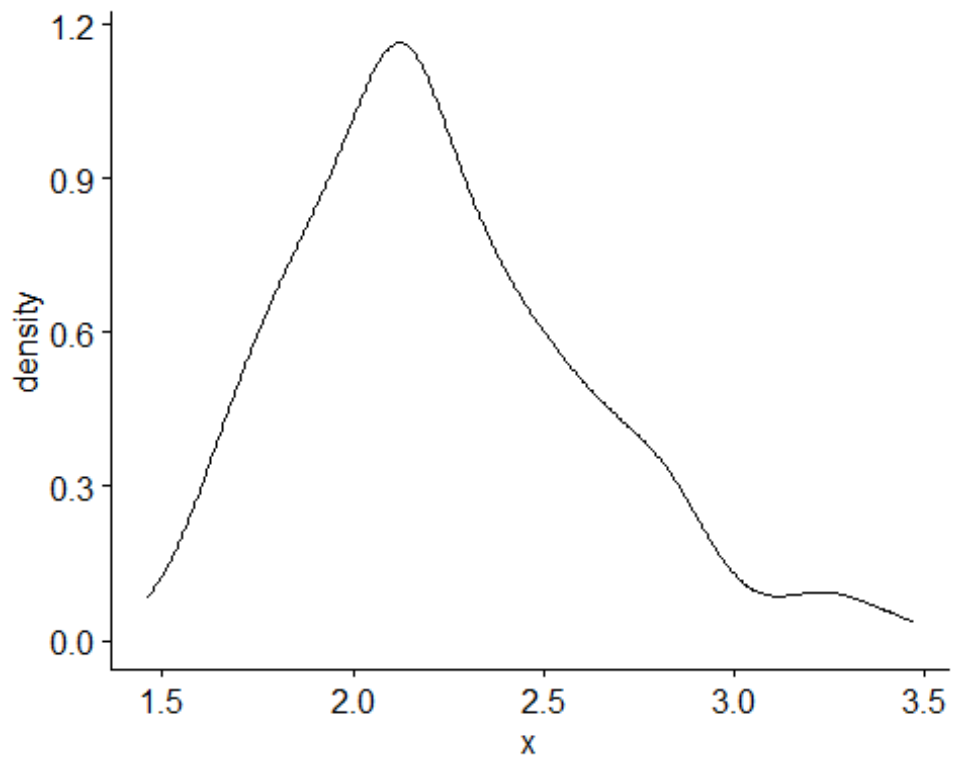
```
                                             "11","12","13","14","15"
```

```
))
```

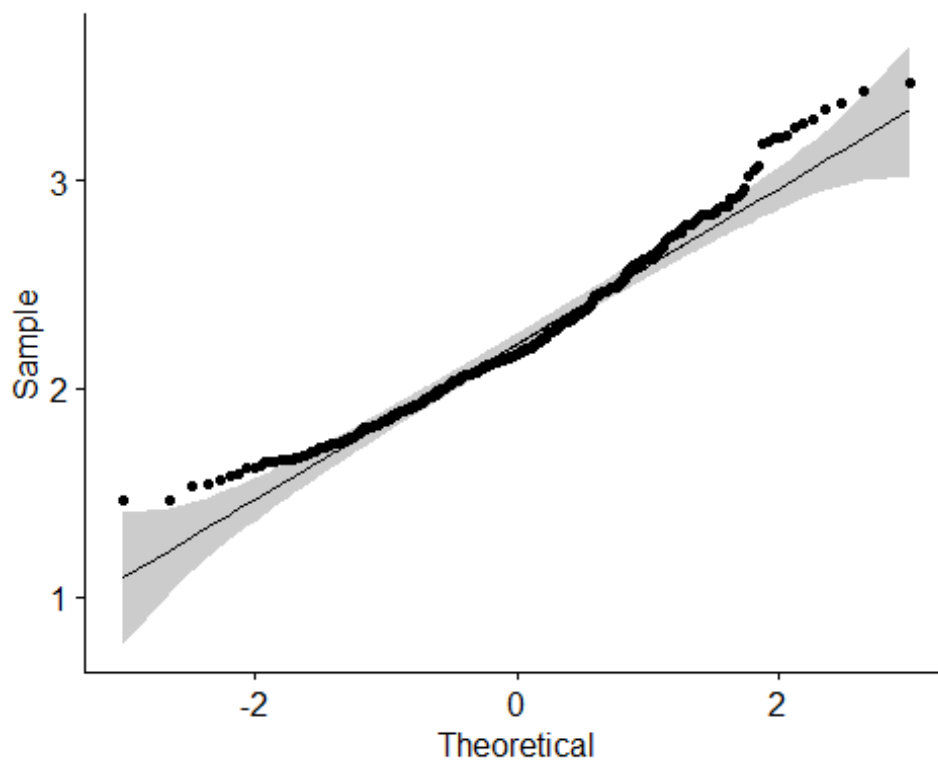
```
vars$month_f <- factor(vars$month, levels = c("1","2","3","4","5","6",
"7",
```

```
"8","9","10","11","12"))
```

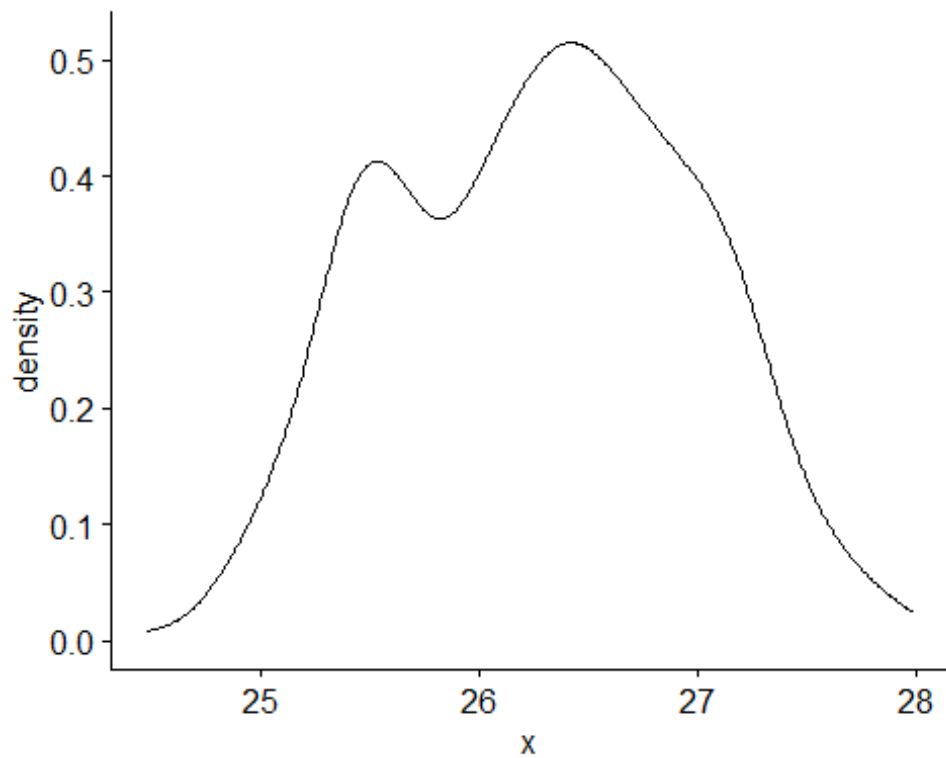
```
# Check response variable distribution and visualise data.  
# Model error  
ggdensity(vars$rms)
```



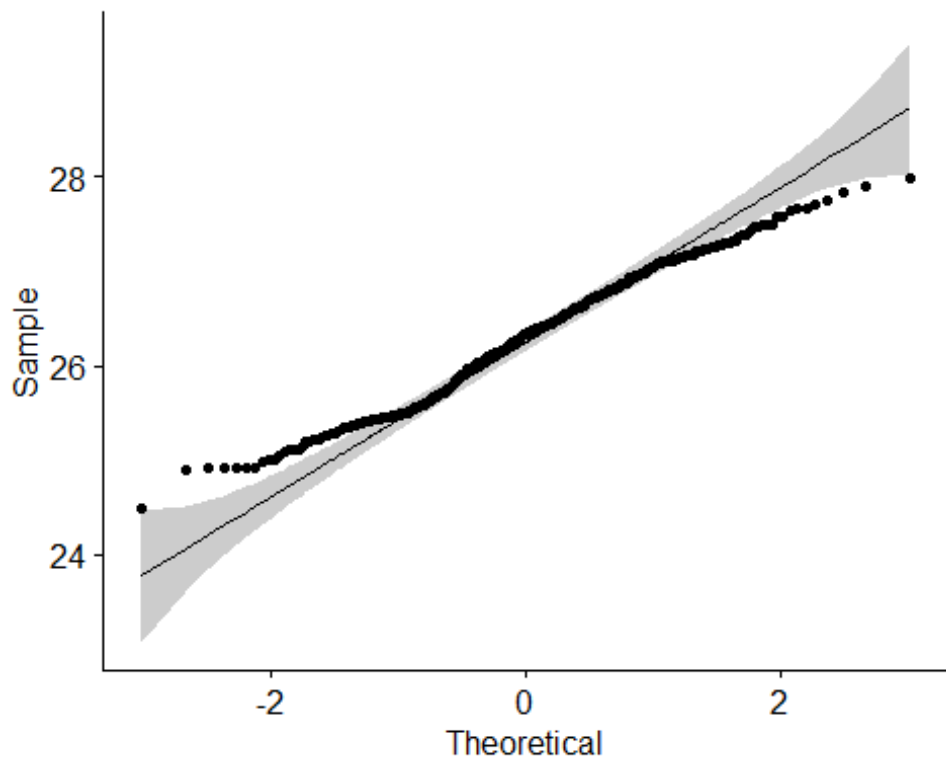
```
ggqqplot(vars$rms)
```



```
# Temperature  
ggdensity(vars$Tmean)
```

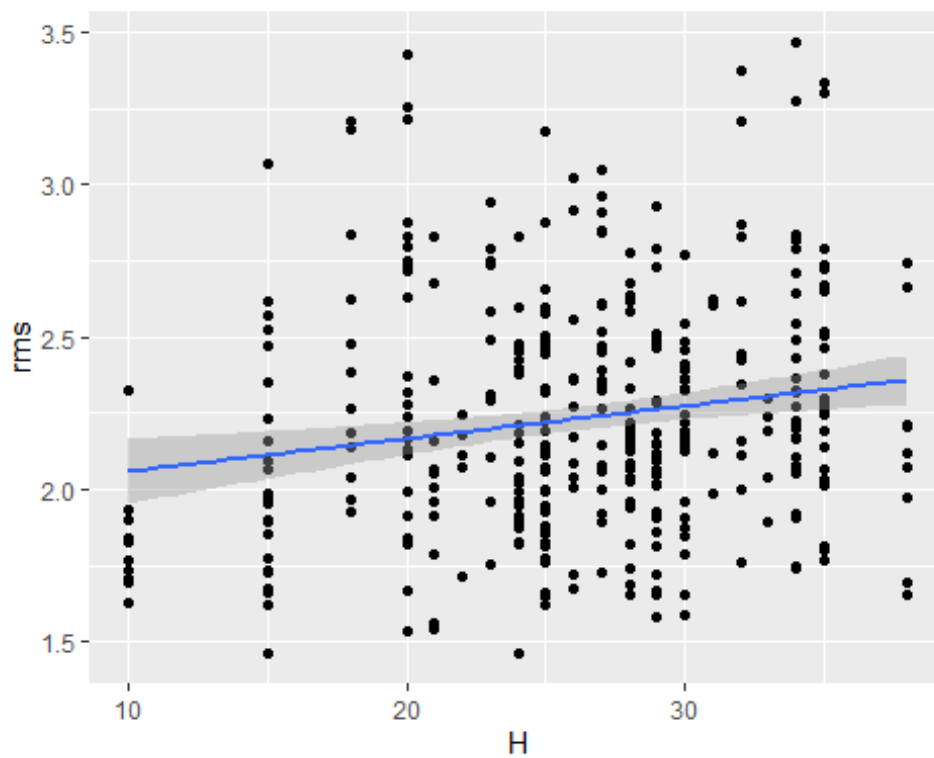


```
ggqqplot(vars$Tmean)
```



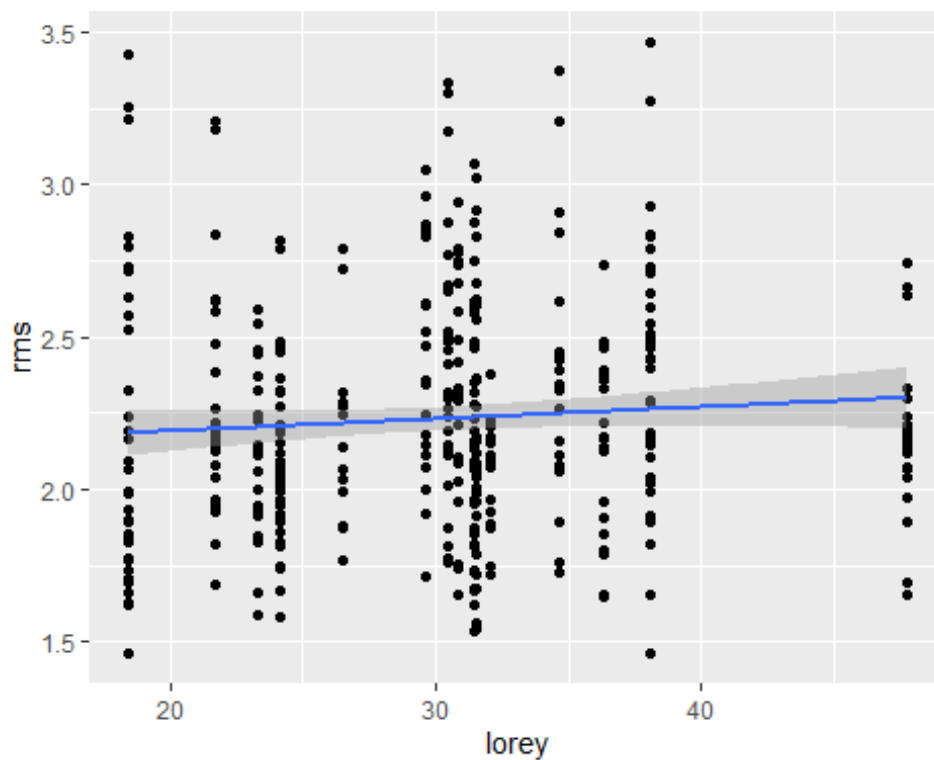
```
(prelim_plot <- ggplot(vars, aes(x = H, y = rms)) +  
  geom_point() +  
  geom_smooth(method = "lm"))
```

```
## `geom_smooth()` using formula 'y ~ x'
```



```
(prelim_plot2 <- ggplot(vars, aes(x = lorey, y = rms)) +  
  geom_point() +  
  geom_smooth(method = "lm"))
```

```
## `geom_smooth()` using formula 'y ~ x'
```



First, build a standard linear model.

```

lm <- lm(rms~H+n+lorey+meanconn+meandepth+month+LocID,data=vars)
lm

##
## Call:
## lm(formula = rms ~ H + n + lorey + meanconn + meandepth + month +
##      LocID, data = vars)
##
## Coefficients:
## (Intercept)          H              n          lorey      meanconn
meandepth
##   37.99594    0.01884   -0.76226   -0.14093   -0.36971
-0.36041
##      month      LocID2      LocID3      LocID4      LocID5
LocID6
##   -0.03053   -3.96933  -14.99030    5.22753    1.71095
1.66169
##      LocID7      LocID8      LocID9      LocID10     LocID11
LocID12
##   -4.20990   -0.40832   -3.28737   -8.53713   -6.08994
NA
##      LocID13     LocID14     LocID15
##           NA           NA           NA

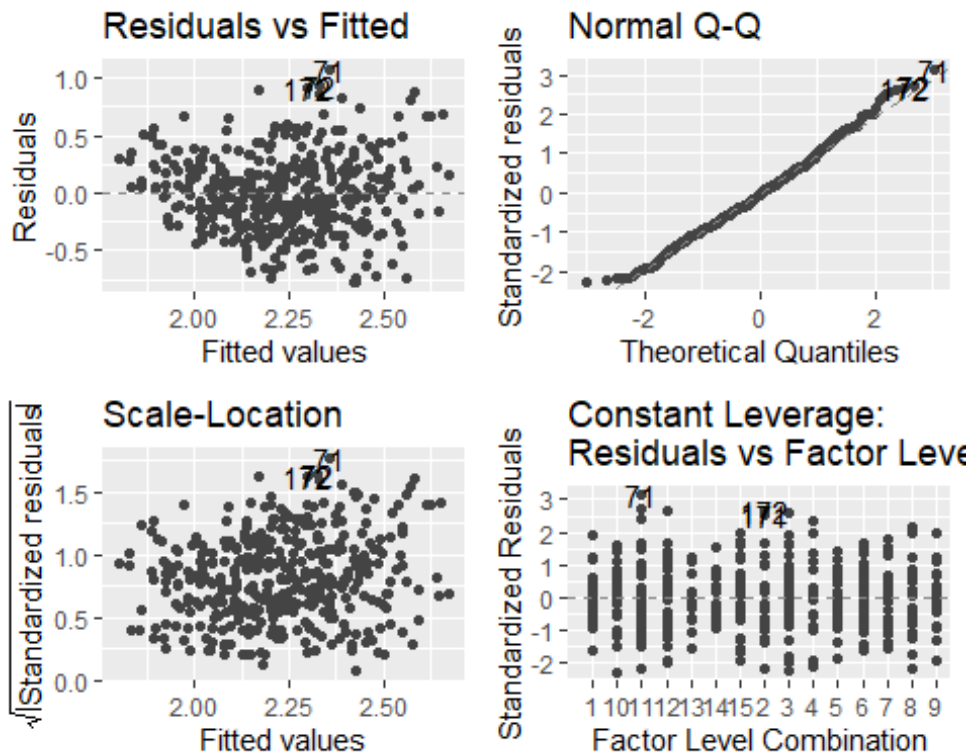
summary(lm)

##
## Call:
## lm(formula = rms ~ H + n + lorey + meanconn + meandepth + month +
##      LocID, data = vars)
##
## Residuals:
##      Min       1Q   Median       3Q      Max
## -0.76978 -0.22946 -0.01966  0.21516  1.06774
##
## Coefficients: (4 not defined because of singularities)
##              Estimate Std. Error t value Pr(>|t|)
## (Intercept)  37.995935  21.486572   1.768  0.0778 .
## H             0.018838   0.004454   4.229 2.96e-05 ***
## n            -0.762257   0.455444  -1.674  0.0950 .
## lorey        -0.140932   0.081306  -1.733  0.0839 .
## meanconn     -0.369711   0.227707  -1.624  0.1053 .
## meandepth    -0.360414   0.185871  -1.939  0.0533 .
## month        -0.030530   0.004838  -6.311 7.96e-10 ***
## LocID2       -3.969332   2.466353  -1.609  0.1084
## LocID3      -14.990296   9.352997  -1.603  0.1099
## LocID4         5.227531   3.027728   1.727  0.0851 .
## LocID5         1.710949   1.068486   1.601  0.1102
## LocID6         1.661694   1.181175   1.407  0.1603
## LocID7        -4.209895   2.752792  -1.529  0.1270
## LocID8        -0.408324   0.346733  -1.178  0.2397
## LocID9        -3.287366   2.071704  -1.587  0.1134
## LocID10       -8.537134   5.340501  -1.599  0.1108
## LocID11       -6.089938   3.734522  -1.631  0.1038
## LocID12              NA              NA      NA      NA
## LocID13              NA              NA      NA      NA

```

```
## LocID14      NA      NA      NA      NA
## LocID15      NA      NA      NA      NA
## ---
## Signif. codes:  0 '***' 0.001 '**' 0.01 '*' 0.05 '.' 0.1 ' ' 1
##
## Residual standard error: 0.3479 on 369 degrees of freedom
## Multiple R-squared:  0.2184, Adjusted R-squared:  0.1845
## F-statistic: 6.443 on 16 and 369 DF, p-value: 8.33e-13

autoplot(lm, smooth.colour = NA)
```



```
#Use dredge for model selection
lmdredge <- dredge(lm, evaluate = TRUE, trace = FALSE)
```

Now, build a mixed effects model, with hour, month and location as ‘random’ effects.

For Root mean square error ~ veg data

```
mixed.lmer <- lmer(rms~H+n+lorey+meanconn+meandepth+
                  (1|LocID_f)+(1|month_f), data=vars,na.action="na.
fail")
summary(mixed.lmer)

## Linear mixed model fit by REML ['lmerMod']
## Formula: rms ~ H + n + lorey + meanconn + meandepth + (1 | LocID_f) +
##       (1 | month_f)
## Data: vars
##
## REML criterion at convergence: 87.2
##
## Scaled residuals:
```

```

##      Min      1Q  Median      3Q      Max
## -3.3309 -0.6443 -0.0873  0.4987  3.7393
##
## Random effects:
## Groups   Name                Variance Std.Dev.
## LocID_f  (Intercept) 0.01608  0.1268
## month_f  (Intercept) 0.08249  0.2872
## Residual                    0.05468  0.2338
## Number of obs: 386, groups: LocID_f, 15; month_f, 12
##
## Fixed effects:
##              Estimate Std. Error t value
## (Intercept)  2.578718   0.450297   5.727
## H              0.017741   0.002895   6.129
## n             -0.009657   0.014201  -0.680
## lorey        -0.007014   0.005503  -1.275
## meanconn     -0.006099   0.003886  -1.569
## meandepth    -0.025819   0.032236  -0.801
##
## Correlation of Fixed Effects:
##              (Intr) H      n      lorey  meancnn
## H              0.030
## n             -0.678 -0.092
## lorey         -0.343 -0.218 -0.081
## meanconn     -0.187 -0.042 -0.357  0.368
## meandepth    -0.754 -0.103  0.636 -0.140 -0.216

```

`tab_model(mixed.lmer)`

rms

Predictors

Estimates

CI

p

(Intercept)

2.58

1.70 – 3.46

<0.001

H

0.02

0.01 – 0.02

<0.001

n

-0.01

-0.04 – 0.02

0.496

lorey

-0.01

-0.02 – 0.00

0.202
 meanconn
 -0.01
 -0.01 – 0.00
 0.117
 meandepth
 -0.03
 -0.09 – 0.04
 0.423
 Random Effects
 σ^2
 0.05
 τ_{00} LocID_f
 0.02
 τ_{00} month_f
 0.08
 ICC
 0.64
 N LocID_f
 15
 N month_f
 12
 Observations
 386
 Marginal R2 / Conditional R2
 0.070 / 0.668

```
dredge(mixed.lmer)

## Global model call: lmer(formula = rms ~ H + n + lorey + meanconn +
##   meandepth + (1 |
##     LocID_f) + (1 | month_f), data = vars, na.action = "na.fail")
## ---
## Model selection table
##   (Intrc)      H      lorey      mncnn      mndpt      n df  lo
gLik AICc
## 2      1.783 0.01664
.890 71.9
## 10     1.892 0.01687
.496 79.2
## 18     1.884 0.01677
.289 80.8
## 6      2.001 0.01641
.496 81.2
## 4      1.885 0.01717 -0.0037880
.963 82.1
## 26     2.347 0.01718
.095 86.5
## 14     2.131 0.01668
-0.005276 -0.015670
7 -37
```

| | | | | | | | | | |
|-------|-------|---------|------------|-----------|-----------|------------|--|---|-----|
| .087 | 88.5 | | | | | | | | |
| ## 12 | 1.969 | 0.01732 | -0.0035180 | | -0.011510 | | | 7 | -37 |
| .581 | 89.5 | | | | | | | | |
| ## 8 | 2.283 | 0.01734 | -0.0075540 | -0.006996 | | | | 7 | -37 |
| .776 | 89.8 | | | | | | | | |
| ## 22 | 2.020 | 0.01659 | | -0.004915 | | -0.0022610 | | 7 | -38 |
| .079 | 90.5 | | | | | | | | |
| ## 20 | 2.016 | 0.01733 | -0.0042990 | | | -0.0081230 | | 7 | -38 |
| .277 | 90.9 | | | | | | | | |
| ## 1 | 2.226 | | | | | | | 4 | -42 |
| .454 | 93.0 | | | | | | | | |
| ## 30 | 2.382 | 0.01700 | | -0.004270 | -0.031700 | -0.0111700 | | 8 | -40 |
| .112 | 96.6 | | | | | | | | |
| ## 28 | 2.449 | 0.01767 | -0.0038820 | | -0.037090 | -0.0177100 | | 8 | -40 |
| .142 | 96.7 | | | | | | | | |
| ## 16 | 2.371 | 0.01750 | -0.0072940 | -0.007036 | -0.011800 | | | 8 | -40 |
| .476 | 97.3 | | | | | | | | |
| ## 24 | 2.307 | 0.01746 | -0.0076100 | -0.006766 | | -0.0024200 | | 8 | -41 |
| .389 | 99.2 | | | | | | | | |
| ## 9 | 2.228 | | | | -0.000183 | | | 5 | -45 |
| .317 | 100.8 | | | | | | | | |
| ## 5 | 2.444 | | | -0.005292 | | | | 5 | -45 |
| .731 | 101.6 | | | | | | | | |
| ## 17 | 2.305 | | | | | -0.0052920 | | 5 | -46 |
| .033 | 102.2 | | | | | | | | |
| ## 3 | 2.135 | | 0.0030050 | | | | | 5 | -46 |
| .713 | 103.6 | | | | | | | | |
| ## 32 | 2.579 | 0.01774 | -0.0070140 | -0.006099 | -0.025820 | -0.0096570 | | 9 | -43 |
| .589 | 105.7 | | | | | | | | |
| ## 25 | 2.461 | | | | -0.012800 | -0.0085820 | | 6 | -48 |
| .543 | 109.3 | | | | | | | | |
| ## 13 | 2.466 | | | -0.005318 | -0.002519 | | | 6 | -48 |
| .668 | 109.6 | | | | | | | | |
| ## 21 | 2.446 | | | -0.005273 | | -0.0002024 | | 6 | -49 |
| .492 | 111.2 | | | | | | | | |
| ## 11 | 2.154 | | 0.0030680 | | -0.002520 | | | 6 | -49 |
| .539 | 111.3 | | | | | | | | |
| ## 7 | 2.434 | | 0.0002342 | -0.005236 | | | | 6 | -50 |
| .217 | 112.7 | | | | | | | | |
| ## 19 | 2.211 | | 0.0027430 | | | -0.0046000 | | 6 | -50 |
| .307 | 112.8 | | | | | | | | |
| ## 29 | 2.502 | | | -0.005188 | -0.004784 | -0.0014970 | | 7 | -52 |
| .130 | 118.6 | | | | | | | | |
| ## 27 | 2.383 | | 0.0029570 | | -0.014680 | -0.0083290 | | 7 | -52 |
| .764 | 119.8 | | | | | | | | |
| ## 15 | 2.457 | | 0.0003031 | -0.005248 | -0.002848 | | | 7 | -53 |
| .103 | 120.5 | | | | | | | | |
| ## 23 | 2.437 | | 0.0002231 | -0.005224 | | -0.0001659 | | 7 | -53 |
| .935 | 122.2 | | | | | | | | |
| ## 31 | 2.493 | | 0.0003601 | -0.005094 | -0.005297 | -0.0016050 | | 8 | -56 |
| .512 | 129.4 | | | | | | | | |
| ## | delta | weight | | | | | | | |
| ## 2 | 0.00 | 0.948 | | | | | | | |
| ## 10 | 7.28 | 0.025 | | | | | | | |
| ## 18 | 8.86 | 0.011 | | | | | | | |

```

## 6  9.28  0.009
## 4  10.21 0.006
## 26 14.55 0.001
## 14 16.53 0.000
## 12 17.52 0.000
## 8  17.91 0.000
## 22 18.52 0.000
## 20 18.91 0.000
## 1  21.08 0.000
## 30 24.67 0.000
## 28 24.73 0.000
## 16 25.40 0.000
## 24 27.22 0.000
## 9  28.85 0.000
## 5  29.68 0.000
## 17 30.29 0.000
## 3  31.65 0.000
## 32 33.72 0.000
## 25 37.37 0.000
## 13 37.62 0.000
## 21 39.27 0.000
## 11 39.36 0.000
## 7  40.72 0.000
## 19 40.90 0.000
## 29 46.62 0.000
## 27 47.89 0.000
## 15 48.57 0.000
## 23 50.23 0.000
## 31 57.47 0.000
## Models ranked by AICc(x)
## Random terms (all models):
## '1 | LocID_f', '1 | month_f'

mixed.lmer2 <- lmer(rms~H+(1|LocID_f)+(1|month_f), data=vars,na.action
="na.fail")
summary(mixed.lmer2)

## Linear mixed model fit by REML ['lmerMod']
## Formula: rms ~ H + (1 | LocID_f) + (1 | month_f)
## Data: vars
##
## REML criterion at convergence: 61.8
##
## Scaled residuals:
##   Min       1Q   Median       3Q      Max
## -3.3125 -0.6415 -0.1151  0.4808  3.8013
##
## Random effects:
##   Groups   Name                Variance Std.Dev.
##   LocID_f  (Intercept) 0.01692  0.1301
##   month_f  (Intercept) 0.08248  0.2872
##   Residual                    0.05473  0.2339
## Number of obs: 386, groups:  LocID_f, 15; month_f, 12
##
## Fixed effects:
##
##           Estimate Std. Error t value

```

```
## (Intercept) 1.783368 0.117172 15.220
## H           0.016643 0.002805 5.932
##
## Correlation of Fixed Effects:
## (Intr)
## H -0.637
```

```
tab_model(mixed.lmer2)
```

rms

Predictors

Estimates

CI

p

(Intercept)

1.78

1.55 – 2.01

<0.001

H

0.02

0.01 – 0.02

<0.001

Random Effects

σ^2

0.05

τ_{00} LocID_f

0.02

τ_{00} month_f

0.08

ICC

0.64

N LocID_f

15

N month_f

12

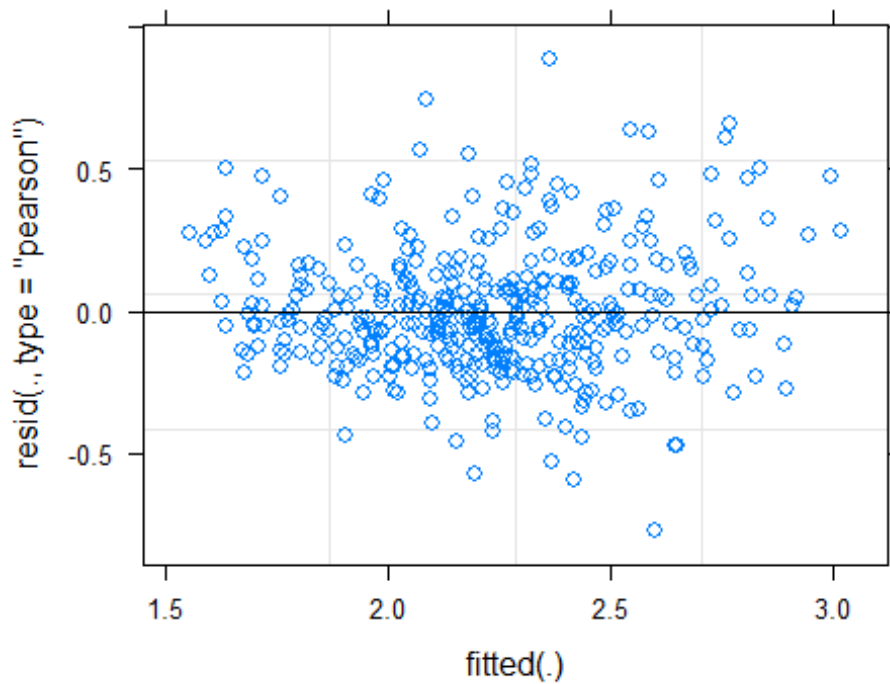
Observations

386

Marginal R2 / Conditional R2

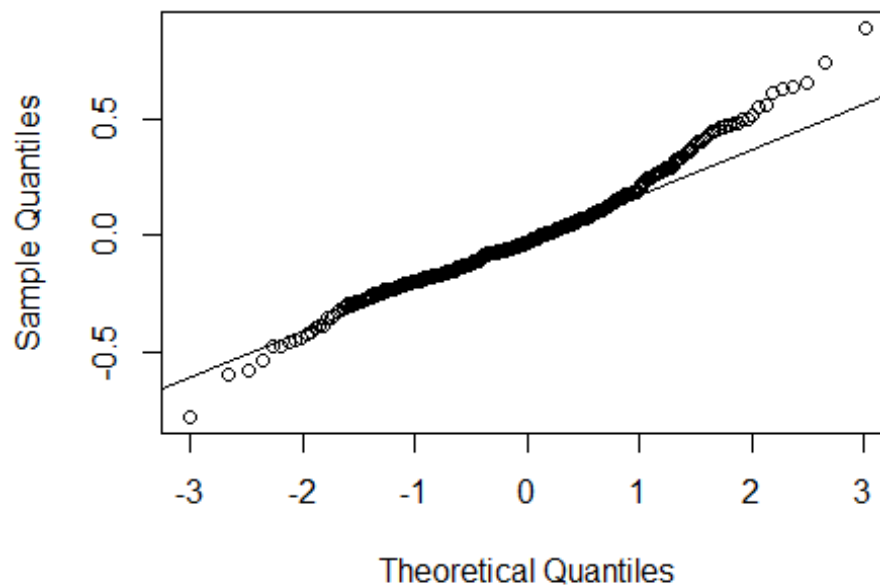
0.066 / 0.668

```
plot(mixed.lmer2)
```



```
qqnorm(resid(mixed.lmer2))
qqline(resid(mixed.lmer2))
```

Normal Q-Q Plot



```
## Plots showing model predictions by Location
pred.mm <- ggpredict(mixed.lmer2, terms = c("H")) # this gives overall
l predictions for the model

# Plot the predictions
(lmer.pred <- ggplot(pred.mm) +
```

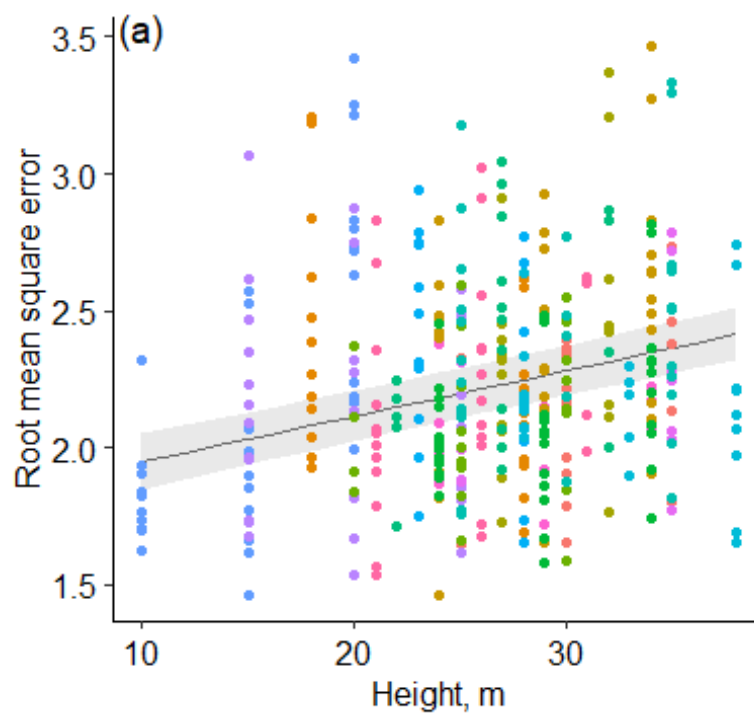
```

geom_line(aes(x = x, y = predicted)) + # slope
geom_ribbon(aes(x = x, ymin = predicted - std.error, ymax = predic
ted + std.error),
          fill = "lightgrey", alpha = 0.5) + # error band
geom_point(data = vars, # adding the raw data (
scaled values)
          aes(x = H, y = rms, colour = LocID_f)) +
labs(x = "Height, m", y = "Root mean square error",
     title = NULL, col="Location") +
theme(axis.title=element_text(size=22),
      legend.title=element_text(size=22),
      legend.text=element_text(size=16)) +
theme_pubr() +
theme(legend.position = "left") +
ggtitle("(a)") +
theme(plot.title = element_text(hjust = 0.01, vjust = - 5))
)

```

Location

- 1
- 2
- 3
- 4
- 5
- 6
- 7
- 8
- 9
- 10
- 11
- 12
- 13
- 14
- 15

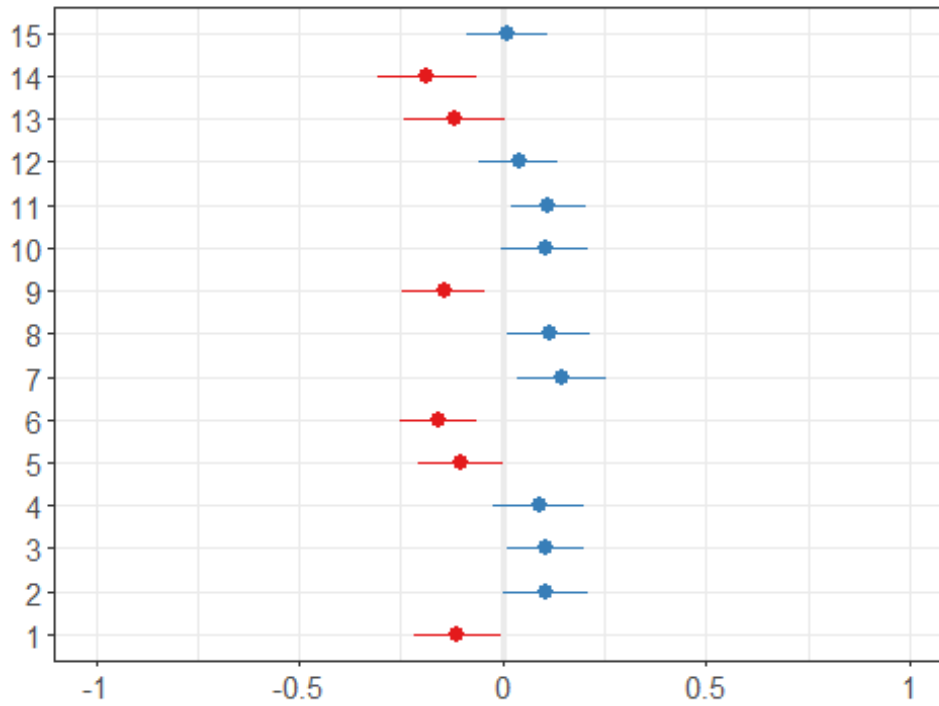


```

set_theme(base=theme_bw())
(re.effects <- plot_model(mixed.lmer2, type="re", show.values=FALSE))
## [[1]]

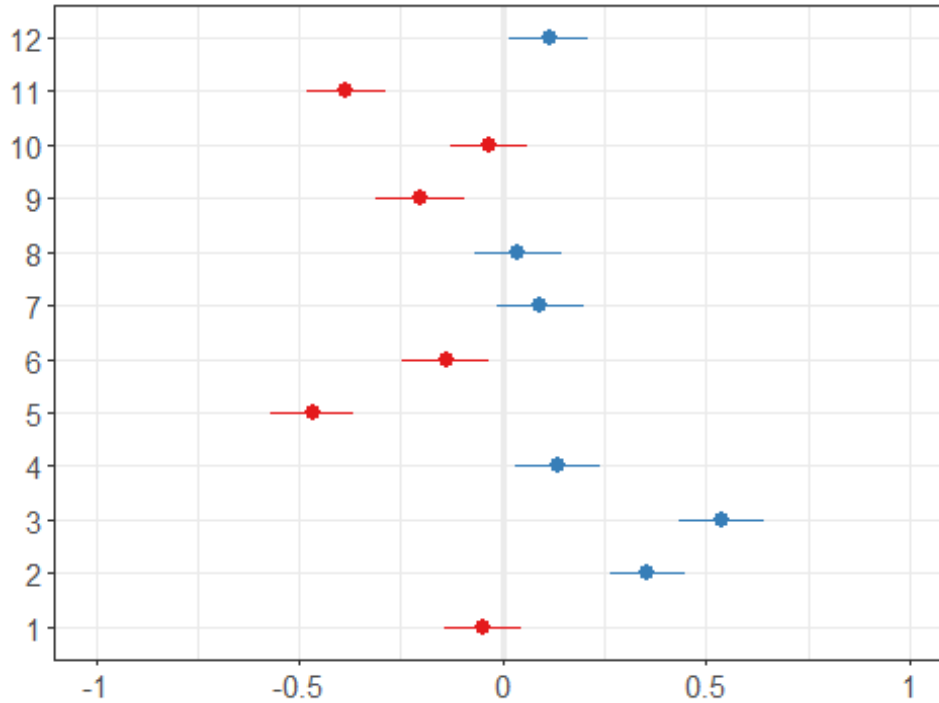
```

Random effects

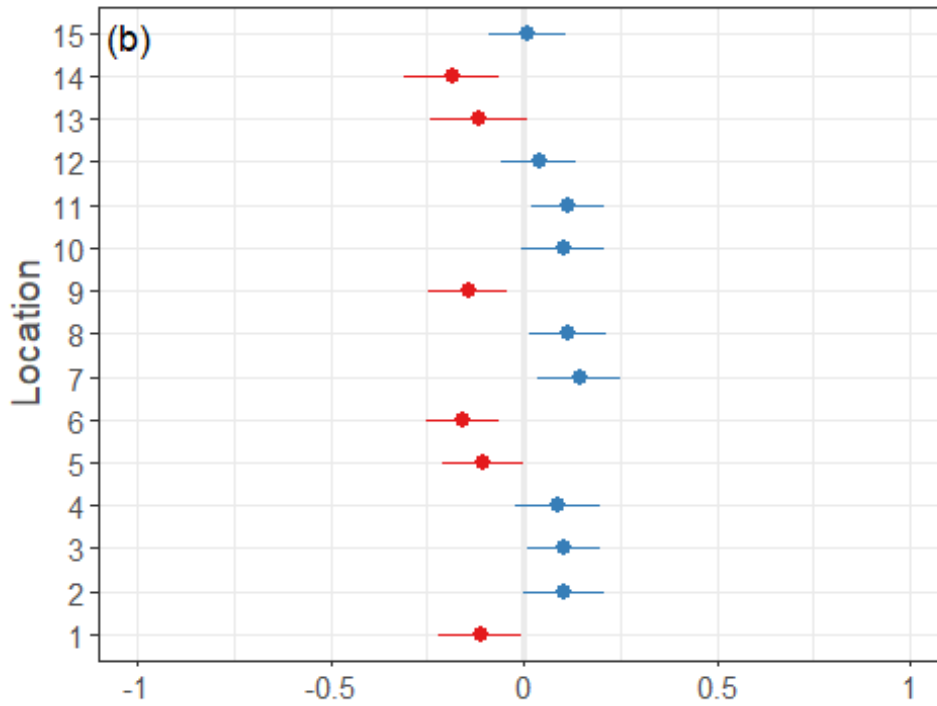


```
##  
## [[2]]
```

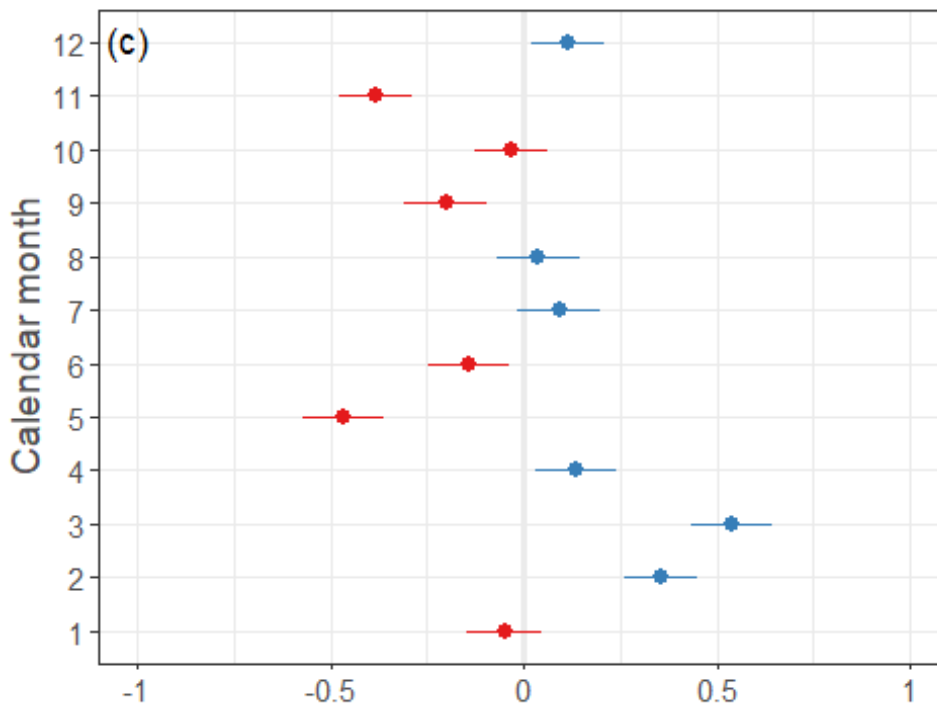
Random effects



```
(re.effects[[1]]<- re.effects[[1]] + labs(title="(b)",x="Location")+  
  theme(plot.title = element_text(hjust = 0.01, vjust = - 7),  
        axis.title = element_text(size=14))
```



```
(re.effects[[2]]<- re.effects[[2]] + labs(title="(c)",x="Calendar month")+
  theme(plot.title = element_text(hjust = 0.01, vjust = - 7),
        axis.title = element_text(size=14)))
```



```
(rms.plots <- arrangeGrob(arrangeGrob(lmer.pred),arrangeGrob(re.effects
s[[1]],re.effects[[2]],ncol=1),
                          ncol=2,widths=c(3,1.5)) )
```

```
## TableGrob (1 x 2) "arrange": 2 grobs
##   z      cells  name      grob
## 1 1 (1-1,1-1) arrange gtable[arrange]
## 2 2 (1-1,2-2) arrange gtable[arrange]

##ggsave("RMSlmerplots.jpg", plot = rms.plots, height = 200, width = 300, units = "mm")
##ggsave("lmerplot.jpg", plot=lmer.pred, height = 150, width = 180, units = "mm")
```

LMM for Mean Absolute Error ~ veg data

```
mixed.mad <- lmer(mad~H+n+lorey+meanconn+
                  (1|LocID_f)+(1|month_f), data=vars,na.action="na.
                  fail")
summary(mixed.mad)

## Linear mixed model fit by REML ['lmerMod']
## Formula: mad ~ H + n + lorey + meanconn + (1 | LocID_f) + (1 | month_f)
## Data: vars
##
## REML criterion at convergence: -68.2
##
## Scaled residuals:
##   Min       1Q   Median       3Q      Max
## -3.3198 -0.6640 -0.1010  0.5332  3.2374
##
## Random effects:
## Groups Name Variance Std.Dev.
## LocID_f (Intercept) 0.01716 0.1310
## month_f (Intercept) 0.08968 0.2995
## Residual 0.03578 0.1891
## Number of obs: 386, groups: LocID_f, 15; month_f, 12
##
## Fixed effects:
## Estimate Std. Error t value
## (Intercept) 1.766332 0.299632 5.895
## H 0.021141 0.002362 8.952
## n -0.001421 0.011061 -0.128
## lorey -0.008308 0.005449 -1.525
## meanconn -0.006028 0.003830 -1.574
##
## Correlation of Fixed Effects:
## (Intr) H n lorey
## H -0.059
## n -0.394 -0.029
## lorey -0.700 -0.193 0.009
## meanconn -0.547 -0.053 -0.290 0.346

tab_model(mixed.mad)
```

mad
Predictors

Estimates
CI
p
(Intercept)
1.77
1.18 – 2.35
<0.001
H
0.02
0.02 – 0.03
<0.001
n
-0.00
-0.02 – 0.02
0.898
lore
-0.01
-0.02 – 0.00
0.127
meanconn
-0.01
-0.01 – 0.00
0.116
Random Effects
 σ^2
0.04
 τ_{00} LocID_f
0.02
 τ_{00} month_f
0.09
ICC
0.75
N LocID_f
15
N month_f
12
Observations
386
Marginal R2 / Conditional R2
0.096 / 0.773

```
dredge(mixed.mad)
```

```
## Global model call: lmer(formula = mad ~ H + n + lorey + meanconn +  
(1 | LocID_f) +
```

```

## (1 | month_f), data = vars, na.action = "na.fail")
## ---
## Model selection table
## (Intrc)      H      lorey      mncnn      n df logLik  AICc de
lta weight
## 2      1.261 0.02051
.00 0.976
## 10     1.334 0.02062
.04 0.011
## 4      1.402 0.02094 -0.004985
.83 0.007
## 6      1.433 0.02045
.13 0.006
## 8      1.752 0.02105 -0.008267 -0.006159
.42 0.000
## 12     1.507 0.02105 -0.005386
.73 0.000
## 14     1.443 0.02058
.31 0.000
## 16     1.766 0.02114 -0.008308 -0.006028 -0.001421
.71 0.000
## 1      1.808
.04 0.000
## 9      1.851
.54 0.000
## 5      1.985
.69 0.000
## 3      1.708
.57 0.000
## 13     1.970
.28 0.000
## 11     1.744
.09 0.000
## 7      1.938
.69 0.000
## 15     1.924
.20 0.000
## Models ranked by AICc(x)
## Random terms (all models):
## '1 | LocID_f', '1 | month_f'

mixed.mad2 <- lmer(mad~H+(1|LocID_f)+(1|month_f), data=vars,na.action=
"na.fail")
summary(mixed.mad2)

## Linear mixed model fit by REML ['lmerMod']
## Formula: mad ~ H + (1 | LocID_f) + (1 | month_f)
## Data: vars
##
## REML criterion at convergence: -89.7
##
## Scaled residuals:
## Min      1Q  Median      3Q      Max
## -3.3054 -0.6636 -0.1208  0.5194  3.2835
##
## Random effects:

```

```

## Groups   Name                Variance Std.Dev.
## LocID_f (Intercept) 0.01792  0.1339
## month_f (Intercept) 0.08969  0.2995
## Residual                0.03580  0.1892
## Number of obs: 386, groups: LocID_f, 15; month_f, 12
##
## Fixed effects:
##              Estimate Std. Error t value
## (Intercept) 1.261289   0.112218  11.240
## H            0.020511   0.002321   8.837
##
## Correlation of Fixed Effects:
##   (Intr)
## H -0.551

tab_model(mixed.mad2)

```

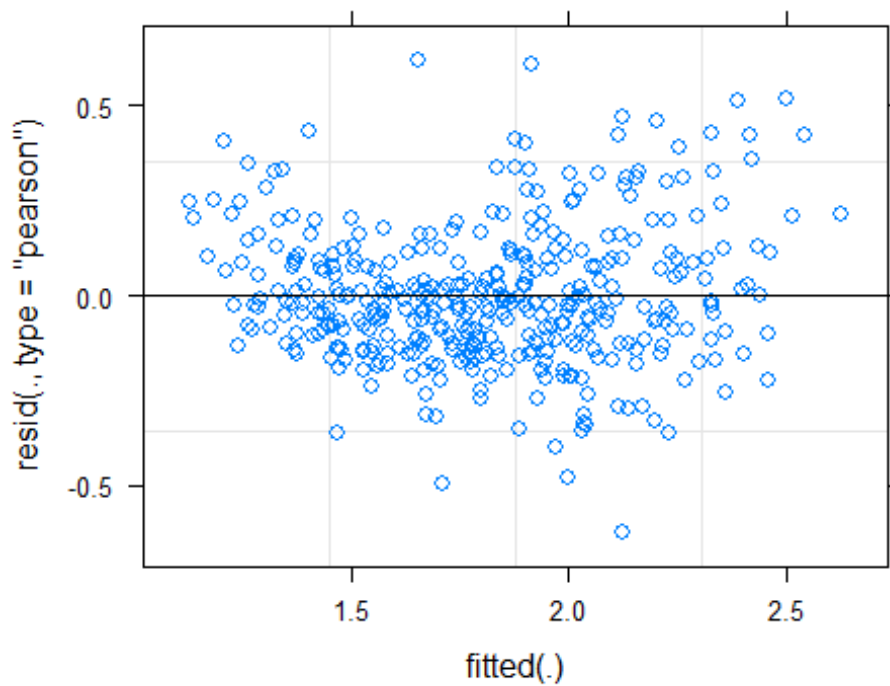
```

mad
Predictors
Estimates
CI
p
(Intercept)
1.26
1.04 – 1.48
<0.001
H
0.02
0.02 – 0.03
<0.001
Random Effects
σ2
0.04
τ00 LocID_f
0.02
τ00 month_f
0.09
ICC
0.75
N LocID_f
15
N month_f
12
Observations
386
Marginal R2 / Conditional R2

```

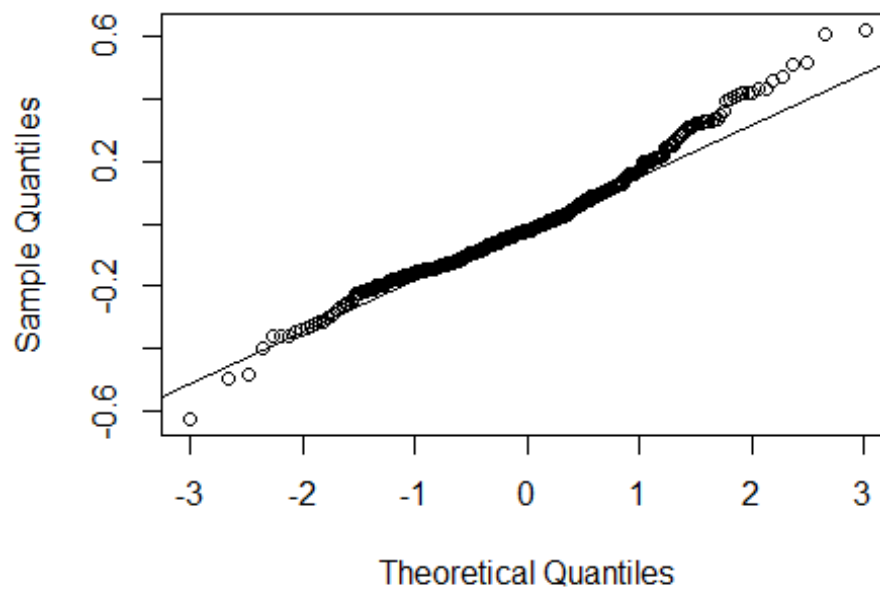
0.103 / 0.776

```
plot(mixed.mad2)
```



```
qqnorm(resid(mixed.mad2))  
qqline(resid(mixed.mad2))
```

Normal Q-Q Plot



```
## Plots showing model predictions by Location  
mad.mm <- ggpredict(mixed.mad2, terms = c("H")) # this gives overall  
predictions for the model
```

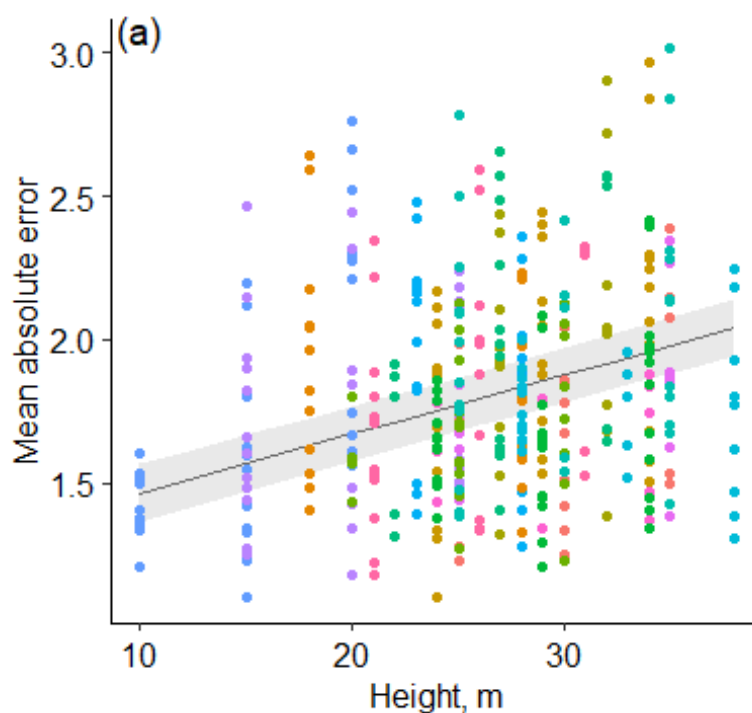
```

# Plot the predictions
(mad.pred <- ggplot(mad.mm) +
  geom_line(aes(x = x, y = predicted)) + # slope
  geom_ribbon(aes(x = x, ymin = predicted - std.error, ymax = predic
ted + std.error),
            fill = "lightgrey", alpha = 0.5) + # error band
  geom_point(data = vars, # adding the raw data (
scaled values)
            aes(x = H, y = mad, colour = LocID_f)) +
  labs(x = "Height, m", y = "Mean absolute error",
       title = NULL, col="Location") +
  theme(axis.title=element_text(size=22),
        legend.title=element_text(size=22),
        legend.text=element_text(size=16)) +
  theme_pubr() +
  theme(legend.position = "left") +
  ggtitle("(a)") +
  theme(plot.title = element_text(hjust = 0.01, vjust = - 5))
)

```

Location

- 1
- 2
- 3
- 4
- 5
- 6
- 7
- 8
- 9
- 10
- 11
- 12
- 13
- 14
- 15

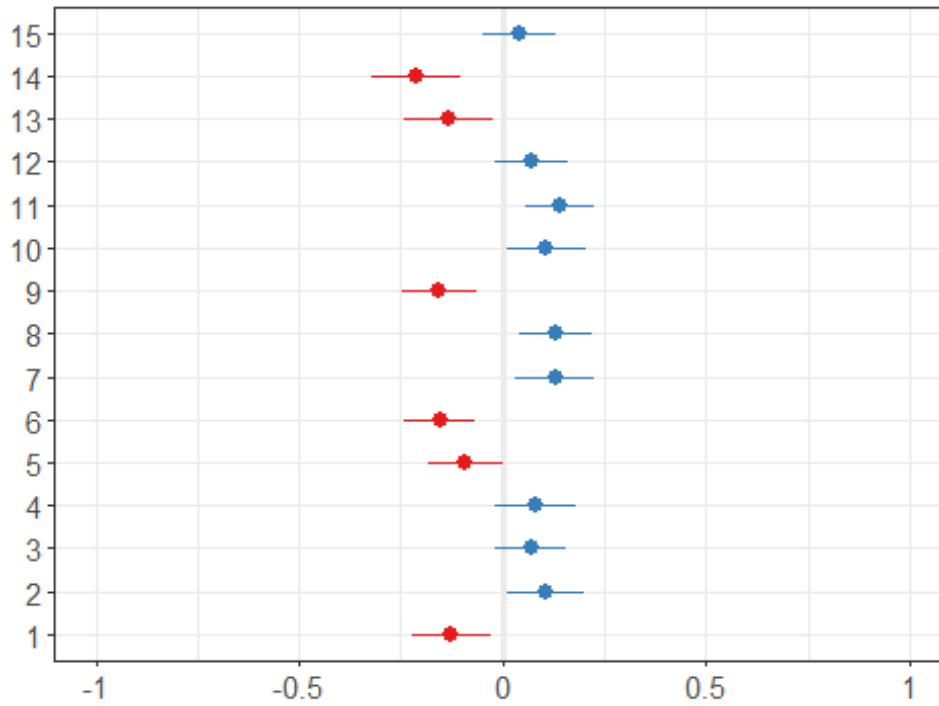


```

set_theme(base=theme_bw())
(mad.effects <- plot_model(mixed.mad2, type="re", show.values=FALSE))
## [[1]]

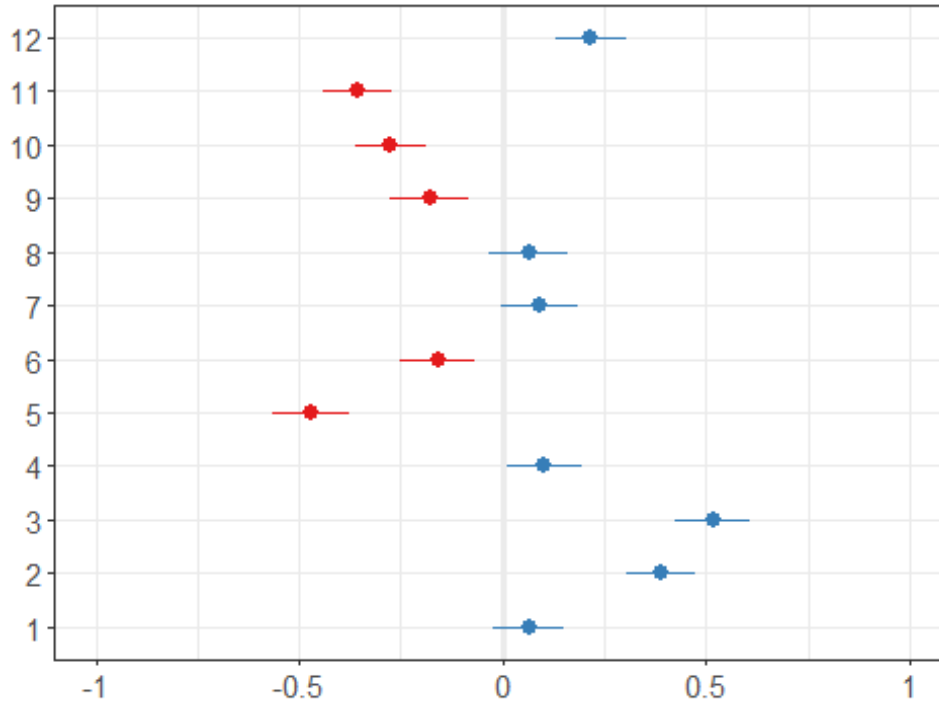
```

Random effects

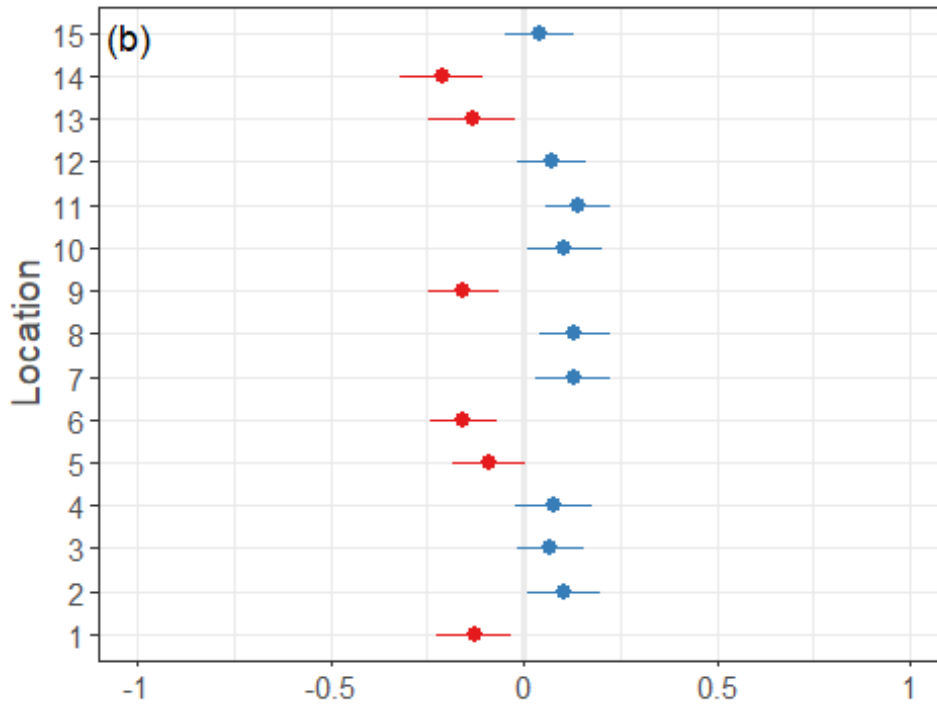


```
##  
## [[2]]
```

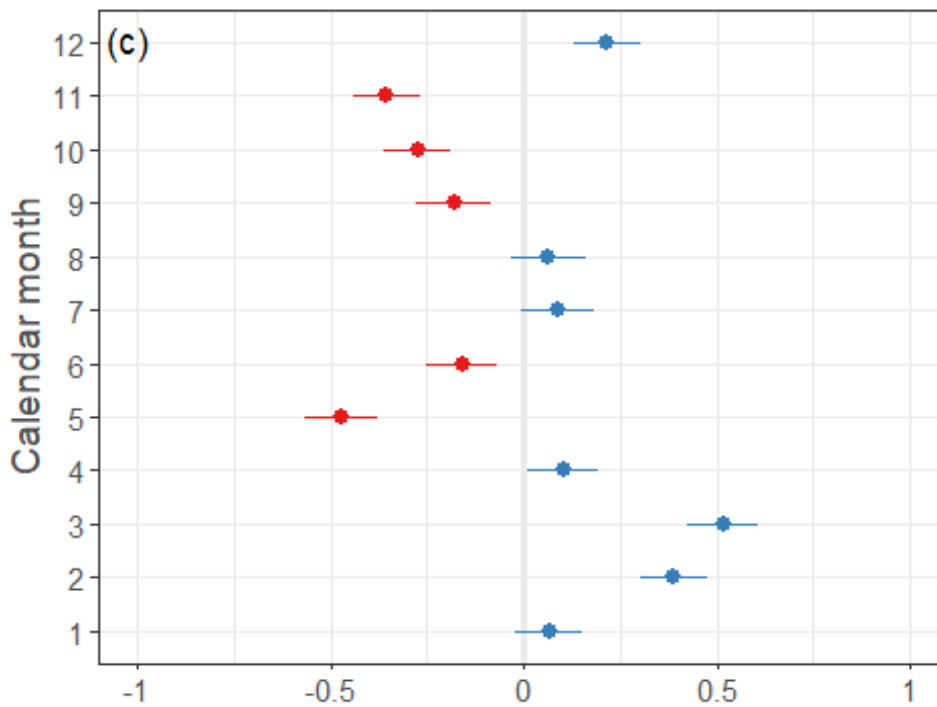
Random effects



```
(mad.effects[[1]]<- mad.effects[[1]] + labs(title="(b)",x="Location")+  
  theme(plot.title = element_text(hjust = 0.01, vjust = - 7),  
        axis.title = element_text(size=14))
```



```
(mad.effects[[2]] <- mad.effects[[2]] + labs(title="(c)", x="Calendar month") +
  theme(plot.title = element_text(hjust = 0.01, vjust = - 7),
        axis.title = element_text(size=14))
```



```
(mad.plots <- arrangeGrob(arrangeGrob(mad.pred), arrangeGrob(mad.effects[[1]], mad.effects[[2]], ncol=1),
                          ncol=2, widths=c(3, 1.5)) )
```

```
## TableGrob (1 x 2) "arrange": 2 grobs
##   z      cells  name      grob
## 1 1 (1-1,1-1) arrange gtable[arrange]
## 2 2 (1-1,2-2) arrange gtable[arrange]

##ggsave("MAElmerplots.jpg", plot = mad.plots, height = 200, width = 300, units = "mm")
##ggsave("madplot.jpg", plot=mad.pred,height = 150, width = 180, units = "mm")
```

LMM for monthly mean temp ~ veg data

```
mixed.temp <- lmer(Tmean~H+n+lorey+meanconn+
                  (1|LocID_f)+(1|month_f), data=vars,na.action="na.
fail")
summary(mixed.temp)

## Linear mixed model fit by REML ['lmerMod']
## Formula: Tmean ~ H + n + lorey + meanconn + (1 | LocID_f) + (1 | month_f)
##   Data: vars
##
## REML criterion at convergence: 337.6
##
## Scaled residuals:
##   Min       1Q   Median       3Q      Max
## -3.7937 -0.5991  0.0290  0.6302  2.7348
##
## Random effects:
##   Groups      Name                Variance Std.Dev.
##   LocID_f     (Intercept)  0.09407  0.3067
##   month_f     (Intercept)  0.27387  0.5233
##   Residual                    0.10176  0.3190
## Number of obs: 386, groups:  LocID_f, 15; month_f, 12
##
## Fixed effects:
##              Estimate Std. Error t value
## (Intercept) 27.126088  0.676589  40.092
## H            0.015036  0.004030   3.731
## n           -0.028990  0.025422  -1.140
## lorey       -0.019025  0.012422  -1.532
## meanconn    -0.004572  0.008801  -0.519
##
## Correlation of Fixed Effects:
##              (Intr) H      n      lorey
## H              -0.045
## n              -0.404 -0.022
## lorey          -0.723 -0.144  0.007
## meanconn      -0.559 -0.040 -0.289  0.343

tab_model(mixed.temp)
```

Tmean

Predictors

Estimates
CI
p
(Intercept)
27.13
25.80 – 28.45
<0.001
H
0.02
0.01 – 0.02
<0.001
n
-0.03
-0.08 – 0.02
0.254
lore
-0.02
-0.04 – 0.01
0.126
meanconn
-0.00
-0.02 – 0.01
0.603
Random Effects
 σ^2
0.10
 τ_{00} LocID_f
0.09
 τ_{00} month_f
0.27
ICC
0.78
N LocID_f
15
N month_f
12
Observations
386
Marginal R2 / Conditional R2
0.046 / 0.793

```
dredge(mixed.temp)
```

```
## Global model call: lmer(formula = Tmean ~ H + n + lorey + meanconn  
+ (1 | LocID_f) +
```

```

## (1 | month_f), data = vars, na.action = "na.fail")
## ---
## Model selection table
## (Intrc)      H      lorey      mncnn      n df      logLik      AICc
delta weight
## 2      25.95 0.01413      5 -160.503 331.2
0.00 0.556
## 1      26.33      4 -161.918 331.9
0.78 0.377
## 10     26.38 0.01418      -0.02866 6 -162.610 337.4
6.28 0.024
## 9      26.73      -0.02704 5 -164.066 338.3
7.13 0.016
## 4      26.39 0.01477 -0.014950      6 -163.217 338.7
7.49 0.013
## 3      26.61      -0.009177      5 -165.168 340.5
9.33 0.005
## 6      26.07 0.01424      -2.849e-03      6 -164.330 340.9
9.72 0.004
## 5      26.45      -2.966e-03      5 -165.822 341.8
10.64 0.003
## 12     26.93 0.01489 -0.016790      -0.03280 7 -165.093 344.5
13.32 0.001
## 11     27.10      -0.010790      -0.02964 6 -167.176 346.6
15.41 0.000
## 14     26.37 0.01431      4.982e-05 -0.02872 7 -166.457 347.2
16.05 0.000
## 8      26.81 0.01496 -0.018930 -7.476e-03      7 -166.679 347.7
16.49 0.000
## 13     26.74      -2.608e-04 -0.02678 6 -168.013 348.2
17.08 0.000
## 7      26.95      -0.012300 -5.980e-03      6 -168.799 349.8
18.65 0.000
## 16     27.13 0.01504 -0.019020 -4.572e-03 -0.02899 8 -168.784 353.9
22.79 0.000
## 15     27.24      -0.012360 -3.277e-03 -0.02688 7 -170.984 356.3
25.10 0.000
## Models ranked by AICc(x)
## Random terms (all models):
## '1 | LocID_f', '1 | month_f'

mixed.temp2 <- lmer(Tmean~H+(1|LocID_f)+(1|month_f), data=vars,na.action="na.fail")
summary(mixed.temp2)

## Linear mixed model fit by REML ['lmerMod']
## Formula: Tmean ~ H + (1 | LocID_f) + (1 | month_f)
## Data: vars
##
## REML criterion at convergence: 321
##
## Scaled residuals:
##      Min       1Q   Median       3Q      Max
## -3.7713 -0.6002  0.0453  0.6409  2.7707
##
## Random effects:

```

```

## Groups Name Variance Std.Dev.
## LocID_f (Intercept) 0.09861 0.3140
## month_f (Intercept) 0.27416 0.5236
## Residual 0.10178 0.3190
## Number of obs: 386, groups: LocID_f, 15; month_f, 12
##
## Fixed effects:
## Estimate Std. Error t value
## (Intercept) 25.952414 0.202582 128.11
## H 0.014133 0.003992 3.54
##
## Correlation of Fixed Effects:
## (Intr)
## H -0.525

tab_model(mixed.temp2)

```

Tmean

Predictors

Estimates

CI

p

(Intercept)

25.95

25.56 – 26.35

<0.001

H

0.01

0.01 – 0.02

<0.001

Random Effects

σ^2

0.10

τ_{00} LocID_f

0.10

τ_{00} month_f

0.27

ICC

0.79

N LocID_f

15

N month_f

12

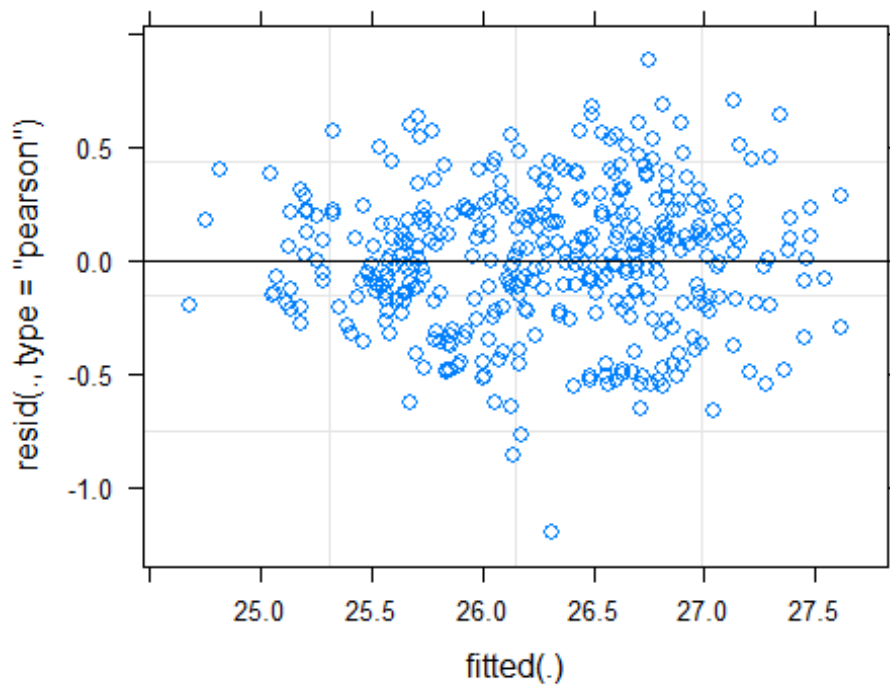
Observations

386

Marginal R2 / Conditional R2

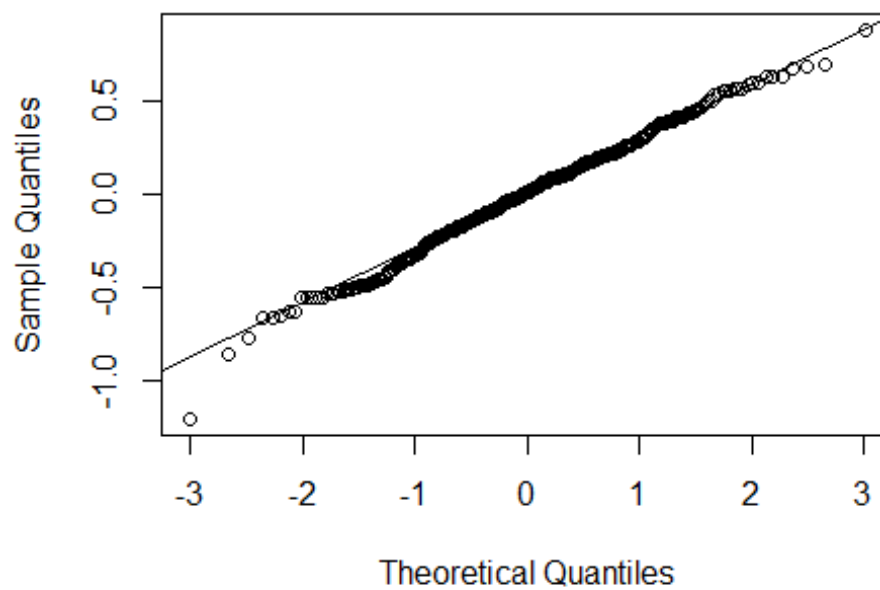
0.016 / 0.789

```
plot(mixed.temp2)
```



```
qqnorm(resid(mixed.temp2))  
qqline(resid(mixed.temp2))
```

Normal Q-Q Plot



```
## Plots showing model predictions by Location  
temp.mm <- ggpredict(mixed.temp2, terms = c("H")) # this gives overall  
L predictions for the model
```

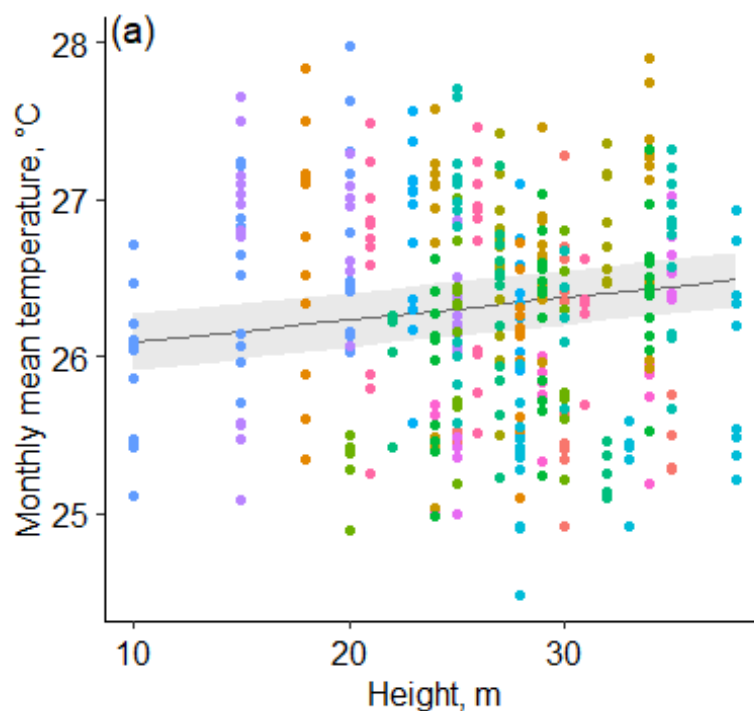
```

# Plot the predictions
(temp.pred <- ggplot(temp.mm) +
  geom_line(aes(x = x, y = predicted)) + # slope
  geom_ribbon(aes(x = x, ymin = predicted - std.error, ymax = predic
ted + std.error),
            fill = "lightgrey", alpha = 0.5) + # error band
  geom_point(data = vars, # adding the raw data (
scaled values)
            aes(x = H, y = Tmean, colour = LocID_f)) +
  labs(x = "Height, m", y = "Monthly mean temperature, °C",
       title = NULL, col="Location") +
  theme(axis.title=element_text(size=22),
        legend.title=element_text(size=22),
        legend.text=element_text(size=16)) +
  theme_pubr() +
  theme(legend.position = "left") +
  ggtitle("(a)") +
  theme(plot.title = element_text(hjust = 0.01, vjust = - 5))
)

```

Location

- 1
- 2
- 3
- 4
- 5
- 6
- 7
- 8
- 9
- 10
- 11
- 12
- 13
- 14
- 15

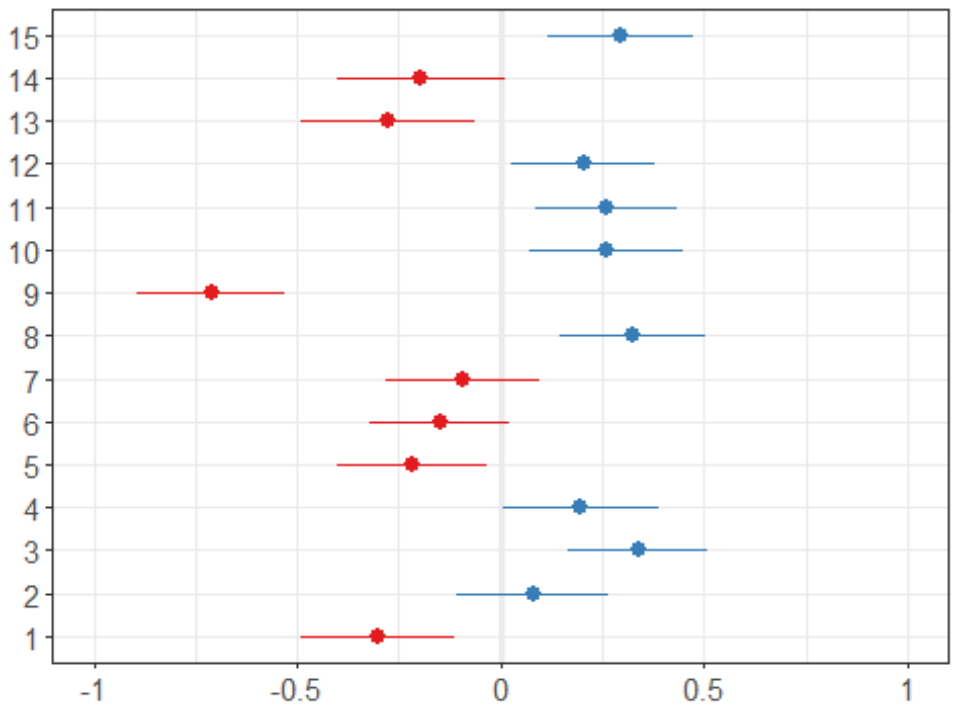


```

set_theme(base=theme_bw())
(temp.effects <- plot_model(mixed.temp2, type="re", show.values=FALSE))
## [[1]]

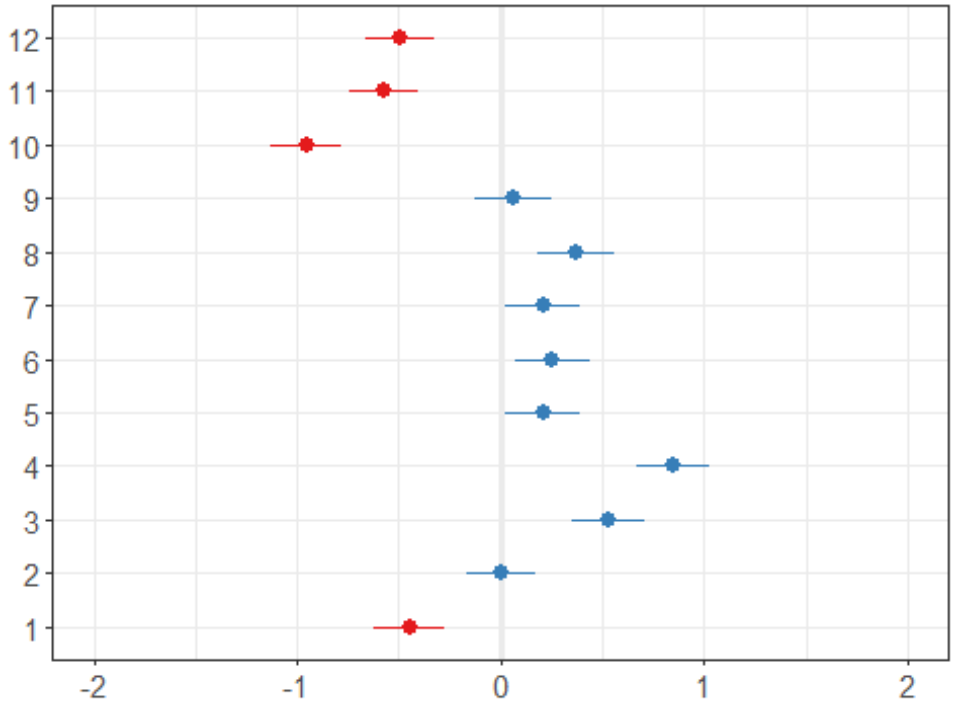
```

Random effects

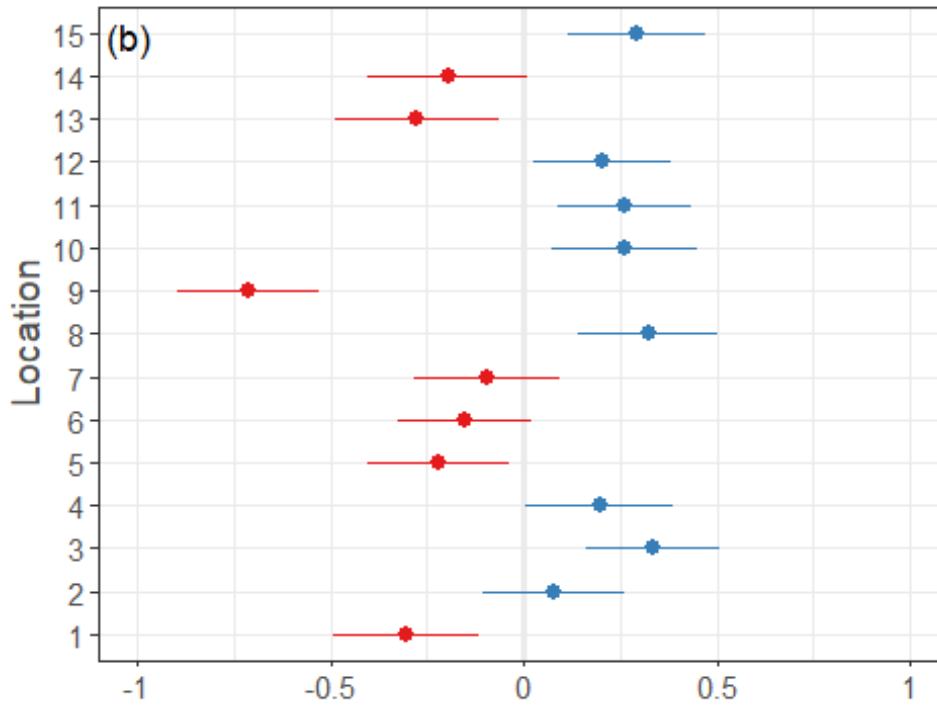


```
##
## [[2]]
```

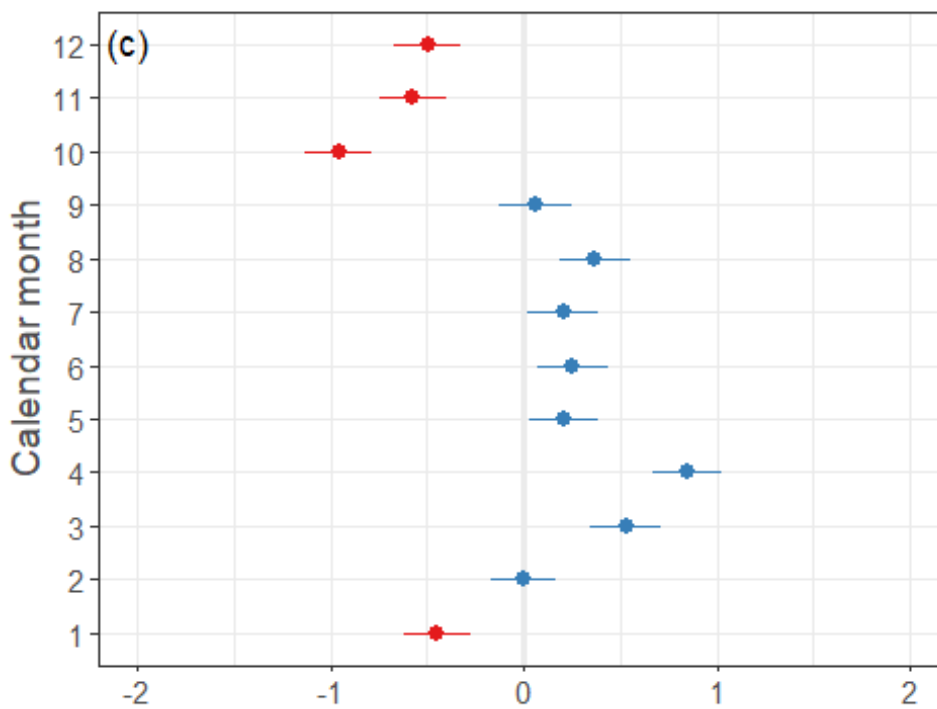
Random effects



```
(temp.effects[[1]]<- temp.effects[[1]] + labs(title="(b)",x="Location"
)+
  theme(plot.title = element_text(hjust = 0.01, vjust = - 7),
        axis.title = element_text(size=14))
```



```
(temp.effects[[2]]<- temp.effects[[2]] + labs(title="(c)",x="Calendar
month")+
  theme(plot.title = element_text(hjust = 0.01, vjust = - 7),
        axis.title = element_text(size=14))
```



```
(temp.plots <- arrangeGrob(arrangeGrob(temp.pred),arrangeGrob(temp.eff
ects[[1]],temp.effects[[2]],ncol=1),
                           ncol=2,widths=c(3,1.5)) )
```

```
## TableGroeb (1 x 2) "arrange": 2 grobs
##   z      cells  name      grob
## 1 1 (1-1,1-1) arrange gtable[arrange]
## 2 2 (1-1,2-2) arrange gtable[arrange]

##ggsave("templmerplots.jpg", plot = temp.plots, height = 200, width =
300, units = "mm")
##ggsave("tempplot.jpg", plot=temp.pred,height = 150, width = 180, unit
s = "mm")
```

LMM for daily maximum temp ~ veg data

```
day <- rawmod%>%
  group_by(LocID,H,month,DOY)%>%
  summarise(rms=rmse(temp,TALOC), mad=mae(temp,TALOC),
            meandiff=mean(diff),maxdiff=max(diff),mindiff=min(diff),
            Tmean=mean(temp),Tmax=max(temp),Tmin=min(temp),
            TALOCmean=mean(TALOC),maxTALOC=max(TALOC),minTALOC=min(TAL
OC))
day2 <- merge(day, veg)
day2$LocID_f <- factor(day2$LocID, levels = c("1","2","3","4","5","6",
"7","8","9","10",
                                           "11","12","13","14","15"
))
day2$month_f <- factor(day2$month, levels = c("1","2","3","4","5","6",
"7",
                                           "8","9","10","11","12"))

mixed.tmax <- lmer(Tmax~H+n+lorey+meanconn+
                  (1|LocID_f)+(1|month_f)+(1|DOY), data=day2,na.act
ion="na.fail")
summary(mixed.tmax)

## Linear mixed model fit by REML ['lmerMod']
## Formula: Tmax ~ H + n + lorey + meanconn + (1 | LocID_f) + (1 | mon
th_f) +
##   (1 | DOY)
##   Data: day2
##
## REML criterion at convergence: 44024.6
##
## Scaled residuals:
##   Min      1Q  Median      3Q      Max
## -7.6440 -0.5580 -0.0483  0.4689  6.5021
##
## Random effects:
##   Groups   Name              Variance Std.Dev.
##   DOY      (Intercept) 2.379      1.542
##   LocID_f  (Intercept) 1.251      1.118
##   month_f  (Intercept) 1.140      1.068
##   Residual                2.474      1.573
## Number of obs: 11391, groups: DOY, 365; LocID_f, 15; month_f, 12
##
## Fixed effects:
##              Estimate Std. Error t value
```

```

## (Intercept) 35.997044  2.380437  15.122
## H           0.062748  0.003719  16.874
## n          -0.090789  0.090908  -0.999
## lorey      -0.056962  0.044008  -1.294
## meanconn   -0.049772  0.031469  -1.582
##
## Correlation of Fixed Effects:
##      (Intr) H      n      lorey
## H      -0.012
## n      -0.414 -0.006
## lorey  -0.749 -0.037  0.006
## meanconn -0.571 -0.010 -0.288  0.339

tab_model(mixed.tmax)

```

```

Tmax
Predictors
Estimates
CI
p
(Intercept)
36.00
31.33 – 40.66
<0.001
H
0.06
0.06 – 0.07
<0.001
n
-0.09
-0.27 – 0.09
0.318
lorey
-0.06
-0.14 – 0.03
0.196
meanconn
-0.05
-0.11 – 0.01
0.114
Random Effects
σ2
2.47
τ00 DOY
2.38
τ00 LocID_f

```

1.25
τ00 month_f

1.14

ICC

0.66

N LocID_f

15

N month_f

12

N DOY

365

Observations

11391

Marginal R2 / Conditional R2

0.064 / 0.680

dredge(mixed.tmax)

```
## Global model call: lmer(formula = Tmax ~ H + n + lorey + meanconn +  
(1 | LocID_f) +  
## (1 | month_f) + (1 | DOY), data = day2, na.action = "na.fail")  
## ---
```

```
## Model selection table
```

| | (Intrc) | H | lorey | mncnn | n | df | logLik | AICc | |
|--------|---------|---------|-----------|----------|-----------|----------|-----------|-----------|---------|
| ## 2 | 30.87 | 0.06262 | | | | 6 | -22008.50 | 44029.0 | |
| 0.00 | | | | | | | | | |
| ## 10 | 32.72 | 0.06262 | | -0.12420 | | 7 | -22009.05 | 44032.1 | |
| 3.11 | | | | | | | | | |
| ## 6 | 32.72 | 0.06257 | | -0.04502 | | 7 | -22009.94 | 44033.9 | |
| 4.89 | | | | | | | | | |
| ## 4 | 31.66 | 0.06270 | -0.026170 | | | 7 | -22010.51 | 44035.0 | |
| 6.03 | | | | | | | | | |
| ## 14 | 33.69 | 0.06259 | | -0.03596 | -0.09014 | 8 | -22010.93 | 44037.9 | |
| 8.87 | | | | | | | | | |
| ## 12 | 33.85 | 0.06272 | -0.033380 | | -0.13230 | 8 | -22010.97 | 44038.0 | |
| 8.95 | | | | | | | | | |
| ## 8 | 35.01 | 0.06273 | -0.056720 | -0.05883 | | 8 | -22011.32 | 44038.7 | |
| 9.66 | | | | | | | | | |
| ## 16 | 36.00 | 0.06275 | -0.056960 | -0.04977 | -0.09079 | 9 | -22012.30 | 44042.6 | |
| 13.62 | | | | | | | | | |
| ## 1 | 32.54 | | | | | 5 | -22143.75 | 44297.5 | |
| 268.50 | | | | | | | | | |
| ## 9 | 34.27 | | | | -0.11680 | 6 | -22144.32 | 44300.6 | |
| 271.64 | | | | | | | | | |
| ## 5 | 34.41 | | | | -0.04537 | 6 | -22144.98 | 44302.0 | |
| 272.96 | | | | | | | | | |
| ## 3 | 32.60 | | | | | 6 | -22146.04 | 44304.1 | |
| 275.08 | | | | | | | | | |
| ## 13 | 35.28 | | | | -0.03717 | -0.08156 | 7 | -22146.07 | 44306.1 |
| 277.14 | | | | | | | | | |
| ## 11 | 34.57 | | | | -0.008615 | -0.11890 | 7 | -22146.61 | 44307.2 |

```

278.24
## 7 35.60 -0.029420 -0.05253 7 -22147.01 44308.0
279.03
## 15 36.48 -0.029630 -0.04436 -0.08189 8 -22148.09 44312.2
283.20
## weight
## 2 0.725
## 10 0.153
## 6 0.063
## 4 0.035
## 14 0.009
## 12 0.008
## 8 0.006
## 16 0.001
## 1 0.000
## 9 0.000
## 5 0.000
## 3 0.000
## 13 0.000
## 11 0.000
## 7 0.000
## 15 0.000
## Models ranked by AICc(x)
## Random terms (all models):
## '1 | LocID_f', '1 | month_f', '1 | DOY'

mixed.tmax2 <- lmer(Tmax~H+(1|LocID_f)+(1|month_f)+(1|DOY), data=day2,
na.action="na.fail")
summary(mixed.tmax2)

## Linear mixed model fit by REML ['lmerMod']
## Formula: Tmax ~ H + (1 | LocID_f) + (1 | month_f) + (1 | DOY)
## Data: day2
##
## REML criterion at convergence: 44017
##
## Scaled residuals:
## Min 1Q Median 3Q Max
## -7.6426 -0.5582 -0.0482 0.4687 6.5024
##
## Random effects:
## Groups Name Variance Std.Dev.
## DOY (Intercept) 2.379 1.542
## LocID_f (Intercept) 1.449 1.204
## month_f (Intercept) 1.140 1.068
## Residual 2.474 1.573
## Number of obs: 11391, groups: DOY, 365; LocID_f, 15; month_f, 12
##
## Fixed effects:
## Estimate Std. Error t value
## (Intercept) 30.868600 0.456303 67.65
## H 0.062616 0.003717 16.85
##
## Correlation of Fixed Effects:
## (Intr)
## H -0.217

```

```
tab_model(mixed.tmax2)
```

Tmax

Predictors

Estimates

CI

p

(Intercept)

30.87

29.97 – 31.76

<0.001

H

0.06

0.06 – 0.07

<0.001

Random Effects

σ^2

2.47

τ_{00} DOY

2.38

τ_{00} LocID_f

1.45

τ_{00} month_f

1.14

ICC

0.67

N LocID_f

15

N month_f

12

N DOY

365

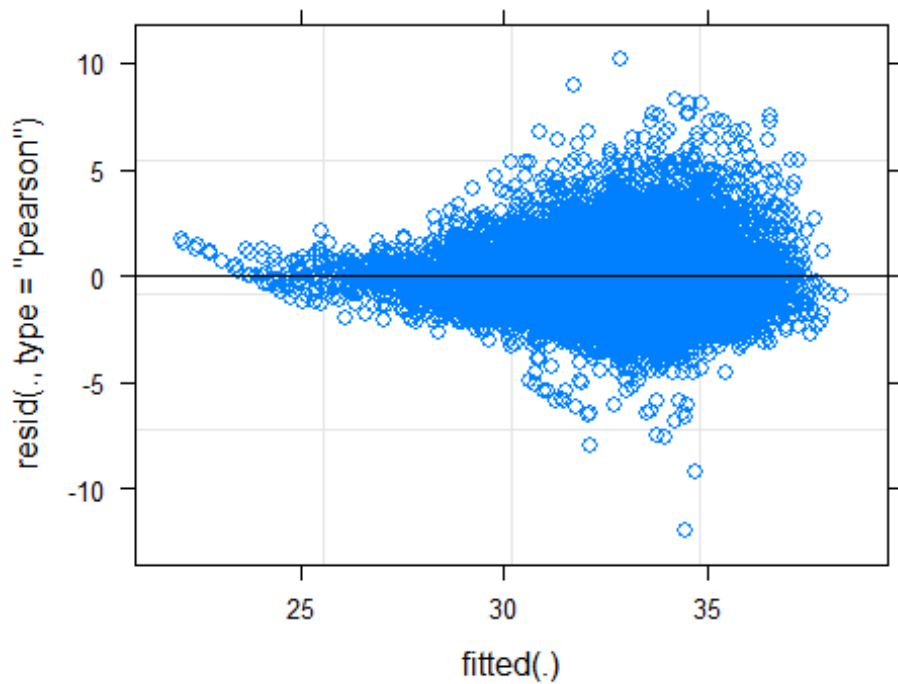
Observations

11391

Marginal R² / Conditional R²

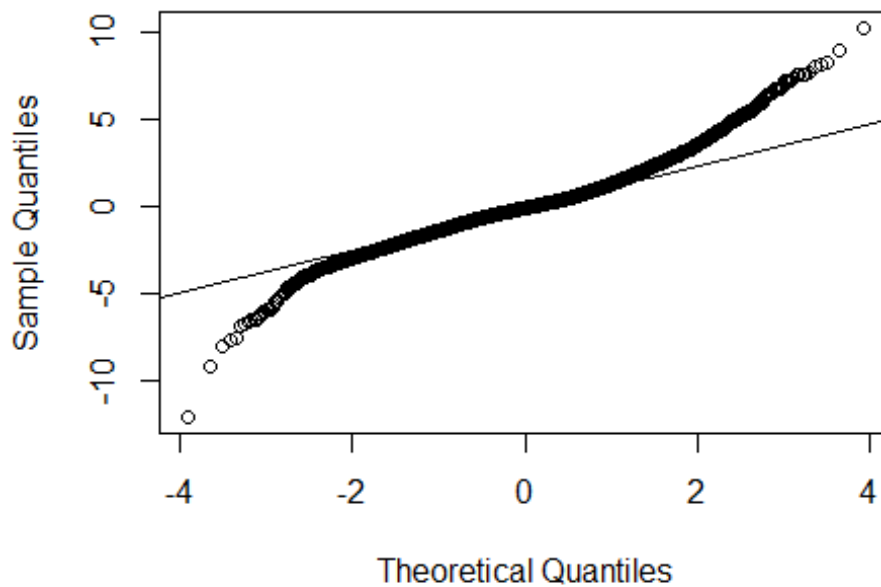
0.020 / 0.674

```
plot(mixed.tmax2)
```



```
qqnorm(resid(mixed.tmax2))
qqline(resid(mixed.tmax2))
```

Normal Q-Q Plot



```
## Plots showing model predictions by Location
tmax.mm <- ggpredict(mixed.tmax2, terms = c("H")) # this gives overall
l predictions for the model

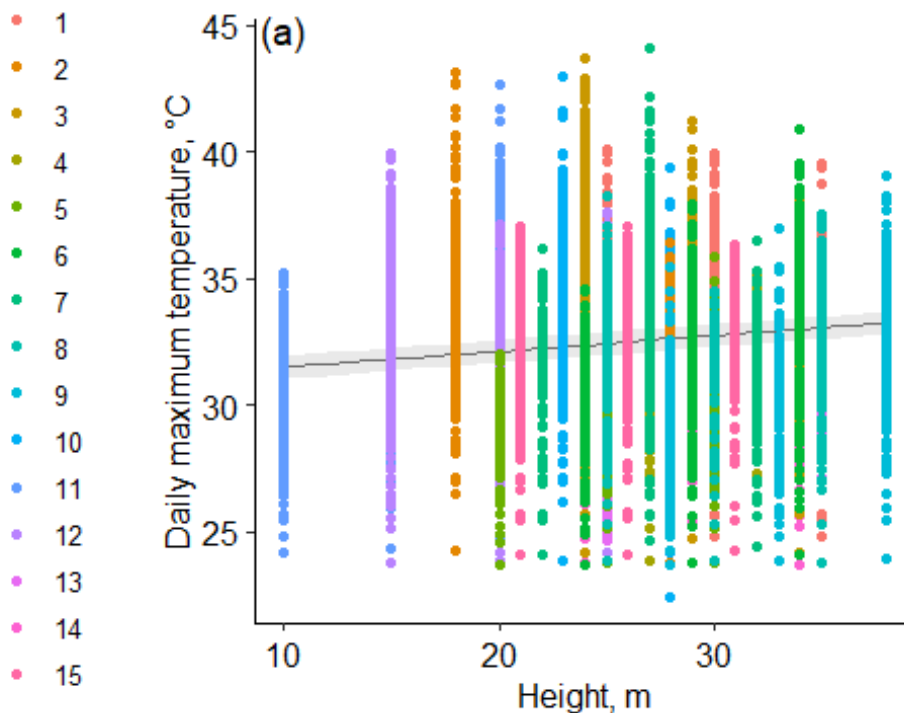
# Plot the predictions
(tmax.pred <- ggplot(tmax.mm) +
```

```

geom_line(aes(x = x, y = predicted)) + # slope
geom_ribbon(aes(x = x, ymin = predicted - std.error, ymax = predic
ted + std.error),
           fill = "lightgrey", alpha = 0.5) + # error band
geom_point(data = day2, # adding the raw data (
scaled values)
           aes(x = H, y = Tmax, colour = LocID_f)) +
labs(x = "Height, m", y = "Daily maximum temperature, °C",
     title = NULL,col="Location") +
theme(axis.title=element_text(size=22),
      legend.title=element_text(size=22),
      legend.text=element_text(size=16)) +
theme_pubr() +
theme(legend.position = "left") +
ggtitle("(a)") +
theme(plot.title = element_text(hjust = 0.01, vjust = - 5))
)

```

Location

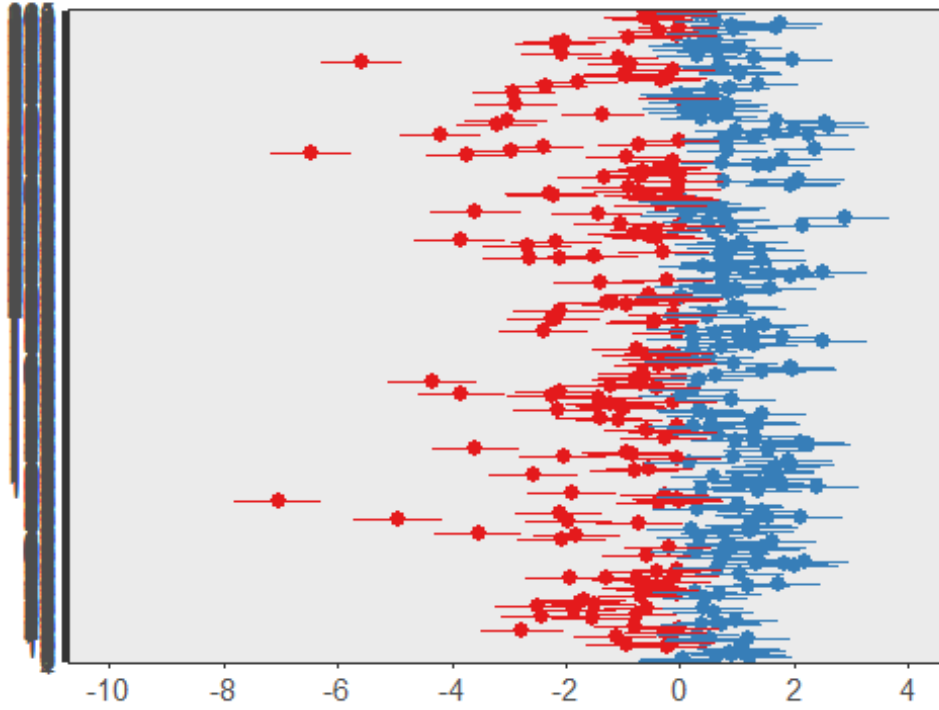


```

set_theme(base=theme_bw())
(tmax.effects <- plot_model(mixed.tmax2,type="re",show.values=FALSE))
## [[1]]

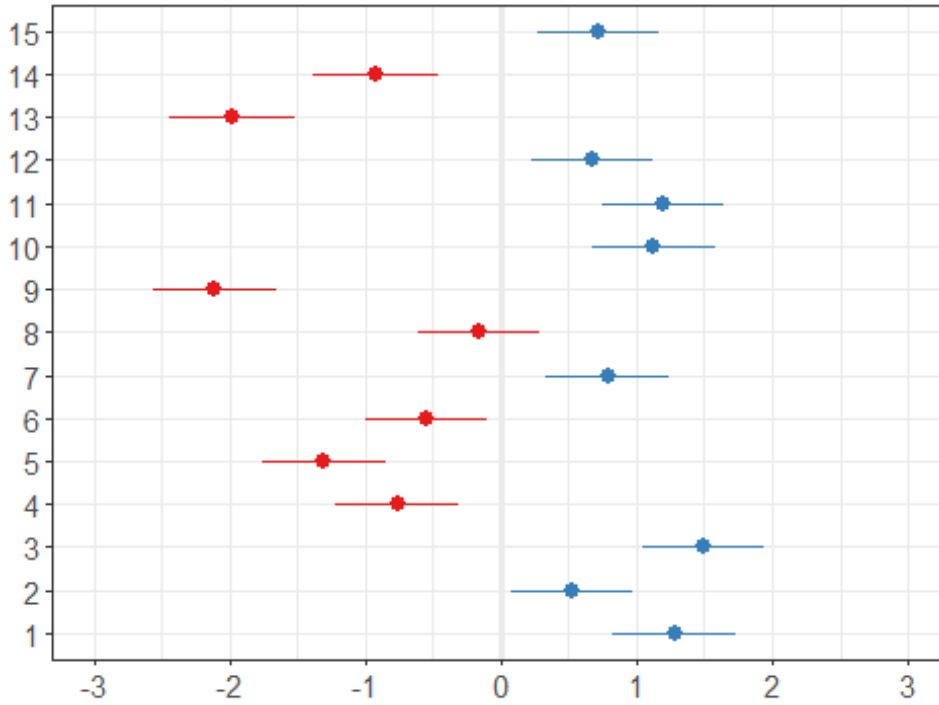
```

Random effects



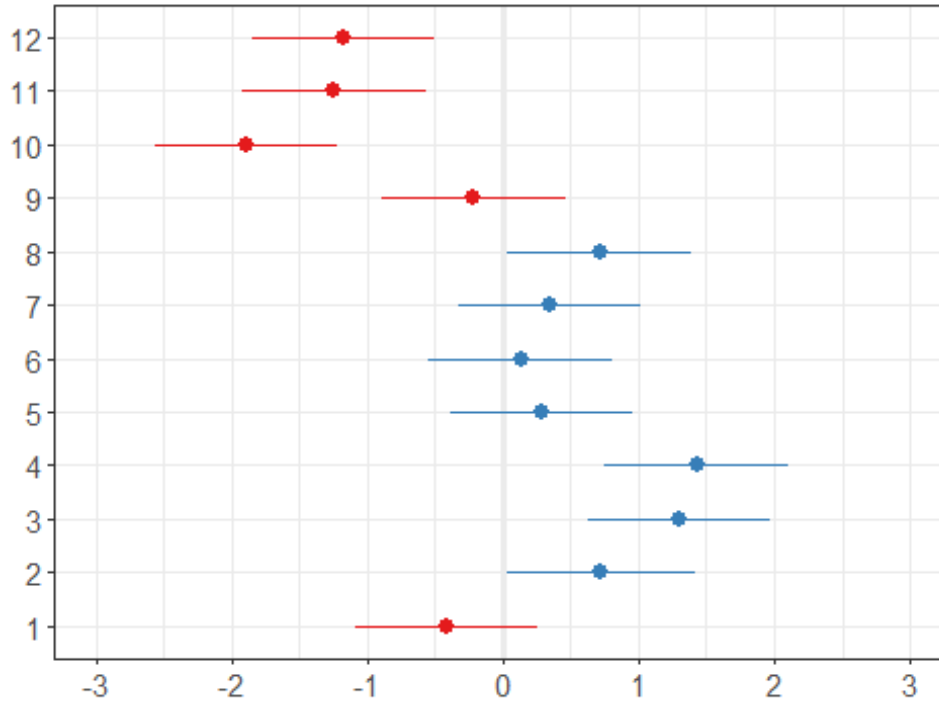
```
##  
## [[2]]
```

Random effects

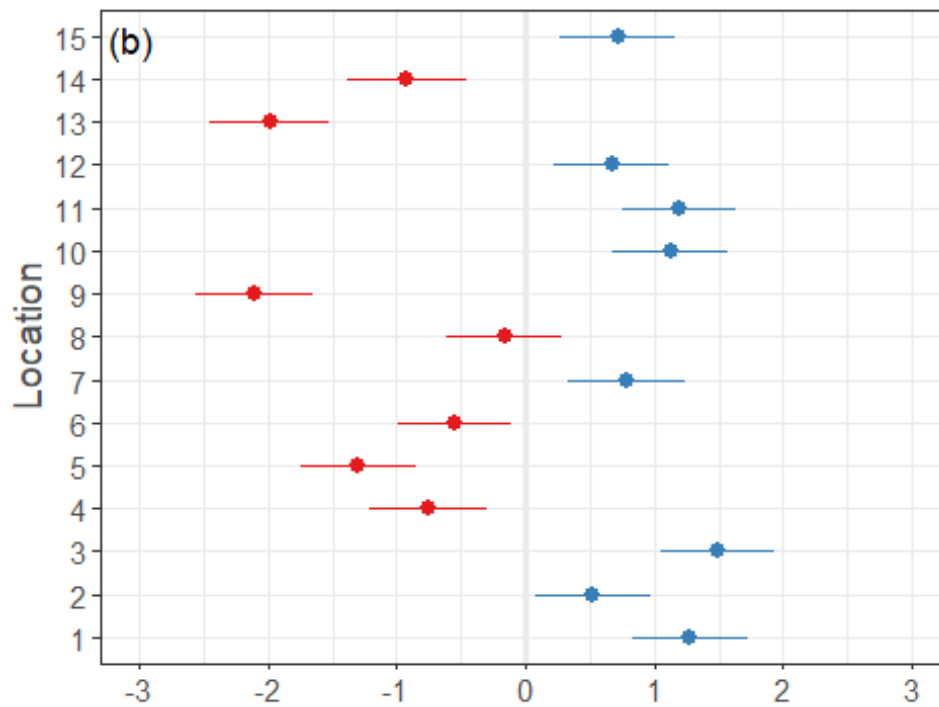


```
##  
## [[3]]
```

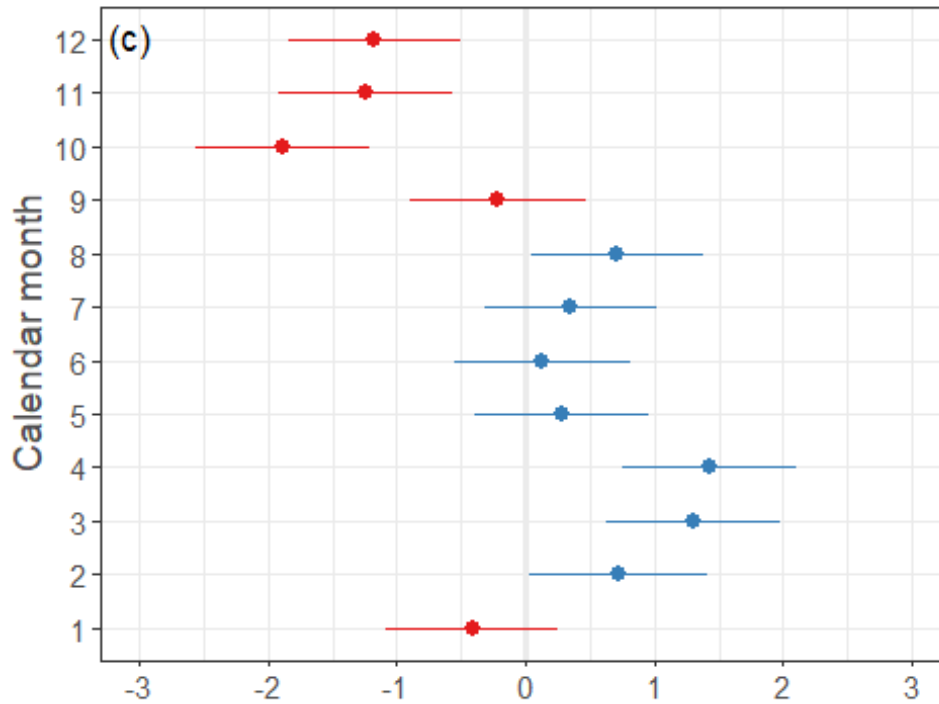
Random effects



```
(tmax.effects[[2]]<- tmax.effects[[2]] + labs(title="(b)",x="Location") +  
  theme(plot.title = element_text(hjust = 0.01, vjust = - 7),  
        axis.title = element_text(size=14)))
```



```
(tmax.effects[[3]]<- tmax.effects[[3]] + labs(title="(c)",x="Calendar  
month") +  
  theme(plot.title = element_text(hjust = 0.01, vjust = - 7),  
        axis.title = element_text(size=14)))
```



```
(tmax.plots <- arrangeGrob(arrangeGrob(tmax.pred),arrangeGrob(tmax.effects[[2]],tmax.effects[[3]],ncol=1),
                          ncol=2,widths=c(3,1.5)) )
```

```
## TableGrob (1 x 2) "arrange": 2 grobs
##   z      cells  name      grob
## 1 1 (1-1,1-1) arrange gtable[arrange]
## 2 2 (1-1,2-2) arrange gtable[arrange]
```

```
##ggsave("tmaxlmerplots.jpg", plot = tmax.plots, height = 200, width = 300, units = "mm")
##ggsave("tmaxplot.jpg",plot=tmax.pred,height = 150, width = 180, units = "mm")
```

Appendix 4.2

R scripts to run the microclimc microclimate model

This document includes the R code, required inputs and model outputs of the microclimc microclimate model for the Sikundur site in North Sumatra, Indonesia, and compares the model output with observed temperatures taken from data loggers for the period October 2018 - October 2019.

Setup for the model

First load the required packages and set the working directory.

```
# Load required packages
library(microclimc)
library(microctools)
library(microclima)

##
## Attaching package: 'microclima'

## The following objects are masked from 'package:microctools':
##
##   difprop, habitats, solalt, solartime, solazi

library(NicheMapR)
library(dplyr)

## Warning: package 'dplyr' was built under R version 4.0.3

##
## Attaching package: 'dplyr'

## The following objects are masked from 'package:stats':
##
##   filter, lag

## The following objects are masked from 'package:base':
##
##   intersect, setdiff, setequal, union

library(ggplot2)

## Warning: package 'ggplot2' was built under R version 4.0.3

library(reshape2)
library(lubridate)

## Warning: package 'lubridate' was built under R version 4.0.3

##
## Attaching package: 'lubridate'
```

```

## The following objects are masked from 'package:base':
##
##   date, intersect, setdiff, union

library(ggpubr)

## Warning: package 'ggpubr' was built under R version 4.0.3

library(gridExtra)

##
## Attaching package: 'gridExtra'

## The following object is masked from 'package:dplyr':
##
##   combine

library(Metrics)
library(ggfortify)

## Warning: package 'ggfortify' was built under R version 4.0.3

library(ggforce)

## Warning: package 'ggforce' was built under R version 4.0.2

library(ggeffects)

## Warning: package 'ggeffects' was built under R version 4.0.3

library(sjPlot)

## Warning: package 'sjPlot' was built under R version 4.0.3

## Registered S3 methods overwritten by 'lme4':
##   method                                from
##   cooks.distance.influence.merMod      car
##   influence.merMod                     car
##   dfbeta.influence.merMod              car
##   dfbetas.influence.merMod             car

## Learn more about sjPlot with 'browseVignettes("sjPlot")'.

library(corrplot)

## Warning: package 'corrplot' was built under R version 4.0.2

## corrplot 0.84 loaded

library(MuMIn)
library(lme4)

## Warning: package 'lme4' was built under R version 4.0.3

## Loading required package: Matrix

library(Hmisc)

## Warning: package 'Hmisc' was built under R version 4.0.3

```

```

## Loading required package: lattice
## Loading required package: survival
## Loading required package: Formula
## Warning: package 'Formula' was built under R version 4.0.3
##
## Attaching package: 'Hmisc'
## The following objects are masked from 'package:dplyr':
##
##   src, summarize
## The following objects are masked from 'package:base':
##
##   format.pval, units

library(tidyverse)

## Registered S3 method overwritten by 'httr':
##   method          from
##   print.cache_info hoardr

## -- Attaching packages ----- tidyverse 1.3.0 --

## v tibble  3.0.6      v purrr   0.3.4
## v tidyr   1.1.2      v stringr 1.4.0
## v readr   1.4.0      v forcats 0.5.1

## Warning: package 'tibble' was built under R version 4.0.3
## Warning: package 'tidyr' was built under R version 4.0.3
## Warning: package 'readr' was built under R version 4.0.3
## Warning: package 'forcats' was built under R version 4.0.3

## -- Conflicts ----- tidyverse_conflicts() --
## x lubridate::as.difftime() masks base::as.difftime()
## x gridExtra::combine()    masks dplyr::combine()
## x lubridate::date()       masks base::date()
## x tidyr::expand()         masks Matrix::expand()
## x dplyr::filter()         masks stats::filter()
## x lubridate::intersect()  masks base::intersect()
## x dplyr::lag()            masks stats::lag()
## x tidyr::pack()           masks Matrix::pack()
## x lubridate::setdiff()    masks base::setdiff()
## x Hmisc::src()            masks dplyr::src()
## x Hmisc::summarize()      masks dplyr::summarize()
## x lubridate::union()      masks base::union()
## x tidyr::unpack()         masks Matrix::unpack()

library(sitreeE)

## Warning: package 'sitreeE' was built under R version 4.0.2

```

```

## Loading required package: sitree
## Warning: package 'sitree' was built under R version 4.0.2
## Loading required package: data.table
## Warning: package 'data.table' was built under R version 4.0.3
##
## Attaching package: 'data.table'
## The following object is masked from 'package:purrr':
##
##   transpose
## The following objects are masked from 'package:lubridate':
##
##   hour, isoweek, mday, minute, month, quarter, second, wday, week
##   yday, year
## The following objects are masked from 'package:reshape2':
##
##   dcast, melt
## The following objects are masked from 'package:dplyr':
##
##   between, first, last
library(ggpointdensity)
## Warning: package 'ggpointdensity' was built under R version 4.0.2
library(viridis)
## Loading required package: viridisLite
# Load location specific info
points <- read.csv("points.csv")

```

1) Download NCEP climate forcing data

```

# Create empty dataframes to store outputs in
M <- vector("list", length = nrow(points))
climdata <- data.frame()

for (a in 1:nrow(points)) {
  start <- if_else(points$type[a] == "plot", as.POSIXlt("2018-09-01"),
), as.POSIXlt("2019-01-01"))
  end <- start + as.difftime(56, units = "weeks")
  interval <- 60
  tme <- seq(from = start, by = interval * 60, to = end)
  climate <- hourlyNCEP(lat = points$lat[a], long = points$long[a],
tme = tme)
  climate1 <- hourlyncep_convert(climate, lat = points$lat[a], long
= points$long[a])

```

```

climate1["Loc"] = points$ID[a]
climdata <- rbind(climdata, climate1)
}

# Save data as csv file write.csv(climdata, file='climNCEPdata.csv')

```

2) Run the microclimc model

```

# Load NCEP data
climdata <- read.csv("climNCEPdata.csv")
# Input Location info
points <- read.csv("points.csv")
# Initialise empty dataframe to store outputs
metout <- data.frame()

for (a in 1:nrow(points)) {
  climate <- filter(climdata, Loc == points$Loc[a])
  tme <- as.POSIXlt(climate$obs_time, format = "%Y-%m-%d %H:%M")
  prec <- dailyprecipNCEP(lat = points$lat[a], long = points$long[a],
, tme)
  vegp <- habitatvars(2, lat = points$lat[a], long = points$long[a],
tme, m = 20)
  vegp$hgt <- points$veghyt[a]
  soilp <- soilinit("Loam")
  # Run model in hourly timesteps for a year using weather dataset i
ncluded
  # with the package
  dataout <- runwithNMR(climate, prec, vegp, soilp, reqhgt = (points
$refhyt[a]),
  lat = points$lat[a], long = points$long[a])
  metout1 <- dataout$metout
  metout1$obs_time <- with_tz(metout1$obs_time, tzone = "Asia/Jakart
a")
  metout1["Loc"] = points$Loc[a]
  metout1["logID"] = points$logID[a]
  metout1["height"] = points$height[a]
  metout <- rbind(metout, metout1)
}

# Reformat dates & convert timezone to Jakarta
metout$obs_time <- parse_date_time(metout$obs_time, "ymd HMS")
metout["hour"] = hour(metout$obs_time)
metout["DOY"] = yday(metout$obs_time)
metout["week"] = week(metout$obs_time)
metout["month"] = month(metout$obs_time)

# Save microclimc predictions as .csv file write.csv(metout,
# file='microclimc_output.csv')

```

Appendix 5.1

R scripts to run the NicheMapR endotherm model

This document provides the R code, required inputs, and outputs of the the NicheMapR microclimate and endotherm models, which is used to calculate heat exchange, metabolism, and water loss for Sumatran orangutan at Sikundur, North Sumatra.

Initial setup

```
# Load packages
library(NicheMapR)
library(ggplot2)
library(dplyr)
library(knitr)
library(tidyr)
library(lubridate)
library(ggpubr)
library(gridExtra)
library(Metrics)
library(reshape2)
library(ggforce)
library(ggpubr)

# Load in datafile for input data points
point <- read.csv("points.csv")
# Filter points df to keep only locations of interest Filter locations for
# points of interest only
filter <- c(1.1, 2.1, 3.1, 4.1, 1.5, 2.5, 3.5, 4.5)
point <- filter(point, ID %in% filter)

# Read in logger data
loggers <- read.csv("clim_hourly.csv")
# Removing rows of data where Lux >32,000, or where temp increased by
>5, plus
# the following two data points (to remove obs where logger was exposed to
direct sunlight resulting in high temp recordings).
loggers <- filter(loggers, keep != "FALSE")
# Convert datetime column to POSIXct format and remove duplicate columns
loggers$datetime <- parse_date_time(loggers$datetime, "dmy HM")
```

1) Run the microclimate model

Run the microclimate model, extract & export outputs:

```
# Create empty data frames where models outputs will be stored.
M <- vector("list", length = nrow(point))
shadmet <- data.frame()
```

```

metout <- data.frame()

# Specify number of days to run model for:
t <- 365

# Run the model using parameters from points data frame. Append Loc,
height &
# date to outputs for both max shade (shadmet) and no shade (metout).
The Loop
# will run the model for each row, and automatically add the output to
the
# dataframes created in the previous step.
for (l in 1:nrow(point)) {
  M[[l]] <- micro_global(loc = c(point$long[l], point$lat[l]), runmo
ist = 0, runshade = 1,
  minshade = 0, maxshade = point$shade[l], timeinterval = t, REF
L = 0.1, elev = point$elevation[l],
  slope = point$slope[l], aspect = point$aspect[l], RUF = 0.02,
D0 = point$D0[l],
  ZH = point$ZH, writecsv = 1, message = 0, Refhyt = point$heigh
t[l], Ushrht = point$midheight[l])
  shad <- data.frame(M[[l]][["shadmet"]])
  shad["LocID"] = point$ID[l]
  shad["height"] = point$height[l]
  shad["date"] <- as.Date(shad$DOY, origin = "2018-12-31")
  shad["month"] = month(shad$date)
  shad["hour"] = shad$TIME/60
  shad["week"] = week(shad$date)
  shadmet <- rbind(shadmet, shad)
  met <- data.frame(M[[l]][["metout"]])
  met["LocID"] = point$ID[l]
  met["height"] = point$height[l]
  met["date"] <- as.Date(met$DOY, format = "%j", origin = "2018-12-3
1")
  met["month"] = month(met$date)
  met["hour"] = met$TIME/60
  met["week"] = week(met$date)
  metout <- rbind(metout, met)
}

# Reorder output dataframes to put Loc and height and date columns fir
st
metout <- metout[, c(20:25, 1:19)]
shadmet <- shadmet[, c(20:25, 1:19)]

# Write output files to .csv in source directory
write.csv(metout, "metout_SRTM.csv")
write.csv(shadmet, "shadmet_SRTM.csv")

```

Plots of observed & predicted values:

Calculate correlation coefficients, RMSE and MAD of model predictions against logger data for each location:

2) Running the endotherm model for a series of ambient temperatures

Run the microclimate model for mid-canopy heights:

```
# Create empty data frames where models outputs will be stored.
M <- vector("list", length = nrow(point))
shadmet <- data.frame()
metout <- data.frame()

# Specify number of days to run model for:
t <- 365

# Run the model using parameters from points data frame. Append Loc,
height &
# date to outputs for both max shade (shadmet) and no shade (metout).
The loop
# will run the model for each row, and automatically add the output to
the
# dataframes created in the previous step.
for (l in 1:nrow(point)) {
  M[[l]] <- micro_global(loc = c(point$long[l], point$lat[l]), runmo
ist = 0, runshade = 1,
  minshade = 0, maxshade = point$shade[l], timeinterval = t, REF
L = 0.1, elev = point$elevation[l],
  slope = point$slope[l], aspect = point$aspect[l], RUF = 0.02,
D0 = point$D0[l],
  ZH = point$ZH[l], writecsv = 1, message = 0, Refhyt = point$he
ight[l], Usrhyt = point$midheight[l])
  shad <- data.frame(M[[l]][["shadmet"]])
  shad["LocID"] = point$ID[l]
  shad["height"] = point$height[l]
  shad["date"] <- as.Date(shad$DOY, origin = "2018-12-31")
  shad["month"] = month(shad$date)
  shad["hour"] = shad$TIME/60
  shad["week"] = week(shad$date)
  shadmet <- rbind(shadmet, shad)
  met <- data.frame(M[[l]][["metout"]])
  met["LocID"] = point$ID[l]
  met["height"] = point$height[l]
  met["date"] <- as.Date(met$DOY, format = "%j", origin = "2018-12-3
1")
  met["month"] = month(met$date)
  met["hour"] = met$TIME/60
  met["week"] = week(met$date)
  metout <- rbind(metout, met)
}

# Reorder output dataframes to put Loc and height and date columns fir
st
metout <- metout[, c(20:25, 1:19)]
shadmet <- shadmet[, c(20:25, 1:19)]

# Save model outputs write.csv(shadmet, 'micro_mid.csv')
```

2a) Using predicted values of orangutan BMR based on the mouse-elephant curve:

Model parameters:

```
cat <- c("adult male", "adult female", "juvenile") # List of age/sex
classes

# core temperature
TC <- 33.4 # core temperature (deg C)
TCMAX <- 35.2 # maximum core temperature (deg C)
RAISETC <- 0.25 # increment by which TC is elevated (deg C)

# size and shape
AMASS <- c(116, 55, 25.5) # mass, kg (adult male, adult female, juven
ile)
SHAPE <- 4 # use ellipsoid geometry
SHAPE_B_REF <- 4 # start off near to a sphere (-)
SHAPE_B_MAX <- 5 # maximum ratio of length to width/depth
UNCURL <- 0.1 # allows the animal to uncurl to SHAPE_B_MAX, the value
being the increment SHAPE_B is increased per iteration
SAMODE <- 2 # surface area relations (2 is mammal, 0 is based on shap
e specified in GEOM)

# fur properties
DHAIRD = 0.00015 # hair diameter, dorsal (m)
DHAIRV = 0.00015 # hair diameter, ventral (m)
LHAIRD = c(0.15, 0.1, 0.05) # hair length, dorsal (m) (adult male, fe
male & juvenile)
LHAIRV = 0.05 # hair length, ventral (m)
ZFURD = 0.03 # fur depth, dorsal (m)
ZFURV = 0.03 # fur depth, ventral (m)
RHOD = 1760000 # hair density, dorsal (1/m2)
RHOV = 9e+05 # hair density, ventral (1/m2)
REFLD = 0.2 # fur reflectivity dorsal (fractional, 0-1)
REFLV = 0.2 # fur reflectivity ventral (fractional, 0-1)

# physiological responses
SKINW <- 0.1 # base skin wetness (%)
MXWET <- 5 # maximum skin wetness (%)
SWEAT <- 0.25 # intervals by which skin wetness is increased (%)
Q10 <- 2.2 # Q10 effect of body temperature on metabolic rate (-)
QBASAL.est <- c(120.18, 68.67, 38.58) # basal heat generation (W) (ma
le, female & juvenile)
DELTAR <- 5 # offset between air tempeprature and breath (°C)
EXTREF <- 20 # O2 extraction efficiency (%)
PANTING <- 0.1 # turns on panting, the value being the increment by w
hich the panting multiplier is increased up to the maximum value, PANT
MAX
PANTMAX <- 15 # maximum panting rate - multiplier on air flow through
the lungs above that determined by metabolic rate
```

Running the model for a series of ambient temps:

```
# environment parameters
TAs <- seq(0, 50, 1) # air temperature (deg C)
VEL <- 1 # wind speed (m/s)
vd <- WETAIR(rh = 30, db = 40)$vd # Weather and Schoenbaechler had 16
.7 mm Hg above 40 deg C = 30% RH at 40 deg C
```

```

vd_sat <- WETAIR(rh = 100, db = TAs)$vd # Weather and Schoenbaechler
had 16.7 mm Hg above 40 deg C = 30% RH at 40 deg C
exp_rh <- vd/vd_sat * 100
exp_rh[exp_rh > 100] <- 100
exp_rh[TAs < 30] <- 15
hum <- exp_rh #rep(humidity,96)
Q10s <- rep(1, length(TAs))
Q10s[TAs >= TCMAX] <- 2 # assuming Q10 effect kicks in only after air
temp rises above TCMAX
# Run the model
endo.TAs <- data.frame()

for (c in 1:3) {
  MASS <- AMASS[c]
  HAIRD <- LHAIRD[c]
  BASAL <- QBASAL.est[c]
  endo.out <- lapply(1:length(TAs), function(x) {
    endoR(TA = TAs[x], VEL = VEL, TC = TC, TCMAX = TCMAX, RH = 90,
AMASS = MASS,
      SHAPE = SHAPE, SHAPE_B_REF = SHAPE_B_REF, SHAPE_B_MAX = SH
APE_B_MAX,
      SKINW = SKINW, SWEAT = SWEAT, MXWET = MXWET, Q10 = Q10s[x]
, QBASAL = BASAL,
      DELTAR = DELTAR, DHAIRD = DHAIRD, DHAIRV = DHAIRV, LHAIRD
= HAIRD, LHAIRV = LHAIRV,
      ZFURD = ZFURD, ZFURV = ZFURV, RHOD = RHOD, RHOV = RHOV, RE
FLD = REFLD,
      RAISETC = RAISETC, PANTING = PANTING, PANTMAX = PANTMAX, E
XTREF = EXTREF,
      UNCURL = UNCURL, SAMODE = SAMODE, SHADE = 80)
  }) # run endoR
  # extract the output
  endo.out1 <- do.call("rbind", lapply(endo.out, data.frame))
  # thermoregulation output
  treg <- endo.out1[, grep(pattern = "treg", colnames(endo.out1))]
  colnames(treg) <- gsub(colnames(treg), pattern = "treg.", replacem
ent = "")
  # morphometric output
  morph <- endo.out1[, grep(pattern = "morph", colnames(endo.out1))]
  colnames(morph) <- gsub(colnames(morph), pattern = "morph.", repla
cement = "")
  # heat balance
  enbal <- endo.out1[, grep(pattern = "enbal", colnames(endo.out1))]
  colnames(enbal) <- gsub(colnames(enbal), pattern = "enbal.", repla
cement = "")
  # mass aspects
  masbal <- endo.out1[, grep(pattern = "masbal", colnames(endo.out1)
)]
  colnames(masbal) <- gsub(colnames(masbal), pattern = "masbal.", re
placement = "")
  QGEN <- enbal$QMET # metabolic rate (W)
  H2O <- masbal$H2OResp_g + masbal$H2OCut_g # g/h water evaporated
  TFA_D <- treg$TFA_D # dorsal fur surface temperature
  TFA_V <- treg$TFA_V # ventral fur surface temperature
  TskinD <- treg$TSKIN_D # dorsal skin temperature

```

```

TskinV <- treg$TSKIN_V # ventral skin temperature
TCs <- treg$TC # core temperature
# Combine outputs into one dataframe
out <- data.frame(TAs, QGEN, H2O, TFA_D, TFA_V, TskinD, TskinV, TC
s)
# Add column for class (adult male/adult female/juvenile)
out["class"] = cat[c]
endo.TAs <- rbind(endo.TAs, out)
}
# write.csv(endo.TAs, 'endo_TAs_predBMR.csv')

```

Plot the results:

```

# Plot TAs vs TCs
TCs <- ggplot(endo.TAs, aes(x = TAs, y = TCs, colour = class)) + geom_
point(aes(shape = class),
      size = 1) + xlim(0, 40) + xlab("Air temperature, °C") + ylab("Core
body temperature, °C") +
  theme_bw() + theme(panel.grid = element_blank()) + theme(legend.ti
tle = element_blank()) +
  theme(axis.title = element_text(size = 12), axis.text = element_te
xt(size = 10))

# Fur temperature
TFA <- ggplot(endo.TAs, aes(x = TAs, y = TFA_D, colour = class)) + geo
m_point(aes(shape = class),
      size = 1) + xlim(0, 40) + xlab("Air temperature, °C") + ylab("Dorsa
l fur temperature, °C") +
  theme_bw() + theme(panel.grid = element_blank()) + theme(legend.ti
tle = element_blank()) +
  theme(axis.title = element_text(size = 12), axis.text = element_te
xt(size = 10))

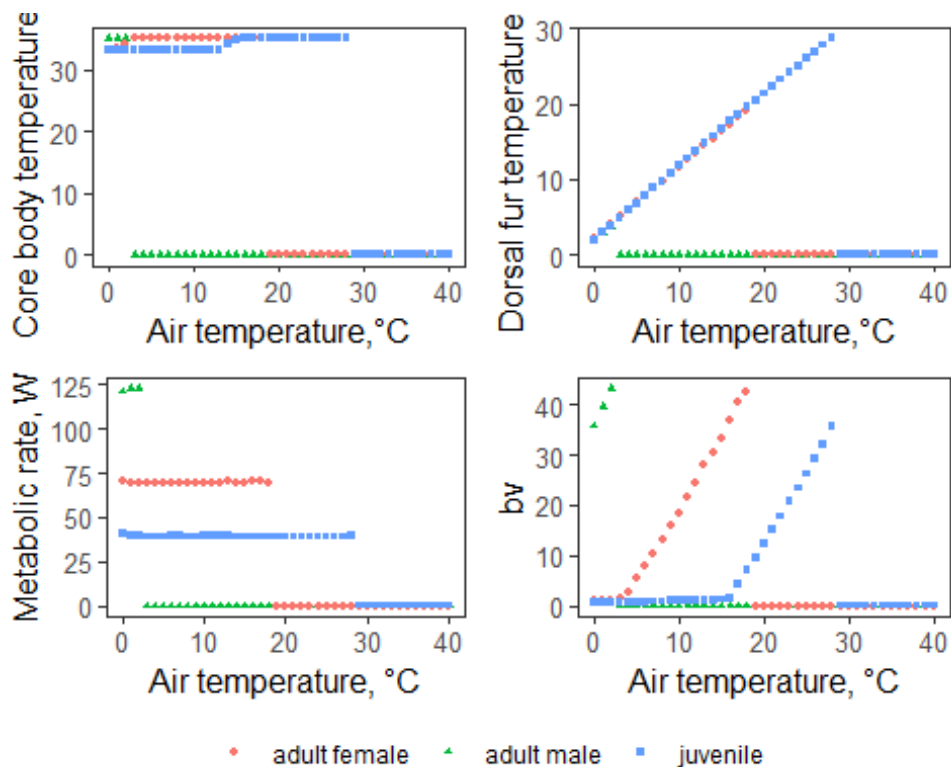
# metabolic rate
MR <- ggplot(endo.TAs, aes(x = TAs, y = QGEN, colour = class)) + geom_
point(aes(shape = class),
      size = 1) + xlab("Air temperature, °C") + ylab("Metabolic rate, W"
) + xlim(0,
      40) + theme_bw() + theme(panel.grid = element_blank()) + theme(leg
end.title = element_blank()) +
  theme(axis.title = element_text(size = 12), axis.text = element_te
xt(size = 10))

# Water Loss
H2Oloss <- ggplot(endo.TAs, aes(x = TAs, y = H2O, colour = class)) + g
eom_point(aes(shape = class),
      size = 1) + xlim(0, 40) + xlab("Air temperature, °C") + ylab("bv")
+ theme_bw() +
  theme(panel.grid = element_blank()) + theme(legend.title = element
_blank()) +
  theme(axis.title = element_text(size = 12), axis.text = element_te
xt(size = 10))

(TAplots <- ggarrange(TCs, TFA, MR, H2Oloss, ncol = 2, nrow = 2, commo

```

```
n.legend = TRUE,
  legend = "bottom"))
```



```
# ggexport(TAPlots,filename='TAPlots_predBMR.pdf')
```

2b) Using observed values of BMR taken from Pontzer et al (2010)

Model parameters:

```
cat <- c("adult male", "adult female", "juvenile") # List of age/sex
classes

# core temperature
TC <- 36 # core temperature (deg C)
TCMAX <- 38 # maximum core temperature (deg C)
RAISETC <- 0.25 # increment by which TC is elevated (deg C)

# size and shape
AMASS <- c(116, 55, 25.5) # mass, kg (adult male, adult female, juven
ile)
SHAPE <- 4 # use ellipsoid geometry
SHAPE_B_REF <- 4 # start off near to a sphere (-)
SHAPE_B_MAX <- 5 # maximum ratio of length to width/depth
UNCURL <- 0.1 # allows the animal to uncurl to SHAPE_B_MAX, the value
being the increment SHAPE_B is increased per iteration
SAMODE <- 2 # surface area relations (2 is mammal, 0 is based on shap
e specified in GEOM)

# fur properties
DHAIRD = 0.00015 # hair diameter, dorsal (m)
DHAIRV = 0.00015 # hair diameter, ventral (m)
```

```

LHAIRD = c(0.15, 0.1, 0.05) # hair length, dorsal (m) (adult male, fe
male & juvenile)
LHAIRV = 0.05 # hair length, ventral (m)
ZFURD = 0.03 # fur depth, dorsal (m)
ZFURV = 0.03 # fur depth, ventral (m)
RHOD = 1760000 # hair density, dorsal (1/m2)
RHOV = 9e+05 # hair density, ventral (1/m2)
REFLD = 0.2 # fur reflectivity dorsal (fractional, 0-1)
REFLV = 0.2 # fur reflectivity ventral (fractional, 0-1)

# physiological responses
SKINW <- 0.1 # base skin wetness (%)
MXWET <- 5 # maximum skin wetness (%)
SWEAT <- 0.25 # intervals by which skin wetness is increased (%)
Q10 <- 2.2 # Q10 effect of body temperature on metabolic rate (-)
QBASAL.obs <- c(77.39, 63.77, 49.96) # basal heat generation (W) (mal
e, female & juvenile)
DELTAR <- 5 # offset between air tempeprature and breath (°C)
EXTREF <- 20 # O2 extraction efficiency (%)
PANTING <- 0.1 # turns on panting, the value being the increment by w
hich the panting multiplier is increased up to the maximum value, PANT
MAX
PANTMAX <- 15 # maximum panting rate - multiplier on air flow through
the lungs above that determined by metabolic rate

```

Running the model for a series of ambient temps:

```

# environment parameters
TAs <- seq(0, 50, 1) # air temperature (deg C)
VEL <- 1 # wind speed (m/s)
vd <- WETAIR(rh = 30, db = 40)$vd # Weather and Schoenbaechler had 16
.7 mm Hg above 40 deg C = 30% RH at 40 deg C
vd_sat <- WETAIR(rh = 100, db = TAs)$vd # Weather and Schoenbaechler
had 16.7 mm Hg above 40 deg C = 30% RH at 40 deg C
exp_rh <- vd/vd_sat * 100
exp_rh[exp_rh > 100] <- 100
exp_rh[TAs < 30] <- 15
hum <- exp_rh #rep(humidity,96)
Q10s <- rep(1, length(TAs))
Q10s[TAs >= TCMAX] <- 2 # assuming Q10 effect kicks in only after air
temp rises above TCMAX
# Run the model
endo.TAs <- data.frame()

for (c in 1:3) {
  MASS <- AMASS[c]
  HAIRD <- LHAIRD[c]
  BASAL <- QBASAL.obs[c]
  endo.out <- lapply(1:length(TAs), function(x) {
    endoR(TA = TAs[x], VEL = VEL, TC = TC, TCMAX = TCMAX, RH = 90,
    AMASS = MASS,
    SHAPE = SHAPE, SHAPE_B_REF = SHAPE_B_REF, SHAPE_B_MAX = SH
    APE_B_MAX,
    SKINW = SKINW, SWEAT = SWEAT, MXWET = MXWET, Q10 = Q10s[x]
    , QBASAL = BASAL,

```

```

        DELTAR = DELTAR, DHAIRD = DHAIRD, DHAIRV = DHAIRV, LHAIRD
= HAIRD, LHAIRV = LHAIRV,
        ZFURD = ZFURD, ZFURV = ZFURV, RHOD = RHOD, RHOV = RHOV, RE
FLD = REFLD,
        RAISETC = RAISETC, PANTING = PANTING, PANTMAX = PANTMAX, E
XTREF = EXTREF,
        UNCURL = UNCURL, SAMODE = SAMODE, SHADE = 80)
    }) # run endoR
    # extract the output
    endo.out1 <- do.call("rbind", lapply(endo.out, data.frame))
    # thermoregulation output
    treg <- endo.out1[, grep(pattern = "treg", colnames(endo.out1))]
    colnames(treg) <- gsub(colnames(treg), pattern = "treg.", replacem
ent = "")
    # morphometric output
    morph <- endo.out1[, grep(pattern = "morph", colnames(endo.out1))]
    colnames(morph) <- gsub(colnames(morph), pattern = "morph.", repla
cement = "")
    # heat balance
    enbal <- endo.out1[, grep(pattern = "enbal", colnames(endo.out1))]
    colnames(enbal) <- gsub(colnames(enbal), pattern = "enbal.", repla
cement = "")
    # mass aspects
    masbal <- endo.out1[, grep(pattern = "masbal", colnames(endo.out1)
)]
    colnames(masbal) <- gsub(colnames(masbal), pattern = "masbal.", re
placement = "")
    QGEN <- enbal$QMET # metabolic rate (W)
    H2O <- masbal$H2OResp_g + masbal$H2OCut_g # g/h water evaporated
    TFA_D <- treg$TFA_D # dorsal fur surface temperature
    TFA_V <- treg$TFA_V # ventral fur surface temperature
    TskinD <- treg$TSKIN_D # dorsal skin temperature
    TskinV <- treg$TSKIN_V # ventral skin temperature
    TCs <- treg$TC # core temperature
    # Combine outputs into one dataframe
    out <- data.frame(TAs, QGEN, H2O, TFA_D, TFA_V, TskinD, TskinV, TC
s)
    # Add column for class (adult male/adult female/juvenile)
    out["class"] = cat[c]
    endo.TAs <- rbind(endo.TAs, out)
}
# write.csv(endo.TAs, 'endo_TAs_obsBMR.csv')

```

Plot the results (point):

```

# Plot TAs vs TCs - scatterplot
TCs <- ggplot(endo.TAs, aes(x = TAs, y = TCs, colour = class)) + geom_
point(aes(shape = class),
      size = 1) + xlim(0, 40) + xlab("Air temperature, °C") + ylab("Body
temperature, °C") +
  theme_bw() + theme(panel.grid = element_blank()) + theme(legend.ti
tle = element_blank()) +
  theme(axis.title = element_text(size = 12), axis.text = element_te
xt(size = 10))

```

```

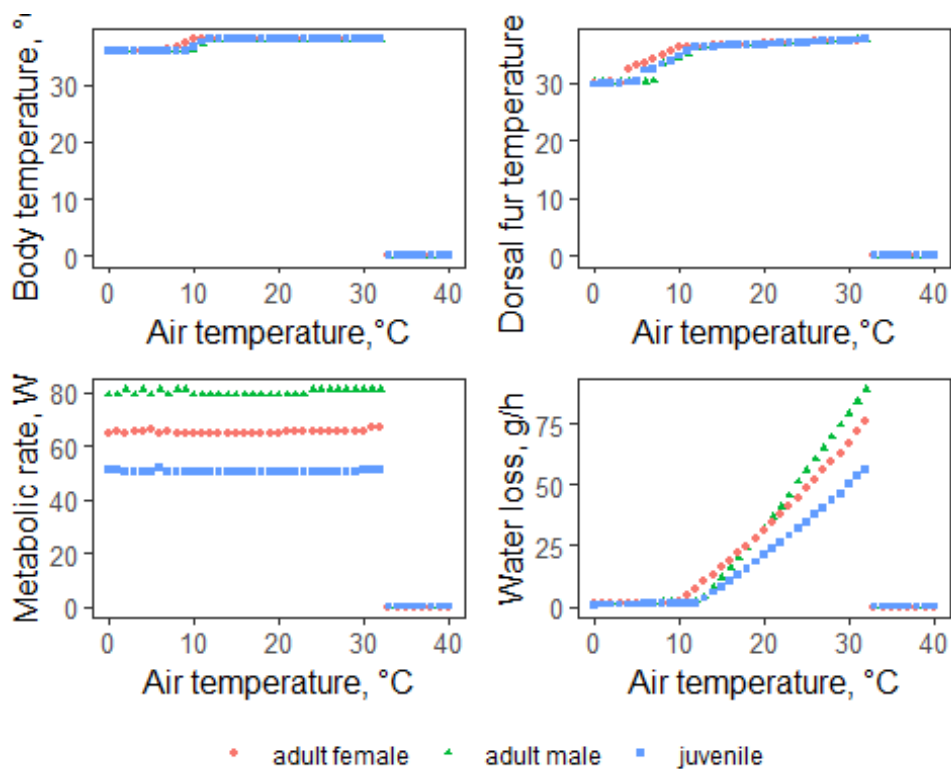
# Fur temperature
TFA <- ggplot(endo.TAs, aes(x = TAs, y = TskinD, colour = class)) + geom_point(aes(shape = class),
  size = 1) + xlim(0, 40) + xlab("Air temperature, °C") + ylab("Dorsal fur temperature, °C") +
  theme_bw() + theme(panel.grid = element_blank()) + theme(legend.title = element_blank()) +
  theme(axis.title = element_text(size = 12), axis.text = element_text(size = 10))

# metabolic rate
MR <- ggplot(endo.TAs, aes(x = TAs, y = QGEN, colour = class)) + geom_point(aes(shape = class),
  size = 1) + xlab("Air temperature, °C") + ylab("Metabolic rate, W") + xlim(0,
  40) + theme_bw() + theme(panel.grid = element_blank()) + theme(legend.title = element_blank()) +
  theme(axis.title = element_text(size = 12), axis.text = element_text(size = 10))

# Water Loss
H2Oloss <- ggplot(endo.TAs, aes(x = TAs, y = H2O, colour = class)) + geom_point(aes(shape = class),
  size = 1) + xlim(0, 40) + xlab("Air temperature, °C") + ylab("Water loss, g/h") +
  theme_bw() + theme(panel.grid = element_blank()) + theme(legend.title = element_blank()) +
  theme(axis.title = element_text(size = 12), axis.text = element_text(size = 10))

(TAplots <- ggarrange(TCs, TFA, MR, H2Oloss, nrow = 2, ncol = 2, common.legend = TRUE,
  legend = "bottom"))

```



```
# ggexport(TApLots,filename='TApLots_obsBMR.pdf')
```

3) Running the model for locations at Sikundur, using the microclimate model as environmental inputs

3a) Using BMR from mouse-elephant curve

```
# run the model for shaded conditions
E <- vector("list", length = nrow(point))
endo.est <- data.frame()

# Use for loop to run for all three classes and all rows in points df
# automatically
for (c in 1:3) {
  MASS <- AMASS[c]
  HAIRD <- LHAIRD[c]
  BASAL <- QBASAL.est[c]
  for (X in 1:nrow(point)) {
    # extract microclimate outputs
    micro <- data.frame(M[[X]][["metout"]]) # unshaded above-ground conditions
    soil <- data.frame(M[[X]][["soil"]])
    micro.shad <- data.frame(M[[X]][["shadmet"]]) # shaded above-ground conditions
    shadsoil <- data.frame(M[[X]][["shadsoil"]])
    dates <- (M[[X]][["dates"]])
    # Location-specific environment parameters
    TAs <- micro.shad$TALOC # air temperatures at height of animal
```

```

L (deg C)
  TAREFs <- micro.shad$TAREF # air temperatures at reference height (deg C)
  TSKYs <- micro.shad$TSKYC # sky temperatures (deg C)
  TGRDs <- shadsoil$D0cm # surface temperatures (deg C)
  VELs <- micro.shad$VLOC # wind speeds at animal height (m/s)
  RHs <- micro.shad$RHLOC # relative humidity at animal height (%)

  SHADE <- (100 - point$shade[X])/100
  QSOLRs <- micro.shad$SOLR * SHADE # solar radiation (W/m2) corrected for shade level
  Zs <- micro.shad$ZEN # zenith angle of the sun (degrees)
  ELEV <- (M[[X]][["elev"]]) # elevation (m)
  ABSSB <- 1 - (M[[X]][["REFL"]]) # substrate solar absorptivity (%)

# Run the model
E[[X]] <- lapply(1:length(TAs), function(x) {
  endoR(TA = TAs[x], TAREF = TAREFs[x], TSKY = TSKYs[x], TGRD = TGRDs[x],
        VEL = VELs[x], RH = RHs[x], QSOLR = QSOLRs[x], Z = Zs[x], ELEV = ELEV,
        ABSSB = ABSSB, TC = TC, TCMAX = TCMAX, AMASS = MASS, SHAPE = SHAPE,
        SHAPE_B_REF = SHAPE_B_REF, SHAPE_B_MAX = SHAPE_B_MAX, SKINW = SKINW,
        SWEAT = SWEAT, Q10 = Q10, QBASAL = BASAL, DELTAR = DELTAR, DHAIRD = DHAIRD,
        DHAIRV = DHAIRV, LHAIRD = LHAIRD, LHAIRV = LHAIRV, ZFURD = ZFURD,
        ZFURV = ZFURV, RHOD = RHOD, RHOV = RHOV, REFLD = REFLD, RAISETC = RAISETC,
        PANTING = PANTING, PANTMAX = PANTMAX, EXTREF = EXTREF, UNCURL = UNCURL,
        SAMODE = SAMODE, SHADE = 0)
})
# Extract the outputs and bind to master dataframe
endo.out <- do.call("rbind", lapply(E[[X]], data.frame))
endo.out["LocID"] = point$ID[X]
endo.out["class"] = cat[c]
endo.out <- cbind(endo.out, TAs)
endo.est <- rbind(endo.est, endo.out)
}
}
# write.csv(endo.est, 'endo_shade_est.csv')

```

3b) observed BMR values from Pontzer et al (2010)

```

# run the model for shaded conditions
E <- vector("list", length = nrow(point))
endo <- data.frame()

# Use for loop to run for all three classes and all rows in points df
# automatically

```

```

for (c in 1:3) {
  MASS <- AMASS[c]
  HAIRD <- LHAIRD[c]
  BASAL <- QBASAL.obs[c]
  for (X in 1:nrow(point)) {
    # extract microclimate outputs
    micro <- data.frame(M[[X]][["metout"]]) # unshaded above-ground
nd conditions
    soil <- data.frame(M[[X]][["soil"]])
    micro.shad <- data.frame(M[[X]][["shadmet"]]) # shaded above-
ground conditions
    shadsoil <- data.frame(M[[X]][["shadsoil"]])
    dates <- (M[[X]][["dates"]])
    # Location-specific environment parameters
    TAs <- micro.shad$TALOC # air temperatures at height of anima
L (deg C)
    TAREFs <- micro.shad$TAREF # air temperatures at reference he
ight (deg C)
    TSKYs <- micro.shad$TSKYC # sky temperatures (deg C)
    TGRDs <- shadsoil$D0cm # surface temperatures (deg C)
    VELs <- micro.shad$VLOC # wind speeds at animal height (m/s)
    RHs <- micro.shad$RHLOC # relative humidity at animal height
(%)
    SHADE <- (100 - point$shade[X])/100
    QSOLRs <- micro.shad$SOLR * SHADE # solar radiation (W/m2) co
rrected for shade level
    Zs <- micro.shad$ZEN # zenith angle of the sun (degrees)
    ELEV <- (M[[X]][["elev"]]) # elevation (m)
    ABSSB <- 1 - (M[[X]][["REFL"]]) # substrate solar absorptivit
y (%)
    # Run the model
    E[[X]] <- lapply(1:length(TAs), function(x) {
      endoR(TA = TAs[x], TAREF = TAREFs[x], TSKY = TSKYs[x], TGR
D = TGRDs[x],
          VEL = VELs[x], RH = RHs[x], QSOLR = QSOLRs[x], Z = Zs[
x], ELEV = ELEV,
          ABSSB = ABSSB, TC = TC, TCMAX = TCMAX, AMASS = MASS, S
HAPE = SHAPE,
          SHAPE_B_REF = SHAPE_B_REF, SHAPE_B_MAX = SHAPE_B_MAX,
SKINW = SKINW,
          SWEAT = SWEAT, Q10 = Q10, QBASAL = BASAL, DELTAR = DEL
TAR, DHAIRD = DHAIRD,
          DHAIRV = DHAIRV, LHAIRD = HAIRD, LHAIRV = LHAIRV, ZFUR
D = ZFURD,
          ZFURV = ZFURV, RHOD = RHOD, RHOV = RHOV, REFLD = REFLD
, RAISETC = RAISETC,
          PANTING = PANTING, PANTMAX = PANTMAX, EXTREF = EXTREF,
UNCURL = UNCURL,
          SAMODE = SAMODE, SHADE = 0)
    })
    # Extract the outputs and bind to master dataframe
    endo.out <- do.call("rbind", lapply(E[[X]], data.frame))
    endo.out["LocID"] = point$ID[X]
    endo.out["class"] = cat[c]
    endo.out <- cbind(endo.out, TAs)
  }
}

```

```

    endo <- rbind(endo, endo.out)
  }
}
# write.csv(endo, 'endo_shaded.csv')

```

Plot endotherm model outputs with estimated BMR input (a) and observed BMR input from Pontzer et al (b).

```

# Add dates to model outputs
dates <- select(shadmet, month, DOY, hour)
dates <- dates %>%
  slice(rep(1:n(), times = 3))

# Endotherm outputs With estimated BMR
endo.est <- cbind(endo.est, dates)

filter1 <- c(1.1, 2.1, 3.1, 4.1)
filter2 <- c(1.5, 2.5, 3.5, 4.5)
endo.est <- endo.est %>%
  mutate(Loc = case_when(LocID %in% filter1 ~ "edge", LocID %in% filter2 ~ "interior"))
# Add total water loss
endo.est["H2O"] = endo.est$masbal.H2OResp_g + endo.est$masbal.H2OCut_g

# Summarise values for average day.
endo.sum <- endo.est %>%
  group_by(class, hour) %>%
  summarise(maxBMR = max(enbal.QMET), meanBMR = mean(enbal.QMET), minBMR = min(enbal.QMET),
            maxH2O = max(H2O), meanH2O = mean(H2O), minH2O = min(H2O), maxCore = max(treg.TC),
            meanCore = mean(treg.TC), minCore = min(treg.TC), maxFur = max(treg.TFA_D),
            meanFur = mean(treg.TFA_D), minFur = min(treg.TFA_D))

# plot values
water <- ggplot(endo.est, aes(x = hour, y = H2O, colour = Loc)) + geom_smooth() +
  xlab("time, hours") + ylab("Water loss, g/h") + ggtitle("(a)") + facet_wrap(~class) +
  theme_pubclean() + theme(legend.title = element_blank(), legend.position = "bottom")

BMR <- ggplot(endo.est, aes(x = hour, y = enbal.QMET, colour = Loc)) + geom_smooth() +
  xlab("time, hours") + ylab("Metabolic rate, W") + ggtitle("(a)") + facet_wrap(~class) +
  theme_pubclean() + theme(legend.title = element_blank(), legend.position = "bottom")

core <- ggplot(endo.est, aes(x = hour, y = treg.TC, colour = Loc)) + geom_smooth() +
  xlab("time, hours") + ylab("Core body temperature, °C") + facet_wrap(~class) +

```

```

    theme_pubclean() + theme(legend.title = element_blank(), legend.po
sition = "bottom")

fur <- ggplot(endo.est, aes(x = hour, y = treg.TFA_D, colour = Loc)) +
geom_smooth() +
  xlab("time, hours") + ylab("Dorsal fur temperature, °C") + ggtitle
("(a)") + facet_wrap(~class) +
  theme_pubclean() + theme(legend.title = element_blank(), legend.po
sition = "bottom")

# With observed BMR

# Add dates to output df
endo <- cbind(endo, dates)
# add column for edge/interior
filter1 <- c(1.1, 2.1, 3.1, 4.1)
filter2 <- c(1.5, 2.5, 3.5, 4.5)
endo <- endo %>%
  mutate(Loc = case_when(LocID %in% filter1 ~ "edge", LocID %in% fil
ter2 ~ "interior"))
# Add column for total water loss
endo["H2O"] = endo$masbal.H2OResp_g + endo$masbal.H2OCut_g

# Summarise values for average day
endo.sum <- endo %>%
  group_by(class, hour) %>%
  summarise(maxBMR = max(enbal.QMET), meanBMR = mean(enbal.QMET), mi
nBMR = min(enbal.QMET),
            maxH2O = max(H2O), meanH2O = mean(H2O), minH2O = min(H2O), max
Core = max(treg.TC),
            meanCore = mean(treg.TC), minCore = min(treg.TC), maxFur = max
(treg.TFA_D),
            meanFur = mean(treg.TFA_D), minFur = min(treg.TFA_D))

# plot values
water.obs <- ggplot(endo, aes(x = hour, y = H2O, colour = Loc)) + geom
_smooth() +
  xlab("time, hours") + ylab("Water loss, g/h") + ggtitle("(b)") + f
acet_wrap(~class) +
  theme_pubclean() + theme(legend.title = element_blank(), legend.po
sition = "bottom")

BMR.obs <- ggplot(endo, aes(x = hour, y = enbal.QMET, colour = Loc)) +
geom_smooth() +
  xlab("time, hours") + ylab("Metabolic rate, W") + ggtitle("(b)") +
facet_wrap(~class) +
  theme_pubclean() + theme(legend.title = element_blank(), legend.po
sition = "bottom")

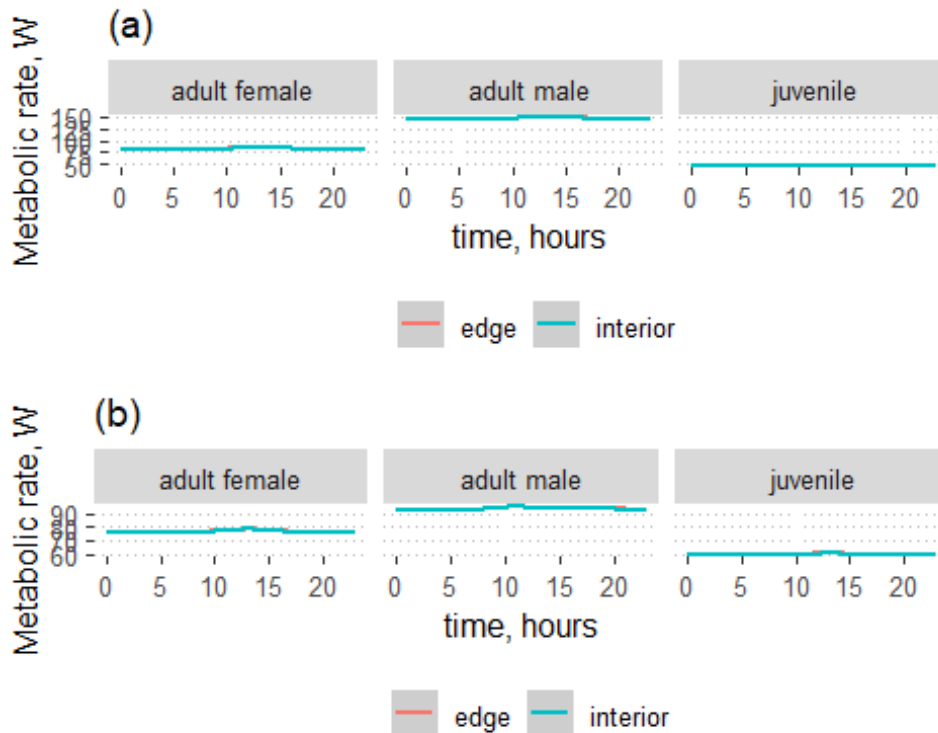
core.obs <- ggplot(endo, aes(x = hour, y = treg.TC, colour = Loc)) + g
eom_smooth() +
  xlab("time, hours") + ylab("Core body temperature, °C") + facet_wr
ap(~class) +
  theme_pubclean() + theme(legend.title = element_blank(), legend.po
sition = "bottom")

```

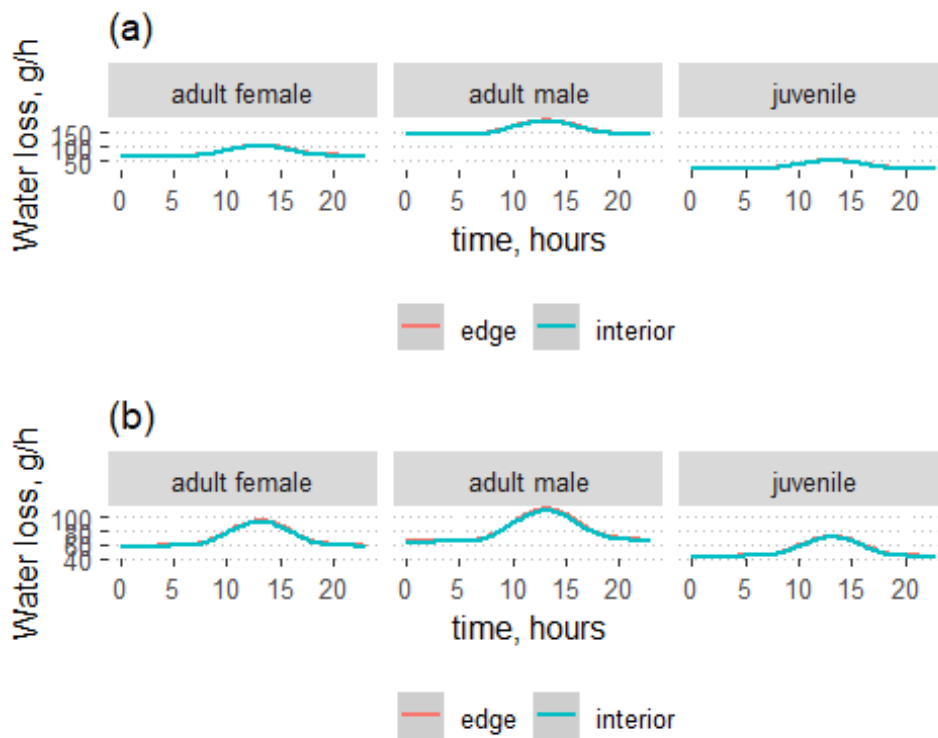
```
fur.obs <- ggplot(endo, aes(x = hour, y = treg.TFA_D, colour = Loc)) +
  geom_smooth() +
  xlab("time, hours") + ylab("Dorsal fur temperature, °C") + ggtitle
  ("(b)") + facet_wrap(~class) +
  theme_pubclean() + theme(legend.title = element_blank(), legend.po
  sition = "bottom")
```

Put figures together and export

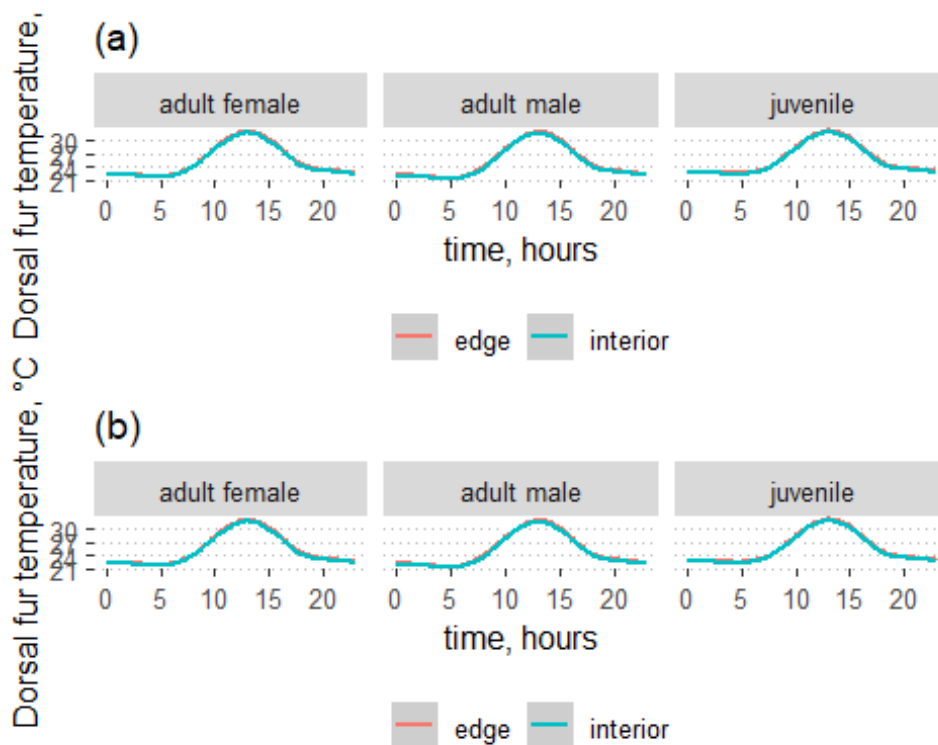
```
BMRplots <- grid.arrange(BMR, BMR.obs, nrow = 2)
```



```
H2Oplots <- grid.arrange(water, water.obs, nrow = 2)
```



```
furplots <- grid.arrange(fur, fur.obs, nrow = 2)
```



```
# ggsave('MRplots.png', plot=BMRplots, height=176, width=176, units='mm')
# ggsave('H2Oplots.png', plot=H2Oplots, height=176, width=176, units='mm')
# ggsave('furplots.png', plot=furplots, height=176, width=176, units='mm')
```